Derivation of Operating Rules for A Multi-Purpose Reservoir Using Soft Computing Techniques

Dr. V. Jothiprakash
Indian Institute of Technology Bombay

DERIVATION OF OPERATING RULES FOR A MULTI-PURPOSE RESERVOIR USING SOFT COMPUTING TECHNIQUES

Project Completion Report

Submitted
to

Indian National Committee on Surface Water
Ministry of Water Resources
Government of India, New Delhi

by

Prof. V. Jothiprakash

Department of Civil Engineering
INDIAN INSTITUTE OF TECHNOLOGY BOMBAY
2014

ABSTRACT

Water is one of the most essential natural resources not only for human survival but also for socio-economic development of a country. The spatial and temporal variation of its availability has necessitated the utilization of available water more efficiently and effectively. Surface water reservoirs play significant role in overcoming this problem apart from serving various purposes like irrigation, hydropower, flood control, industrial and domestic water supply, navigation, etc. The intra basin water sharing in a multi-reservoir system forces the water resources planners to have an integrated operation of multi-reservoir system rather than operating them as a single reservoir system. Thus, optimizing the operations of a multi-reservoir system for an integrated operation is gaining importance, especially in developing countries in India. Optimizing the operations of a multi-reservoir for various purposes requires systematic study. Over the decades, several conventional optimization techniques had been developed and applied for the optimization of complex water resources system. These include techniques such as linear programming (LP), dynamic programming (DP), non-linear programming (NLP), goal programming, etc. However, these conventional techniques have their own advantages and disadvantages.

Recently, evolutionary algorithm (EA) based soft computing techniques have been applied to overcome the drawbacks of conventional techniques in optimizing complex water resources systems. These techniques include genetic algorithm (GA), differential evolution algorithm (DE), ant colony optimization (ACO), particle swarm optimization (PSO) and many more. The major difference between the conventional optimization techniques and soft computing is that in the former case, the optimal solution is derived where as in the soft computing techniques; it is searched from a randomly generated population of possible solutions. Thus, EAs searches the optimal solution from the randomly generated initial population and attains the global optimum over the generation. However, these EAs results in premature convergence and slower iteration to reach global optimal solution for problems having complex hard bound constraints, when the initial population is not so good. Recently, chaos algorithm has been used by researchers to overcome these problems and to enhance the search in EAs.

In the present study, the EAs such as GA and DE are coupled with chaos to enhance the search and applied for optimizing complex multi-reservoir systems having hard bound constraints. The chaos algorithm is used to generate initial population and also in other steps of evolutionary optimization techniques to enhance the search and increase the convergence rate. The proposed techniques are applied for both single and multi-objective optimization of complex multi-reservoir systems, namely, Kukadi Irrigation Project (KIP) and Koyna Hydro-Electric Project (KHEP).

The KIP is a complex multi-reservoir irrigation system with five reservoirs is considered as a case study for multi-objective optimization of a multi-reservoir system. Among five reservoirs in the system, four upstream reservoirs are in parallel and one is in series at the downstream. In order to meet the demand at the downstream reservoir, water is being transferred from the upstream reservoir through rivers and canals. Thus, the complexity of the system is to find the optimal quantity of water transfer to the downstream reservoir at appropriate time. Hence, in this study, an optimal cropping pattern is derived for the sustainable integrated operation of KIP multi-reservoir system. The behaviour of the multiple reservoirs in the KIP is assessed using a simulation model and the performance is evaluated using indices such as reliability, resilience and vulnerability. An optimal crop planning model is developed with the objective of maximizing the net benefits and maximizing the crop production. Initially, a sustainable crop plan is derived for the KIP using MOFLP showed a satisfaction level of 0.46 for the integrated operation of multi-reservoir system with an irrigation intensity of 102.18%. The same model is solved using chaotic non-dominated genetic algorithm-II (CNSGA-II) and chaotic multi-objective differential evolution algorithm (CMODE). The parameters of the multi-objective evolutionary algorithms are fixed based on sensitivity analysis. On comparing all the techniques, it is found that CMODE has resulted in slightly higher net benefits of Rs. 1921.77 Million ($ 31.96 Million) and crop production of 1201.55 thousand tonnes. CMODE resulted in a crop area of 88678.46 ha during Kharif and 66562.98 ha during Rabi with an irrigation intensity of 106.29%. It is also found that CMODE resulted in optimal intra basin water transfer both spatially and temporally compared to MOFLP. The simulation of optimal results showed that CMODE polices performed better for longer run with less deficits compared to MOFLP policies.

The KHEP is one of the major hydropower projects in India and is considered as a case study of single objective optimization. It has four powerhouses, among which three are in the

Western side and one is at the Eastern side, through which irrigation releases are made. The complexity of the system is that the power releases (towards Western side) and irrigation releases (towards Eastern side) are in the opposite direction and cannot be complemented due to the topology. There is a need to optimize the operation of KHEP such that the power production and irrigation demands are met satisfactorily. Hence in this study, the KHEP operations are optimized with the objective of maximizing the hydropower production. Initially, the behaviour of the KHEP is assessed using a simulation model for various cases based on the duration of operation of hydropower plants. The statistical performance indicators such as reliability, resilience and vulnerability are used to evaluate the performance of the system. An optimization model is developed with the objective of maximising the hydropower production subject to satisfying the irrigation demands and other constraints. Thus, irrigation demands are given higher priority by making it as a separate constraint. The developed optimization model is solved using both conventional NLP and EAs coupled with chaos for four different operating policies. On comparing with NLP, simple genetic algorithm and differential evolution algorithm, it is found that hybrid chaotic differential evolution (HCDE) algorithm and hybrid chaotic genetic algorithm (HCGA) resulted better. Among the four policies assessed, the Policy 1 has resulted in maximum power production of 5195.39 × 10^6 kWh from HCDE. However, this Policy 1 has not resulted in irrigation release. The Policy 3 has resulted 3950.93 × 10^6 kWh hydropower is a feasible option, since it satisfied the monthly demand as well as produced 22% more hydropower than Policy 4. The performances of Policy 3 are evaluated using a simulation model for longer run. The simulation results showed that Policy 3 satisfied the irrigation demand in most of the time period (only 8 months deficit out of 588 months) and the average annual irrigation deficit is only 12.63 × 10^6 m^3.

Keywords: Simulation, Optimization, Evolutionary Algorithms, Chaos, Multi-reservoir System

CONTENTS

LIST OF FIGURES

LIST OF TABLES

LIST OF ABBREVIATIONS

AAID	Annual Average Irrigation Deficit
ACO	Ant Colony Optimization
AFID	Annual Frequency of Irrigation Deficit
AI	Artificial Intelligence
AIC	Akaike information criterion
ANFIS	Adaptive Neuro-Fuzzy Interactive System
ANN	Artificial Neural Network
APM	Augmented Price Method
ARIMA	Auto Regressive Integrated Moving Average
BCGA	Binary Coded Genetic Algorithm
BIC	Bayesian information criterion
BPTT	Back Propagation Through Time
BSDP	Bayesian Stochastic Dynamic Programming
CCGP	Chance Constrained Goal Programming
CCLP	Chance Constrained Linear Programming
CDDD	Constrained Differential Dynamic Programming
CDE	Chaotic Differential Evolution
CDF	Cumulative Distribution Function
CGA	Chaotic Genetic Algorithm
CMODE	Chaotic Multi-Objective Differential Evolution
COA	Chaos Optimization Algorithm
CS-MODE	Chaotic Sequences Based Multi-Objective Differential Evolution
DDDP	Discrete Deterministic Dynamic Programming
DE	Differential Evolution
DLBC	Dimbhe Left Bank Canal
DP	Dynamic Programming
DPR	Deterministic Dynamic Programming with Regression
DRBC	Dimbhe Right Bank Canal
DSGA	Direct Search Genetic Algorithm
EA	Evolutionary Algorithm

FDE	Fuzzy Differential Evolution
FDP	Folded Dynamic Programming
FIS	Fuzzy Interface System
FLP	Fuzzy Linear Programming
FM	Fuzzy Mamdani
FMOO	Fuzzy Multi-Objective Optimization
FSDP	Fuzzy Stochastic Dynamic Programming
GA	Genetic Algorithm
GAMS	General Algebraic Modelling System
GBC	Ghod Branch Canal
GP	Genetic Programming
GSI	Generalized Shortage Index
HCDE	Hybrid Chaotic Differential Evolution
HCGA	Hybrid Chaotic Genetic Algorithm
HEC	Hydrologic Engineering Centre
IDP	Incremental Dynamic Programming
IMSCOA	Improved Mutative Scale Chaos Optimization Algorithm
IPD	Iterated Prisoner's Dilemma
KDPH	Koyna Dam Power House
KHEP	Koyna Hydro Electric Project
KIP	Kukadi Irrigation Project
KLBC	Kukadi Left Bank Canal
KRL	Koyna Reduced Level
KWDT	Krishna Water Dispute Tribunal
LINGO	Language for Interactive General Optimization
LP	Linear Programming
MA	Moving Average
MAE	Mean Absolute Error
MAID	Monthly Average Irrigation Deficit
MBC	Meena Branch Canal
MCOA	Multi-Objective Chaotic Optimization Algorithm
MDDL	Minimum Draw Down Level
MFC	Meena Feeder Canal

MFID	Monthly Frequency of Irrigation Deficit
MIMO	MULTI-input Multi-output
MLBC	Manikdoh Left Bank Canal
MLP	Multi Layer Perceptron
MMGA	Macro-Evolutionary Multi-Objective Genetic Algorithm
MOCA	Multi-Objective Constrained Algorithm
MOCDE	Multi-Objective Cultured Differential Evolution
MODE	Multi-Objective Differential Evolution
MOEA	Multi-Objective Evolutionary Algorithms
MOFLP	Multi-Objective Fuzzy Linear Programming
MOGA	Multi-Objective Genetic Algorithms
MSE	Mean Square Error
MSL	Mean Sea Level
MT	Model Tree
MW	Mega Watt
NIR	Net Irrigation Requirement
NLP	Non-Linear Programming
NSGA	Non-Dominating Sorting Genetic Algorithm
NSP	Nagarjuna Sagar Project
PAES	Pareto Archived Evolution Strategy
PAID	Percentage Annual Irrigation Deficit
PC	Pushpawathi Canal
PLBC	Pimpalgaon Joge Left Bank Canal
PMID	Percentage Monthly Irrigation Deficit
PSO	Particle Swarm Optimization
R	Correlation Coefficient
RBS	Reliability Based Simulation
RBSIM	Rule Based Simulation
RCGA	Real Coded Genetic Algorithm
RMSE	Root Mean Square Error
SA	Simulated Annealing
SBX	Simulated Binary Crossover
SDP	Stochastic Dynamic Programming

SLGA	Self-Learning Genetic Algorithm
SLP	Successive Linear Programming
SOM	Self-Organizing Map
SOMA	Self-Organizing Migrating Algorithm
SOP	Standard Operating Policy
SPEA	Strength Pareto EA
SQP	Sequential Quadratic Programming
SRSP	Sri Ram Sagar Project
SSR	Sum of squared residuals
TLRN	Time Tagged Recurrent Network
VLGA	Varying Chromosome Length Genetic Algorithm
VNS	Variable Neighbourhood Search
WRBC	Wadaj Right Bank Canal

Chapter 1

Introduction

1.1 General

Water is one of the most essential natural resources for human survival. Globally, only 2.7% of the total water available on the earth is fresh, out of which about 75.2% lies frozen in Polar regions and another 22.6% is present as groundwater (Jain *et al.*, 2007). The rest is available in lakes, rivers, atmosphere, and soil moisture. Thus, the available fresh water for human consumption is a very small proportion, which is in rivers and lakes and also rapidly diminishing over the year (Kumar *et al.*, 2005). Moreover, this available water significantly varies in spatially and temporally causing optimal allocation problems to water resources managers. Surface water reservoirs play a significant role in supplying water for various purposes and to some extent solves the problem of spatial and temporal variation of water availability (Simonovic, 1992). The various purposes served by the surface water reservoirs are irrigation, hydropower, industrial and domestic water supply, flood control, navigation, recreation, etc. In order to achieve maximum benefits, these reservoirs are needed to be operated in such a way that the available water is allocated optimally for various purposes. However, optimal operation of a reservoir is a challenging task for water resources planners and managers as the demand increases day-by-day from various sectors. This necessitated the need to operate the surface water resources optimally by allocating the available water for various inter-sectoral demands.

1.2 Surface Water Reservoir Systems

A surface water reservoir is a storage structure that stores water during the periods of excess inflow (monsoon season) in order to best meet the demands during the periods of low flow (non-monsoon season) (Vedula and Mujumdar, 2005). The state of the surface water reservoir system in a period is generally defined by the reservoir storage at the beginning of a period and the inflow into the reservoir during that period. The operating policy of a reservoir is a sequence of release decisions during the operational periods (such as months) specified as a function of the state of the system. The optimal reservoir operation policies should be derived such that constraints including physical characteristics of the reservoir, land and water availability, demands for various purposes, mass balances and other socio-economical issues related to a reservoir are not violated. Thus, the decision variables are typically releases and end-of-period storage volumes for the reservoir operation problem (Wurbs, 1993).

1.2.1 Issues in Surface Water Reservoir Systems

In India, most of the reservoir operation policies are based on thumb rule and are devised long back. The other criticism of these operating rules is that they are derived without understanding the behaviour of the system. The ever increasing water demand for various purposes, and other practical and environmental constraints in constructing new reservoirs (Chang and Chang, 2009) necessitated the conversion of a single purpose single reservoirs into a multi-purpose as well as multi-reservoir system. The conversion of single purpose to multi-purpose operation resulted in conflicts among various purposes and also resulted in dispute between different stake holders in sharing the available water. A major conflict issue in the operation of reservoir systems arises when the reservoir is not capable of supplying all the demands (Karamouz *et al.*, 2003). Irrigated agriculture is the largest consumer of water and surface water reservoirs play a major role in supplying the irrigation water. However, varying crop water requirement for multiple crops under different command area makes the system complex for effective crop planning. There are some reservoirs having more command area and could not cater the irrigation demand on its own. In such cases, water will be transferred from the upstream reservoir to supplement the demands at the downstream reservoir. The conversion of single reservoir to multi-reservoir and water transfer from one reservoir to other reservoir makes the system operation more complicated. Hence, an

integrated planning and operation considering all the reservoirs in the system as a component is required for the optimal integrated operation of a multi-reservoir system.

1.2.2 Issues in Optimization Techniques

Optimizing the operations of a reservoir are complex because of the uncertainty in the input variables, non-linear relationship between the variables, conflicting and competing multiple objectives, non-convexity of the problem, and discontinuity of the solution space (Loucks *et al.*, 1981; Simonovic, 1992). Thus, reservoir optimization requires a systematic study (Simonovic, 2009). One of the important advancement made in systems engineering is the development and application of various optimization techniques to solve the complex problems. The optimization techniques can be broadly classified into two categories namely (i) conventional techniques and (ii) artificial intelligence based soft computing techniques. The conventional techniques are linear programming (LP), non-linear programming (NLP), dynamic programming (DP), and goal programming, etc. For the past several decades these techniques have been widely used in reservoir optimization (Yeh, 1985). However, these conventional techniques have certain drawbacks in solving complex large scale multi-purpose multi-reservoir systems with hard bound constraints. Some of the complexities of conventional techniques are:

1. The LP is used to solve problems having linear objectives with linear constraints. However, in real life most of the water resources systems are non-linear in nature. Sometimes, piecewise linear approximations have been used for non-linear functions; however linearization increases the problem size extensively and also fails to guarantee the global optimal solution (Labadie, 2004).

2. The gradient based NLP techniques are applied for non-linear objective functions and constraints, especially for hydropower optimization problems. However, the complexity increases with the degree of non-linearity. They also often get trapped to local optima for highly complex hard bound non-convex problems.

3. The DP is widely seen as a suitable alternative for NLP techniques. In general, the DP decomposes the original problem into different sub-problems (discretization of the variables of the model in to different states) and is solved sequentially (stages) (Bellman,

1957). The accuracy of the solution in DP depends on the number of discretization of the states and stages. However, the major limitation of DP is that with large number of discretization, the computational times increases exponentially and results in curse of dimensionality. In addition, the formation of recursive equation also changes for various applications.

4. The conventional optimization techniques have limitation in handling multi-objective optimization problems. In conventional techniques, the multiple objectives are handled either by constraint method or weight method (Mays and Tung, 2002). Both of these methods convert the multi-objective optimization problem into a single objective optimization problem to give only one optimal solution in each iteration and do not produce a Pareto optimal front. To generate multiple optimal solutions and to form Pareto optimal front, the conventional optimization techniques need to be run for several times. However, problems having multiple conflicting objectives should be considered simultaneously for generating true Pareto optimal front having large number of optimal solutions. Hence, these conventional techniques may not be suitable for multi-objective problems with conflicting objectives.

To overcome these drawbacks of applying conventional techniques in water resources, recently, artificial intelligence (AI) based soft computing techniques are widely used in optimizing water resources systems. These AI techniques are mostly search techniques that search the optimal solution from a possible solution space, where as the conventional method derives the optimal solution. Some of the widely used soft computing techniques are genetic algorithm (GA), differential evolution algorithm (DE), ant colony optimization (ACO), particle swarm optimization (PSO), simulated annealing (SA), etc. The evolutionary algorithms (EA) that works on principle of natural genetics '*survival of the fittest*' are GA and DE algorithms. These techniques start their search from a randomly generated initial population of possible solutions to attain the global optimal solution over the generation. Hence, the results of the evolutionary algorithms mainly depend on the randomly generated initial population for the effective search and faster convergence. However, it is reported that the simple evolutionary algorithms are slower in convergence and may results in sub-optimal solutions for a complex problems having hardbound constraints (Yuan *et al.*, 2002; Chen and Chang, 2007; Cheng *et al.*, 2008).

1.3 Motivation of the Study

The systems engineering is a promising approach and useful for optimizing the problems dealing with management of scarce resources (Jain and Singh, 2003). Fairly large number of conventional and soft computing techniques has been reported for the optimization of water resources systems. However, the changing scenario of conversion of single purpose reservoir into multi-purpose and single reservoir to multi-reservoir system necessities the optimal planning of reservoir operation. The water is being transferred from one reservoir to other in the same basin as well as to other adjacent basins to cope up the demand and to solve spatial variation of water availability. In such cases, the operation of one reservoir affects the other reservoir and makes the system complex. Hence, the intra basin water transfer in a multi-reservoir requires an integrated operational planning considering all the reservoirs in the system.

Many of the real life problems involve conflicting and competing objectives. For example, hydropower and irrigation are conflicting objectives. Hydropower production requires high head in the reservoir for effective operation and more power production whereas crop production demands more irrigation releases. In some peculiar cases, hydropower and irrigation releases are in opposite direction in which the power releases cannot be utilized further. Thus, conflict arises when the hydropower is not produced through irrigation releases and requires separate release which does not cater the irrigation requirements. In such cases, a suitable trade-off needs to be arrived so as to satisfy both the irrigation and hydropower demands. All these issues in reservoir operation, especially in developing country like India motivated to take up a study to optimize the operations of multi-reservoirs systems having intra basin water transfer.

1.4 Scope of the Study

Most of the reservoirs in India are still operated using the rule curves derived during the design of the reservoir or based on thumb rules and past experience. Wurbs and Carriere (1993) reported that modifying the operational policies of a reservoir in response to changing conditions and increasing demand is always beneficial to the limited surface water resources. Optimal water resource systems planning, management, and operation is far more complex

because of the multiple interdependent physical, biochemical, ecological, social, legal and political (human) processes that govern the behaviour of the water resource systems (Loucks, 1992). In addition, many water resource systems are characterized by multiple objectives that often conflict and compete with one another (Chang and Chang, 2009). However, the advancement in system engineering and computation made the complex water resource systems problems to simple.

Several systems optimization techniques have been developed over the years and successfully applied for optimizing the reservoir operations. Recently, modern heuristic search techniques were developed and more frequently used by the researchers for the optimisation of reservoir operation problems due to their ability to handle the nonlinear and non-convex characteristics of the reservoir operation problems (Reddy and Nagesh Kumar, 2012). Among the heuristic search techniques, the genetic algorithm and differential evolution algorithm are more efficient and robust for reservoir operation due to their simplicity. However, with the increase in the complexity of larger scale water resources system, simple search techniques results in premature convergence, slow iterations to reach the global optimal solution and getting stuck at a local optimum. To overcome this drawback; recently, the chaos algorithm is coupled with evolutionary search technique (Yuan *et al.*, 2002; Cheng *et al.*, 2008).

Chaos is a universal non-linear phenomenon in nature (May, 1976) and is having highly unstable motion of deterministic systems in finite phase space (Williams, 1997). Some special characteristics of chaos are ergodicity, regularity, randomicity, and highly sensitive to initial condition (May, 1976). Because of these properties, the general optimization technique can obtain the global optimal solution more readily and rapidly than other previously adopted methods (Li and Jiang, 1998; Cheng *et al.*, 2008; Han and Lu, 2008). Also, it can more easily escape from local minima than other stochastic algorithms and retain diversity in the population (Davendra *et al.*, 2010a). Cheng *et al*. (2008) states that a nonlinear system is said to be chaotic if it exhibits sensitive dependence on initial conditions and has an infinite number of different periodic responses. Most of the water resources systems are non-linear and the modelling of the system is highly depends on the initial condition. In addition, the search of evolutionary algorithms depends on initial population that are randomly generated. Hence, there is a scope to apply chaos algorithm not only in initial population generation but also in other optimization steps to enhance the search of the evolutionary algorithm for solving real world problem having hard bound constraints.

1.5 Objectives of the Study

In view of the aforementioned problems, the broad objective of the present study is to formulate an optimal crop-planning model with reservoir inflow forecast information to implement the same to develop optimal reservoir operating rule curves using soft computing techniques.

The specific objectives of the present research are:

1. To derive optimal cropping pattern and optimal reservoir operating policies for a multipurpose reservoir system
    a. The irrigation requirements in the basin will be estimated using FAO Modified Penman method and FAO Penman – Monteith method.
    b. The optimal cropping pattern will be arrived using a Fuzzy optimization model.
    c. The optimal operating policies will be derived by developing a Fuzzy-Genetic Algorithm model.
    d. The complimentary and conflicting objectives will be evaluated using multi objective analysis.
2. To predict the important input variable, namely inflow into the reservoir, Artificial Intelligence techniques such as ANN and Genetic Programming models will be developed.
3. To compare the results obtained using soft computing techniques with that of conventional systems approach techniques, stochastic dynamic programming model and also with the field conditions.

1.6 Organisation of the Report

The report is organized in seven chapters in the following manner. In the chapter 1, the concepts of water resources system, problems associated with reservoir system and optimization techniques, motivation, scope and the objectives of the study are described in detailed. A comprehensive literature review depicted in Chapter 2 highlights the various conventional and soft computing techniques used for single and multi-objective optimization

of reservoir operations. The limitations and advantages of various models reported in literature are also discussed in detail. Based on the literature review, the various stages of the present work are given at the end of the chapter. The Chapter 3 briefly describes the techniques used in the present study for the optimization of reservoir operations. The concepts, steps, and working principle of genetic algorithm and differential evolution algorithm for both single and multi-objective optimization are given in detail. The basis and characteristics of chaos technique and procedure for coupling chaos with evolutionary algorithm is also given. To evaluate the described methodology in Chapter 3, it is applied to complex multi-reservoir systems in Maharashtra, India. The details of the multi-reservoir system and their complexities are given in Chapter 4. Single and Multi-reservoir inflow prediction model is given in Chapter 5. In Chapter 6, the results of multi-objective optimization of multi-reservoir system is presented and discussed. A complex multi-reservoir system with five reservoirs having multiple canals and water transfer among the reservoirs is selected for deriving optimal multi-crop planning for integrated operation. The results from single objective optimization of multi-reservoir system using evolutionary algorithm coupled with chaos are discussed in Chapter 7. In the single objective optimization, the proposed techniques are used for maximizing the hydropower production from a complex multi-reservoir hydropower system. The summary of the work done and the conclusion arrived from the present study is discussed point by point in Chapter 8. The research contribution and scope for future work is also reported in Chapter 8. The literatures referred in the report are given as a separate chapter followed by the awards and publications from this work.

Chapter 2

Literature Review

2.1 General

Optimal reservoir operation is needed for efficient utilization of the available water resources, especially for a water sharing multi-reservoir system. Deriving an optimal operation plans for a multi-reservoir system is a complex process and it requires a systematic study (Loucks *et al.*, 1981). Systems analysis has emerged as one of the best tools for solving complex water resources planning and management problems. Over the decades, several system optimization techniques have been developed and applied for solving the complex water resources problems. These optimization techniques have evolved from optimal solution deriving technique to optimal solution searching techniques. Most of the conventional methods are optimal solution deriving techniques. These include linear programming (LP), non-linear programming (NLP), goal programming, dynamic programming (DP), etc. Recently, the optimization technique have taken diversion from solution deriving technique to optimal solution searching technique mostly based on bio-mimic processes (Reddy and Nagesh Kumar, 2012). These techniques are classified as evolutionary algorithm (EA) based soft computing techniques. Some of the most widely used soft computing techniques are genetic algorithm (GA), differential evolution algorithm (DE), etc. The application of these techniques is very wide in water resources, especially in the optimization of complex reservoir operation. Yeh (1985) presented a detailed review about the application of LP, DP, NLP and simulation models on reservoir operation. Simonovic (1992) reviewed various

mathematical optimization and simulation models used in reservoir management and operations. It was reported that new technologies like expert systems must be integrated with the existing simulation and optimization tools for reservoir analysis for closing the gap between theory and practice. Similarly, Wurbs (1993) carried out a comprehensive review about various simulation and optimization models with an emphasis on practical applications. Later, Labadie (2004) presented a state-of-art of review on various conventional and heuristic technique like GA for optimal operation of multi-reservoir systems. The various simulation, optimization and combined simulation-optimization models and their applications were reported by Rani and Moreira (2010), Fayaed *et al.* (2013) and Hossain and El-Shafie (2013). Recently, Singh (2014) reviewed various techniques used for planning and management of irrigation reservoir systems. In this chapter, the review of these techniques is further extended based on the motivation and objectives of the present study. This literature review is broadly presented in two topics based on number of objectives, single objective and multi-objective studies and for each topic; the review is presented technique wise.

2.2 Single Objective Optimization

In a single objective optimization problem, among various purposes of a reservoir, only a specific purpose is considered as decision variable and included in the objective for optimization. Other purposes of the reservoir are mostly considered as constraints in the optimization problem.

2.2.1 Conventional Methods

The conventional optimization methods has been classified into two distinct groups, direct and gradient based methods (Deb, 2001). In direct methods, only objective function and constraint values are used to guide the search, whereas the gradient based methods uses the first and/or second order derivatives of the objective function and/or constraints to guide the search process. Many conventional techniques such as LP, NLP, DP, etc. had been successfully used for optimizing the reservoir operations with single objective. Among these, LP is the simplest technique, which assumes the objectives and constraints are linear in nature. The LP technique has been extensively used in water resources planning, especially for deriving optimal cropping pattern, system capacity expansion studies and to explore

various design parameters in connection with feasibility studies, where details in storage variation are not important (Barros *et al.*, 2003). The NLP technique is widely applied for optimizing hydropower systems (Gagnon *et al.*, 1974; Tejada-Guibert *et al.*, 1990), since it involves no approximation and uses the physically based non-linear function (Barros *et al.*, 2003). NLP technique is also used for optimal cropping pattern (Paudyal and Das Gupta, 1990), multi-purpose reservoir optimization (Sinha *et al.*, 1999), and optimal design and operation of pumping stations (Moradi-Jalal *et al.*, 2003) apart from hydropower optimization. The Bellman's (1957) dynamic programming (DP) is recognized as a suitable alternative to NLP and is considered as one of the powerful technique for optimization of water resource systems. The DP splits a problem of '*n'* decision variables in to '*n'* sub-problems having one decision variable and each sub-problem is referred to as a stage. Thus, decisions are taken stage by stage, until the final results are obtained.

All the above techniques can be solved either deterministically or stochastically. The deterministic method does not consider the uncertainties and inaccuracies involved in the variables. However, the real-life reservoir operation involves lot of uncertainty in inflow and other variables. Hence, stochastic models were developed by researchers to overcome the limitations of the deterministic models. The uncertainty can be included in model either implicitly or explicitly. In an implicit model, the stochastic nature of inputs is incorporated through sensitivity analysis. Optimization is performed with different scenarios of stochastic data to evaluate their impact on the operation policy. In explicit stochastic modelling, the uncertainty is directly incorporated in to the problem using transition probabilities. Alternatively, the uncertainty can also be considered as chance constraint. The chance constraint is converted into its deterministic equivalent using a linear decision rule and probability distributions. However, these approaches can handle only the statistical uncertainty and not the non-statistical uncertainty namely vagueness or impreciseness present in the data (Mohan and Jothiprakash, 2000). In such cases, the fuzzy set theory developed by Zadeh (1965) has been proved as a robust where these kinds of uncertainties can be modelled as fuzzy variables (Zimmermann, 1996). Some of the application of these conventional techniques on reservoir optimization is discussed in the following section.

2.2.1.1 Linear Programming

A linear programming (LP) problem may be defined as the problem of maximizing or minimizing a linear objective function subject to linear constraints. The variables may be either negative or non-negative and the constraints may be equal or unequal. Maji and Heady (1980) analysed the optimal cropping pattern of Mayurakshi project in India using deterministic and chance-constrained LP (CCLP) model. It was reported that both the deterministic and CCLP models resulted in more intensive cropping pattern with more dependence on Rabi than Kharif crops in the region. A LP model was formulated by Vedula *et al*. (1986) to study the Bhadra reservoir project based on the concept of over year and within year storages. The reservoir operations were evaluated by simulating thirteen different policies using both historic and synthetically generated monthly stream flows. On comparing the results with the actual operation for 11 years, it was reported that the hydropower generation could be substantially increased using the derived policies without any irrigation deficits.

Liang and Hsu (1994) developed a fuzzy linear programming (FLP) model for optimal hydroelectric generation scheduling in the Taiwan power system. The hourly loads, the hourly natural inflows and the cost were expressed in fuzzy set notations. On comparing the results with conventional LP model, it was reported that FLP model resulted in less total cost for the generation schedule, since the uncertainties in load, demands and natural inflows were taken into account in the FLP model. It was concluded that the FLP is very effective in obtaining proper hydropower generation schedules.

Sreenivasan and Vedula (1996) developed a CCLP model for the optimal operation of a multi-purpose reservoir with the objective of maximizing the annual hydropower production while meeting the irrigation demands for a specified reliability level. The irrigation releases were defined as chance constraint and converted into its deterministic equivalent using a linear decision rule. The model was solved for different reliability levels with an increment of 0.05 from 0.50. It was reported that the maximum possible reliability for meeting the irrigation demand was 0.65 and the corresponding maximum annual hydropower produced by the bed turbine was 5.68 M kWh.

Mohan and Jothiprakash (2000) developed a FLP model for conjunctive use operation of Sri Ram Sagar Project (SRSP) in India and compared the results with classical LP model. The fuzziness involved in the inflow and groundwater pumping is considered using a linear membership function in the FLP model. It was reported that the fuzziness in groundwater pumping played a prominent role in deriving optimal crop plan with 0.78 degree of satisfaction. It was reported that the increase in fuzziness increases the degree of satisfaction.

An irrigation planning model was developed by Raju and Nagesh Kumar (2000a) using LP for the evaluation of irrigation development strategies of SRSP, India. The objective of the model was to maximize the net benefits. The stochastic nature of inflows was considered through chance constrained and the model was solved for various dependable inflows. It was reported that the net benefits obtained for 75% dependable inflow level is 68.8% more than at 90% dependable inflow level and concluded that LP is a more versatile technique for deriving optimal crop planning.

A LP model was formulated by Singh *et al*. (2001) to derive optimal cropping pattern for the command area of Shahi distributory of Sharda canal command located in Bareilly, Uttar Pradesh, India. The objective of the model was to maximize the net return subject to various physical and socio-ecological constraints. It was reported that the model has resulted in an optimal crop area of 11,818 ha with a maximum net return of Rs. 185 million for 100% water availability.

Sethi *et al.* (2002) developed a LP model for deriving optimal crop planning for a coastal river basin in India with the objective of maximizing the economic net returns from various crops, excluding the irrigation cost. The developed model was subjected to various constraints such as surface and groundwater availability and their mass balance, cropping pattern restrictions, etc. Upon evaluating the model for nine different exceedance probability of net irrigation requirements (NIR), it was reported that the optimal annual net return increases with decrease in the probability levels of NIR.

A combined optimization-simulation approach was used by Mohan and Jothiprakash (2003) to derive the optimal cropping pattern for SRSP, India. The optimal cropping pattern was derived using LP model with and without conjunctive use. Three policies were evaluated, (i) irrigation with surface water only, (ii) irrigation with conjunctive use of surface and

groundwater, without socio-economic constraint and (iii) irrigation with conjunctive use operation, with socio-economic constraint. The policies derived from the optimization model were evaluated using a simulation model for a longer series of inflow data. It was reported that the conjunctive operation of surface and groundwater is essential in the command area.

Moradi-Jalal *et al*. (2007) developed a deterministic LP model to derive optimal multi-cropping pattern. The reservoir operations were related to release policy, water allocations and reservoir spills in a monthly operating time. The objective of the study was set to maximize the annual benefit from the system considering the monthly water balance, water demand, evaporation loss and governing equations for reservoir release and operations. It was reported that the variations in monthly inflow caused very little change in the optimum benefits of the system. It was reported that the variable cropping patterns increased the benefit due to the flexibility of the system for adapting to different inflow regimes.

Valunjkar (2007) compared the optimal cropping pattern resulted from LP, FLP and fuzzy interface system (FIS) techniques applied to the command area of Pench irrigation project in Maharashtra, India for different reliable flow conditions. The FLP and FIS were constructed with fuzziness involved in constraint coefficients and available surface water. It was reported that the FIS resulted a maximum net benefits of Rs. 655.13 million and Rs. 389.60 million for normal and critical rainfall year, respectively. It was concluded that the FLP and FIS were more suitable and superior to conventional techniques for deriving optimal crop planning.

A LP model was developed by Bozorg Haddad *et al.* (2009) for deriving optimal annual cultivation rules in a multi-crop irrigation area with the objective of maximizing the annual benefits from the reservoir–irrigation system. In this study, the annual irrigation areas were considered as a linear function of storage at the end of the last operating year and the average inflow rate of the current year. It was reported that the developed cultivation rules showed a 40% decrease in the value of the objective function compared to the previous study by Moradi-Jalal *et al*. (2007) for the same study area. However, by analysing the rules curves for five-year generated inflow series, it was stated that the developed rule curves will be helpful for planners and/or stakeholders to decide at the beginning of each year how much and which type of product should be cultivated.

Jothiprakash *et al.* (2011a) developed a CCLP for deriving an optimal cropping pattern for SRSP, India. The CCLP model was solved for various dependable inflows levels obtained from monthly and annual inflow series. It was reported for the probability of model time period (monthly) should be considered rather than planning time period (annual).

A weekly irrigation planning model was developed by Srinivasa Prasad *et al*. (2011) to derive optimal cropping pattern for Nagarjuna Sagar Project (NSP), Andhra Pradesh, India. The objective of the model was to maximize the annual net benefits to obtain optimal cropping pattern and weekly releases to the crops grown in each sub area under each canal. The model was solved for four levels (90%, 85%, 80% and 75%) of reliability of weekly inflow to account the uncertainty. It was reported that the total annual benefit and total allocated area for 75% reliability was higher compared to 90% reliability for all states of initial storage of reservoir. It was also stated that the initial storage of the reservoir at the beginning of the season influenced the cropping pattern and water allocations. Hence, a minimum carry over year storage of 1000×10^6 m^3 was recommended to get maximum annual benefit.

Tzimopoulos *et al*. (2011) derived optimal cropping pattern of an irrigation area with the objective of maximizing the net benefits. It was reported that the LP model provided the optimal cropping pattern for the region with highest profit, both for the cultivator and the water resources managers. Alabdulkader *et al.* (2012) developed a LP model for deriving the optimal cropping pattern in Saudi Arabia with the objective of maximizing the net annual return. The developed model was aimed to efficiently allocate the scarce water resources and arable land among the competing crops in Saudi Arabia. It was reported that the results showed the potential to generate a net return equivalent of about 2.42 billion US $ per year.

A LP model was developed by Singh and Panda (2012) to optimally allocate the land and water for maximizing net annual returns from an irrigated area in Haryana, India. The yield, price and production cost of crops, unit costs of canal water, groundwater, quality of the mixed canal water and groundwater and NIR of crops were considered in the model. It was reported that the model resulted in 26% increase in net annual return from the study area. However, the crop area for rice, mustard, barley and gram were decreased while cotton, sugarcane, wheat, millet and sorghum were increased. It was also reported that the model resulted in an increased groundwater use to mitigate the water logging and salinity problems.

The study recommended the conjunctive use of canal water and groundwater to maximize the farm income and also to alleviate water logging problems.

2.2.1.2 Non-Linear Programming

A non-linear programming (NLP) model is also similar to LP, consists of objective function, constraints and variables. The difference is that a NLP includes at least one non-linear function, which could be the objective function, or some constraints. Many real world water resources systems are inherently non-linear in nature. Simonovic and Srinivasan (1993) developed a NLP model for optimal operation a multi-purpose reservoir for hydropower generation and flood control. This model determined the optimal reservoir release policy along with the optimal reliabilities of satisfying hydropower demand and flood control storage requirements. It was reported that the reliabilities of reservoir system performance for flood control and hydropower production were 0.7789 and 0.8307 respectively.

Sinha *et al*. (1999) developed a non-linear optimization model for a multi-purpose multi-reservoir operation in India. In this study, a modified sequent peak algorithm is used to determine the storage capacity of the reservoirs. The gradient-based optimization algorithm was employed to integrate the simulation into an optimal screening model. It was reported that the developed model successfully integrated the behaviour analysis algorithm, automatic differentiation and sequent peak algorithm. It was reported that the model resulted in 11.10% cost saving and 8.72% reduction in land submergence. It was concluded that the model provided a compact representation of the screening algorithm and could be used to screen large reservoir systems efficiently.

Ailing (2004) optimized the operations of two hydroelectric reservoirs in series on the upper reaches of the Yellow River in China using a NLP model. The decomposition–coordination method was used to simplify the complexity of the problem. It was reported that the model resulted in a total annual electricity production of 7.983 billion KWh, which is 6.3% higher than the actual. It was concluded that the method is even more applicable for real time optimal operation of multiple reservoir systems. Devamane *et al*. (2006) developed a NLP model for a multi-reservoir system in upper Krishna basin and solved using General Algebraic Modelling System (GAMS) package. The objective of the study was to maximize the irrigation, municipal and industrial releases, and power production. The results were

compared with LP model. It was reported that the NLP model resulted in less irrigation deficit with more power production than LP model.

Barros *et al.* (2009) studied the impacts of the upstream storage reservoirs on the hydropower production of Itaipu hydropower plant, which is a run-of-river reservoir and does not have storage capacity. The analyses were carried out using the HIDROTERM (combination of hydro model (HIDRO) and a thermal model (TERM)), which is basically a non-linear optimization model written using the GAMS package. The model was optimized using three decades of historical inflow data and reported 14% higher power production through regularization of upstream reservoirs. Thus, it was concluded that the upstream reservoirs impacts significantly on the hydropower production of Itaipu hydropower plant.

Devamane *et al.* (2009) developed a storage based optimal operational policies for multi-reservoir system using a NLP model. The NLP model was solved year by year using GAMS-Minos package for 37 years historic data. The effect of storage on the release rules was considered to derive monthly reservoir operational rules. Based on the results of optimization model, two set of relationships, (1) relationship between individual storage versus total system storage and (2) relationship between optimal releases versus the individual reservoir available water were studied. By using regression analysis, a set of storage allocation functions and release rule equations are derived. The rules derived from optimization model are evaluated using a rule based simulation (RBSIM) model for 5 years of historic data to assess the improvement in the performance. It was reported that the RBSIM model (5117 GWh) produced higher hydropower than the NLP model (5063 GWh).

The non-linear functions also can be handled using DP technique. Different types of DP like deterministic dynamic programming (DP) (Karamouz and Houck, 1982, 1987; Boehle *et al.*, 1983; Karamouz *et al.*, 1992; Jothiprakash and Mohan, 2003), stochastic dynamic programming (SDP) (Karamouz and Houck, 1987; Vedula and Mohan, 1990; Braga Jr *et al.*, 1991; Ben Alaya *et al.*, 2003; Jothiprakash and Shanthi, 2004; Gakpo *et al.*, 2005), fuzzy stochastic dynamic programming (FSDP) (Tilmant *et al.*, 2002; Mousavi *et al.*, 2004), bayesian stochastic dynamic programming (BSDP) (Mujumdar and Nirmala, 2007), folded dynamic programming (FDP) (Nagesh Kumar and Baliarsingh, 2003), incremental dynamic programming (IDP) (Kim *et al.*, 2001; Yurtal *et al.*, 2005), etc. were also used of deriving optimal reservoir operation policies.

2.2.2 Simple Evolutionary Algorithms

Many conventional deterministic and stochastic LP, NLP and DP models have been developed extensively to derive the operating rules for single as well as multi-reservoir system with single objective. However, these conventional techniques may result in local optimal solution or slower iteration for complex problems. LP models are not suitable for non-linear problems and linearization increases the complexity of the problem. Some of the disadvantages of NLP are time consuming, iterative processing, requirement of large storage space and may results in local optimal solution (Sinha *et al.*, 1999). The DP may result in curse of dimensionality for large number of discretization. To overcome these drawbacks of conventional techniques, soft computing techniques are used and proved to be more efficient for optimization problems. Among different soft computing techniques, application of evolutionary algorithm (EA) to water resources system engineering have been discussed in the following section, particularly literature on genetic algorithm (GA) and differential evolution (DE) algorithm. Ranjithan (2005) emphasised the role of evolutionary computation in environmental and water resources systems analysis. Savic (2008) reported that EAs are more suitable for complex water resources system optimization problems that are difficult to evaluate through iterations. Reddy and Nagesh Kumar (2012) discussed key features of various bio-inspired computational algorithms and their scope for application in science and engineering fields. One of the significant advantages of soft computing techniques is that they can handle any type of objective function.

2.2.2.1 Genetic Algorithms

Genetic algorithm (GA) is a powerful global optimization search technique and has a wide spectrum of application in problems of engineering and science (Goldberg, 1989). The working principle of GA mimics the processes of biological evolution in order to solve problems and to model evolutionary systems. Basically, it is search based optimization techniques, which searches the optimal solution from a population of possible solutions. GA uses the probabilistic rules in the search process, and they can generally outperform the conventional optimisation techniques on difficult, discontinuous and multimodal functions (Solomatine *et al.*, 2008). Chang and Chen (1998) reported that the GA is a very promising technique for solving the water resource management models. GAs have been increasingly applied to various search and optimization problems (Deb, 1999). Mohan and Vijayalakshmi (2009) and Rani *et al*. (2013) presented a detailed review and application of GA in water

resources. Nicklow *et al*. (2010) presented a state-of-art review about application of GA in water resources planning and management. A detailed review about the application of GA for reservoir optimization is discussed in this section.

Chen (1997) demonstrated the application of GA for the management of ShiJing irrigation network using sequence crossover, multi-points crossover and multi-points mutation methods. Chang and Chen (1998) compared the performance of the binary coded genetic algorithm (BCGA) and real coded genetic algorithm (RCGA) for the flood control operation of a reservoir system in Taiwan. It was reported that the RCGA obtained better results than the BCGA, in terms of higher mean objective function values with smaller standard deviation and converges quickly.

Wardlaw and Sharif (1999) developed a GA model for a four reservoir system and compared the results with the discrete deterministic dynamic programming (DDDP). The developed GA model employs real value coding, tournament selection, uniform crossover, and modified uniform mutation. The crossover probability was fixed as 0.70 after sensitivity analysis by trial and error method. It was reported that the four reservoir problem achieved the near global optimum within 500 generations with a population size of 200. The same code was used to solve a ten reservoir problem with some modification to the evaluation function. The same parameters of GA used in the four reservoir problem were used here also. The maximum return achieved for ten reservoir problem was 1190.25, which is 99.7 % of the known global optima. It was concluded that GA was capable of addressing large complex water resources problems.

Further, Sharif and Wardlaw (2000) extended the application of GA model developed by Wardlaw and Sharif (1999) for a multi-reservoir system in Brantas Basin, Indonesia. The GA model followed the set up of tournament selection, elitism, uniform crossover and modified uniform mutation. The constraints were handled by using quadratic penalty equation. Four different cases were analysed and the results of the GA model were compared with the results of DDDP. It was reported that GA achieved 99.84, 99.98 and 99.07% of DDDP results for the first three cases. It was also stated that GA performs better than the DDDP in terms of delta water supply.

Wardlaw and Bhaktikul (2001) developed a GA model to derive optimal operating rules for Upper Wardha reservoir in Maharashtra, India. The fitness function was minimizing the squared deviation of monthly irrigation demand. The decision variables were monthly releases for irrigation from the reservoir and initial storages in the reservoir at beginning of the month. It was reported that even during the low flow condition, the GA model satisfied the downstream irrigation demand. It was concluded that GA model has the capability to perform efficiently for the real world reservoir operation problems.

Chen (2003) applied RCGA to derive the 10-day operating rule curves for a reservoir in Taiwan. The parameter of the RCGA was determined by testing different parameters and reported that macro evolutionary selection and blend-α crossover were better. It was also reported that the solutions were very close to the optimum value and achieved within 200 generations with a population of 100. The rule curve resulted by RCGA maintained higher water level in the reservoir and water deficits were lower than the original rule curve. It was concluded that RCGA was a most promising technique and very efficient for optimizing highly nonlinear systems.

Raju and Nagesh Kumar (2004) developed a GA model to derive efficient cropping pattern for maximizing benefits for SRSP in India and compared the results with LP model. The penalty function method was used to convert the constrained problem into an unconstrained problem with a reasonable penalty coefficient. The GA parameters were optimized by running the model for various values of population, generations, crossover and mutation probabilities and reported that 50, 200, 0.6 and 0.01, respectively were found to be better. The optimal cropping pattern was derived for 90% dependable inflow level. It was reported that the irrigated area and net benefits obtained by GA have deviated by 5.15 and 3.97% as compared to LP results. It was concluded that GA was an effective optimization tool for irrigation planning and the results can be utilized for efficient planning of the irrigation system.

Ahmed and Sarma (2005) developed a GA model for deriving the optimal operating policy of a multi-purpose reservoir and compared its performance with the SDP model. Both the GA and SDP models were developed with the objective of minimizing the squared deviation of irrigation releases. Four policies were developed assuming the irrigation release as piecewise linear functions. The model performance was evaluated using a simulation model for 20

years of historic monthly stream flow. It was reported that the policies derived by GA model were efficient than SDP model for irrigation, however the SDP model produced more hydropower than GA model. However, it was also reported that GA model releases were nearer to the required demand and concluded that GA model was advantageous over SDP model in deriving the optimal operating polices. Based on the simulation results, policy derived by GA model was recommended because of its overall better performance. It was concluded that the operating policy derived using GA was promising and competitive and can be efficiently used for deriving operating policy for a multi-purpose reservoir.

Chang *et al*. (2005) compared the BCGA and RCGA model for deriving optimal operating rule of the Shih-Men reservoir, Taiwan. The rule curves were assumed to be piecewise linear functions and the coordinates of the inflection points in the rule curves were optimized. It was reported that both BCGA and RCGA reached steady state solution after 10 generations. It was reported that the operating rule curves obtained from both the GA models performed better in terms of water release and hydropower production. However, it was concluded that RCGA was slightly better than BCGA in terms of objective function value.

Jian-Xia *et al.* (2005) compared the performance of BCGA and RCGA model with DP model and disaggregation and aggregation method for hydropower generation. The GA models were developed with ranking selection, two-point crossover with 0.75 probability, uniform mutation with 0.05 probability and population size as 100. It was reported that the RCGA was two times faster than the BCGA based on the convergence to the optimal solution. It was also concluded that GA could be easily applied to complex nonlinear systems.

Jothiprakash and Shanthi (2006) developed a GA model to derive optimal operating rules for the Pechiparai reservoir in Tamil Nadu, India. The objective function was to minimize the annual sum of squared deviation from desired irrigation release and desired storage volume. The decision variables were release for irrigation and other demands (industrial and municipal demands) from the reservoir. The GA model was developed using roulette wheel selection method, uniform crossover and modified uniform mutation operator. Based on sensitivity analyses, population size, crossover probability and number of generations were fixed as 150, 0.76 and 175 respectively. It was reported that the GA model resulted in irrigation releases equal to irrigation demand.

Nagesh Kumar *et al.* (2006) developed a GA model for deriving optimal operational policy and optimal crop water allocations of the Malaprabha single-purpose irrigation reservoir in Karnataka State, India. The objective was to maximize the sum of the relative yields from all crops in the irrigated area. The model takes into account reservoir inflow, rainfall on the irrigated area, intra-seasonal competition for water among multiple crops, the soil moisture dynamics in each cropped area, the heterogeneous nature of soils, and crop response to the level of irrigation applied. It was reported that the optimal operating policy obtained using the GA was similar to LP. Also stated that GA model can be used for optimal utilization of the available water resources of any reservoir system to obtain maximum benefits.

An indirect penalty method of constraint handling was proposed by Chang (2008) for the flood control optimization of Shihmen reservoir, Taiwan. A suitable penalty parameter was proposed to reach a solution without violating the constraints. The constraints were divided into bound constraints, soft constraints and hard constraints. The bound constraints were used to confine the search space. The soft constraints were allowed to violate while the hard constraints were not allowed to violate the search space by imposing severe penalty. On comparing the results for 29 typhoon events, it was reported that the Simplex method unsatisfied the constraints where as the penalty type GA converged to the feasible solution space. It was concluded that the penalty type GA provided rational hydrographs to reduce flood damage during the flood operation and increased the final storage for future usages.

Karamouz *et al.* (2008) developed a GA model to optimise the cropping pattern of eight irrigation networks in Tehran province in Iran for the conjunctive use of surface and groundwater. The GA model was developed with real value encoding, tournament selection and single point crossover. The model was formulated in such a way that both cropping pattern and water allocation from surface or groundwater resources are simultaneously optimized. The GA parameters such as population size, crossover and mutation probabilities were fixed as 100, 0.9 and 0.003, respectively based on sensitivity analysis. On comparing with the existing cropping pattern, it was reported that there was significant change in the cropping area for different crops for achieving higher total benefit.

A monthly time step GA model was developed by Jothiprakash and Shanthi (2009) with the objective of minimizing the squared deviation of monthly irrigation deficit. The optimal results from the GA model were compared with the conventional SDP model. Both the

models were solved with same objective function and constraints. Based on the performance, it was reported that the GA model satisfied the demand to a greater extent, whereas SDP model resulted in irrigation deficit. It is reported that GA models are better suited than conventional optimization techniques for self sufficient systems. It was concluded that the GA model is a robust optimization technique for solving complex problems.

Zahraie and Hosseini (2009) developed a GA model for optimizing the Zayandeh-Rud reservoir operations in Iran considering the variation in water demands. In order to incorporate the demand uncertainties in the optimal operation policies, different types of linear equations were developed using different combinations of inflow, initial storage and water demands. The optimum values for crossover probability, mutation probability, population size, and number of generations were estimated as 0.60, 0.008, 1800 and 112, respectively. It was reported that the fuzzy linear regression equations with asymmetric membership function resulted the best long-term performance in meeting variable demands.

Chang *et al.* (2010) extended the constrained GA model developed by Chang (2008) for developing an optimal operational strategy for the Shih-Men Reservoir considering the ecological base flow. The ecological base flow requirements are considered as constrains in the GA model while minimizing the generalized shortage index (GSI). The constrained GA results were compared with the historical operations for three cases of ecological base flow requirements. It was reported that the constrained GA model performed better compared to current M5 operation rule cures and significantly improved the efficiency and effectiveness of reservoir operations for multiple water users.

Garudkar *et al.* (2011) developed an optimization model to derive optimal reservoir releases of Waghad Irrigation Project in upper Godavari basin of Maharashtra, India. An elitist GA model was developed considering the heterogeneity of crops in the command area with the objective of maximizing the net benefits. In this study, tournament selection with uniform crossover and uniform mutation was used in GA. The constraints were handled using penalty function method. On comparing the results with present practice, it was reported the GA model resulted 19% increase in total net benefits and net irrigated area increased to 50% of irrigable command area.

Hınçal *et al.* (2011) explored the efficiency and effectiveness of GA technique for optimizing multi-reservoir system. Three reservoirs in the Colorado River Storage Project were optimized for maximization of energy production. The constraint on storages was embedded into the objective function as penalty terms. The results obtained were compared with the real operational data and it was reported that GA was found to be effective technique and can be utilized as an alternative technique to other traditional optimization techniques.

Jothiprakash *et al.* (2011b) compared the performance of GA and SDP models in deriving the optimal operational rules for a multi-reservoir system in India. The population size, crossover probability and number of generations of the GA model were fixed as 150, 0.84 and 275 respectively based on sensitivity analyses. The penalty function method was used to handle the constraints. On comparing the results with single reservoir system (Jothiprakash and Shanthi, 2006, 2009), it was stated that the increase in complexity due to increase in number of variables for the multi-reservoir system can be easily handled by increasing the probability of crossover and increasing the number of generation in GA technique. Finally, it was concluded that GA is a robust technique and provides better solution than SDP models.

2.2.2.2 Differential Evolution Algorithm

Differential evolution (DE) algorithm is one of the most recent global optimization technique developed by Storn and Price (1995). Mayer *et al.* (2005) reported DE algorithm as a simple variant of an evolutionary algorithm. Like other evolutionary algorithms, DE is also a population based technique that searches the global optimum by evaluating the objective function using the randomly generated initial population (Price *et al.*, 2005). Some of the applications of DE pertains to reservoir operation is discussed in this section.

Vasan and Raju (2007) applied DE algorithm to derive optimal irrigation planning for Mahi Bajaj Sagar Project, India. Ten different strategies of DE were analyzed with various population sizes, crossover factor (*CR*) and weighting factors (*F*) and the results of DE models were compared with LP model. Based on sensitivity analyses on ten different strategies of DE, it was reported that *DE/rand-to-best/1/bin* strategy performed better with maximum benefits of Rs. 113.15 crores and less CPU time for a population size of 1100, *CR* as 0.9 and *F* as 0.6. It was reported that both the results of DE and LP models were comparable for high dimensional problems.

Pant *et al.* (2008) applied DE to determine optimal cropping pattern for Pamba-Achankovil-Vaippar link project command area in India. The objective was to maximize the net irrigation benefit from the crops cultivated in the area subjected to various constraints. The model was evaluated for a population size of 30, crossover constant as 0.5, and scale factor as 0.5 for 1000 generations. The model was optimized for 50%, 75% and 90% dependable inflow. On comparing the results with LP model, it was reported that the DE performed better for 75% and 90% water year dependable flows. However, both the LP and DE resulted in same net benefits and crop area for 50% dependable inflow level. It was concluded that DE could be considered as an alternative for LP.

Adeyemo and Otieno (2009a) derived optimal crop planning using DE algorithm and compared the results with LP model. The problem was solved for 10 different strategies of DE with the objective of maximizing the total income. The constraints of the problem were handled using penalty function method. It was stated that the *DE/rand-1-bin* strategy performed better for a population size of 160, crossover as 0.95 and scale factor as 0.5. It was reported that both the techniques resulted in same area for almost all the crops and same total volume of water to irrigate the crops. It was concluded that DE is capable of obtaining the global optimal solution.

Regulwar *et al*. (2010) applied DE algorithm to derive optimal operation of multipurpose reservoir with the objective of maximizing the hydropower production and compared it with the results of GA model. The control parameters such as population size, crossover constant and the weight were fixed according to their fitness value. Based on sensitivity analysis, it was reported that the *De/best/1/bin* strategy performed better among the ten strategies of DE. It was reported that the DE model resulted in a maximum hydropower production of 30.885×10^6 kWh with an irrigation release of 928.44×10^6 m^3. Based on the results, it was concluded that both the GA and DE are comparable and performing equally better.

2.2.3 Hybrid Evolutionary Algorithms

Simple EAs often suffer the problems of premature convergence and evolving too slowly often exist when initial population is not so good (Li and Jiang, 1998; Yuan *et al.*, 2002; Cheng *et al.*, 2008). Cheng *et al*. (2008) reported that with the increase in the complexity of larger scale water resources system, GAs frequently face the problems of premature

convergence, slow iterations to reach the global optimal solution and getting stuck at a local optimum.

In order to generate a good initial population, recently chaotic technique is employed to utilize its merits. Chaos is the existence of unpredictable or random behaviour that often occurs in non-linear systems (Williams, 1997). The characteristics of chaos are highly sensitivity to the initial value, ergodicity and randomness (May, 1976). Li and Jiang (1998) proposed chaos optimization algorithm (COA) and demonstrated its effectiveness through five complex functions. Lü *et al*. (2003) stated that the chaotic algorithm is very efficient in maintaining the population diversity during the evolution process of GA technique. The advantages of the chaos characteristics along with optimization algorithm will more likely result in global optimum solution with higher search speed than some stochastic optimization algorithms (Li and Jiang, 1998; Cheng *et al.*, 2008; Han and Lu, 2008). Tavazoei and Haeri (2007) compared ten one-dimensional mapping methods which is used as search patterns in the COA. It was reported that the search patterns differed with each method in view of convergence rate, algorithm speed and accuracy. Finally, it was concluded that choosing the best map for optimizing is a problem-based subject. Some of the hybrid EAs is reviewed in this section.

Yuan *et al*. (2002) proposed a hybrid chaotic genetic algorithm (HCGA) model for a short-term hydropower scheduling. In their study, the initial population was generated as chaotic sequence using one-dimensional logistic map method and they introduced a self-adoptive error back propagating mutation in order to prevent premature convergence. It was reported that HCGA was feasible and effective method for solving the large scale constrained non-linear optimization problems. Caponetto *et al*. (2003) used chaotic sequence instead of a random numbers in the selection, crossover and mutation operations to improve the performance of EAs in solving a salesman problem. Methods such as one-dimensional logistic map, tent map, sinusoidal iterator, gauss map and lozi map were used to generate the chaotic sequences. The proposed method was tested on problems like De Jong functions, LMI eigen value problem, Iterated Prisoner's Dilemma problem and Travelling Salesman Problem. A statistical analysis using t-test was performed to validate performance of the EAs. It was reported that the EAs showed improvement when chaos sequences were used instead of random numbers.

Chen and Chang (2007) proposed a real-coded hypercubic distributed genetic algorithm (HDGA) for optimizing reservoir operation to prevent premature convergence and to obtain near global optimal solutions. The HDGA was designed to have various sub-populations that are processed using separate and parallel GA. Genetic operators such as linear ranking selection, blend-α crossover and Gaussian mutation were applied to search the optimal reservoir releases. The HDGA was then applied to a multi-reservoir system in northern Taiwan. It was reported that the HDGA minimized the water deficit of the reservoir system and provided much better performance than the conventional GA in terms of obtaining lower values of the objective function and avoided local optimal solutions.

Momtahen and Dariane (2007) developed a direct search genetic algorithm (DSGA) model. The model was extended to multi-reservoir system with some modification by Dariane and Momtahen (2009) to enhance the computational efficiency. Initially, the DSGA was applied to a three reservoir problem and then applied to seven reservoir system with some modifications. Finally, the model was applied to 16 reservoir systems with the objective of minimizing the overall operation costs. The GA parameters used in the model were tournament selection, arithmetic crossover, and arithmetic mutation. The best population size of 200, crossover and mutation probabilities of 0.80 and 0.05 were found to best using trial and error method. On comparing the results with SDP and DPR results, it was reported that the GA model performed better than other two conventional models. It was concluded that GA models were capable of optimizing large and complex multi-reservoir systems and can optimize any type of objective function.

A novel HCGA based on the COA and GA was developed by Cheng *et al.* (2008) for optimizing a hydropower reservoir. The one-dimensional logistic map was used to generate initial population as chaotic sequence. Annealing chaotic mutation operation was proposed to maintain the population diversity and to avoid the local optimum. Upon testing with standard benchmark problems, it was reported that the HCGA improved convergence speed and solution accuracy. Furthermore, the developed model was applied for the monthly operation of a hydropower reservoir with a series of monthly inflow of 38 years. For both GA and HCGA, a crossover probability of 0.80, mutation probability as 0.10, population size as 100 were used and the results were compared. It was reported the long term average annual energy production was the best in HCGA and also it converged faster than DP and the

standard GA. It was concluded that HCGA is feasible and effective method for optimal operations of complex reservoir systems.

Han and Lu (2008) proposed a Improved Mutative Scale Chaos Optimization Algorithm (IMSCOA) for the economic load dispatch problem. The proposed algorithm has modification in selecting initial value, search configuration and convergence criteria to stop the search. It was reported that IMSCOA obtained better optimal value than other algorithms regardless of the scale and nonlinearity of the problem. It was concluded that the application of the chaos optimization algorithm in power systems will bring enormous economic benefit.

A new improved chaotic DE algorithm was proposed by Yuan *et al.* (2008) to optimize the daily hydropower production and the results were compared with the conjugate gradient and two-phase neural network methods. The crossover '*CR*' and mutation factor '*F*' is represented as chaotic sequence using one-dimensional logistic map method. The objective of the study was to minimize the summation of the deviation between the hourly load demand and hydropower generation subject to satisfying all kinds of physical and operational constraints. The DE parameters such as population size, initial mutation factor, crossover factor and maximum generation were set as 80, 0.40, 0.90 and 2000 respectively. The model was run for 20 times for different initial populations in succession and the best result was selected as the final optimization solution. It was reported that the final optimal result obtained by chaotic DE was better than the two-phase neural network and conjugate gradient method.

Zahraie *et al.* (2008) proposed a varying chromosome length genetic algorithm (VLGA) model for optimal reservoir operation. In the VLGA model, the chromosome length was sequentially increased to obtain good initial solution. Based on hydrologic characteristics, two models, VLGA-I and VLGA-II were proposed. The VLGA-I model used previous year best solutions as the initial solutions, where as the VLGA-II chooses the initial solutions using the K-nearest neighbour algorithm. All the models were applied to three case studies of Zayandeh-Rud Reservoir, Karoon-I Reservoir, and the system of Bakhtiari (upstream) and Dez (downstream) Reservoirs in Iran to evaluate their performance. It was reported that all the models showed an improvement in the convergence speed for all case studies.

To increase the rate of convergence in DE Algorithm, Yin and Liu (2009) modified the mutation operator by randomly selecting four different individuals from population instead of two. The modified DE algorithm was applied to optimize the hydropower production. On comparing with a DP model, it was reported that the DE algorithm was superior in calculation speed and provided a new approach for optimal operation of multi-reservoir to overcome the curse of dimensionality of DP model.

Chen *et al.* (2010) developed an adaptive GA model with double dynamic mutation operator to prevent the premature convergence and local optima. The model was applied for the eco-friendly operation of cascade reservoirs in the Southwest of China. It was reported that the adaptive GA resulted in higher upstream water level and 4% more power generation than simple GA model. It was concluded that the adaptive GA with the dynamic mutation operator fulfilled the goal of eco-friendly reservoir operation and enhanced the global search accuracy in comparison with simple GA model.

Davendra *et al*. (2010a) analysed the population dynamics in EAs and its relation to chaotic systems. A dynamic population was generated using the basic chaotic principles to induce and retain diversity in the population. The model was simulated using GA, DE and Self-Organizing Migrating Algorithm (SOMA) on the combinatorial problem of quadratic assignment. Each simulation was repeated 10 times with the same control parameters and reported that there were very good improvement in the results.

Ebrahimzadeh and Jampour (2013) used Lorenz chaotic system to generate pseudo random numbers for operators of GA to avoid local convergence. A population size of 40, crossover probability of 0.6 and mutation probability of 0.02 are fixed as the GA model parameters. Upon testing benchmark problems, it was reported that Chaos GA model resulted 34% improvement in Schaffer function and 54% improvement in Clonalg function. It was concluded that the proposed method converged quickly and much more efficient than traditional GA in solving optimization problems.

Vucetic and Simonovic (2013) proposed a novel Fuzzy Differential Evolution (FDE) algorithm to consider the vague information on the search space and to deliver a more focused search. The proposed FDE algorithm utilized the fuzzy triangular membership function for variable initialization and random alpha-cut membership function to create alpha-cut intervals

to be perturbed through mutation by fuzzy arithmetic. Upon demonstrating the algorithm on several benchmark problems, the algorithm was used for flood control operation of Wildwood reservoir in the Upper Thames River basin, Canada. It was reported that the FDE algorithm performed better than the classical DE in terms of convergence speed.

2.3 Multi-Objective Optimization

A surface water reservoir serves multiple purposes such as irrigation, hydropower, industrial and domestic water supply, flood control, navigation, recreation, etc. These purposes may conflict and/or compete with each other. For example, crop production requires more releases from the reservoir where as the hydropower production requires more storage to maintain the head in the reservoir. Therefore, it is very much essential to consider all the objectives simultaneously to arrive an optimal trade-off among the conflicting objectives so as to satisfy all the demands. The literature review on various multi-objective optimization models using conventional and soft computing techniques are presented in this section.

2.3.1 Conventional Multi-Objective Optimization Methods

The conventional techniques solve the multi-objective problem either by weighting or constraint method. In the weighting method, a relative weight is assigned to each objective function and converted into a single objective by adding all the objectives. A given set of weight will give only a single set of non-inferior solution and the relative weights are need to be varied systematically to produce a pareto-optimal front. In the constraint method, a single objective is optimized by considering all other objectives as constraints. Thus, both these methods convert the multi-objective optimization problem is into a single objective optimization problem to generate only a single pareto-optimal solution in a single iteration. Hence, to generate the pareto-optimal front, the conventional optimization model has to be solved for several times. Some of the multi-objective studies carried out using conventional methods are discussed in this section.

2.3.1.1 Weighting or Constraint Method

Dauer and Krueger (1980) developed a methodology for solving multi-objective water resources problems. The proposed method decomposed the system into groups of objectives

according to their priority in the model. The goal programming was then used to analyse the groups and the solution of each individual group was arrived using the method of constraints. The proposed methodology was demonstrated using multi-period screening model for a river basin development. The constraint method was used by Yeh and Becker (1982) to develop the trade-off between different objectives of California Central Valley Project. The five objectives considered were (1) hydropower production, (2) fish protection, (3) water quality maintenance, (4) water supply, and (5) recreation. The multi-objective model was solved using modified LP and DP techniques for various combinations. Two sets of monthly historical stream flows corresponding to a drought year and an excess water year were used to develop the corresponding non-inferior solution sets. It was concluded that the constraint method of multi-objective optimization can be practically applied to multi-reservoir system optimization.

A chance constrained goal programming model (CCGP) was developed by Changchit and Terrell (1989) for a three reservoir system which is a portion of the Red River reservoir system in Oklahoma, U.S.A. The objective was to minimize the undesirable deviations from the goals and goals were water supply, downstream flow, hydropower generation, recreation and flood protection. All these goals were expressed either deterministically or probabilistically depending on the inflow and were converted to their deterministic equivalents. The inflow was assumed to be normally / log normally distributed and the conditional cumulative distribution function was determined with known conditional mean and conditional standard deviation of inflows. It was reported that the use of conditional cumulative distribution function; which considered the correlation between inflows, improved the accuracy of the results.

A multi-objective LP model was developed by Mohan and Raipure (1992) to derive the optimal release policy of a large-scale multi-reservoir system in Chaliyar River basin in Kerala, India. The five reservoirs in the basin were considered as a single system and the optimal monthly releases from the reservoirs were derived with the objective of maximizing the irrigation releases and hydropower production using LP technique. The constraint technique was used to handle the multiple objectives and three series of inflow sequences representing the normal, drought, and excess flow conditions were used in the model. It was reported that the normal and excess flow conditions satisfied all the demands, whereas the

drought flow condition resulted in deficit. From the trade-off analysis, it was reported that the power production decreased when there is an increase in irrigation release.

Barros *et al.* (2003) developed a monthly NLP model for the management and operations of the Brazilian hydropower system. The NLP model considered six objectives such as (1) minimizing the loss of the stored potential energy, (2) minimizing storage deviations from targets, (3) maximizing total energy production, (4) minimizing spilled energy, (5) minimizing energy complementation and (6) maximizing the profit derived from secondary energy and handled using weighting approach. The formulated NLP model was first linearized by two different linearization methods and solved by LP technique. The outputs from the LP were then used as the initial policy for the successive linear programming (SLP) and NLP techniques. All the three techniques, LP, SLP and NLP were solved using the linear and nonlinear solvers in GAMS-MINOS. A comparative analysis was made between the linearized and the NLP models. It was reported that the LP model produced 0.6% less total energy and storage varied more frequently in the NLP model than the LP model. On comparing with the historical operational records, it was reported that the NLP model performance were superior.

The HIDROTERM model was used by Zambon *et al.* (2012) to optimize the management and operations of the Brazilian hydrothermal system. The developed model was solved for different scenarios of inflow, demand, and installed capacity to demonstrate the efficiency and utility of the model. It was reported that HIDROTERM model was suitable for different applications such as planning operation, capacity expansion, and operational rule studies, and trade-off analysis among multiple water users.

2.3.1.2 Multi-Objective Fuzzy Linear Programming

The other way to solve a multi-objective optimization problem is to convert the multiple objectives as fuzzy variables and solve it for certain level of satisfaction. Thus, the uncertainty and fuzziness are accounted in fuzzy multi-objective optimization (FMOO).

A multi-objective fuzzy linear programming (MOFLP) model was developed by Gupta *et al.* (2000) for optimal area allocation in Narmada river basin. Initially, the monthly operations of the reservoir are simulated for 30 years and the resulted optimal monthly irrigation releases were used as inputs to the MOFLP area allocation model. It was reported that the minimum

area crop plan based on 25 years of historical period should to be adopted to avert the risk. It was concluded that the fuzzy-compromise cropping pattern obtained with 80% dependable releases and rainfall could be the best cropping pattern with small risk.

Raju and Nagesh Kumar (2000b) developed a MOFLP model to evaluate the management strategies of SRSP, India. Maximizing the net benefits, maximizing the crop production and maximizing the labour requirement were the three objectives considered in MOFLP. Initially all the objectives were optimized using crisp LP and from the results of LP, the objectives were fuzzified. The fuzzified multi-objectives were solved for maximizing the degree of satisfaction using 90% dependable inflow. It was reported that the net benefits, crop production and labour employment obtained using MOFLP were lesser by 2.38%, 9.6% and 7.22% compared to that of crisp LP model. A similar methodology was used by Raju and Duckstein (2003) for evaluating the management strategies of Jayakwadi irrigation project, Maharashtra, India using MOFLP approach. While achieving a 0.57 level of satisfaction, it was stated that the net benefits, agricultural production, labour employment have decreased by 4.13, 5.39 and 3.4% compared to the crisp LP model. Finally, both the studies concluded that MOFLP is a simple and suitable tool for multi-objective optimal crop planning.

Mehta and Jain (2009) developed an operational policy for a multi-purpose Ramganga reservoir in India using MOFLP with the objective of maximizing the release with several constraints and solved it in an iterative manner. The model was set to minimize the damage due to floods and droughts and determines optimum releases against demands for domestic supply, irrigation, and hydropower generation during monsoon and non-monsoon periods. The fuzzy rules were formulated from actual releases and three fuzzy rule based models were reported separately for monsoon and non-monsoon periods. All the models were developed using Fuzzy Mamdani (FM) and Adaptive Neuro-Fuzzy Interactive System (ANFIS) – Grid and Cluster techniques and results were compared. It was reported that ANFIS cluster gave the best results but FM was more users friendly. It was concluded that ANFIS cluster method was more efficient with highest correlation coefficient but FM method was recommended for site use.

Sahoo *et al.* (2006) developed a MOFLP to derive planning and management strategies of available land-water-crop system of Mahanadi-Kathajodi delta in Eastern India. The objective was set to optimize the economic return, production and labour utilization subject to specified

land, water, fertilizer and labour availability, and water use pattern constraints. All the three objectives of the LP model were given the same priority level to obtain the compromised solution in a fuzzy environment. Based on the study, conjunctive use of water was recommended to restrict further depletion of groundwater. It was concluded that for optimal land-water-crop system planning, the LP model are best suited for single criteria decision making and the fuzzy models are best for multi-criteria decision making.

Zeng *et al.* (2010) developed a MOFLP model with triangular fuzzy numbers for optimal crop planning of Liang Zhou region, Gansu province of northwest China. The optimal cropping pattern was derived for different water saving levels and different satisfaction grade. It was reported that the increase in water saving level increased the crop area and net benefits. On comparing the results with multi-objective LP model, it was reported that MOFLP results are more stable when uncertain coefficients were involved in the crop area planning. A MOFLP model was developed by Choudhari and Raj (2010) for a four-reservoir system to derive optimal operating policy considering the uncertainty in resources, technological coefficients, objective function coefficients. The objectives were maximizing the returns from irrigation release and maximizing the returns from power releases. In addition, the effect of fluctuations in irrigation demand and release, power demand and release and available storage volume were considered. It was reported that the feasibility value increased with decrease in the corresponding satisfaction level. It was also stated that the fuzzification of various parameters in the optimization problem will result in different operation policies, giving more flexibility to the policy maker. It was concluded that the multi-objective fuzzy optimization has robust applications in water resources engineering in general and reservoir operation, in particular.

Regulwar and Gurav (2010) developed an irrigation planning model to derive optimal crop planning in command area of Jayakwadi Project, Maharashtra, India using MOFLP approach. Four LP models were developed with the objective of optimizing the net benefits, crop production, employment generation and manure utilization. Then, the MOFLP model was formulated using the linear membership function from the results of crisp LP models. It was reported that the MOFLP model resulted in a degree of satisfaction of 0.58. The model was further extended by Regulwar and Gurav (2011, 2012) by considering the uncertainty in objectives, resources, technological coefficients using fuzzy. Both these studies concluded that MOFLP was a promising technique for sustainable irrigation planning as it incorporates the fuzziness in both resources and decision variables simultaneously.

Morankar *et al.* (2013) applied MOFLP to a case study of Khadakwasla complex irrigation project in Maharashtra, India. Three objectives, namely, maximization of net benefits, crop production and labour employment were considered. In this study, objective functions were considered as fuzzy in nature using different membership functions, namely, nonlinear, hyperbolic and exponential and 75% dependable inflow was used to derive the optimal crop planning. It was reported that all the membership functions resulted in higher irrigation intensity than the current irrigation intensity. It was concluded that the exponential and hyperbolic membership functions provided similar cropping pattern whereas non-linear membership function provided different cropping pattern.

Mirajkar and Patel (2013) developed a MOFLP model to study the sustainable irrigation planning of Ukai reservoir, Gujarat, India. The objectives such as maximizing the net benefits, employment generation, revenue generation from municipal and industrial water supply and minimization of cost of cultivation were considered. Initially all these four objectives were solved individually using LP technique for 75% exceedance inflow and the pay-off matrix is created. From the pay-off matrix the MOFLP model is formulated and solved for four inflow conditions viz, most critical year (90% exceedance probability), critical year (85% exceedance probability), normal year (75% exceedance probability), and wet year (60% exceedance probability). It was reported that the 75% dependable inflow was only marginally sufficient to meet the requirement and 85% dependable inflow resulted in deficit in water availability in the command area.

2.3.2 Evolutionary Algorithms based Multi-Objective models

The conventional optimization methods have their own merits and demerits in handling multi-objective optimization problems. The major drawback of conventional methods for multi-objective optimization is that they result in a single pareto-optimal solution rather than a pareto-optimal front having multiple solutions. Hence, the conventional optimization techniques need to be run for several times to generate multiple optimal solutions and to form pareto-optimal front. This can be overcome by applying multi-objective evolutionary algorithm (MOEA), which produces a true pareto-optimal front with multiple non-dominated solutions in a single run. Coello *et al*. (2007) discussed various evolutionary algorithms for solving multi-objective problems. Adeyemo (2011) reviewed the applications of evolutionary algorithms for multi-objective optimization of reservoir operations. It was reported that the

MOEA are most suitable for solving complex, non-linear, convex and multi-objective reservoir problems, since they produce tradeoffs to reservoir operation problems from which a reservoir operator can choose a suitable solution.

2.3.2.1 Multi-Objective Genetic Algorithms

In many real-life problems, multiple objectives may conflict with each other, and optimizing a particular single objective may result in unacceptable solution with respect to the other objectives. Hence, a reasonable solution to a multi-objective problem is to generate a set of non-inferior solutions, which satisfies the objectives without being dominated by any other solution. Konak *et al*. (2006) presented an overview and tutorial about multi-objective genetic algorithms (MOGA).

Kuo *et al*. (2003) used the weight method to derive the optimal rule curves of a multi-reservoir system in Chou-Shui River Basin, Taiwan under multipurpose operation using a GA model. The weight method was used to arrive at a trade-off between water supply and hydropower production. A penalty coefficient was added in the objective function to improve searching process in GA. Upon analysing six cases, it was reported that GA efficiently obtained different shapes of rule curves using different weight factors. Similarly, Louati *et al.* (2011) used the weight method to form a single objective from two objectives. The two objectives considered were minimizing the water allocation to demand centers and the salinity level of the water supply to end users within a complex multiple reservoir system located in Tunisia. However, the weight method could not provide multiple non-dominated solutions and Pareto optimal front in a single run. The non-dominated sorting GA-II (NSGA-II) developed by Deb *et al*. (2002) produced the Pareto optimal solution in single run and overcome the computation difficulties of other multi-objective evolutionary algorithms.

The NSGA-II was applied by Kim and Heo (2004) for the multi-objective optimization of a multi-reservoir system in Han River basin, South Korea. The multi-objectives that were considered in the study were to maximize the storages and minimize the water shortages. In this the study, simulated binary crossover (SBX) with a probability of 0.9 and mutation rate as 1/36 with a population of 500 were used for 500 generations. The problem was optimized with two distribution indices, 3.0 and 3.8 of SBX. It was reported that both the distribution indices resulted varying co-efficient of variation values for all the reservoirs in the system. It was concluded that NSGA-II could be efficiently used to identify Pareto optimal solutions.

Kim and Heo (2006) applied NSGA-II to optimize the multi-objectives of multi-reservoir system in the Han River basin. Two different cases were analysed, in case 1 only the storage and release limits constraints of each reservoir in the Han River basin were considered where as in case 2 constraint on storage, release limits, water supply demand and end of month water level were considered. The simulation model was applied to evaluate the performance of the model and the results were compared with the historical reservoir operation records. It was reported that the NSGA-II resulted in more releases to downstream and maintaining the storage in reservoir better than the historical releases. The study was further extended by Kim *et al*. (2006) for three cases having different constraint conditions. Both these studies concluded that NSGA-II performed well for the optimization of multi-reservoir system having multi-objectives.

The real coded NSGA-II was used by Reddy and Nagesh Kumar (2006) to generate a pareto-optimal set for Bhadra Reservoir system, India. The multi-objectives considered were minimizing the irrigation deficits and maximizing the hydropower generation. The model was solved for three inflow scenarios representing dry, normal and wet seasons, with a population size of 200 using SBX and polynomial mutation for 1000 generations. The clustering technique was used to sort out the best solution among the many alternatives. It was reported that storage and release policies obtained from MOGA would help the reservoir operator in making a suitable decision for different inflow scenarios. It was concluded that the MOGA was very much useful in producing a well defined non-dominated solution set for conflicting objectives.

Kim *et al.* (2008) developed a piece-wise-linear operating rule for the Soyanggang reservoir using the NSGA-II. Minimizing the shortage index and maximizing the hydropower production were the two objectives considered. Initially, a piecewise-linear operating rule consisting of 4 and 5 linear lines was derived using the implicit stochastic optimization from 100 years of generated inflow. Then, the coordinates of the linear operating rules were coded as chromosomes and optimized using NSGA-II. The optimal results were further evaluated using a simulation model with six years of historical inflow data. It was reported that the piecewise-linear operating rules performed well at the same time satisfied all the constraints.

Yang *et al.* (2009) developed a methodology by integrating the MOGA, constrained differential dynamic programming (CDDD) and the groundwater simulation model for the

conjunctive use of surface and subsurface water in southern Taiwan. The MOGA was used to minimize the fixed costs and pumping cost, generate a pattern of pumping/recharge and estimate the non-inferior solutions set. The shortage index was used to estimate the water deficit cost. The groundwater simulation model was used to handle the complex dynamic relationship between the groundwater level and the pumping/recharge pattern. The CDDP model was adopted to distribute the optimal releases among multi-reservoirs. It was reported that the final non-inferior solutions set with fixed costs ranged from 4,578,260,000 N.T. dollars to 3,366,480,000 N.T. dollars with the shortage index from 18.29 to 28.02.

Darshana *et al.* (2012) used the CROPWAT simulation model and MOGA optimization model to derive optimal releases for the irrigation system in Holeta catchment, Ethiopia. The CROPWAT simulation model was used to estimate the crop water requirement and to develop water–yield relationships among various crops. The NSGA-II was used to derive the optimal crop planning with the objectives of maximizing the net benefits and minimizing the irrigation water requirements. The NSGA-II was applied with a population size of 150, a multi-point crossover with probability of 0.8, mutation with probability of 0.01 and 3000 generations. It was reported that 23% of water could be saved by varying the crop area.

Kumphon (2013) applied the MOGA to determine the optimal operation of a multi-reservoir system in the Chi River Basin, Thailand. Two competing objective functions such as release and storage were considered for the multi-objective analysis. The GA model parameters considered were crossover probability as 0.9, mutation probability as 0.2, population size as 100 and maximum generation as 300. It was reported that the predicted values of reservoir releases and storage were mostly lower than the actual values. The reliability of non-inferior solutions was determined using the root mean square error. It was reported that the root mean square error were very low for storage (17.05) and release (3.65).

2.3.2.2 Multi-Objective Differential Evolution Algorithms

The multi-objective differential evolution (MODE) is also very similar to the MOGA in its working principle. The non-dominated sorting, ranking and selection procedure reported by Deb *et al*. (2002) for MOGA was adopted in MODE along with basic DE working principle. However, the application of multi-objective differential evolution (MODE) is very minimal compared to NSGA-II and some of the literatures are reviewed in this section.

Reddy and Nagesh Kumar (2007) applied multi-objective differential evolution (MODE) algorithm for optimizing the operation of Hirakud Reservoir, Orissa, India. The multiple objectives were minimizing flood risk, maximizing hydropower production, and minimizing the irrigation deficits in a year, subject to various physical and technical constraints. Based on test problem results, *MODE/rand-to-best/1/bin* strategy was selected as best and applied with a population size of 200, crossover as 0.3 and mutation constant as 0.5 for 500 generations for optimizing the reservoir operations. On comparing the results with NSGA-II, it was reported that the MODE resulted in many pareto-optimal solutions in a single run. The MODE algorithm was further extended by Reddy and Nagesh Kumar (2008) to evolve optimal strategies for irrigation crop planning of Malaprabha reservoir system for four different hydrologic scenarios. It was reported that the changes in the hydrologic conditions over a season has considerable impact on the cropping pattern and net benefits from the irrigation system. From these studies, it was concluded that the MODE algorithm performed better than NSGA-II and could be used for optimal irrigation planning also for optimization of reservoir operations.

Adeyemo and Otieno (2009b) used MODE algorithm for deriving optimal cropping pattern for Vaalhart Irrigation Scheme in South Africa. The multiple objectives considered were maximizing the total net profit, maximizing the total planning area and minimizing the irrigation water. The DE parameters used were population size 100, crossover as 0.95 and scaling factor as 0.5 for 1000 generations. It was reported that MODE resulted a good trade-off between conflicting objectives and all the solutions on the Pareto front were good. Adeyemo and Otieno (2010) further extended the MODE algorithm to solve multi-objective crop planning model with multiple constraints. The multi-objectives considered in their study were minimizing the total irrigation water, maximizing net income and total agricultural output. Four different strategies such as *DE/rand/1/bin*, *DE/rand/2/bin*, *DE/rand/1/exp* and *DE/rand/2/exp* were used. The parameters such as scale factor, crossover rate and population size were fixed as 0.50, 0.95 and 100 respectively based on trial and error. It was reported that MODE with binomial crossover resulted more non-dominated solutions than exponential crossover. It was concluded that MODE is a good algorithm for solving crop planning problem especially in water deficient areas.

Raju *et al*. (2012) applied MODE algorithm for the irrigation planning of Mahi Bajaj Sagar Project, Rajasthan, India using 75% dependable inflow scenario. Maximizing the net benefits,

agricultural production and labour employment were the three objectives considered in the multi-objective environment. The K-means cluster analysis was used to reduce non-dominated alternatives generated by MODE to manageable groups. Optimal number of groups was determined based on the Davies–Bouldin and Dunn's cluster indices. It was concluded that selection of suitable parameters is necessary for effective implementation in real-world planning situations.

Schardong *et al*. (2013) derived the optimal operation policy for a complex multipurpose reservoir system in Brazil using MODE algorithm and compared with NSGA-II. The objectives were minimizing the shortage demand, maximizing the water quality and minimizing the pumping cost. The developed model was applied to the two inflow scenarios representing drought period (inflows below historical average) and wet period (inflows above historical average). It was reported that MODE algorithm outperformed NSGA-II and it converged closer to optimal solution with better spread coverage of the true Pareto front.

2.3.3 Multi-Objective Hybrid Evolutionary Algorithms

The simple MOEAs results in premature convergence and local optimal solution for complex non-linear multi-objective optimization problems (Chen *et al.*, 2007; Hakimi-Asiabar *et al.*, 2009; Huang *et al.*, 2010). In order to overcome this drawback of simple MOEAs, few researchers proposed several changes and modification in MOEA to improve their performance. Some of literatures, pertaining to the modified MOEAs otherwise termed as hybrid MOEAs are discussed in this section.

Macro-evolutionary multi-objective genetic algorithm (MMGA) model was developed by Chen *et al.* (2007) to avoid premature convergence of conventional GA. The developed model was applied to derive the rule curves of a multi-purpose reservoir in Taiwan serving water supply and hydropower generation. It was reported that the MMGA yielded better spread solutions and converged closer to the true Pareto frontier than the NSGA-II. Xianfeng *et al*. (2008) proposed a multi-objective chaotic optimization algorithm (MCOA) to solve multi-objective non-linear water resources deployment problem. The proposed algorithm magnified the chaotic series generated by logistic mapping to the feasible region and searched the best results by iterative comparison. Based on the results, it was reported that the MCOA

is a very useful global optimization algorithm for solving optimal water resources deployment and has high efficiency.

Hakimi-Asiabar *et al.* (2009) developed a Self-Learning Genetic Algorithm (SLGA) model to derive the operating policies of a multi-objective multi-reservoir system. The SLGA used Self-Organizing Map (SOM) and Variable Neighbourhood Search (VNS) algorithms to add memory to the GA and to improve its local search accuracy. The multi-objectives considered in the study were supplying water demands, generating hydropower energy and controlling water quality in downstream river. It was reported that, SLGA showed tangible improvements in the convergence rate, diversity of solutions, quality of solutions and running time. It was also shown that the SLGA has the capability of solving large scale multi-reservoir, multi-purpose reservoir operation optimization problems. The algorithm was further improved by Hakimi-Asiabar *et al.*, (2010) and applied to derive optimal operating policies of a multi-reservoir system. It was reported that the SOM has significantly increased the number of non-dominated solutions in the last generation. Also, it was stated that the total run-time of the SLGA is less than NSGA-II due to its higher convergence rate.

Sarker and Ray (2009) proposed a multi-objective constrained algorithm (MOCA) and compared the results with the conventional constraint method and NSGA-II for deriving optimal crop planning. The main difference between the NSGA-II and MOCA was in the process of population reduction in the selection process. It was reported that the proposed method maintained the end points of the objective space as well as the maximum and minimum values of the variables in the process of population reduction and maintained the diversity in the population. It was concluded that the MOCA resulted superior solutions than NSGA-II for the non-linear version of the optimal crop planning model.

A new multi-objective cultured differential evolution (MOCDE) was proposed by Qin *et al.* (2010) for reservoir operation flood control problem. The multi-objectives considered were maximizing the upstream water level and maximizing the discharge to downstream protected areas. The crossover parameter, scale factor and population size was set as 0.2, 0.1 and 50 respectively and solved for 1000 generations. On comparing the results with constrained DP, it was reported the computational time in MOCDE is much lesser that DP. Also, it was stated that the solutions obtained using MOCDE converged well to the true pareto front and

distributed uniformly. It was concluded that MOCDE can be a viable alternative for generating optimal trade-offs in reservoir multi-objective flood control operation.

Huang *et al.* (2010) developed a chaotic GA (CGA) model to solve a multi-objective optimization of hydropower system with ecological consideration. The multi-objectives were converted in to a single objective using constraint method. In the proposed CGA, chaotic variables were introduced using one dimensional logistic method into the optimization variables. The proposed CGA was applied for the optimal operation of a hydroelectric reservoir and the results were compared with GA, COA and DP. Based on the results, it was reported that CGA had performed better than other methods and has high search efficiency, good convergence performance, faster pace converge to the global optimal solution.

Wu *et al*. (2011) developed a CGA model to optimize the operations of a hydropower reservoir considering the ecological flow. The population was initialized using one dimensional logistic mapping method. The multi-objectives considered were maximizing the annual power generation and output of the minimal output stage in the year and minimizing the shortage of eco-environment water demand in the reservoir region and downstream river. It was reported the model resulted in 8 million kWh annual generation and concluded that the model was worthy to derive the optimal operation of hydropower reservoir since it considered river ecological flow and promote the sustainable utilization of water resources.

Shokri *et al.* (2013) combined ANN and NSGA-II to reduce the number of simulations required in EAs for multi-objective optimization problems. In the proposed algorithm, the ANN was used to train and update only the required areas in the decision space. The proposed NSGA-II - ANN methodology was examined using three standard test problems and one real-world problem with two objectives namely, meeting the demand and flood control. It was reported that the hybrid NSGA-II - ANN algorithm extracted the pareto front with in less simulation time compared to simple NSGA II algorithm. On comparing the results of test problem and real world problem, it was concluded that the proposed algorithm showed similar performance despite lower computational-time.

In order to avoid premature convergence, Zhang *et al*. (2013) proposed chaotic sequences based multi-objective differential evolution (CS-MODE) to solve optimal short-term hydrothermal scheduling. The proposed algorithm utilized the elitist archive mechanism to

retain the non-dominated individuals and a heuristic two-step constraint-handling technique to handle complex equality and inequality constraints. A new mutation operator was proposed by modifying mutation parameter using chaotic sequence generated by three mappings methods namely logistic mapping, circle mapping and tent mapping. On comparing the results with simple MODE, it was reported that CS-MODE resulted in lower thermal cost with less emission rate.

2.4 Closure

A detailed literature review related to the objectives of the present study is reported in this chapter. Both, single objective and multi-objective optimization models pertaining to reservoir operation has been reviewed. From the literature review, it is observed that the conventional optimization techniques were widely used to derive the optimal policies till recent past. Especially, LP has been used for deriving the optimal crop planning and NLP is used for non-linear hydropower production functions. Later, DP was used as a suitable alternative to NLP. All these techniques were solved either deterministically or stochastically. In order to consider the vagueness or impreciseness, fuzzy technique has been employed in reservoir optimization. Few authors have modelled the uncertainty in the inflow as chance constraint and solved using LP or NLP techniques. Even though lots of modifications have been made to conventional techniques, there exist many difficulties in solving large scale complex water resources problems.

Some of the disadvantages of conventional techniques are time consuming work, iterative process, requirement of large storage space, single solutions and may results in local optimal solution. The DP may end up in curse of dimensionality. Thus, it was reported that the conventional techniques are not suitable for multi-objective optimization problems, since it results in a single solution and need to be solved repeatedly to evolve a Pareto optimal front. For multi-objective optimization, among conventional methods most of the studies adopted MOFLP approach for optimal crop planning. However, most of the studies are for single reservoir system and the fuzziness are mostly considered only in the objective function. To overcome the drawbacks of conventional techniques, soft computing optimization techniques were developed and applied to solve single as well as multi-objective problems.

The evolutionary algorithm based soft computing techniques were recently used by researchers for optimizing the reservoir operations. Among various evolutionary algorithms, it is found that GA has been widely used for single objective optimization of water resources systems and this indicates wide range of application of GA in reservoir operation. Another evolutionary algorithm namely differential evolution (DE) algorithm is used as an alternative to GA because of its simplicity and faster convergence, especially for large scale complex problems having more variables. Among various soft computing techniques, NSGA-II and MODE algorithm have been used for optimization of water resources system especially to solve multi-objective optimization. However, it is found that most of the studies reported pertain to single reservoir system having no hard binding constraints. These EAs, search the global optimum from the randomly generated initial population. It has been reported that these EAs often suffer the problems of premature convergence and evolve too slowly to reach the global optimal solution. This is especially true, when the initial population is not so good for problems having complex hard bound constraints. Few studies have been reported on hybrid optimization algorithms, to overcome this drawback of GA and DE.

Recently, chaos algorithm has been used by researchers to overcome the convergence problem. In most of the studies, chaos algorithm has been found in generating the initial population. It is reported that combining chaos with evolutionary algorithm improved the performance of soft computing techniques. Application of this chaotic evolutionary algorithm is very scanty in reservoir operation and it is not reported for multi-objective multi-reservoir system. In a multi-reservoir system, all the reservoirs need to be considered simultaneously for sustainable integrated operation. In addition, there is a good possibility of intra sub-basin water transfer from a reservoir to another system. This type of temporal transfer of water from one reservoir to other reservoir to satisfy the demand of other reservoir, makes the water resources system more complicated. Hence, an integrated planning is required for the optimal operation of a multi-reservoir system and also for sustainable crop production, especially in developing countries like India. Also, real life reservoir operation involves multiple objectives, which are conflicting in nature.

Chapter 3

Materials and Methods

3.1 General

A systematic study to derive optimal operational plans of a reservoir necessitates the water resources modeller to have a complete knowledge and understanding about its behaviour. A simulation model provides more useful insights about the systems behaviour when its operations are simulated for various scenarios for longer period. Thus, simulation of the existing policies of a reservoir is essential for the effective planning and operation (Mays and Tung, 2002). If the simulation results show that the existing reservoir operation policies are not adequate to meet the demands, then there is a need to optimize its operation. Optimization is the process of finding the best feasible solution subject to various set of constraints. Over the decades, several conventional and soft computing techniques have been developed and applied to derive the optimal operational policies for a complex water resources system. The conventional techniques are prone to local optimal solution for complex problems having non-linearity, non-convexity, and multi-objectives. In such cases, the evolutionary algorithms are reported as a suitable alternative to conventional techniques. The results of the evolutionary algorithm mainly depend on the randomly generated initial population that is arrived based on the probabilistic theory. However, the simple evolutionary algorithms are slower in convergence and results in sub-optimal solutions for complex water resources problems with hardbound constraints. Very recently, to overcome this drawback, the chaos algorithm is coupled with evolutionary optimization technique (Yuan *et al.*, 2002;

Cheng *et al.*, 2008). Most of the hydrological variables exhibit chaotic behaviour, which is a projection that depends upon the initial condition (Sivakumar, 2000). Hence in the present study, the chaos algorithm is coupled with evolutionary algorithm for achieving better performance. In this chapter, development of simulation model and chaos based single and multi-objective GA and DE techniques are discussed in detail.

3.2 Simulation Model

In spite of development of various optimization techniques, simulation technique remains as a primary tool for reservoir planning and management studies in practice (Koutsoyiannis *et al.*, 2002). Simulation technique has a wide range of application and remains as an effective tool for evaluating a system to improve its performance through the analyses for various scenarios. Reservoir simulation is used to determine whether the operation policy of a reservoir system is adequate to meet its demands or not. It is also used to determine reservoir storage requirements at the end of the season. In some cases, before arriving a detailed operational plan, the behaviour of the system need to be studied using the standard operating policy (SOP). This will help the modeller to understand the system components, their importance and their responses for various input scenarios. In general, the simulation is accomplished by routing the flow through a reservoir using the continuity equation (Mays and Tung, 2002). In the present research, before developing a detailed optimization model, it is aimed to study and evaluate the behaviour of two complex multi-reservoir systems using a monthly time step simulation model. The first system is having hydropower production as major objective and the second system is having irrigation planning as major objective.

The multi-reservoir hydropower production is simulated for different operating scenarios, as well as for various duration of operation of hydropower plants. Similarly, the operation of another multi-reservoir irrigation system is simulated to study the irrigation releases and intra basin water transfer in the system. The broad steps involved in the development of simulation model are given in Figure 3.1. As a first step, the inputs such as inflow, initial storage and various physical parameters are read from the user. The next step is to estimate the evaporation losses, other demands and available storage in the reservoir for releases. After checking the constraints, the releases are made as per standard operating policy (SOP). After estimating the releases, the overflow and final storage levels are estimated. The procedure is

repeated for the next time step and continued until the total duration of the simulation period. Further, the output from the simulation model is used to study the behaviour of the system. This is achieved by analysing the releases and other outputs through statistical performance indicators such as reliability, resilience and vulnerability. After the SOP, the simulation is repeated by using present policy.

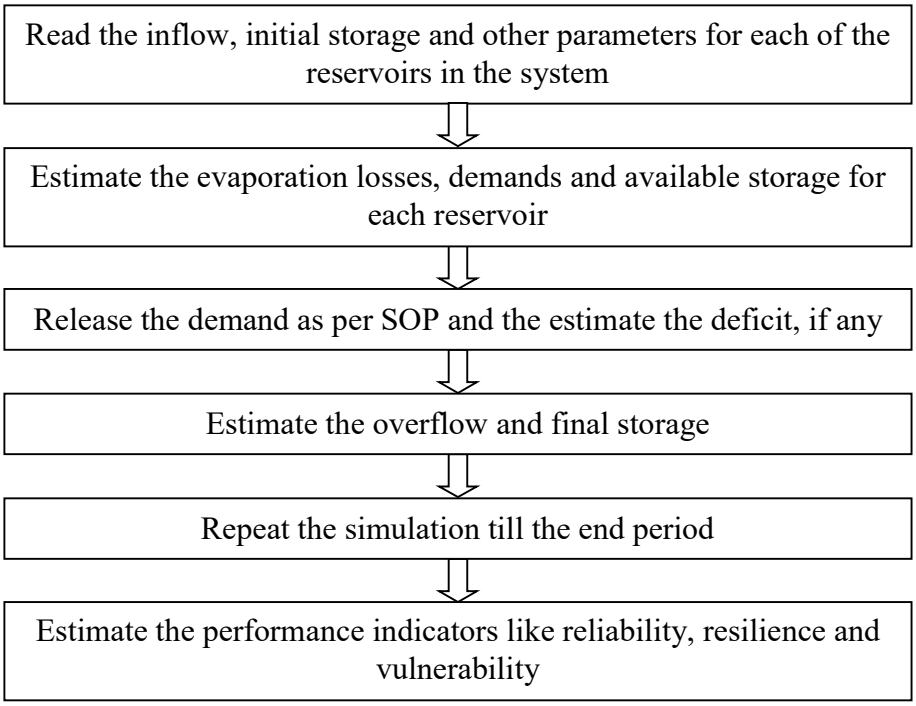

Figure 3.1. Broad steps of the simulation models used in the present study

Karamouz *et al*. (2003) reported that reliability is an important indicator for measuring the performance of the water resources systems in meeting the demands. In order to estimate dependability of the system, the time and volume reliabilities are estimated. The time reliability is the probability of the state of the system (x_t) that occurs in satisfactory state (S) (i.e. number of time the demand is satisfied during the total simulation period) (Loucks, 1997). Conversely, it is also estimated by deducting the number of failure periods out of the total simulation period from one. Thus, the reliability can be computed as:

$$Rel_t = 1 - \frac{F_n}{T} \qquad 0 \le Rel_t \le 1;\ F_n \le \mathrm{T} \qquad (3.1)$$

where Rel_t is the time reliability, F_n is the number of failure periods during the total simulating time period 'T'. In addition to the time reliability, volume reliability (Rel_v) is also computed which specifies the volume of the total demand that is released from the reservoir during the simulation period. The volume reliability is given as:

$$Rel_v = \frac{\sum_{t=1}^{T} R_t}{\sum_{t=1}^{T} D_t} \qquad 0 \le Rel_v \le 1 \tag{3.2}$$

where R_t is the release from the reservoir during the time period 't' and D_t is the demand of during the time period 't'. For a given system, the volume reliability will be higher than time reliability. Since in time reliability, releases less than the demand during a time period 't' is considered as failure for that time period 't', whereas in volume reliability, the releases are accounted for calculation.

Resilience describes how quickly a system recovers from the failure state after the occurrence of failure. Basically, it is a measure of the duration of the system in the unsatisfactory state. Resilience is an important indicator to assess the damages caused by droughts and floods (Karamouz *et al.*, 2003). It is also the probability that a satisfactory state (S) follows an unsatisfactory state (F) (Loucks, 1997). Thus, resilience is given as:

$$Res = Pr\{x_{t+1} \in S | x_t \in F\} \tag{3.3}$$

Kjeldsen and Rosbjerg (2004) redefined the resilience as the inverse of the mean value of the time spent by the system in an unsatisfactory state. It can be given as:

$$Res_{mean} = \left\{ \frac{1}{M} \sum_{j=1}^{M} d_j \right\}^{-1} \tag{3.4}$$

where M is the number of failure events and d_j is the duration of the failure event 'j'.

The maximum resilience is given as

$$Res_{max} = \left\{ \max_{j} \left(d_j \right) \right\}^{-1} \tag{3.5}$$

In the present study, Res_{mean} and Res_{max} given in Eq. 3.4 and Eq. 3.5 are used as the resilience performance indicators.

Vulnerability is the measure of magnitude of the failure events that occurred during the simulation period. Kjeldsen and Rosbjerg (2004) simplified the vulnerability measure stated by Hashimoto *et al*. (1982) and redefined the vulnerability as the mean value of the deficit events. Thus, mean vulnerability is expressed as:

$$Vul_{mean} = \frac{1}{M} \sum_{j=1}^{M} v_j \tag{3.6}$$

where v_j is the deficit volume of the failure event j.

The maximum vulnerability is estimated using the following equation:

$$Vul_{max} = \max_{j} \left\{ v_j \right\} \tag{3.7}$$

The behaviour of the system based on its long term operation can be assessed for various scenarios of simulation using these indicators. These three statistical performance indicators were widely used by many researchers to assess the performance of reservoir operations (Burn *et al.*, 1991; Loucks, 1997; Kjeldsen and Rosbjerg, 2004; McMahon *et al.*, 2006; Jain, 2009; Umadevi *et al.*, 2013).

3.3 Chaotic Evolutionary Algorithm for Single Objective Optimization

Recently, the evolutionary algorithms were widely applied to overcome the shortcomings of the conventional techniques, particularly in optimizing large scale complex water resources systems. Among various evolutionary algorithms, it reported that genetic algorithm (GA) and differential evolution (DE) algorithm are very versatile and more robust. However, simple

GA and DE often suffer the problems of premature convergence and evolving too slowly for complex problems with hard bound constraints when initial population is not so good (Li and Jiang, 1998; Yuan *et al.*, 2002; Cheng *et al.*, 2008). Hence, chaos technique is coupled with EAs to improve its search and convergence rate. Caponetto *et al*. (2003) reported that the chaotic sequences increased the performance of evolutionary algorithm and its convergence. The chaotic sequences improves the diversity in the population in evolutionary algorithm, (Davendra *et al.*, 2010a).

In the present study, the chaos algorithm is coupled with evolutionary algorithms and is applied for optimizing complex multi-reservoir systems having both linear and non-linear objective function. It is proposed to apply chaos algorithm not only in initial population generation but also in other optimization steps. The methodologies of these techniques are discussed in this section.

3.3.1 Hybrid Chaotic Genetic Algorithm

Genetic algorithm (GA) is a search based optimization technique developed by Holland (1975) that works on the principle of natural genetics (Goldberg, 1989; Deb, 2001; Reeves, 2003). In contrast to conventional optimization techniques, GA searches the optimal solution from a population of possible solutions. Each potential solution in the search space is represented through a set of randomly generated chromosome (also called as string) made of discrete units called genes (also called as sub-strings). Each sub-string controls one or more features of the string (Deb, 2001) and the collection of strings is called as population. The fitness of each string in the population is evaluated using an appropriate fitness function to select the strings for the next generation. The selected strings are subjected two genetic operators namely crossover and mutation to create a new population for the next generation. Thus, new population is created by swapping the sub-strings of the strings. Then, the mutation is applied to reintroduce the genetic diversity that might have lost during reproduction and crossover (Reeves, 2003). This process is continued till the termination criteria are reached.

In the present study, the chaos is coupled with GA to enhance the performance of the search and to increase the convergence rate. Chaos often exists in non-linear systems (Williams, 1997), and as reported by Li and Jiang (1998), chaos exhibits many good properties such as

ergodicity, stochastic properties, and irregularity. May (1976) proposed a one-dimensional logistic mapping equation to generate a chaotic sequence and is given as:

$$Y_{j+1} = \lambda Y_j (1 - Y_j) \qquad j = 1, 2, 3\ldots \tag{3.8}$$

where λ is a control parameter, varies between $0 \leq \lambda \leq 4$. The above equation is a deterministic without any stochastic disturbance (May, 1976). However, the long-term behaviour of the system changes significantly with the change in λ. When λ is 4, the system becomes chaotic. In Eq. 3.8, Y_1 is the initial chaotic variable randomly generated between 0 and 1. From this initial variable (Y_1), the chaotic sequence (a series of chaotic numbers) is generated using the logistic Eq. 3.8. A sample chaotic sequence is shown in Figure 3.2, for all sequence λ is 4. Figure 3.2(a) shows a sample chaotic sequence generated using the Eq. 3.8 with an initial value as 0.70953. Thus, each variable in the sequence is dependent on initial variable and a small change in initial value causes a large difference in its long-time behaviour, which is the basic characteristic of chaos. This can be correlated with the releases in reservoir operation, such that the releases in the subsequent months depend on previous month releases. Hence, the decision variables (releases) are generated as chaotic sequence to achieve a better initial population. May (1976) reported that, if the randomly generated initial variable (Y_1) is equal to 0.25, 0.5, and 0.75, the logistic Eq. 3.8 leads to deterministic series rather than a chaotic series. Figure 3.2(b), (c) and (d) shows that the Eq. 3.8 leads to a deterministic series when the initial value is equal to 0.25, 0.50 and 0.75, respectively. Hence, the initial variable (Y_1) should not be equal to the above mentioned values.

The working principle of hybrid chaotic GA (HCGA) proposed in the present study is given in Figure 3.3. As seen in Figure 3.3, the chaotic algorithm is used in initial population generation, crossover and mutations. In that way the probabilistic based genetic algorithm can be now called as chaos based genetic algorithm. The step by step procedure adopted in the hybrid chaotic genetic algorithm is explained in the following section.

3.3.1.1 Chaotic Initial Population

Most of the evolutionary algorithms are probabilistic based search techniques that depend upon the initial population. The two important aspects of the search are (1) initial population and (2) population size.

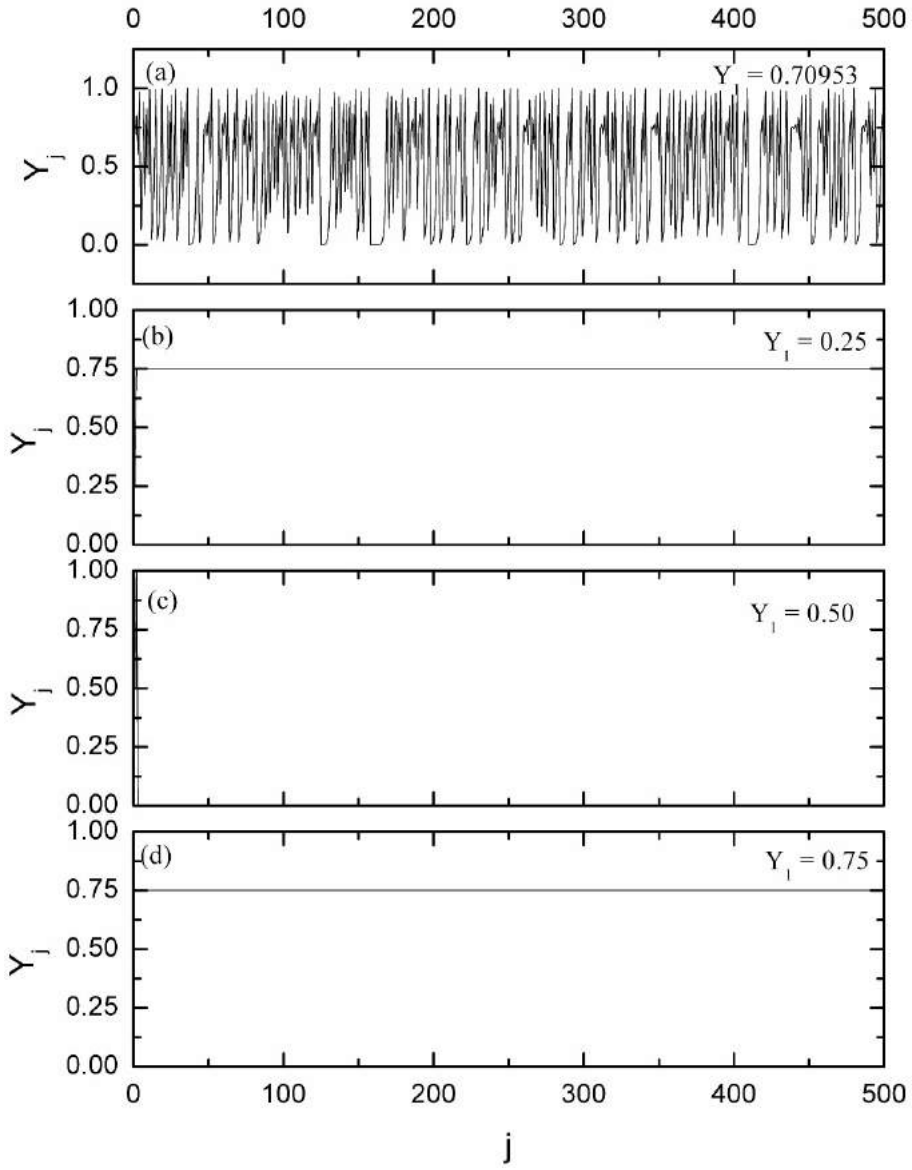

Figure 3.2. Illustration of Chaotic Sequence (Arunkumar and Jothiprakash, 2013)

The initial population is often randomly generated within the lower and upper bounds of the variables. The genes of the chromosome in the population can be represented in any specific format using bits, floating point numbers, trees, arrays, or any other objects (Sivanandam and Deepa, 2007). The representation of chromosomes as floating point numbers by integers is termed a real value encoding. In real coded GA (RCGA), each string is coded as a floating point numbers of the same length as the number of decision variables. Real value coding is more effective than binary coding in terms of precision, efficiency and flexibility (Oliveira and Loucks, 1997; Chang and Chen, 1998; Wardlaw and Sharif, 1999; Chang *et al.*, 2005), since there is no discretization of decision variable (Haupt and Haupt, 2003). Dhar and Datta

(2008) reported that the solutions obtained using a BCGA were inferior than RCGA for same population size and number of generations. Hence, in the present study, RCGA is used.

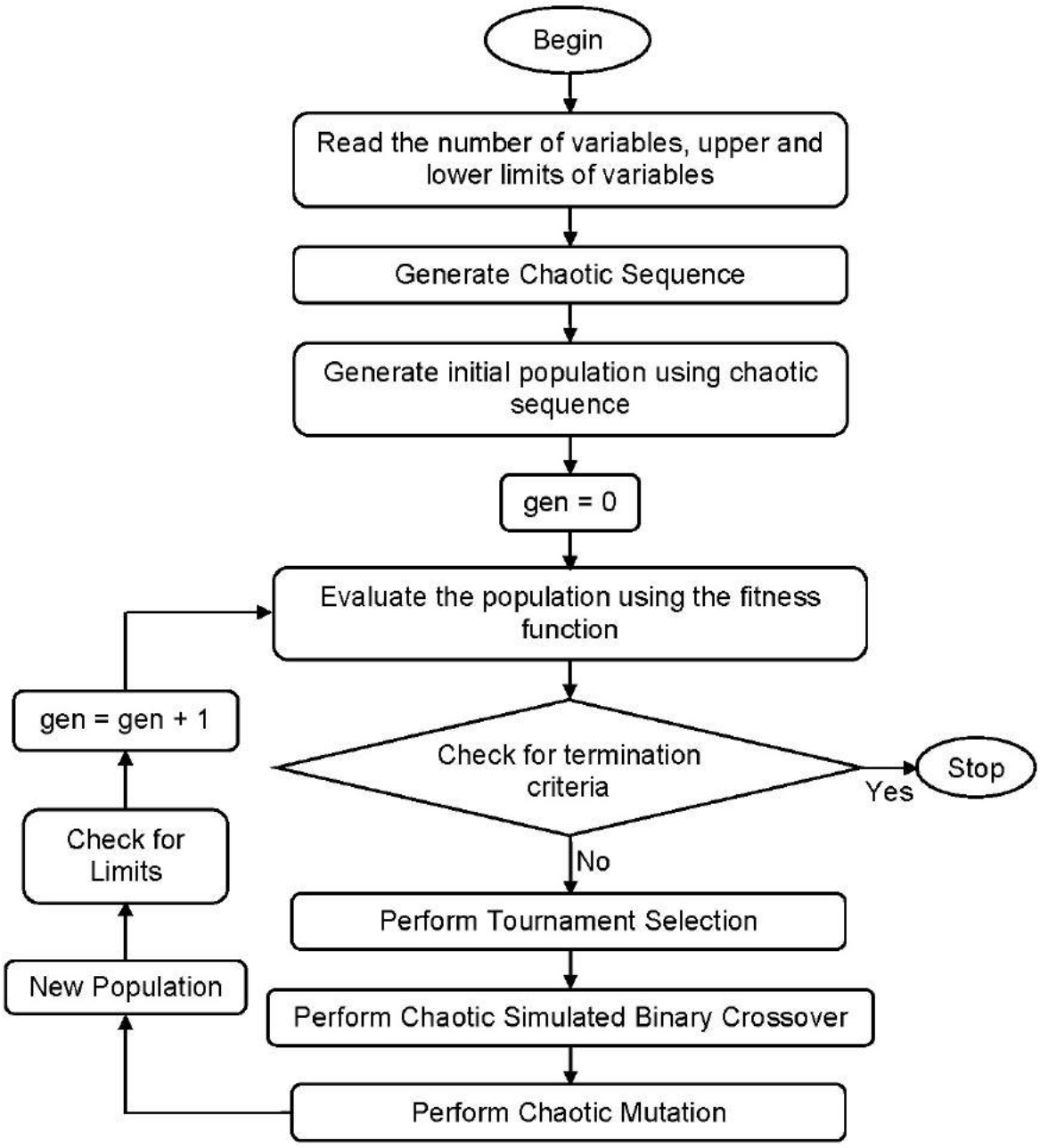

Figure 3.3. Working principle of Hybrid Chaotic Genetic Algorithm

In the RCGA, each gene is represented as a floating point value that is randomly generated within the upper ($UB_{i,j}$) and lower bounds ($LB_{i,j}$) of each variables. Thus, in a real coded

genetic algorithm, the sub-strings of each string in a population are initiated (Haupt and Haupt, 2003) as:

$$X_{i,j} = Y_{i,j} \times (UB_{i,j} - LB_{i,j}) + LB_{i,j} \qquad i = 1, 2 \ldots N_p;\ j = 1, 2, \ldots, N_v; \tag{3.9}$$

where $X_{i,j}$ is the 'j^{th}' sub-string of 'i^{th}' string; N_p is the population size and N_v is the number of variables. In the present study, chaos is used in the generation of initial population. Here, $Y_{i,j}$ is the chaotic variable generated using the one dimensional logistic Eq. 3.8. Thus, the generated initial population is a chaotic sequence that exhibits the properties of chaos.

3.3.1.2 Chaotic Simulated Binary Crossover

As explained in the previous section, selection of strings makes copies of good strings but does not create new ones (Deb, 2001; Sivanandam and Deepa, 2007). The new population is created by randomly crossing the strings in the mating pool with each other and hence the crossover is the most important step in GA as the search for global optimal depends on it. Generally, in crossover two parent chromosomes from the mating pool are combined together to form new chromosomes called offsprings. The offsprings are expected to inherit good genes, since the parents with better fitness values are selected among existing chromosomes in the population. By iteratively applying the crossover operator, genes of good chromosomes are expected to appear more frequently in the population, eventually leading to converge to an overall good solution. In order to preserve some good strings selected during the reproduction, not all strings in the population are used for crossover (Deb, 2001). This process of retaining some of the parent strings for the next generation without undergoing crossover and mutation is known as elitism. The crossover probability is an important parameter, which describes how often crossover is performed. If crossover probability is 100%, then all offspring are made by crossover. If it is 0%, the whole new generation is made from exact copies of chromosomes from old population.

The simulated binary crossover (SBX) developed by Deb and Agrawal (1995) that simulates the working principle of single point crossover in BCGA has been modified and used in the present study. In the present study, chaos sequence is introduced into the simulated binary crossover (SBX) to maintain the population diversity. The following steps were performed during SBX operation (Deb, 2001). Deb and Agrawal (1995) used a random number (u_j) to

estimate the spread factor (β_j) in the simulated binary crossover. In the present study, the random number (u_j) is generated as a chaotic sequence and the spread factor is computed using the Eq. 3.10.

$$\beta_j = \begin{cases} (2u_j)^{\frac{1}{\eta_c+1}} & if \quad u_j \le 0.5 \\ \left(\frac{1}{2(1-u_j)}\right)^{\frac{1}{\eta_c+1}}, & otherwise \end{cases} \tag{3.10}$$

where η_c is the distribution index and non-negative real number . Deb (Deb, 2001) reported that larger value of η_c produced 'near-parent' offsprings and vice versa. If $X_{1,j,t}$ and $X_{2,j,t}$ are the parent string with j^{th} sub-string in the t^{th} generation, then the offsprings $X_{1,j,t+1}$ and $X_{2,j,t+1}$ for the next generation are computed using the equations 3.11 and 3.12 respectively,

$$X_{1,j,t+1} = 0.5\{(1+\beta_j)X_{1,j,t} + (1-\beta_j)X_{2,j,t}\} \tag{3.11}$$

$$X_{2,j,t+1} = 0.5\{(1-\beta_j)X_{1,j,t} + (1+\beta_j)X_{2,j,t}\} \tag{3.12}$$

The new two offsprings will be symmetric about the parents to avoid bias towards any particular parent. After crossover, the strings are subjected to mutation.

3.3.1.3 Chaotic Mutation

The mutation operator introduces random changes in to the characteristic of strings to reintroduces the genetic diversity into the population and assists the search to escape from local optima (Deb, 2001). Mutation is generally applied at the sub-string level at very small rate. If there is no mutation, offsprings generated using crossover are directly used for next generation without any change. If mutation is performed, one or more parts of a string are changed. Like crossover probability, the mutation probability is also an important parameter and decides how often parts of string is mutated. The probability is usually taken about 1/L, where L is the length of the string or number of decision variables (Deb, 2001). Different forms of mutation are available for different kinds of representation. Uniform mutation (Sharif and Wardlaw, 2000; Jian-Xia *et al.*, 2005; Jothiprakash and Shanthi, 2006, 2009), non-

uniform mutation (Tospornsampan *et al.*, 2005), normal distribution mutation (Dariane and Momtahen, 2009), Gaussian mutation (Chen and Chang, 2007) were the different types of mutation used in solving complex water resources problems.

In the present study, chaotic mutation is proposed to assists the search to escape from the local optimal solution. In the chaotic mutation, randomly chosen substrings are muted with a chaotic sequence using Eq. 3.9 to introduce the diversity in the population. Thus, the chaos properties are maintained in the population. After the mutation process, new population for the next generation is created. This new population is used to evaluate the fitness function in the next generation. The fitness of the newly created population will be evaluated and the procedure is continued until the termination criteria are reached. The termination criteria used in this study are given in section 3.5.

3.3.2 Hybrid Chaotic Differential Evolution Algorithm

Differential Evolution (DE) algorithm is another type of EA developed by Storn and Price (1995) as an improved version of GA for faster convergence (Price *et al.*, 2005). Feoktistov (2006) stated that DE is one of the most powerful tools for global optimization, easy to implement and converges faster than GA. Price *et al*. (2005) reported that simplicity, easy to use, speed and robustness as the advantages of DE. The key parameters that control the search in DE are the population size (N_p), crossover constant (CR) and the scale factor (F) (Price *et al.*, 2005). The search for global optimum in DE is dependent on mutation unlike GA that is highly depended on crossover. Similar to GA, DE is also a population based technique that searches the global optimum over the generations. Usually, the initial population (group of vectors) is randomly generated within the specified upper and lower limits of the variables. Once the initial population is generated, the fitness of each vector is evaluated. Like other population based methods, the new population for the next generation is created using mutation and crossover in DE. DE mutation adds the scaled difference of two randomly selected vectors to the third vector in the population to generate a new trial vector. Then, DE employs uniform crossover, also referred as discrete recombination. The new population is created by comparing the trial vectors with the vectors of the old population of the same index. This procedure is repeated until all population vectors have competed against a randomly generated trial vector. Skanderova *et al*. (2013) studied the effect of different random numbers generators on the course of evolution and the speed of convergence to the

global solution in DE algorithm. It was reported that the evolution convergence was faster with the random numbers generated using chaos (Davendra *et al.*, 2010b). In the present study, a hybrid chaotic DE (HCDE) algorithm is developed by coupling the general DE algorithm with chaos technique. The detailed methodology adopted in developing HCDE algorithm is discussed in the following section.

3.3.2.1 Population Initialization

DE encodes all variables as floating point numbers. Price *et al*. (2005) states that the variables are initialized as a real value numbers even if it is discrete or integral, since DE internally treats all variables as floating point values regardless of their type and to add diversity to their different distributions. The initial population is generated within the upper ($UB_{i,j}$) and lower limits ($UB_{i,j}$) of the variables. Once limits are specified, a random number is assigned to each variable of vector within the prescribed range. In the present study, the chaotic logistic mapping method given by May (1976) is used to generate a chaotic sequence instead of random numbers to create the vectors to form the initial population. The Eq. 3.9. is used to generate the chaotic initial population. Thus, the generated initial population is a chaotic sequence, which exhibits the properties of chaos. Then, the fitness of each vector in the population is evaluated using a fitness function. The objective function of the optimization problem is used as the fitness function in this study to evaluate the population. The new population for the next generation is created using mutation and crossover in DE.

3.3.2.2 DE Mutation

Once the population is initialized, DE mutates and recombines the population to produce a population of trial vectors. In particular, DE mutation adds the scaled difference of two randomly selected vectors to a third vector in the population to create the trail vector. The third vector may be a random vector or the best vector of old population. Equation 3.7 shows three different, randomly chosen vectors to create a mutant trail vector.

$$V_{i,t} = X_{r1,t} + F \times (X_{r2,t} - X_{r3,t}) \qquad i = 1,2,\ldots,N_p; \quad r_1 \neq r_2 \neq r_3 \qquad (3.13)$$

Where $V_{i,t}$ is the new trail vector of i^{th} population of t^{th} generation; $X_{r1,t;}$ $X_{r2,t;}$ $X_{r3,t}$ are the randomly selected vectors from the population and F is the scale factor. The scale factor (F) is a positive real number that controls the rate at which the population evolves in DE. Storn

and Price (1997) stated that F should not be greater than 1 for effective optimization, even though there is no upper limit on F. Also, the scale factor ensures that the random vectors does not duplicate the existing vectors and also shifts the focus of the search from local to global optima. This procedure is repeated until new trail vector of population size (N_p) is created.

3.3.2.3 Crossover

Next to mutation, DE employs uniform crossover which is also referred as discrete recombination. The DE crossover creates trial vectors from the variable that have been copied from two different vectors. Thus, the DE mutation is carried out among the vectors of the population where as the crossover is carried out between each variable of the vector in the population. Thus, DE crosses each vector with a mutant vector. In DE crossover, the user defined crossover constant (CR) is compared with uniform random number (r_j) generated between 0 and 1. If the generated random number is less than or equal to CR, the variable (v_j) from the mutant trial vector is selected; otherwise, the variable (x_j) from the vector of old population is selected to trail vector. In addition, the trial parameter with randomly chosen index, j_{rand}, is taken from the mutant to ensure that the trial vector does not duplicate x_i. Mathematically it is given as:

$$U_{i,t} = u_{j,i,t} = \begin{cases} v_{j,i,t} & if \;\; r_j \le CR \;\; or \;\; j = j_{rand} \\ x_{j,i,t} & otherwise \end{cases} \tag{3.14}$$

Once the new trial population is created using mutation and crossover, the fitness of the each vector in the trial population is evaluated.

3.3.2.4 Selection

The vector for creating new population for the next generation is created by comparing the fitness value of trial population vectors with that of the old population vectors of same index. If the trial vector ($U_{i,t}$) has an equal or lower fitness value (for minimization problem) than that of its target vector ($X_{i,t}$) of old population, then the trail vector is selected for the next generation; else, the old vector is retained in the population for next generation. The selection process is carried out as using the Eq. 3.15.

$$X_{i,t+1} = \begin{cases} U_{i,t} & if \ f(U_{i,t}) \leq f(X_{i,t}) \\ X_{i,t} & otherwise \end{cases} \tag{3.15}$$

Price *et al*. (2005) stated that DE algorithm more tightly integrates recombination and selection than other EA by comparing each trial vector with the target vector of old population from which it inherits parameters. The process of mutation, crossover and selection is repeated until the optimum value is achieved or a pre-specified termination criterion is satisfied.

3.4 Chaotic Evolutionary Algorithm for Multi-Objective Optimization

Most of the real world problems are characterized by the presence of many complementing and conflicting objectives. Therefore, it is necessary to solves them as a multi-objective optimization problem rather than a single objective problem to arrive at an optimal trade-off between various objectives. In multi-objective optimization problems, there is often a dilemma as how to determine if one solution is better than another. Deb (Deb, 2001) reported that constructing pareto-optimal front is the best way to select the optimal solution for multi-objective optimization. This pareto-optimal front is referred as non-inferior solutions that are not dominated by other solutions in the search space. Conventional techniques have limitation in handling multi-objective optimization problems and will not generate multiple pareto-optimal solutions in a single run. Generally, the conventional optimization techniques convert the multi-objective optimization problem into single objective optimization problem to generate only a single pareto-optimal solution. To generate multiple optimal solutions, the conventional optimization techniques have to be used for several times. To overcome these limitations, several multi-objective evolutionary algorithms (MOEA) were reported. Some of them were niched pareto genetic algorithm (NPGA) (Horn *et al.*, 1994), non-dominating sorting genetic algorithm (NSGA) (Srinivas and Deb, 1994), pareto archived evolution strategy (PAES) (Knowles and Corne, 1999), strength pareto EA (SPEA) (Zitzler and Thiele, 1999), non-dominating sorting genetic algorithm-II (NSGA-II) (Deb *et al.*, 2002), etc. The main advantage of these techniques over other conventional optimization is that these MOEAs can generate the whole pareto-optimal solutions in a single run. Deb *et al*. (2002) compared NSGA-II with PAES and SPEA for various complex multi-objective functions and

reported that NSGA-II outperformed both the algorithms in terms of diverse set of solutions and in converging to the true pareto-optimal set.

3.4.1 Multi-Objective Hybrid Chaotic Genetic Algorithms

The elitist non-dominated sorting genetic algorithm-II (NSGA-II) developed by Deb *et al*. (2002) is used in the present study to solve the multi-objective optimization problem of reservoir operation. Also, the chaos algorithm is coupled with NSGA-II in each and every operation for efficient multi-objective optimization and to increase the convergence rate. The step by step methodology adopted in hybrid chaotic NSGA-II is given in Figure 3.4.

3.4.1.1 Population Initialization

Similar to single objective HCGA, the population is initialized as a chaotic sequence using one dimensional logistic mapping method developed by May (1976) as discussed in section 3.3.1.1. Then, each objective of the optimization problem is evaluated to find fitness of the chromosomes in the population. In multi-objective optimization, the fitness function is more difficult to determine (Sivanandam and Deepa, 2007). In the present study, the objective function is used to estimate the fitness value and the population is sorted based on non-domination into different fronts.

3.4.1.2 Non-Dominated Sorting

Once, the objective values are estimated, the strings are sorted based on non-domination. Here, the objective values are termed as solutions. In order to identify solutions of the first non-dominated front, each solution is compared with every other solution in the population to find if it is dominated. For each solution '*X*' in the population, the number of solutions which dominates the solution '*X*' (domination count) and a set of solutions that the solution '*X*' dominates are estimated. It the domination count is zero for a solution '*X*', then it is put in the first non-dominated front and assigned as rank one. In order to find the individuals in the next non-dominated front, the solutions of the first front are discarded temporarily and the above procedure is repeated until all the solutions are sorted in to different fronts. The solution in the first front are completely non-dominated by the other solutions in the population and the solutions in the second front are dominated only by the solutions in the first front. All the solutions in a front are ranked based on front in which they belong to. The solutions in the first front are ranked 1 and the solutions in the second front are ranked as 2 and so on.

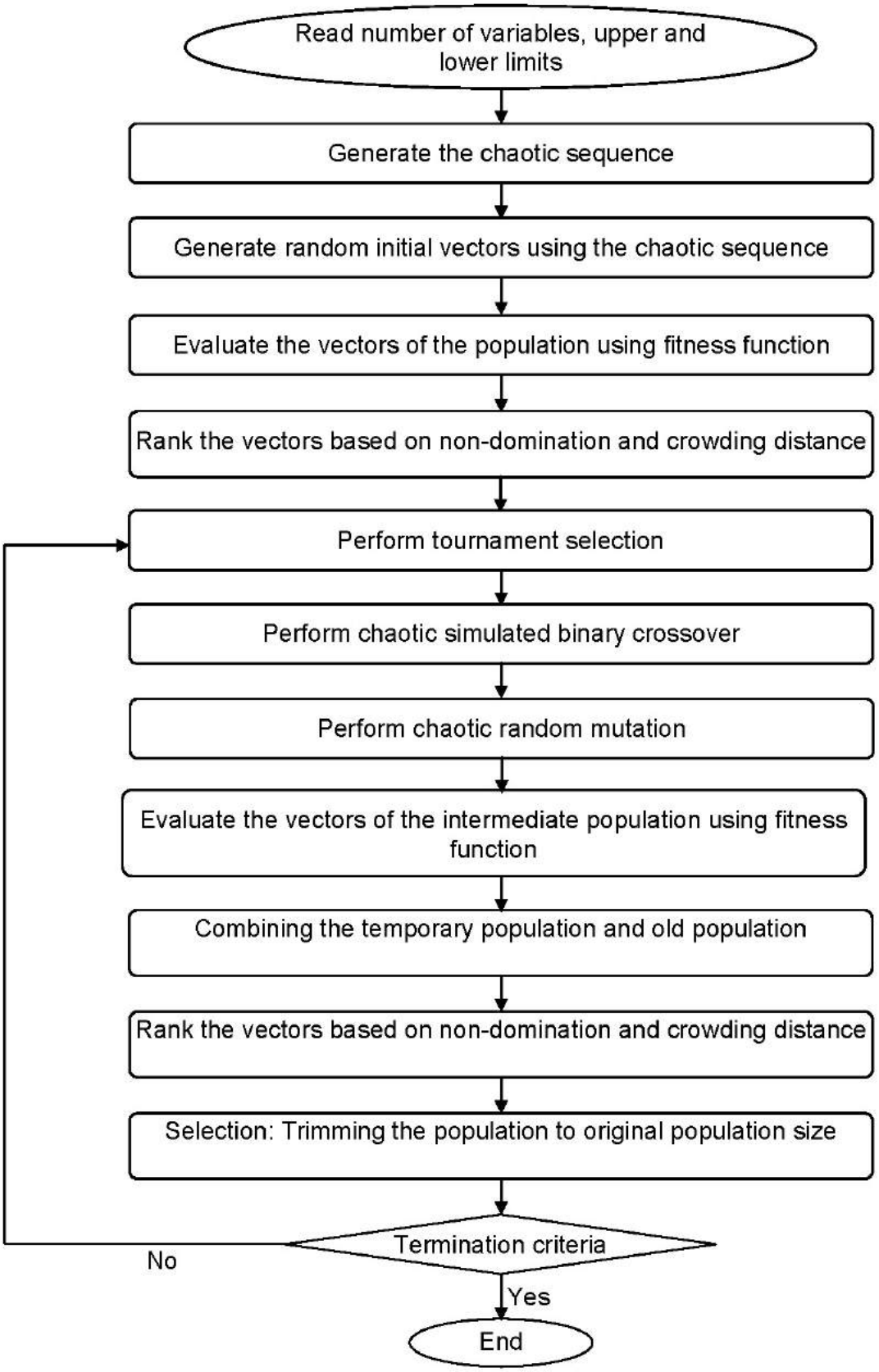

Figure 3.4. Step by step methodology of Chaotic NSGA-II adopted in the present study

In case of constrained multi-objective optimization, Deb *et al*. (2002) reported three more criteria for non-dominated sorting. It is stated that a solution '*X*' is said to constrained dominate a solution '*Y*', if (i) solution '*X*' is feasible and solution '*Y*' is infeasible (ii) both the solutions are infeasible, but solution '*X*' has a smaller overall constraint violation than solution '*Y*' and (iii) both solutions are feasible and solution '*X*' dominates solution '*Y*'. Deb *et al*. (2002) described that the above criteria is based on the principle that the feasible solution has a better non-domination rank than the infeasible solution. Thus, all feasible solutions are ranked according to their non-domination level based on the objective function values. However, among two infeasible solutions, the solution with a smaller constraint violation has a better rank.

3.4.1.3 Crowding Distance Estimation

After sorting the solutions into various fronts based on non-domination, the crowding distance is estimated, since the solutions are selected based on rank and crowding distance. The crowding distance is assigned front wise and is calculated for each solution to measure how close a solution is to its neighbours. Deb *et al*. (2002) stated that the basic idea behind the crowding distance is to find the euclidian distance between each solution in a front based on their objective values in the solution space. The crowding distance of a solution in a front is the average side length of the cuboid formed by connecting the adjacent solutions as shown in Figure 3.5. In Figure 3.5, the dark rounded circles are solutions of first front and hollow circles are solutions are second front. To calculate the crowding distance, the solutions in a front are sorted in ascending order based on the objective function value and each objective function is normalized before calculating the crowding distance. For all the solutions, the crowding distance ($I_{x,m}$) is first initialized as zero. Then, the solutions with smallest and largest objective function values (x-1 and x+4) are assigned an infinite distance value. For all other intermediate solution '*x*', the crowding distance (I_x) is estimated using the equation (Deb *et al.*, 2002):

$$I_{x,m} = I_{x,m} + \frac{I_{(x+1).m} - I_{(x-1).m}}{f_{\max,m} - f_{\min,m}} \tag{3.16}$$

where $I_{(x+1).m}$ and $I_{(x+1).m}$ are the crowding distance of solution '*x+1*' and '*x-1*' for the objective function '*m*'; $f_{max,m}$ and $f_{min,m}$ are the maximum and minimum objective values for

the objective function '*m*'. This calculation is continued with other objective functions. The overall crowding distance value is calculated as the sum of individual distance values corresponding to each objective. In order to maintain the population diversity, the solution with higher crowding distance value will have chance for selection for the next generation. Thus, the solutions in the boundary are always selected; since, they have higher crowding distance value. The solutions of chromosomes are selected for crossover and mutation using a selection operator based on the rank and crowding distance.

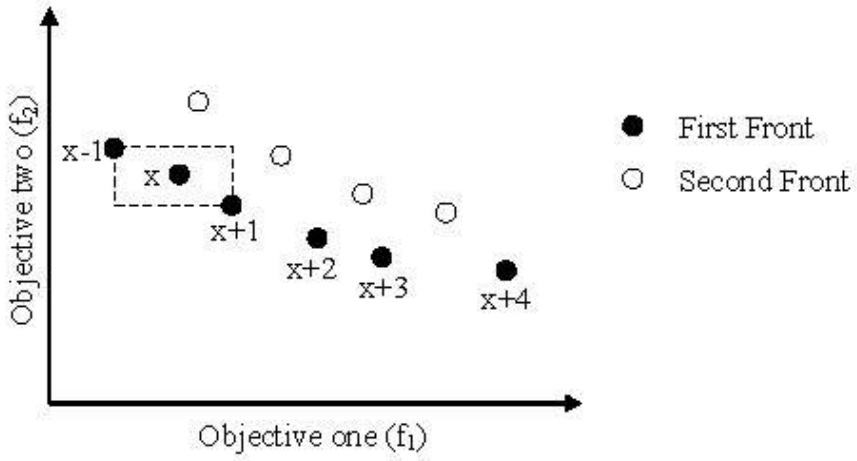

Figure 3.5. Calculation of crowding distance

3.4.1.4 Selection

The chromosomes for crossover and mutation are selected according to the rank and crowding distance. Deb *et al*. (2002) developed a crowding distance operator which conducts tournament and select the chromosomes based on rank and crowding distance. In this process, two solutions are randomly chosen from the population and are compared. A solution '*X*' wins the tournament, if (i) solution '*X*' has better rank than solution '*Y*' or (ii) if both the solutions '*X*' and '*Y*' have same rank then the solution having higher crowding distance is selected. In this present study, in addition to these criteria, three more criteria discussed in section 3.4.1.2 for constrained multi-objective optimization is also considered during the selection process. The chromosomes of selected solutions are crossed each other to generate new chromosomes and are subjected to mutation. In the present study, the chaotic simulated binary crossover discussed in section 3.3.1.2 is used for crossover and the chaotic random mutation discussed in section 3.3.1.3 is used for mutation. Thus, the new population is created based on the chaotic simulated binary crossover and chaotic mutation.

3.4.1.5 Recombination and Selection

Once, the new population are created, the fitness values of each objective function are estimated. Both the old and new populations will be combined and thus the population size is doubled. Deb *et al*. (2002) stated that the elitism is ensured in recombination, since all the previous and current best individuals are added in the population. Again, the population is sorted based on non-domination in to various fronts and crowding distance is estimated. Figure 3.6 shows the recombination and selection of chromosomes in NAGA-II. In the selection process, both the old population (OP) and new population (NP) are combined and sorted in to different fronts (F1, F2, F3, etc) based on non-domination. The new population for the next generation is filled by front wise starting from the first front until the population size reaches the defined population size. If adding all the individuals in a front exceeds the defined population size, then remaining individuals in that front are selected based on the crowding distance. In Figure 3.6, all the chromosomes in first three fronts (up to F3) are selected and remaining chromosome from F4 is selected based on crowding distance. The unselected chromosomes in F4 will be discarded. Thus, only the best individuals are selected as new population based on rank and crowding distance for the next generation. Again fitness of the new population is evaluated and this procedure is continued till the termination criteria are reached.

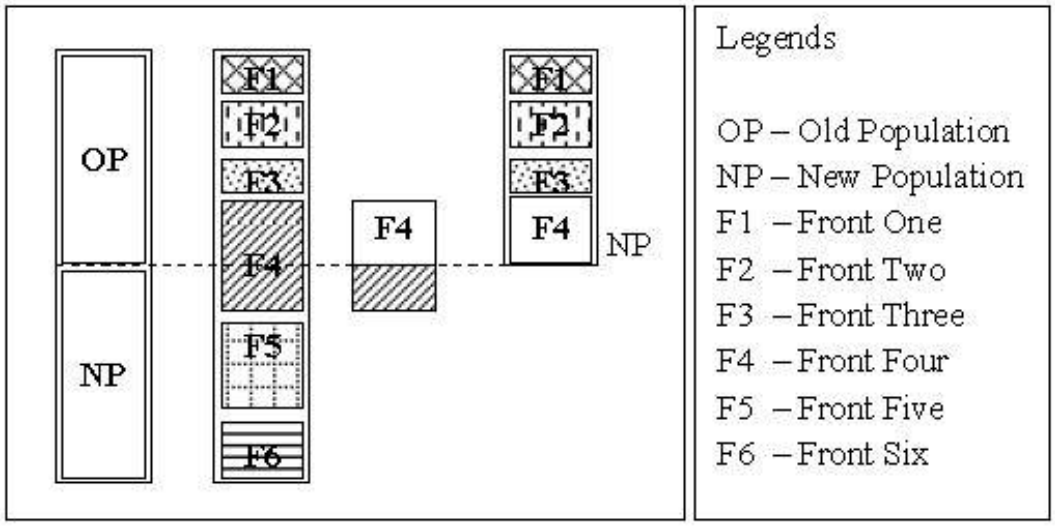

Figure 3.6. Recombination and selection of new population

3.4.2 Multi-Objective Chaotic Differential Evolution Algorithms

The chaotic differential evolution (CDE) developed for single objective optimization is suitably modified in line with NSGA-II for multi-objective optimization. In multi-objective differential evolution algorithm (MODE) also, the chaos technique is used to generate initial population and thus making chaotic multi-objective differential evolution algorithm (CMODE). The non-dominated sorting, crowding distance operator, recombination and selection developed by Deb *et al*. (2002) is incorporated with DE to generate the pareto-optimal front. The step by step methodology of the CMODE is given in Figure 3.7. The major difference between the CNSGA-II and CMODE is that crossover influences the search process in GA whereas mutation carries the search in DE. Hence in DE, mutation is performed earlier than crossover.

3.4.2.1 CMODE Parameter and Population Initialization

As a first step in CMODE, the main algorithm is initialized by reading the DE parameters such as scale factor, crossover factor, population size, number of objectives and number of variables. Then, the vectors of the population are generated within the upper and lower bound of the variables using the chaotic sequence as discussed in section 3.3.2.1. The fitness of each objective of the vectors is estimated using the objective function.

3.4.2.2 Non-dominated Sorting and Crowding Distance Estimation

The vectors are sorted into different fronts based on the non-domination and the crowding distance. The non-dominated sorting procedure explained in section 3.4.1.2 and the crowding distance estimation procedure explained in 3.4.1.3 is used in CMODE.

3.4.2.3 CMODE Mutation and Crossover

After sorting the vectors into various fronts, the DE mutation described in section 3.3.2.2 and crossover described in section 3.3.2.3 is performed to create the temporary population. The vectors in first front are non-dominated by other vectors of the population and hence they are chosen as best vectors for DE mutation. If more than one vector is in first front, then the crowding distance is compared and the vector having larger crowding distance is marked as best vector.

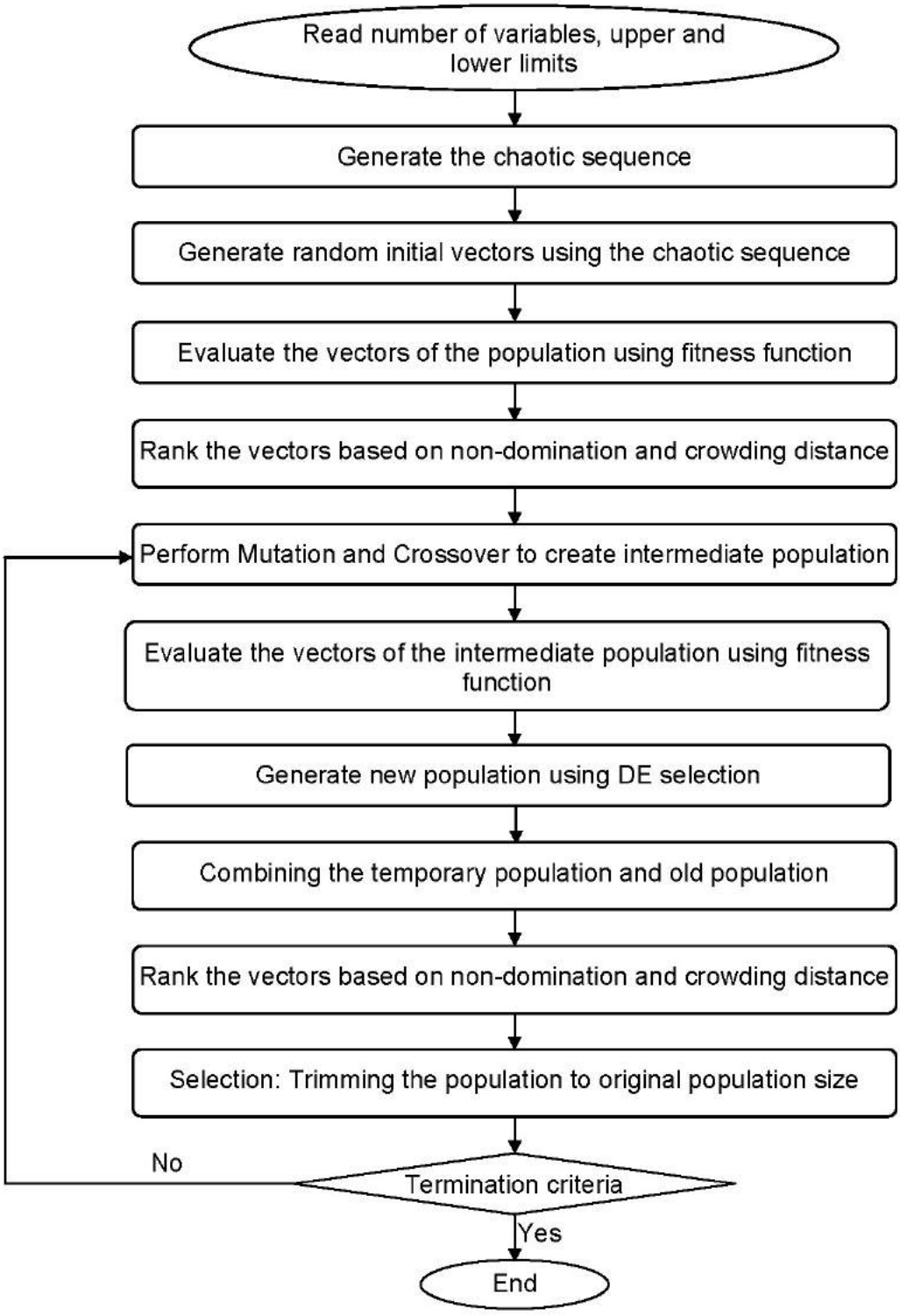

Figure 3.7. Step by step methodology of chaotic MODE adopted in the present study

3.4.2.4 CMODE Selection

Once the temporary population is created using mutation and crossover, the CMODE selection is carried out to select new population for next generation. In CMODE selection, the criteria used by Deb *et al*. (2002) for constrained multi-objective optimization is suitably combined with DE selection. In CMODE selection, the objective value of same index of temporary and old population is compared and the better one is selected for the next generation. However, in CMODE selection, the same index of temporary population and old population is compared based on three criteria. A vector '*X*' of temporary population is selected over vector '*Y*' of old population, if (i) vector '*X*' is feasible and vector '*Y*' is infeasible, or (ii) both vectors '*X*' and '*Y*' are infeasible, but vector '*X*' has less constraint violation, or (iii) both vectors '*X*' and '*Y*' are feasible, but vector '*X*' dominated the vector '*Y*'. Thus, based on these criteria, the new temporary CMODE population is created.

3.4.2.5 Recombination and Selection

After creating a new temporary population using CMODE selection, both the old population and new temporary population are combined. Then, the vectors are again sorted and ranked into various fronts based on non-domination criteria. The crowding distance is estimated for the vectors in each front. The vectors for next generation are selected from the first front subsequently until the population size. This procedure is explained in section 3.4.1.5. This procedure is continued till the termination criteria are satisfied.

3.5 Termination Criteria

An optimization algorithm is terminated when all the constraints are satisfied in a constrained problem. However, different objectives may often conflict in a multi-objective optimization. In such cases, satisfying one objective may result in an unsatisfactory state of other objectives. Thus, it is not always clear when to stop the search for a better trade-off solution. Various termination criteria are available to stop the search and are as follows:

Number of Generations: Usually, the objective function is not known in advance for a real world problem. Hence, optimization can be terminated after reaching a maximum number of generations. Thus, the algorithm stops when the specified number of generations has evolved.

No change in fitness: The algorithm stops if there is no significant improvement in the objective function value (fitness value) for a sequence of consecutive generations.

The termination criterion finally brings the search of the evolutionary algorithm based optimization to halt. In this study, both the number of generations and no change in fitness value are used as termination criteria (whichever is satisfied first) to stop the algorithm.

3.6 Closure

In this chapter, the methodology and working principle of two evolutionary algorithms, namely genetic algorithm and differential evolution algorithm are discussed in detailed for single objective and multi-objective optimization to be applied for multi-reservoir systems. Both the GA and DE are coupled with chaos. The chaos is introduced in generating initial population, crossover and mutation in genetic algorithm. In DE, the chaos is used for generating only the initial population. The procedure for coupling chaos algorithm in various steps of EA is presented. The same procedure is extended to multi-objective EA and is described in detail. It is aimed to compare the performance of proposed chaos based EAs with that of conventional optimization techniques. After deriving the optimal solution, it is aimed to check the performance of the optimal solution for a longer period using a simulation model. The multi-reservoir system selected as case studies for applying the single objective and multi-objective optimization techniques are described in the next chapter.

Chapter 4

Study Area

4.1 General

The techniques proposed and discussed in previous Chapter 3 are applied for the optimization of complex surface water reservoir systems. Two complex multi-reservoir systems in Maharashtra, India are selected as case studies. The first one is Kukadi Irrigation Project (KIP), a large scale five reservoir irrigation system having multiple command area under various canals and irrigating multiple crops. The second one is Koyna Hydro Electric Project (KHEP), a complex multi-purpose multi-reservoir system with hydropower production as a major objective. This system has two reservoirs and four hydropower plants at various locations and direction also. Both these cases are complex in their own way. In this chapter, the details of these study areas, their complexities and data collected are discussed in detail.

4.2 Kukadi Irrigation Project

Kukadi Irrigation Project (KIP) is one of the major irrigation projects in Maharashtra comprising of five dams namely, Dimbhe, Wadaj, Manikdoh, Pimpalgaon Joge and Yedgaon. These five reservoirs combinedly irrigates a total area of 1,46,053 ha in Pune, Ahmednagar and Solapur districts of Maharashtra, India (KIPR, 1990). The geographical location of Kukadi Irrigation Project dams and canals are shown in Figure 4.1. The salient features of

Kukadi project dams are given in Table 4.1. Dimbhe reservoir is the largest reservoir in the system having a high live storage followed by Manikdoh. These two reservoirs get maximum inflow and significantly contribute to the water transfer in the system. The Wadaj and Manikdoh are just sufficient reservoirs. Yedgaon is comparatively smaller capacity reservoir having a storage lesser than Dimbhe and Manikdoh, however it has an area about 60% of the total area of KIP.

Table 4.1. Salient features of Kukadi Project dams

Details	Dimbhe	Wadaj	Manikdoh	Pimpalgaon Joge	Yedgaon	Total
River	Ghod	Meena	Kukadi	AR	Kukadi	
Gross Storage (10^6 m^3)	382.06	35.94	307.91	217.92	93.43	1037.26
Dead Storage (10^6 m^3)	28.30	2.83	19.81	125.16	14.15	190.25
Live Storage (10^6 m^3)	353.76	33.11	288.10	92.76	79.28	847.01
Irrigable Command Area (ha)	36524	3925	2265	13250	90089	146053

The schematic sketch of reservoirs and ten canals of Kukadi irrigation project are given in Figure 4.2 along with the irrigable crop area. All the four upstream reservoirs are in parallel to each other and Yedgaon is in series to all the upstream reservoir. There are about tens canals in the entire KIP system and all are contour canals. The water is transferred to the Yedgaon reservoir through canals and rivers from the upstream reservoir. The water from Dimbhe and Wadaj is transferred through canals and from Manikdoh and Pimpalgaon Joge is transferred through rivers.

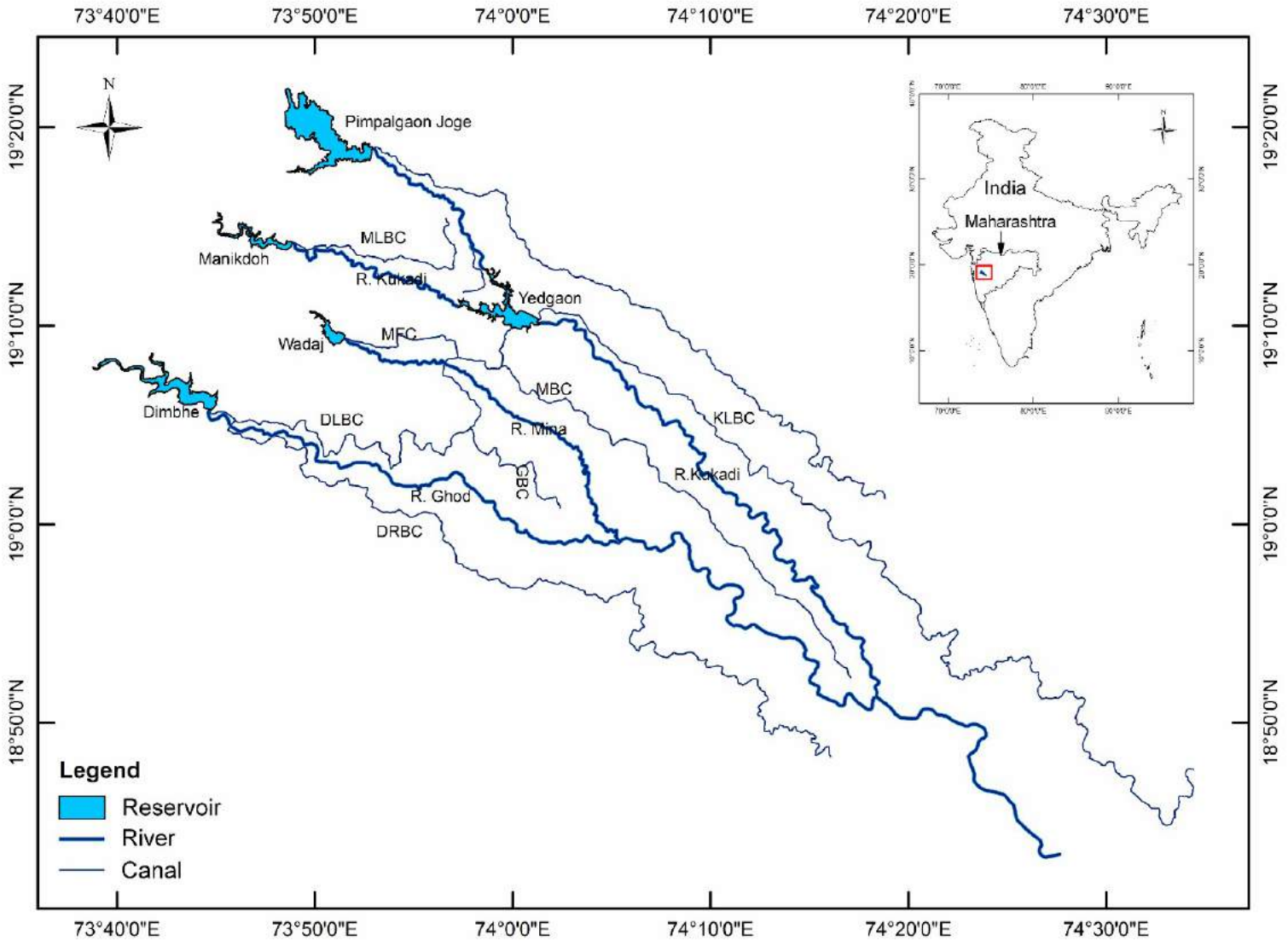

Figure 4.1. Location of KIP dams and canals

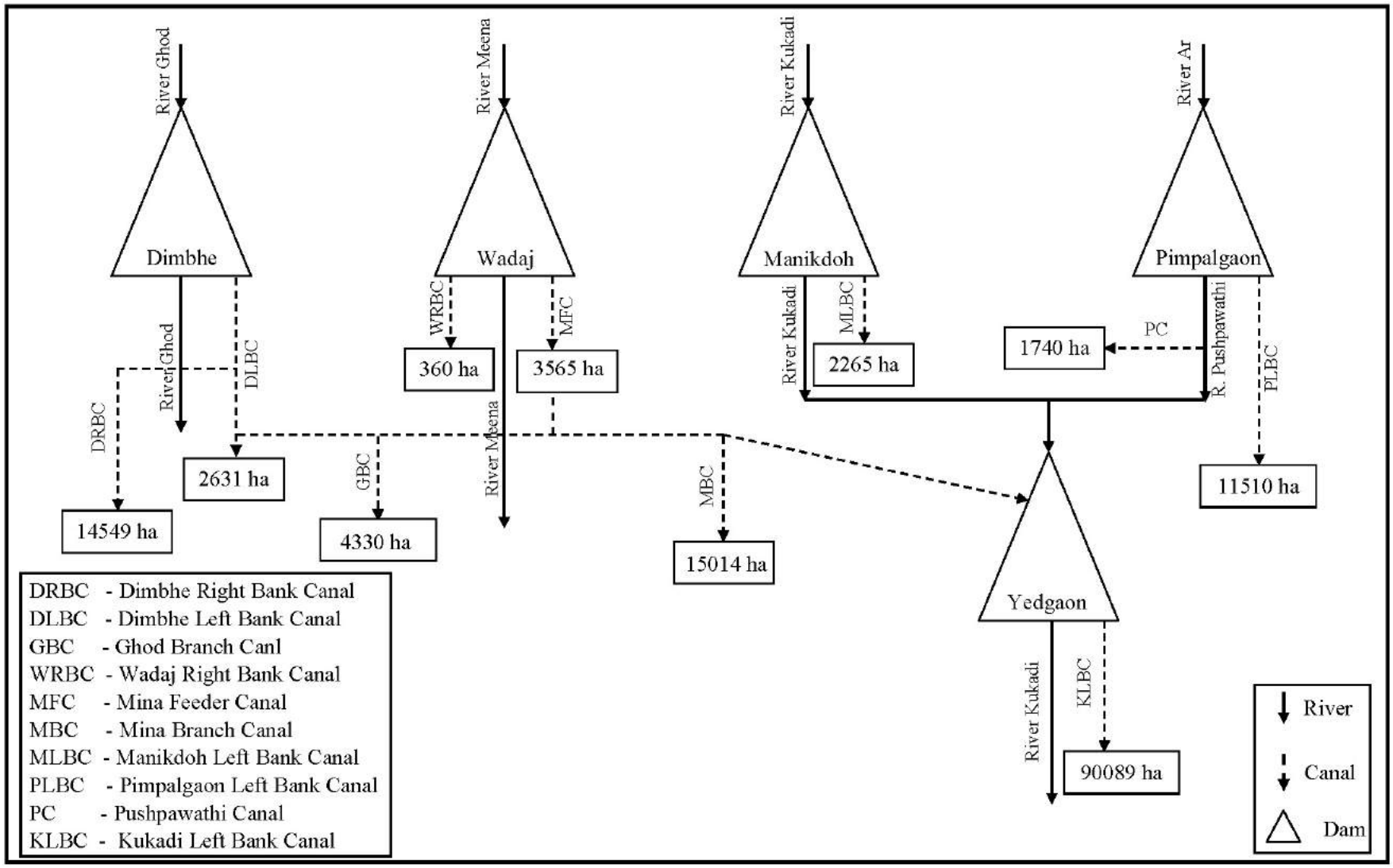

Figure 4.2. Schematic sketch of canal system of KIP

4.2.1 Dimbhe Dam

Dimbhe is a masonry dam across river Ghod near village Dimbhe with the global coordinates of 19° 6′ N latitude and 73° 43′ E longitude and impounds a gross storage of 382.22 × 10^6 m^3. Maximum height of the dam is 72.10 m. It has a spillway portion (five gates of size 12 × 8.50 m each) with a designed discharge capacity of 2122 m^3/s. The irrigable command area of Dimbhe reservoir is 36,524 ha through four canals. The Dimbhe Left Bank Canal (DLBC) takes off directly from the dam and irrigates an area of 2,631 ha. The Dimbhe Right Bank Canal (DRBC) takes off from DLBC at the third kilometre through an aqueduct across Ghod River and irrigates an area of 14,549 ha. The Ghod Branch Canal (GBC) takes off from the DLBC and irrigates an area of about 4,330 ha. The Meena Branch Canal (MBC) also takes off from DLBC and irrigates an area of about 15,014 ha. The balance available water is transferred to Yedgaon reservoir through the extended Dimbhe Left Bank Canal ending into Yedgaon reservoir.

4.2.2 Wadaj Dam

Wadaj is a composite small earth dam across river Meena, impounds a gross storage of 48.13 × 10^6 m^3. The global coordinates are 19°8′ N latitude and 73° 54′ E longitude. Maximum height is 26.42 m and length 1830 m. Its spillway has five gates of size 12 × 5 m each with designed discharge capacity of 1426 m^3/s. The Wadaj Right Bank canal (WRBC) takes off from the dam and irrigates an area of about 360 ha. The Meena Feeder Canal (MFC) takes off from the Wadaj dam and joins DLBC after irrigating an area of 3,565 ha. The length of MFC is 14 km and discharge capacity is 20.81 m^3/s. The remaining water is fed into the Kukadi Project (i.e. Yedgaon reservoir through Meena Feeder Canal). MFC takes off from left bank of Wadaj and joins DLBC before Meena branch canal. Thus, MBC receives water from both Dimbhe as well as Wadaj reservoirs.

4.2.3 Manikdoh Dam

Manikdoh is masonry dam across Kukadi river with a gross storage of 308.00 × 10^6 m^3. The maximum height of the dam, above the riverbed is 51.80 m and length of dam is 930 m. The entire storage is proposed to be utilized for irrigation through the Manikdoh Left Bank Canal (MLBC) taking off from the left bank of dam and irrigates an area of about 2,265 ha. The

remaining water is transferred to Yedgaon reservoir by letting down the water into Kukadi river through irrigation outlet and river sluice of the Manikdoh Dam.

4.2.4 Pimpalgaon Joge Dam

Pimpalgaon Joge dam is a mixed type, the main dam is of earthen type and spillway is in concrete. The dam is constructed on Ar River, a tributary of the Kukadi river near village Pimpalgaon Joge and a bund near continental divide line. It is an earthen dam, with gated spillway on left bank saddle. Maximum height of dam is 28.97 m and length is 1490 m. Pimpalgaon Joge dam has two irrigation canals, Pimpalgaon Joge Left Bank Canal (PLBC) and Pushpawathi canal (PC). The PLBC takes off directly from Pimpalgaon Joge dam and irrigates an area of 11,510 ha. The PC irrigates an area of about of 1,740 ha. The excess water is transferred to Yedgaon reservoir by letting down the water in the Pushpawathi river which joins the Yedgaon reservoir.

4.2.5 Yedgaon Dam

The Yedgaon dam is constructed across the Kukadi river at Yedgaon, with a gross capacity of 93.45×10^6 m^3. The KLBC is the main canal in the system takes off directly from the Yedgaon dam and irrigates an area of about 90,089 ha, largest area under a canal in this integrated system. The command area under KLBC is high and Yedgaon dam alone cannot satisfy the irrigation requirement. Hence, the excess water from all the upstream reservoirs is transferred to Yedgaon dam through canals and rivers to cater the irrigation needs of command area under KLBC (Siddamal and Birajdar, 2012). This shows that KLBC receives water from upstream reservoirs.

4.2.6 Data Pertaining to KIP

The data required for the study has been collected from the Office of the Executive Engineer, Kukadi Irrigation Circle 1, Naranyangaon, Maharashtra, India. The data includes salient hydraulic features of the dam and canals, reservoir inflow, evaporation losses, area-capacity-elevation table, water demand data and operational records of the reservoir. All these data are collected for eleven years from 2001 to 2012, since the last dam is completed in the year 2000. The command area details include cultivable area under each canal, type of crops grown in the command area.

The historical inflow into each reservoir of KIP is given in Figure 4.3. From the figure, it is observed that the inflow into the reservoir is intermittent and occurs only during the monsoon period every year. It is also observed that the inflow to Dimbhe and Manikdoh is comparatively higher than other reservoirs in the system.

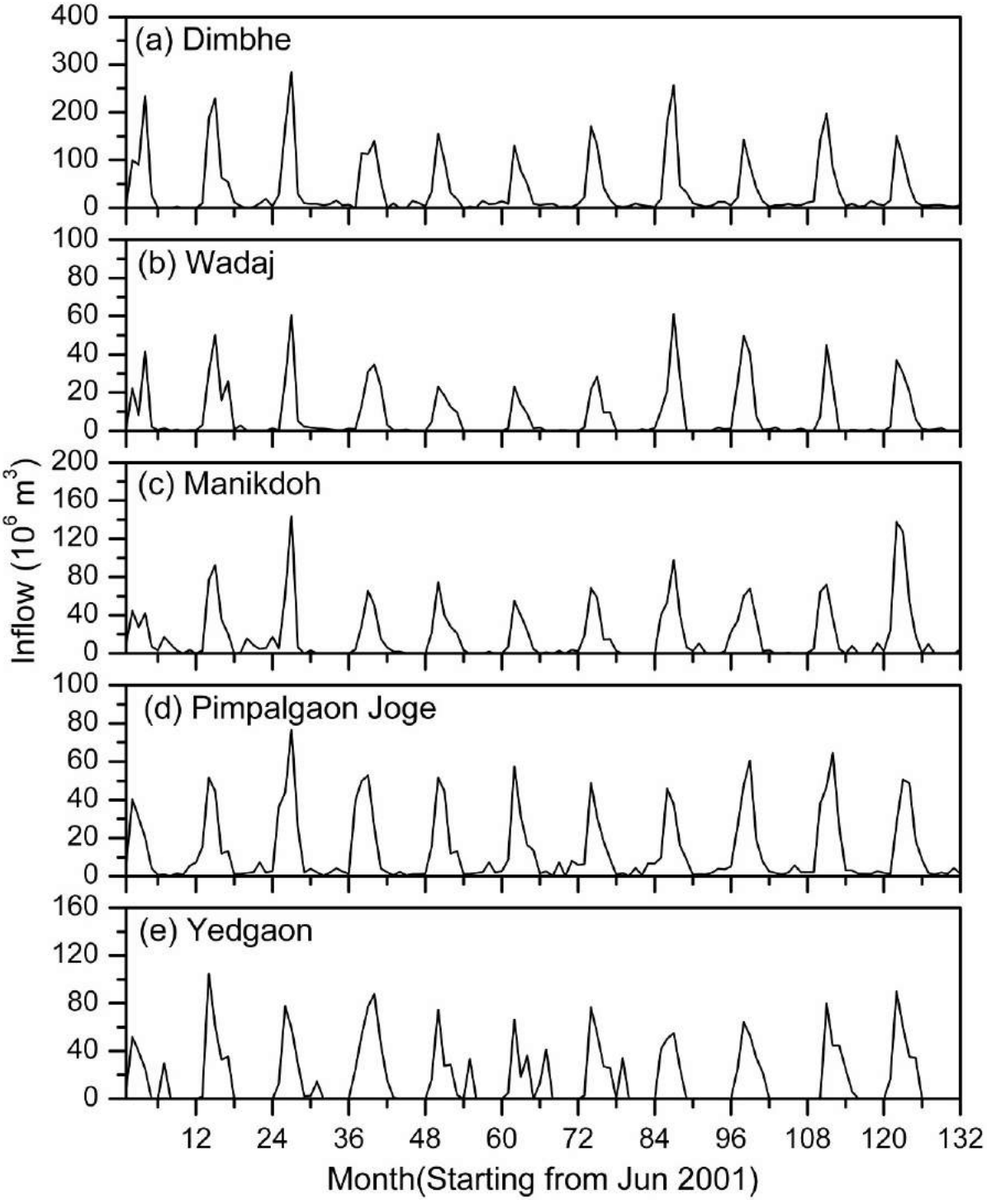

Figure 4.3. Historical monthly inflow into Kukadi project dams

4.2.7 Canal System and Existing Cropping Pattern

The particulars of canals and water requirement for each canals is given in Table 4.2. The KLBC is the longest canal in the system, followed by DRBC. The average annual rainfall in this area varies from 3810 mm to 5080 mm. The cropping pattern practiced in the Kukadi command area is given in Figure 4.4. Kharif and Rabi are the two major seasons during which crops are cultivated. During Kharif season crops such as Jowar Hybrid, Bajra Hybrid, Paddy drilled, Groundnut, Chillies, and Vegetables are grown. The major crops cultivated during Rabi season are Wheat, Jowar Local Rabi, Jowar Hybrid Rabi, Jowar Rabi (Rattoon), Peas, Vegetables/Onion and Potatoes. In the present study, the irrigation water requirement of different crops is estimated using FAO Modified Penman Method and by incorporating the transmission losses as suggested by KIPR (1990). Thus, the net water requirement at the canal head is estimated by considering the field efficiency as 65% and transmission efficiency as 75% (KIPR, 1990). It is observed that the water requirement during Rabi season is higher than Kharif season, due to non-availability of rainfall. Also, the water requirement at KLBC is much higher compared to other canals due to larger area. Hence, transfer of water from upstream reservoirs to Yedgaon reservoir is very much necessary, which makes the system complex. The net water requirements of each crop for different months are given in Table 4.3. Among Kharif crops, Paddy requires more water for irrigation. Similarly, Wheat requires more water among Rabi crops. The water requirement during the Rabi season is higher than Kharif season, particularly during the months of November and December.

Table 4.2. Particulars of canals of KIP and water requirement

Canal	Dam	Length	Canal Carrying Capacity	Irrigation Area	Water requirement at canal head*		
					Kharif	Rabi	Total
		(km)	(m^3/s)	(ha)		(10^6 m^3)	
DRBC	Dimbhe	132.00	8.42	14549.00	38.25	66.64	104.89
DLBC	Dimbhe	55.00	35.00	2631.00	6.92	10.23	17.15
GBC	Dimbhe	13.00	2.50	4330.00	11.40	16.33	27.73
MBC	Dimbhe/Wadaj	40.00	8.68	15014.00	39.45	58.32	97.77
WRBC	Wadaj	10.00	0.20	360.00	0.93	1.40	2.33
MFC	Wadaj	14.00	21.05	3565.00	9.37	13.86	23.23
MLBC	Manikdoh	23.50	1.31	2265.00	5.94	8.80	14.74
PLBC	Pimpalgaon	71.00	6.65	11510.00	30.26	44.71	74.97
PC	Pimpalgaon	16.00	0.90	1740.00	4.57	6.74	11.31
KLBC	Yedgaon	249.00	52.12	90089.00	236.73	350.00	586.73
Total		623.50		146053.00	383.82	577.03	960.85

*As per Project Design

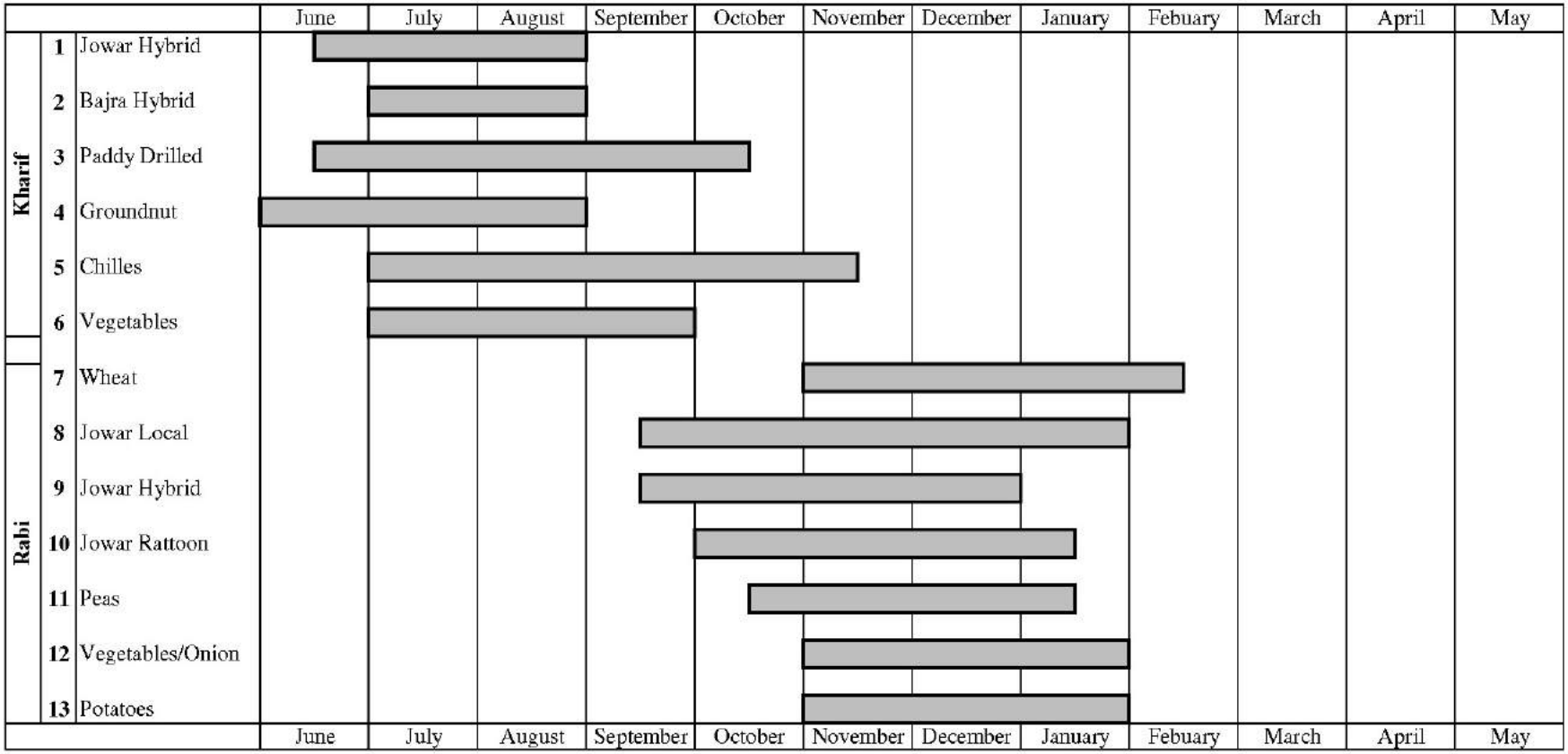

Figure 4.4. Existing cropping pattern in the command area of Kukadi Irrigation Project

Table 4.3. Net water requirement (mm) of each crop during different time period

	Crop	Jun	July	Aug	Sep	Oct	Nov	Dec	Jan	Feb	Mar	Apr	May	Total
Kharif	Jowar Hybrid	76.00	115.00	139.00	–	–	–	–	–	–	–	–	–	330.00
	Bajra Hybrid	–	162.00	84.00	–	–	–	–	–	–	–	–	–	246.00
	Paddy Drilled	100.00	165.00	147.00	106.00	27.00	–	–	–	–	–	–	–	545.00
	Groundnut	184.00	77.00	136.00	–	–	–	–	–	–	–	–	–	397.00
	Chilles	–	141.00	87.00	97.00	182.00	50.00	–	–	–	–	–	–	557.00
	Vegetables	–	96.00	101.00	79.00	–	–	–	–	–	–	–	–	276.00
Rabi	Wheat	–	–	–	–	–	149.00	176.00	242.00	113.00	–	–	–	680.00
	Jowar Local	–	–	–	16.00	90.00	165.00	206.00	124.00	–	–	–	–	601.00
	Jowar Hybrid	–	–	–	18.00	121.00	189.00	99.00	–	–	–	–	–	427.00
	Jowar Rattoon	–	–	–	–	137.00	181.00	98.00	1.00	–	–	–	–	417.00
	Peas	–	–	–	–	56.00	123.00	194.00	8.40	–	–	–	–	381.40
	Vegetables/Onion	–	–	–	–	–	130.00	156.00	211.00	–	–	–	–	497.00
	Potatoes	–	–	–	–	–	156.00	196.00	197.00	–	–	–	–	549.00
	Total	360.00	756.00	694.00	316.00	613.00	1143.00	1125.00	783.40	113.00	0.00	0.00	0.00	5903.40

4.2.8 Complexities of KIP

At the outset, KIP looks like a self sufficient system, (i.e.) inflow is more or less equal to demand. But the type of crops grown in the command area is not same as the project crop and thus the demand is increasing. Secondly, the spatial and temporal variation in the availability calls for a better optimal solution. Thus, the complexity of the KIP is such that there is a need to find intra basin temporal distribution of water availability over space. Most of the command is under KLBC due to topology. However, the water availability at Yedgaon is very less. Hence, transfer of water from other reservoirs to Yedgaon is very much need and calls for an optimal water transfer, both spatially and temporally. It is also to be taken care such that the water transfer from one reservoir should not affect the cropping area under its own command area and at appropriate time, since more water could not be stored at Yedgaon due to its smaller capacity. Altogether, the spatial and temporal water availability and multiple crops, multi-reservoir systems calls for an appropriate cropping pattern under different canals and operating policies for appropriate spatial and temporal water transfer.

4.3 Koyna Hydro Electric Project

The Koyna Hydro Electric Project (KHEP) is considered as the case study for the model having single objective optimization of a multi-reservoir system. The KHEP is located in the Sahyadri ranges of Maharashtra, India as shown in Figure 4.5. The Sahyadri ranges serves as a continental divide with 1000 m high head at Krishna river basin and suddenly tapers down to Arabian sea from peak within 50 km on Western side (Thatte, 2012). This has lead to the design and operation of KHEP by utilizing the naturally available head for hydropower production (KHEP, 2005). KHEP has four powerhouses and integrates the operation of two reservoirs, namely Koyna reservoir and Kolkewadi reservoir.

4.3.1 Koyna Dam

The Koyna Dam is one among the 23,000 large dams in the world and is situated across Koyna river with a global co-ordinate of 17°24'N latitude and 73°45'E longitude. The Koyna river is a major tributary to river Krishna. The Koyna river rises at Mahabaleshwar at an altitude of about 1,600 m above mean sea level (MSL) in Sahyadri hill range, Maharashtra

and flows north to south direction almost parallel to the Arabian Sea. The catchment is elongated, hilly with steep slopes with an area of about 891.78 km^2. The average width of the catchment is 14 km and average length is 64 km with a hill slope of 1 in 100. The average annual rainfall is around 5000 mm and this water is impounded by the Koyna Dam.

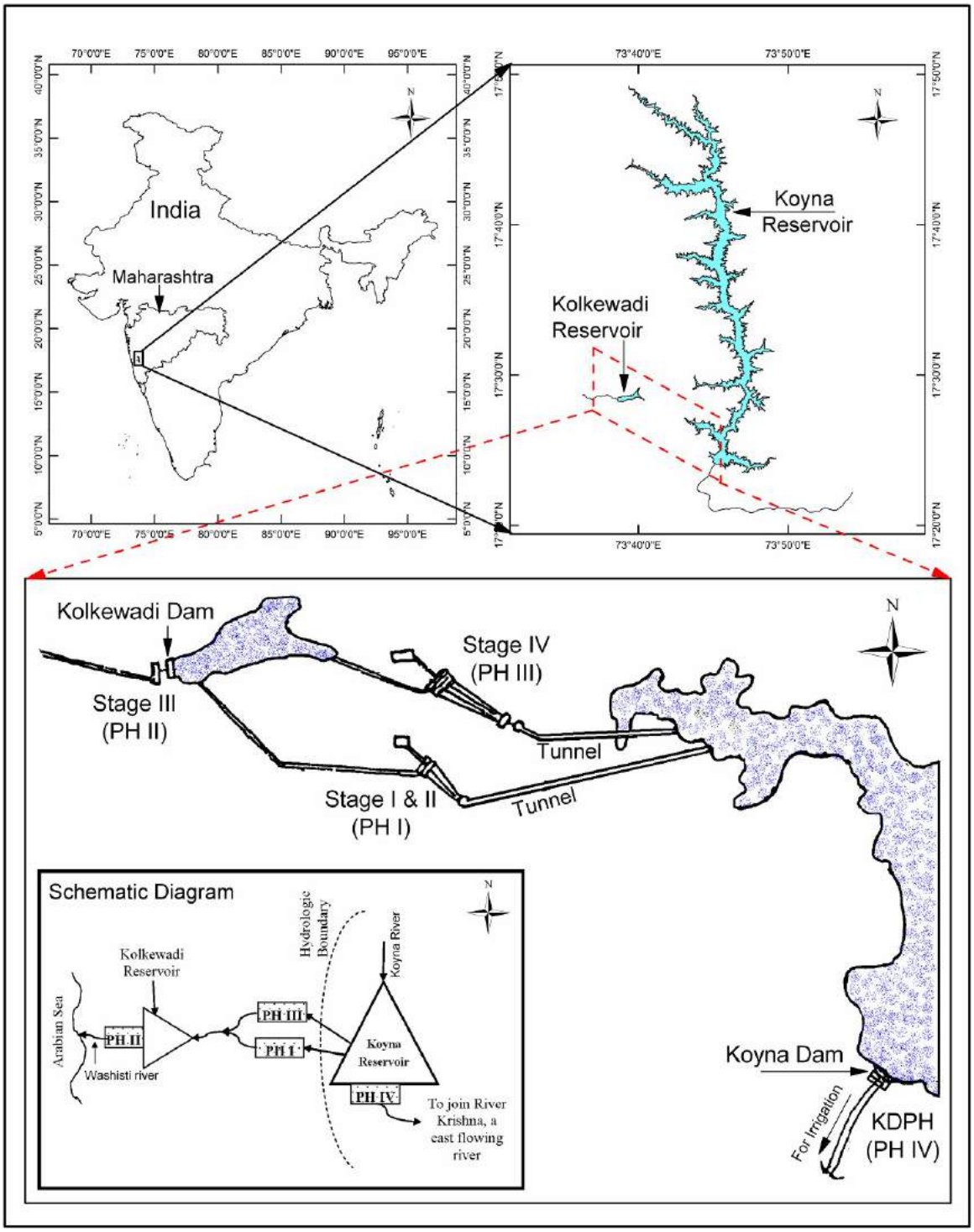

Figure 4.5. Location of KHEP and its powerhouses

The salient features of Koyna dam is given in Table 4.4. The gross storage capacity of the reservoir is 2797.40 × 10^6 m^3. The water spread area at full reservoir level is about 13% of the catchment area. The inflow to the Koyna dam is estimated based on reservoir levels and outflow (Thatte, 2012). The Koyna reservoir has three powerhouses, two on Western side, and one on Eastern side at the foot of the dam. Although Koyna dam is basically built for generating hydropower, it also serves irrigation purposes like most of the other dams in the subcontinent (Thatte, 2012). The periodically release of water (usually twice in a month) from the Koyna reservoir made the Koyna as a perennial river, whereas its tributaries are mostly ephemeral (Naik *et al.*, 2001). Thus, various lift irrigation schemes have been developed along the Koyna river and sugarcane is the main crop cultivated in the area. Other crops grown include upland paddy, sorghum, wheat and pulse. The irrigation releases are on the Eastern side of the reservoir, which has fertile land as compared to barren exposed rock covers, and undulating terrain on Western side, where the major powerhouses are located.

4.3.2 Kolkewadi Dam

The Kolkewadi dam is located in the Konkan region of Maharashtra, India with global co-ordinates of 17.29°N and 73.39°E. The salient features of Kolkewadi dam is given in Table 4.4. The length of the dam is 497 m and height is 66.3 m. The gross storage capacity of Kolkewadi reservoir is 36.22 × 10^6 m^3 and the net storage is 11.22 × 10^6 m^3 (KHEP, 2005). The average annual rainfall near the dam site is about 4000 mm in the catchment area of about 25.40 km^2. However, the Kolkewadi reservoir receives most of its inflow from tail water of powerhouse of Koyna reservoir and regulates the flow to another powerhouse (PH III). The discharge from PH III joins the Washisti river and finally confluences with the Arabian sea through Boladwadi nalla.

4.3.3 Powerhouses of KHEP

The KHEP has four powerhouses and their details are given in Table 4.5. The locations of the powerhouses are given in Figure 4.5. The Koyna stage – I was the first station with 4 × 70 MW capacity. The second stage with a capacity of 4 × 80 MW was designed with the same head works. Thus, the headrace tunnel, surge well pressure shafts and tailrace are common for these two stages and hence both Stage I and Stage II is together referred as PH I.

Table 4.4. Salient features of Koyna and Kolkewadi Dams

Details	Koyna Reservoir	Kolkewadi Reservoir
River	Koyna	Boladwadi Nalla
Purpose	Hydropower and partly for Irrigation	Hydropower
Catchment area (km^2)	891.78	25.40
Length of Dam (m)	807.72	497.00
Gross Storage (10^6 m^3)	2797.40	36.22
Net Storage (10^6 m^3)	2652.40	11.22
Dead Storage (10^6 m^3)	145.00	25.00
Water Spread at FRL (km^2)	115.35	1.67
Maximum Height above river bed (m)	85.35	56.80
Maximum Height above foundation (m)	103.02	66.30
MWL (KRL) (m)	659.90	137.16
FRL (KRL) (m)	657.90	135.40
MDDL (KRL) (m)	609.60	130.10
KRL – Koyna Reduced Level, KRL = MSL + 9.43 m		

The stage – IV (henceforth referred as PH III) is the major powerhouse in KHEP with a capacity of 1000 MW and is also on the Western side of the reservoir. The water released through tailrace from PH I and PH III is collected in a pickup dam named Kolkewadi reservoir which acts as balancing reservoir to maintain head Stage III of KHEP. The Stage III at Kolkewadi dam is having a capacity of 4 × 80 MW (hereafter Stage III is referred as PH II). The Koyna Dam Power House (KDPH) (hereafter referred as PH IV) was constructed with a capacity of 2 × 20 MW to utilize the head available in the reservoir and to generate hydropower through irrigation releases and further flow towards Eastern side to join river Krishna. It is worth mentioning that irrigation releases through PH IV flows East side of the dam, the flow from PH I, PH II and PH III flow towards Western side of the dam and confluences in the Arabian Sea without any further utilization. The full installed capacity of all the powerhouses supplying base power in the grid is not sufficient to cope up with the peak demand of Maharashtra during morning and evening peak hours of every day. Hence, the demands during peak hours are satisfied by converting the hydropower stations into peaking stations (Thatte, 2012). All the powerhouses in the system are peak stations and are operated only for producing the peak demands. However, the power production at the dam foot powerhouse (PH IV) is incidental, which generates hydropower only through irrigation releases.

Table 4.5. Details of powerhouses of KHEP (Jothiprakash and Arunkumar, 2014)

Powerhouses	Stages I & II (PH I)		Stage III (PH II)	Stage IV (PH III)	KDPH (PH IV)
Dam	Koyna		Kolkewadi	Koyna	Koyna
No. of Turbines	4 + 4		4	4	2
Headrace tunnel Length (m)	748		4,351	4,225	–
Maximum discharge (m^3/s)	164.00		170.00	260.00	67.96
Design head (m)	475	490	109.70	500.00	59.00
Generator (MW)	280 (4 × 70)	320 (4 × 80)	320 (4 × 80)	1000 (4 × 250)	40 (2 × 20)
Speed (rpm)	300	375	214	375	250

4.3.4 Data Pertaining to KHEP

The data pertaining to KHEP has been collected from the Sub-divisional Engineer office, Koyna Dam Maintenance section, Koyna Nagar and Kolkewadi Dam Maintenance section, Alore, Maharashtra, India. The data such as reservoir details, working table of the reservoir, catchment details, various demand details, powerhouse details and reservoir operation policies were collected from Irrigation Department, Koyna Dam Circle, Pune, Maharashtra, India. The historical monthly inflow into Koyna and Kolkewadi reservoir is given in Figure 4.6. Figure 4.6(a) shows the historical observed monthly inflow time series to the Koyna reservoir for 49 years from 1961. It is observed there is a cyclic pattern in the observed data. A maximum inflow of 6748.37×10^6 m^3 has been observed during the year 2005. The average annual inflow in to Koyna reservoir is estimated as 4172.06×10^6 m^3 over the 49 years data. Figure 4.6(b) shows the historical observed monthly inflow time series to the Kolkewadi reservoir. The average annual monthly inflow in to Kolkewadi reservoir is 9.69×10^6 m^3. Both the reservoirs are intermittent in nature and receive inflow during monsoon periods only.

The historical end month storage level of Koyna reservoir is given in Figure 4.7. It is found that there is large variation in storage level over the period of time. Initially, the storages are very less and over the period of time, Koyna reservoir attained maximum storage levels frequently. It is also evident from the figure that the reservoir has reaches the minimum storage level during very few months. It is observed that the storage is very high during recent time period, continuously reaching the maximum storage level every year. Thus, the reservoir is always maintained at high storage levels.

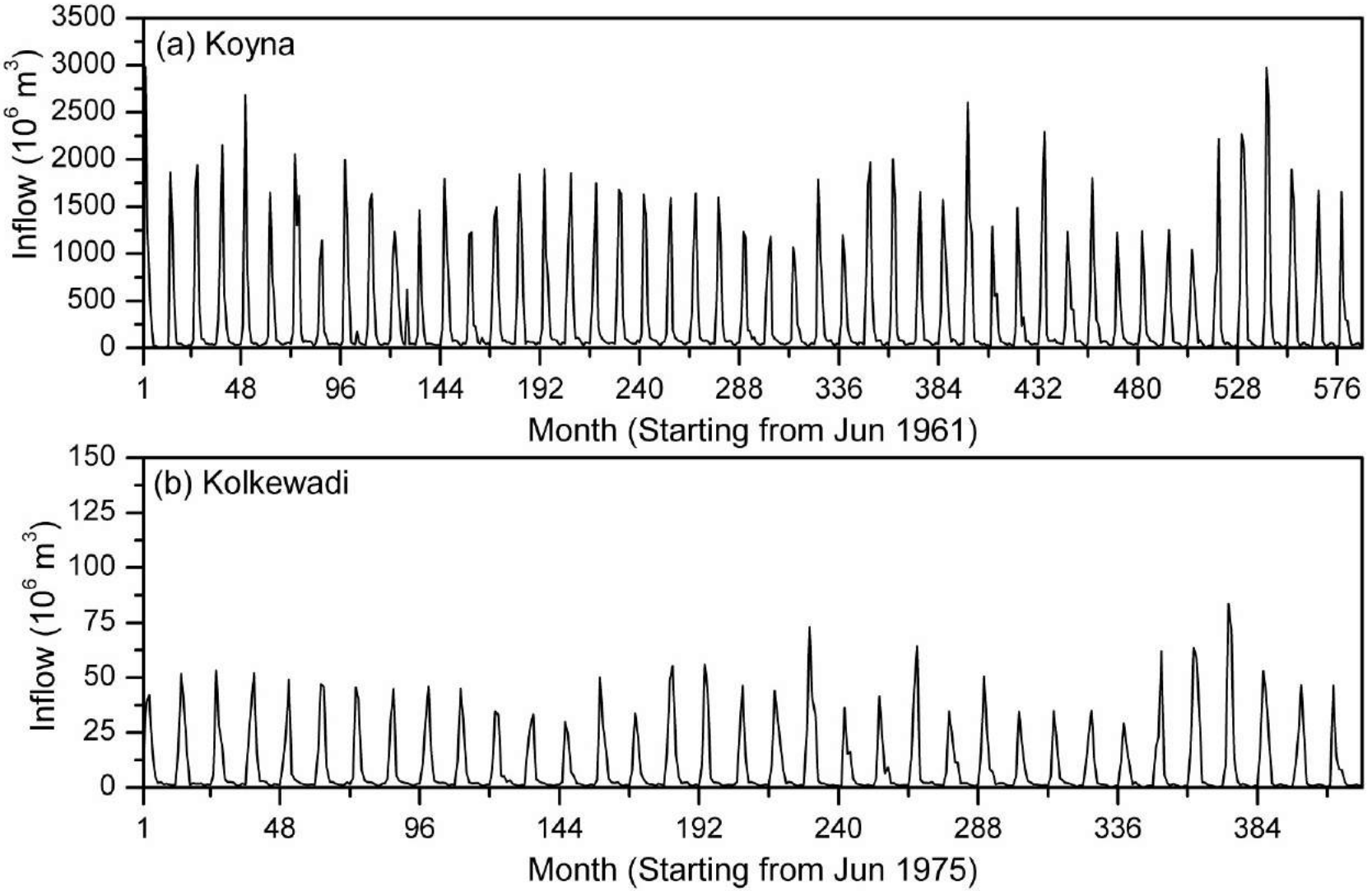

Figure 4.6. Historical monthly inflow into (a) Koyna reservoir and (b) Kolkewadi reservoir

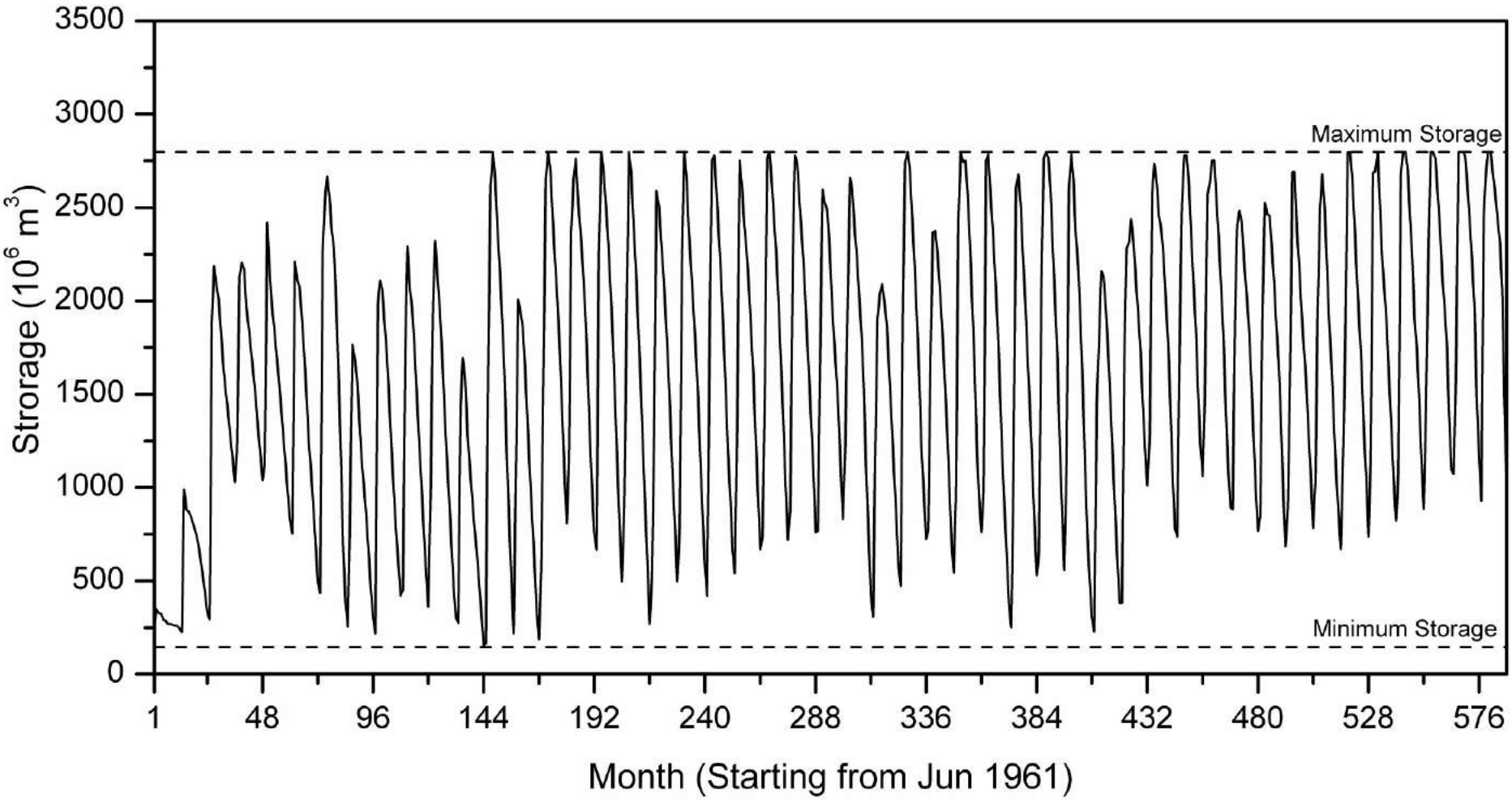

Figure 4.7. Historical end month storage of Koyna reservoir

4.3.5 Complexities in the KHEP System

Usually, hydropower releases are termed as non-consumptive, since the water can be used for some other purpose after power generation, mostly for irrigation. However in KHEP, the releases to major powerhouses and irrigation are in the opposite direction which makes the operation of the system very complex. Also, the water diverted to the major powerhouses (Western side) will never meet back the originated river. This means that the water diverted for hydropower production never meets Krishna river, but are let into Arabian sea. Diverting large quantity of water to the major powerhouses on the Western side of the reservoir resulted in serious disputes among different stakeholders, especially from Eastern side. Thus, Krishna Water Dispute Tribunal (KWDT) was constituted to resolve the water sharing disputes in Krishna basin and has issued order in sharing the maximum water to hydropower generation and irrigation from Koyna reservoir. Since, the power releases and irrigation releases are separate and in opposite direction, the KWDT limited the diversion of large quantity of water towards the Western for power production (KWDT, 2010). Apart from this sociological issue, there also exist conflicts among the powerhouses, since they are located at different levels and have different capacity of power generation. The same quantities of releases to different powerhouses will produce varying hydropower due to varying net head and capacity. Thus, there is a need to optimally utilize the available water both for hydropower generation and irrigation for maximizing their benefits.

4.4 Closure

In this chapter the details of the study area, Koyna Hydro Electric Project and Kukadi Project are given. Koyna hydroelectric project is one the major hydroelectric project of India. It caters the peak power demand need of Maharashtra state. Kukadi project is one of the major irrigation projects of Maharashtra state. It comprises the integrated operation of five reservoirs. Thus, these study area are having greater importance in their specific purposes. Hence, there is much scope to optimize the operation of these reservoirs.

Chapter 5

Single and Multi-Reservoir Inflow Prediction Model

5.1 Kukadi Irrigation Project

Multi-reservoirs located in the upper reaches of the Bhima river basin have been studied for concurrent forecasting of future inflows for both full year and seasonal conditions. The models are developed using common time period of data; because the reservoirs are constructed and started operating at differ time periods. Initially, conventional as well as AI techniques are applied to predict inflow into each reservoir independently. Secondly, conventional stochastic and ANN models are developed for multi-variate predictions into the multi-reservoirs concurrently without considering the exogenous inputs like upstream releases, surplus and import from adjacent watershed. This multi-reservoir system imports water from adjacent watersheds during Kharif and Rabi seasons which are considered in the final part of the study for concurrent predictions into the reservoirs. Model Tree (MT) and Genetic Programming (GP) techniques are not applied to these multi-variate concurrent predictions due to inherent limitations.

All the models are developed using daily data except stochastic concurrent model. The conventional stochastic modelling is limited to monthly inflow data series, because for daily data it is felt increasingly difficult to manage the curse of dimensionality. Yedgaon reservoir is the distribution reservoir from where all the demands are met. Thus, apart from one-day-ahead prediction, multi-time-step-ahead prediction is also attempted for this reservoir. The

concurrent prediction of inflows into the multi-reservoirs including multi-step-ahead prediction for Yedgaon reservoir is the major aim of this part of study.

5.1.1 Multi-reservoir System Considering Each Reservoir Independently

Fairly large amount of research has been reported on application of conventional stochastic and AI techniques for a single reservoir system without explicitly indicating whether the case study reservoir considered is reservoir in series or in parallel, imports water from adjacent watersheds or receives surplus from adjacent watersheds. Thus, as a first step in this multi-reservoir case study, all the three reservoirs are considered as individual reservoir system and conventional stochastic model and AI techniques are applied to predict the future inflows into each reservoir separately. The daily time series data available for Manikdoh, Pimpalgaon Joge and Yedgaon reservoirs are 1st June 1985 - 31st May 2008, 1st June 2000 - 31st May 2008 and 1st June 1977 - 31st May 2008 respectively. Since the data available is for different time periods, the common time period data availability from 1st June 2000 - 31st May 2008 is considered for modelling. Thus the total length of daily data used is for 8 years. For this data length, different modelling techniques such as stochastic and AI techniques like ANN, MT and GP are applied. The raw data has not performed better and hence data scaling, normalization and transformations such as logarithmic, exponential and square root are tried. The performance is found to be poor which may be due to large length of zero values in the data set, large variation in observed data points and also may be due to lack of pattern in the inflow of the reservoir in series. For daily inflow data series, the data pre-processing in the form of moving average (MA) (window, k = 3) performed exceptionally better and hence the same data pre-processing technique is used in the multi-reservoir study also. Out of 8 years of inflow data 70% (1937) of data is used for training and 30% (831) is used for testing for all the techniques. Three separate daily inflow prediction models (one for each reservoir) are built with full year and seasonal data to predict next days' inflow for each inflow series.

5.1.1.1 Auto Regressive Integrated Moving Average (ARIMA) Model

Multi-reservoir prediction is first dealt by considering each reservoir system as an individual system by developing three different models for bench marking purpose. Daily full year and seasonal models are evolved for the reservoirs using ARIMA modelling approach. Standard evaluation measures are then assessed for better model in each category and shown in Table 5.1. The table indicates that ARIMA(2,1,2) and ARIMA(1,1,1) are the better models for pre-

processed full year data and seasonal data respectively. It is found that the performance of the models are poor indicating that efficient modelling approach is required for daily inflow predictions into independent reservoir system.

Table 5.1. Summary of performance of independent daily ARIMA models with data pre-processing during training and testing period

Phase	Error criteria	ARIMA(2,1,2) model with full year data			ARIMA(1,1,1) model with seasonal data		
		Manikdoh	Pimpalgaon Joge	Yedgaon	Manikdoh	Pimpalgaon Joge	Yedgaon
Training	MSE, 10^{12} m^6	4.632	5.259	4.392	4.224	3.406	3.277
	MAE, 10^6 m^3	1.155	1.500	1.278	1.003	0.774	0.530
	R	0.650	0.672	0.664	0.712	0.658	0.731
	AIC	5599	5380	6480	3944	4137	5135
Testing	MSE, 10^{12} m^6	5.647	6.037	5.392	5.224	5.236	5.237
	MAE, 10^6 m^3	4.155	3.590	3.278	2.130	2.174	1.210
	R	0.502	0.534	0.571	0.662	0.658	0.671
	AIC	5305	5017	5744	5303	6020	5737

5.1.1.2 ANN Model

The same pre-processed data series for same number of inputs used in ARIMA model has been used in AI models also. A simple MLP model is first developed for full year and seasonal data by optimizing hidden nodes while training the network with BP algorithm and hyperbolic-tangent as transfer function. The network is trained for several epochs for achieving best performance. The dynamic time tagged recurrent network (TLRN) has exhibited good performance for daily data and is thus tried in this case. The summary of best ANN model for full year and seasonal data showing various performance measures is displayed in Table 5.2 during training and testing.

For full year data, MLP ANN(2-2-1) has shown better performance for Pimpalgaon Joge and Yedgaon reservoir inflow prediction with R = 0.771 and 0.899 respectively during testing,

while, TLRN has modelled Manikdoh reservoir with R = 0.660 much inferior to the seasonal data models. Seasonal data ANN(2-2-1) model trained with TLRN with 2 inputs having gamma memory structure displayed good error statistics for Manikdoh, Pimpalgaon Joge and Yedgaon reservoirs with R = 0.954, 0.971, 0.960 respectively during testing of the network. Considering all the performance measures including MSE = 0.708, 0.452, 0.730 and MAE = 0.514, 0.465, 0.689, the seasonal data model performance is better than full year data model performance, thus it can be seen that the large number of zero inflow values in full year could not be modelled better even with sophisticated TLRN network using MA data pre-processing. The next AI technique of MT is then tried in order to improve the performance, especially for the full year data.

Table 5.2 Summary of performance of independent daily ANN models with data pre-processing during training and testing period

Phase	Error criteria	ANN(2-2-1) models with full year data			ANN(2-2-1) models with seasonal data		
		Manikdoh (TLRN)	Pimpalgaon Joge (MLP)	Yedgaon (MLP)	Manikdoh (TLRN)	Pimpalgaon Joge (TLRN)	Yedgaon (TLRN)
Training	MSE, 10^{12} m^6	2.218	0.794	1.521	0.554	0.494	0.958
	MAE, 10^6 m^3	0.718	0.378	0.792	0.515	0.494	0.752
	R	0.751	0.902	0.914	0.972	0.971	0.972
Testing	MSE, 10^{12} m^6	2.182	3.098	0.924	0.708	0.452	0.730
	MAE, 10^6 m^3	0.635	0.427	0.670	0.514	0.465	0.689
	R	0.660	0.771	0.899	0.954	0.971	0.960

5.1.1.3 Model Tree (MT) Model

The MT models developed are pruned and smoothed till SDR reduced substantially. The summary of best MT models for full year and seasonal data during training and testing is displayed in Table 5.3. With 2 antecedent inflow series i.e. MT 2 model with 2 input data has shown improved performance over ANN model for full year data (R = 0.910, 0.880, 0.936, MSE = 0.699, 1.341, 0.602 and MAE = 0.198, 0.278, 0.306) whereas seasonal MT 2 model

has not shown any improvement over ANN model. The higher MSE values indicate that the peak inflows are not captured by MT 2 model for seasonal data. However, the MT 2 model has improved the performance of full year data over the corresponding ANN model.

Table 5.3 Summary of performance of independent daily MT models with data pre-processing during training and testing period

Phase	Error criteria	MT 2 models with full year data			MT 2 models with seasonal data		
		Manikdoh	Pimpalgaon Joge	Yedgaon	Manikdoh	Pimpalgaon Joge	Yedgaon
Training	MSE, 10^{12} m^6	0.516	0.523	0.990	0.939	1.320	1.295
	MAE, 10^6 m^3	0.234	0.250	0.399	0.415	0.507	0.487
	R	0.949	0.939	0.943	0.958	0.920	0.925
Testing	MSE, 10^{12} m^6	0.699	1.341	0.602	1.994	1.501	1.295
	MAE, 10^6 m^3	0.198	0.278	0.306	0.455	0.456	0.487
	R	0.910	0.880	0.936	0.878	0.913	0.925

5.1.1.4 LGP Model

To achieve higher accuracy in peak inflow prediction, the well-proven GP modelling technique is taken up for independent reservoir inflow prediction for full year and seasonal data. LGP 2 model with 2 inputs has resulted in the best performance measures, R is ranging from 0.957 to 0.979, MSE and MAE is in the range of 0.167 to 0.509 and 0.169 to 0.428 respectively. All the statistics displayed in Table 5.4 are best for LGP 2 model as compared to ANN and MT models.

Time series and scatter plot during testing for LGP 2 model, which exhibited best results for full year and seasonal data for the three reservoirs, is shown in Figure 5.1(a) – (f) and Figure 5.2(a) – (f) respectively. From Figure 5.1 and Figure 5.2 it is very clear that whether the data is full year or seasonal, LGP 2 model is performing better and it can be clearly seen that even though there is a pattern in Manikdoh and Pimpalgaon Joge reservoirs, there is a changing

pattern for controlled inflow into Yedgaon reservoir. However, the LGP model has predicted even this data also accurately for all magnitudes of observed inflows.

Table 5.4 Summary of performance of independent daily LGP models with data pre-processing during training and testing period

Phase	Error criteria	LGP 2 models with full year data			LGP 2 models with seasonal data		
		Manikdoh	Pimpalgaon Joge	Yedgaon	Manikdoh	Pimpalgaon Joge	Yedgaon
Training	MSE, 10^{12} m^6	0.176	0.212	0.692	0.378	0.439	0.930
	MAE, 10^6 m^3	0.205	0.226	0.358	0.336	0.354	0.571
	R	0.983	0.976	0.961	0.981	0.975	0.973
Testing	MSE, 10^{12} m^6	0.167	0.294	0.414	0.325	0.381	0.509
	MAE, 10^6 m^3	0.169	0.270	0.273	0.301	0.297	0.428
	R	0.977	0.976	0.957	0.979	0.975	0.970

Even though there is inter-dependency among the reservoirs and the time step considered is short, AI models have predicted better. From the results, it is found that LGP model has performed exceptionally better for different reservoirs at different time steps. It is to be remembered that data pre-processing plays a vital role in achieving the good performance. Thus, it may be concluded that if the time step is shorter (daily), LGP 2 model with data pre-processing technique may be used in real life rather than stochastic and other AI techniques such as ANN and MT.

The results of independent AI models are convincing from the point of view of individual dam authority. However, regional water manager in a reservoir system is more concerned about concurrent inflow prediction. Thus the second case is of concurrent inflow prediction without considering the exogenous inputs.

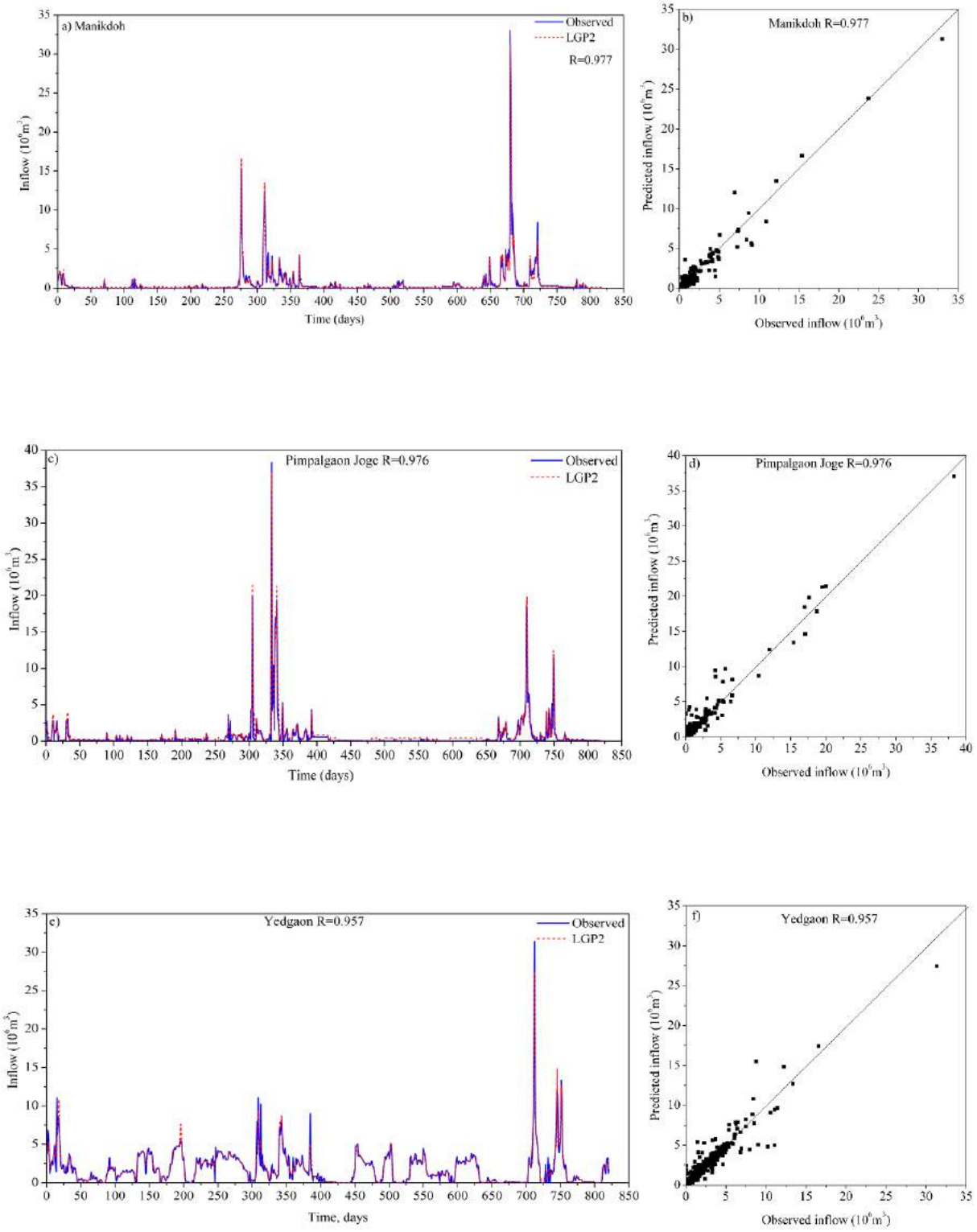

Figure 5.1(a) – (f) Time series and scatter plot of independent daily full year LGP 2 model during testing period

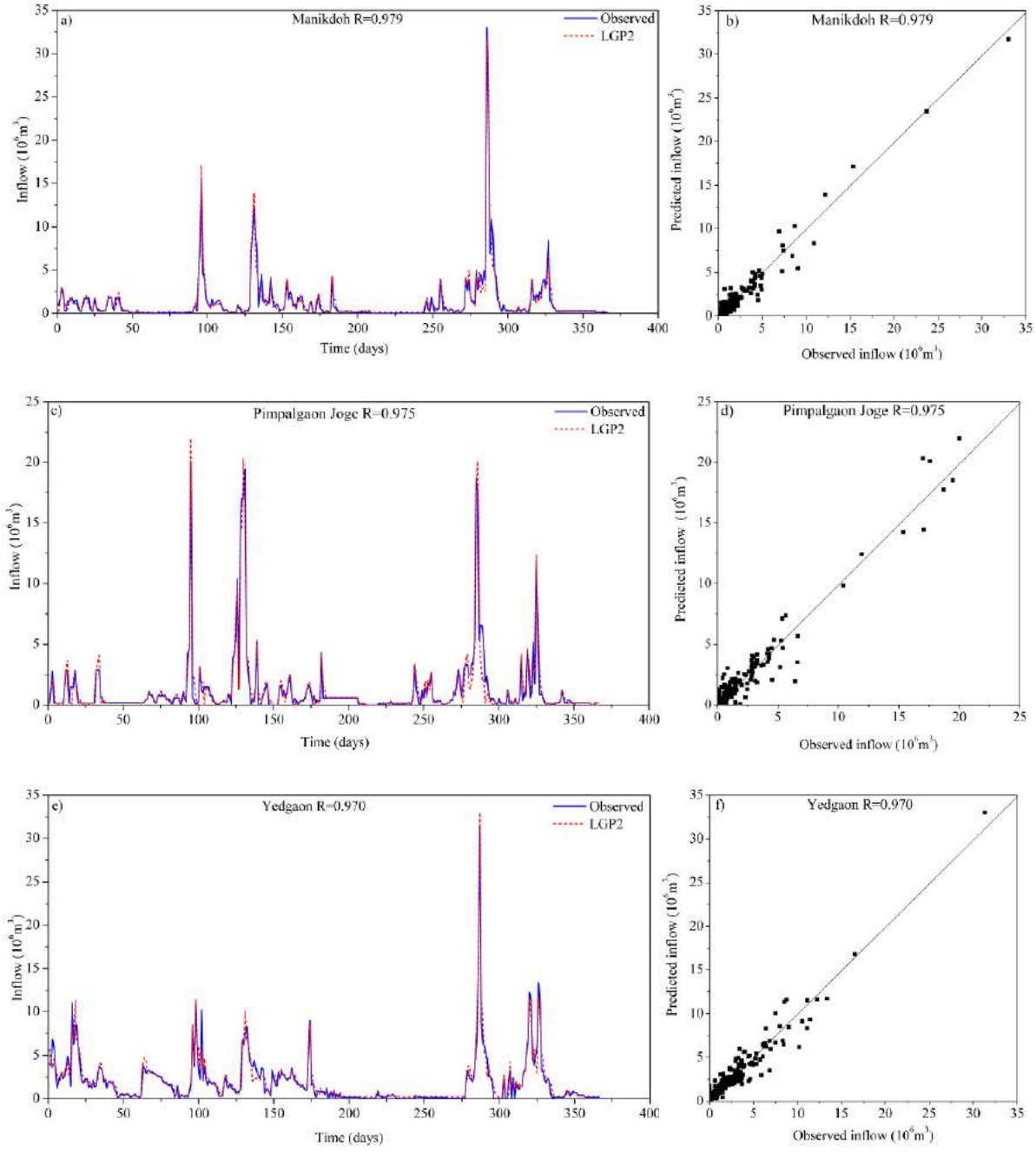

Figure 5.2(a) – (f) Time series and scatter plot of independent daily seasonal LGP 2 model during testing period

5.1.2 Concurrent Multi-reservoir Model without Exogenous Inputs

As a second case, the concurrent inflow prediction into multi-reservoirs are aimed at by considering only antecedent inflow into the reservoir and without considering exogenous inputs (upstream releases and import from nearby watersheds). In this case, concurrent inflow prediction with stochastic AR(p) model could not be carried out for daily time step due to the

curse of dimensionality. In daily ANN models: concurrent multi-reservoir inflow case, a multi-input multi-output (MIMO) structured ANN model has been developed using monthly as well as daily inflow data and are discussed. In this modelling, tri-variate time series corresponding to the three reservoirs are analysed utilizing their interdependences for one-step-ahead forecast.

5.1.2.1 Concurrent Monthly Full Year Stochastic AR(p) Model

The AR(p) models up to p = 10 are developed for monthly full year data to predict multi-reservoir inflows. Summary of the performances of four AR(p) models are presented in Table 5.5. It is noticed that all the models showed very poor predictions, some models have shown negative correlation thereby indicating the in-capabilities in modelling complex multi-reservoir monthly data by AR(p) models. However, AR(5) model showed slightly better prediction, and the scatter plot of the observed and predicted inflows into the three reservoirs is displayed in Figure 5.3(a) – (c). The data points available for modelling full year inflow for a period of 8 years is very less (96). This may be another reason for poor performance of the AR(p) model. The seasonal data points are still less i.e. only 40 data points in the inflow series. Therefore, the concurrent monthly seasonal inflow prediction could not be carried out. In order to model the monthly data better the non-linear ANN technique is attempted.

Table 5.5 Summary of performance of concurrent monthly full year AR(p) models during testing period

Model	Manikdoh			Pimpalgaon Joge			Yedgaon		
	MSE, 10^{12} m^6	MAE, 10^6 m^3	R	MSE, 10^{12} m^6	MAE, 10^6 m^3	R	MSE, 10^{12} m^6	MAE, 10^6 m^3	R
AR(1)	2085	21.143	-0.046	4057	32.891	0.013	8280	68.605	0.111
AR(2)	2036	19.41	-0.08	3984	31.386	-0.077	7542	64.294	0.281
AR(5)	1850	4.97	-0.167	3449	19.323	-0.064	4402	33.234	0.394
AR(8)	5315	-39.251	-0.119	7373	-21.103	-0.135	14393	-73.906	-0.201

5.1.2.2 Concurrent Monthly Full Year ANN Model

Concurrent ANN prediction models for transformed monthly full year data are developed using MLP network. Predictive capability of TLRN with different memory structures is checked for the complex data series as the standard MLP has shown poor predictions.

Initially, all the models are developed with antecedent inflow into the three reservoirs as the input. Thus, ANN models with multiples of three input nodes indicate that there are no exogenous inputs. However, the performances are poor. In order to improve the performance, the river releases from upstream reservoirs are added as the inputs. Thus ANN model with sum of multiples of 3 and multiples of 2 is the number of nodes used in the input layer. Monthly seasonal models are not developed due to less number of data points for model training and testing. The model was trained using 70:30% of data length for training and testing monthly data sets. ANN architecture for feed forward MLP and feed back TLRN with one or more hidden layers and varying number of nodes are developed.

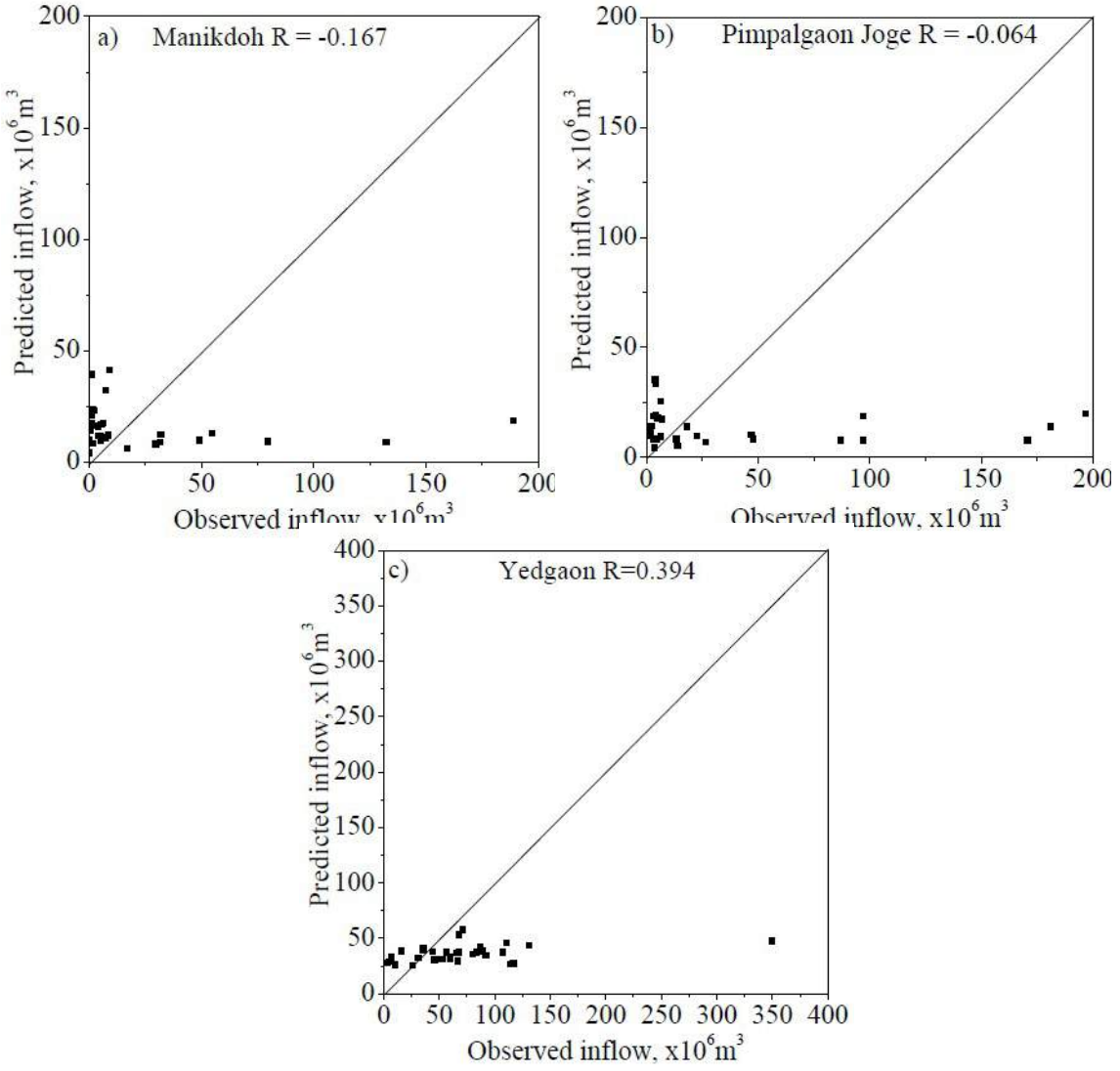

Figure 5.3 (a) – (c) Scatter plots of concurrent monthly full year stochastic AR(5) model during testing period

The effect of hidden neurons in the network is identified by various trials. Number of training cycles is varied from 1000 to 30,000 in order to achieve better results. The ANN configuration which has resulted in minimum MSE is selected for further model evaluation. As stated earlier, TLRN which is better suited for time series prediction has exhibited better error statistics as compared to standard MLP networks. The performance measures for the better models resulting from logarithmic-transformed data are summarized in Table 5.6.

Table 5.6 Summary of performance of concurrent monthly full year ANN models with data-transformations during testing period

Model	Manikdoh			Pimpalgaon Joge			Yedgaon		
	MSE, 10^{12} m^6	MAE, 10^6 m^3	R	MSE, 10^{12} m^6	MAE, 10^6 m^3	R	MSE, 10^{12} m^6	MAE, 10^6 m^3	R
ANN(10-4-3) {MLP}	3113	30.654	0.325	5265	42.768	0.215	5302	52.996	0.277
ANN(7-4-4-4-3) {TLRN with time delay memory}	975	21.335	0.747	1613	24.963	0.694	2265	32.376	0.602
ANN(8-4-4-3) {TLRN with time delay memory}	1144	22.694	0.756	1845	23.987	0.642	2866	35.517	0.476
ANN(7-6-4-3) {TLRN with time delay memory}	896	21.077	0.704	1855	25.29	0.630	2259	32.135	0.623
ANN(5-4-4-3) {TLRN with time delay memory}	1196	22.716	0.718	1764	26.552	0.705	2410	31.421	0.575
ANN(10-4-3) {TLRN with time delay memory}	3190	31.842	0.276	5523	44.137	0.131	5999	52.053	0.182
ANN(10-4-3) {TLRN with time delay memory}	1967	30.913	0.456	3211	35.962	0.362	2897	32.618	0.454
ANN(15-10-3) {TLRN with time delay memory}	2492	33.328	0.366	4624	49.785	0.193	6156	57.255	0.203
ANN (15-15-3) {TLRN with gamma memory}	1311	25.34	0.779	3558	38.50	0.495	7835	67.59	0.266
ANN(15-15-3) {TLRN with Laguerre memory}	1896	23.265	0.785	2727	36.129	0.582	5669	57.377	0.382

One can observe that only TLRN with time delay memory structure could capture the pattern in the observed inflows. All these models are similar and perform satisfactorily. Concurrent predictions for the three reservoirs with ANN(7-6-4-3) model exhibited better correlation with the observed series 0.704, 0.630 and 0.623 respectively. Seven input variables and two to three hidden layers with few hidden nodes are required to learn the complex and non-linear observed data sets. The other statistics are also close to the best statistics. This model has 3 inflows and 2 lag upstream releases as the input. In continuation with the model selection, scattered plots of the predicted inflows with the corresponding observed series are displayed for each reservoir in Figure 5.4. From Figure 5.4 it can be seen that ANN model is also poorly performing with full year data, except Manikdoh reservoir.

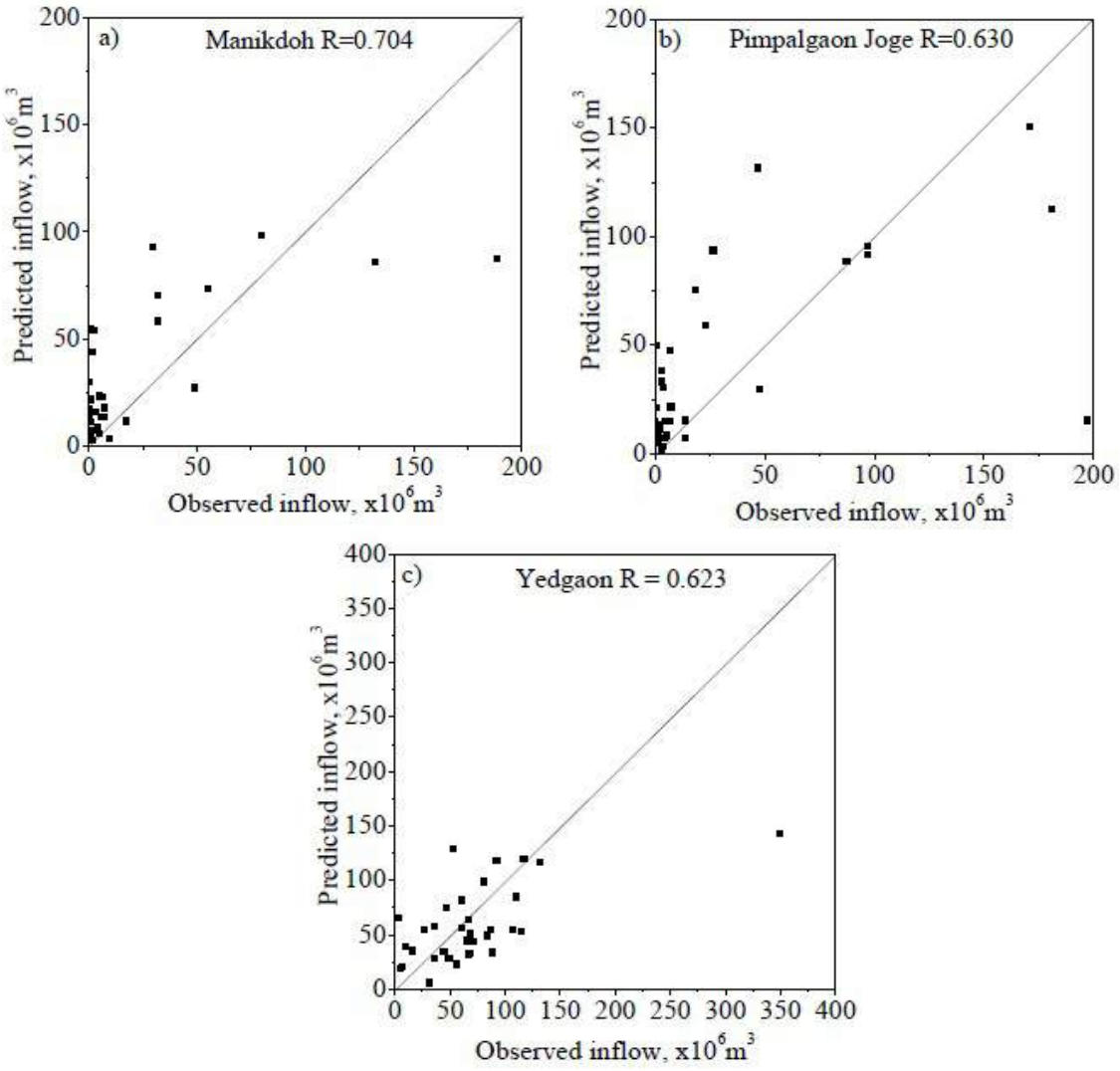

Figure 5.4(a) – (c) Scatter plot of concurrent monthly full year ANN(7-6-4-3) model with data-transformation during testing period

The reason may be due to shorter length of data since the number of pattern is only 8, thus making the network incapable. Thus from previous runs, it is found that the raw data, scaled and transformed data could not be modelled well. The concurrent predictions with MLP and TLRN networks for monthly full year data, pre-processed with MA are disclosed and the performance of this model is displayed in Table 5.7. Concurrent predictions with MLP and TLRN networks for monthly seasonal data have displayed average performances as compared to corresponding full year predictions.

Memory structures of time delay and gamma are combined with TLRN resulting in better performance as compared to traditional MLP models. ANN(5-4-3) model with TLRN and time delay memory structure has shown better results for seasonal data in most of the error statistics as shown in Table 5.7 as compared to other models. In this case also, traditional MLP model has not resulted in better fit but TLRN networks having time delay and gamma memory structures has resulted better than transformed-data ANN model as well as data pre-processed seasonal models. Amongst all the models, ANN(3-4-3) model having an input of only previous time step inflow into a reservoir has predicted the concurrent inflow into the reservoir better as shown in Table 5.7. The time series and scatter plot of observed and predicted inflow during testing period is shown in Figure 5.5(a) – (c).

Table 5.7 Summary of performance of concurrent monthly ANN models with data pre-processing during testing period

Performance of monthly full year inflow data									
Model	Manikdoh			Pimpalgaon Joge			Yedgaon		
	MSE, 10^{12} m^6	MAE, 10^6 m^3	R	MSE, 10^{12} m^6	MAE, 10^6 m^3	R	MSE, 10^{12} m^6	MAE, 10^6 m^3	R
ANN(3-3-3) {MLP}	1287	20.351	0.468	2442	29.670	0.471	2921	32.771	0.546
ANN(3-3-3) {TLRN with time delay memory}	427	12.493	0.863	1189	17.139	0.780	1984	30.401	0.773
ANN(3-2-3) {TLRN with gamma memory}	652	16.081	0.799	889	17.908	0.870	1027	24.546	0.695
ANN(3-3-3) {TLRN with gamma memory}	270	10.281	0.929	1390	17.543	0.763	1779	33.582	0.588
ANN(3-4-3) {TLRN with gamma memory}	222	9.469	0.937	1164	15.327	0.804	678	20.575	0.830

Performance of monthly seasonal inflow data									
Model	Manikdoh			Pimpalgaon Joge			Yedgaon		
	MSE, 10^{12} m^6	MAE, 10^6 m^3	R	MSE, 10^{12} m^6	MAE, 10^6 m^3	R	MSE, 10^{12} m^6	MAE, 10^6 m^3	R
ANN(5-4-3)	3756	49.928	0.642	8034	75.329	0.120	13629	85.261	0.621
ANN(5-4-3) {TLRN with time delay memory}	827	17.399	0.808	2259	30.708	0.602	2109	34.448	0.407
ANN(5-3-3) {TLRN with gamma memory}	1788	33.266	0.660	1894	30.742	0.670	6779	53.130	0.356
ANN(5-4-3) {TLRN with gamma memory}	2733	41.470	0.534	1520	27.912	0.775	5135	47.857	0.537

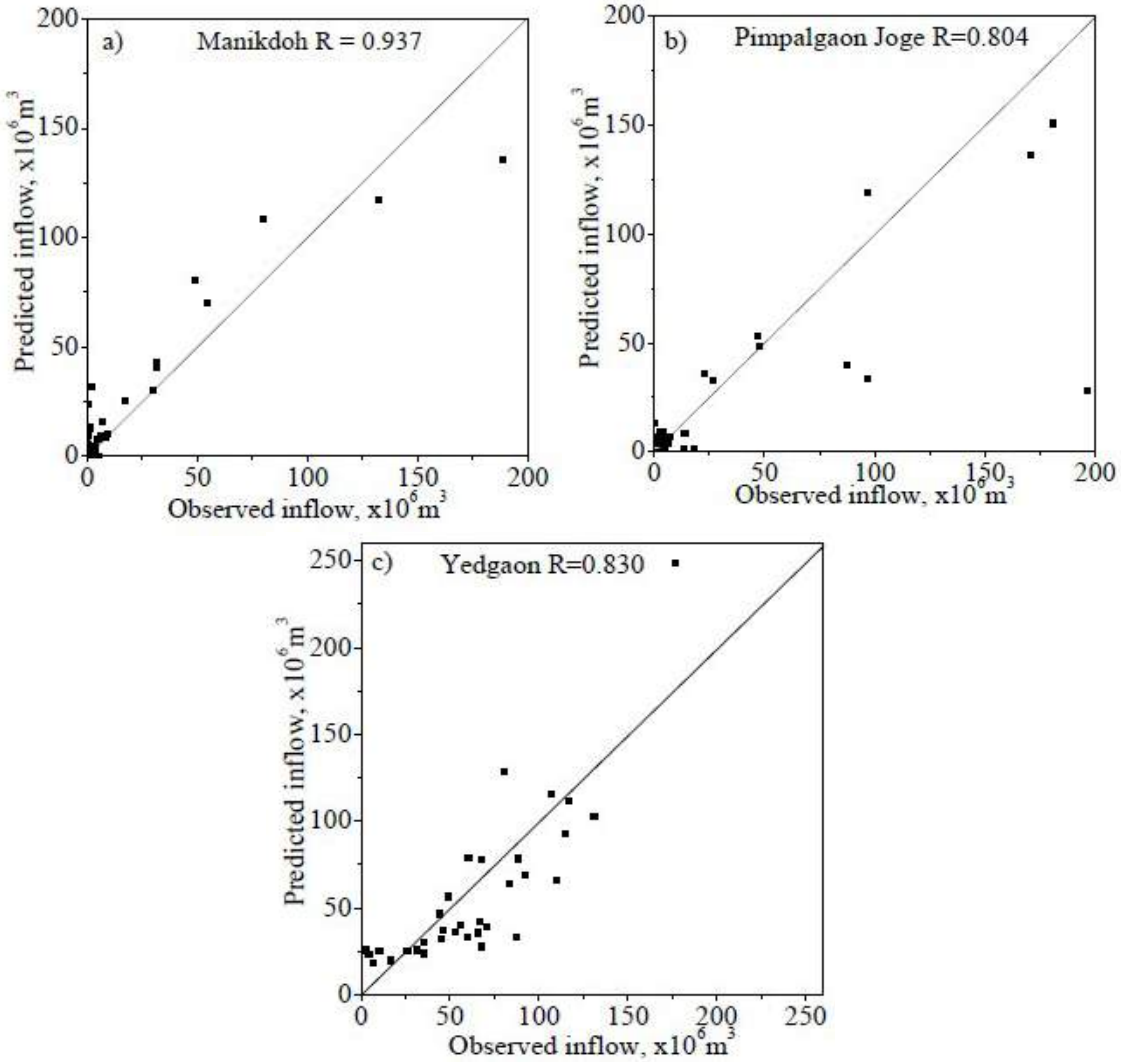

Figure 5.5(a) – (c) Scatter plot of concurrent monthly full year ANN(3-4-3) model with data pre-processing during testing period

5.1.2.3 Concurrent Daily ANN Model

From the previous section, it is seen that multi-reservoir inflows with monthly time-stepped stochastic and ANN models could not predict the concurrent reservoir inflow better (because of lesser length of data set). Hence the prediction is tried with daily data set. The stochastic daily model could not be carried out due to the curse of dimensionality. The daily full year and seasonal ANN models are developed using 70% of data length for training and 30% of data length for testing. The inputs to the network are the lagged inflows and upstream releases to predict one-day-ahead inflow. ANN models are developed using MLP and TLRN networks with varying hidden nodes. Training is stopped when the pre-determined minimum error is reached. The effect of hidden neurons in the network training is identified by various trials.

From the numerous models developed with MLP and TLRN networks, it is found that with logarithmic-transformed full year data, both the models exhibited average and similar performances. The performance of sigmoid transfer function on data sets containing varying degrees of noise and non-linearity are tried. The number of hidden layers and hidden nodes are changed and found that the addition of hidden layer only increases the complexity of the network (increasing the number of parameters) and does not necessarily enhance the model performance.

Numerous models developed with standard MLP and TLRN networks for logarithmic-transformed seasonal data are trained with varying algorithms like BP, BPTT, LM and CG. Both the networks resulted in good performance during training period but showed average error statistics during validation tests. Randomization of one peak value in testing set is done with training set for improvement in peak inflow value. This resulted in over-estimation during testing. Being the daily seasonal data, there are large variations in the magnitudes of data points. In order to reduce these variations, normalization of the data set is done prior to feeding the data into the network. The data is normalized before training and testing between 0 and 1 by dividing all the inflow values with maximum inflow. For comparison of the models, four better models in this case are short-listed during validation and summary is displayed in Table 5.8. All the models displayed are developed with logarithmic-transformed data except ANN(3-14-3) model which is normalized data model.

Table 5.8 Summary of performance of concurrent daily ANN models with data transformation during testing period

Performance of daily full year inflow data									
Model	Manikdoh			Pimpalgaon Joge			Yedgaon		
	MSE, 10^{12} m^6	MAE, 10^6 m^3	R	MSE, 10^{12} m^6	MAE, 10^6 m^3	R	MSE, 10^{12} m^6	MAE, 10^6 m^3	R
ANN(5-10-3) {TLRN with gamma memory}	1.864	0.557	0.707	6.612	0.700	0.416	2.510	1.050	0.665
ANN(5-15-3) {TLRN with gamma memory}	2.006	0.546	0.686	6.730	0.728	0.381	3.508	1.181	0.542
ANN(5-24-3) {MLP}	1.422	0.404	0.784	6.300	0.61	0.430	1.276	0.638	0.846
ANN(5-30-3) {MLP}	1.362	0.450	0.799	6.500	0.570	0.419	1.721	0.678	0.801
Performance of daily seasonal inflow data									
Model	Manikdoh			Pimpalgaon Joge			Yedgaon		
	MSE, 10^{12} m^6	MAE, 10^6 m^3	R	MSE, 10^{12} m^6	MAE, 10^6 m^3	R	MSE, 10^{12} m^6	MAE, 10^6 m^3	R
ANN(5-10-15-3) {TLRN with gamma memory}	5.885	1.031	0.637	5.8	1.096	0.568	4.987	1.181	0.712
ANN(5-10-5-4-3) {MLP}	3.652	1.174	0.769	5.508	1.469	0.619	3.149	1.315	0.842
ANN(5-25-3) {MLP}	3.183	0.793	0.786	4.862	1.059	0.606	3.23	1.063	0.792
ANN(3-14-3) {MLP}	3.279	0.717	0.780	4.927	0.846	0.650	5.518	0.971	0.746

In the first glance, all the seasonal data models are performing similar to full year data models. The simple MLP ANN(3-14-3) model (normalized data) has better performance amongst all the models developed and the time series and scatter plot of this model is shown in Figure 5.6(a) – (f). The scatter plot showed that the higher inflows are over-predicted resulting in lowering of R statistics for this model. Thus it may be concluded that in case of concurrent inflow prediction into multi-reservoir system also, ANN models require better data pre-processing technique rather than identifying the best ANN structure. In this case, the MA series with k = 3 has been derived for individual reservoirs in the multi-reservoir system

which constitutes as the input to the ANN model. It is found from the numerous models developed with MLP and TLRN type of networks that by using pre-processed inputs both the networks exhibited improved performances. The number of hidden nodes is also reduced considerably thereby reducing the complexity of the model. Best performance of each type of network selected and is shown in Table 5.9.

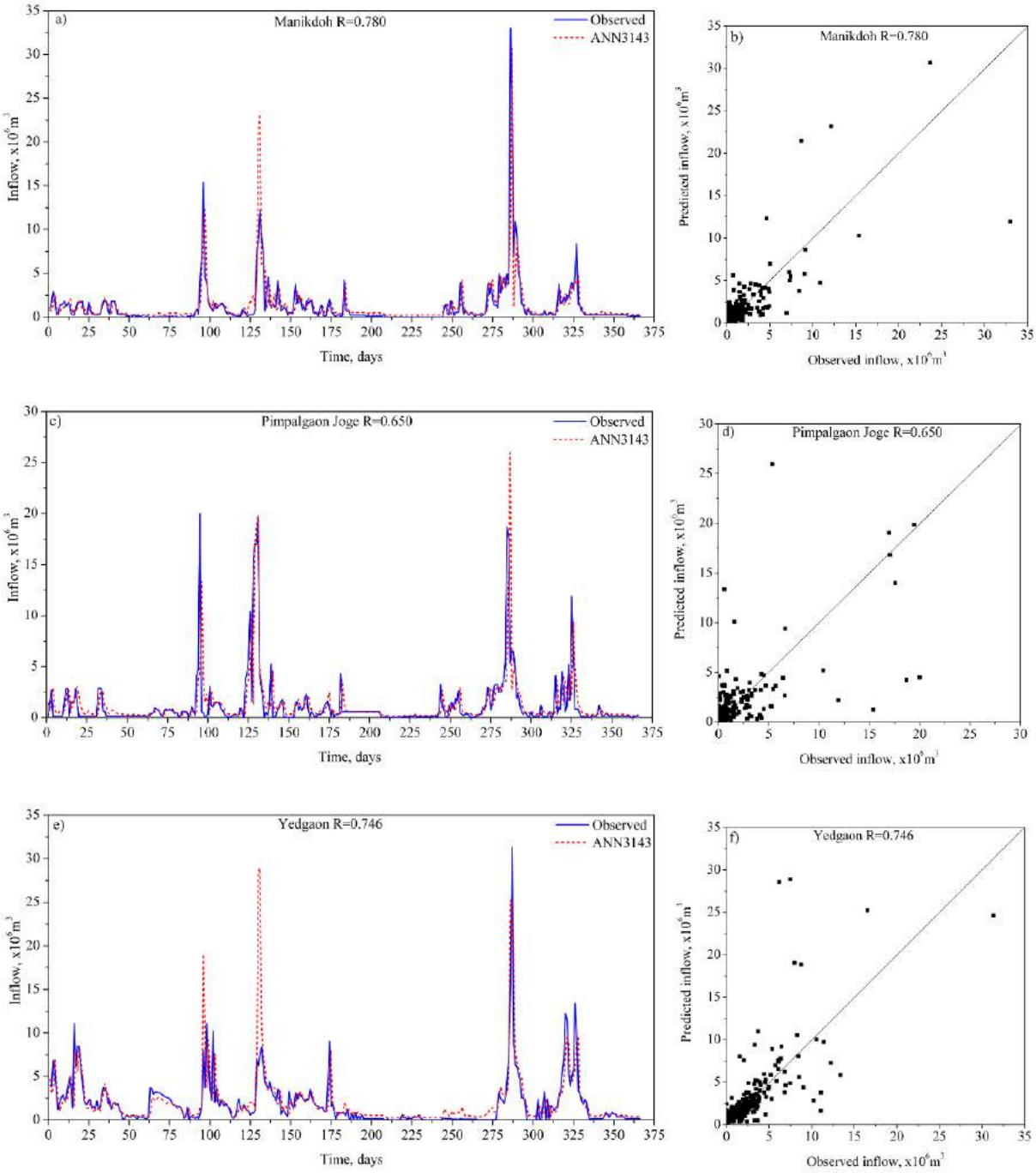

Figure 5.6(a) - f) Time series and scatter plot of concurrent daily seasonal ANN(3-14-3) model with data transformation during testing period

Table 5.9 Summary of performance of concurrent daily ANN models with data pre-processing during training and testing period

Performance of daily full year inflow data							
Data phase	Error criteria	ANN(6-5-3) {MLP}			ANN(3-3-3) {TLRN with gamma memory}		
		Manikdoh	Pimpalgaon Joge	Yedgaon	Manikdoh	Pimpalgaon Joge	Yedgaon
Training	MSE, 1012 m6	1.615	1.152	1.542	0.512	0.362	0.976
	MAE, 106 m3	1.096	0.812	0.939	0.436	0.388	0.679
	R	0.880	0.879	0.931	0.950	0.959	0.952
Testing	MSE, 1012 m6	2.257	1.654	1.654	0.696	1.091	0.652
	MAE, 106 m3	1.172	0.819	0.871	0.435	0.438	0.567
	R	0.768	0.855	0.875	0.910	0.897	0.936
Performance of daily seasonal inflow data							
Data phase	Error criteria	ANN(6-4-3) {MLP}			ANN(6-3-3) {TLRN with gamma memory}		
		Manikdoh	Pimpalgaon Joge	Yedgaon	Manikdoh	Pimpalgaon Joge	Yedgaon
Training	MSE, 1012 m6	3.069	4.814	38.480	0.573	0.543	1.130
	MAE, 106 m3	1.247	1.987	5.915	0.513	0.576	0.843
	R	0.779	0.879	0.861	0.971	0.971	0.973
Testing	MSE, 1012 m6	4.078	4.423	36.703	0.745	0.635	1.011
	MAE, 106 m3	1.376	1.879	5.756	0.486	0.573	0.813
	R	0.794	0.864	0.723	0.950	0.966	0.954

At a glance, it is found that the full year and seasonal daily data concurrent models are performing equally better with R value in the range of 0.950 during testing and 0.970 during training. However, TLRN with gamma memory with lesser hidden nodes i.e. ANN(6-3-3) model using seasonal data has resulted in better forecasting for all the error statistics. The corresponding network configuration is shown in Figure 5.7. The results indicate that one-day antecedent inflow in each reservoir along with only 3 hidden nodes (as against 14 nodes with data-transformed model) is necessary to build the model for next day's inflow into each

reservoir. The R value during testing period for these reservoirs are 0.950, 0.966 and 0.954 respectively and their other error statistics (MSE = 0.745, 0.635, 1.011 and MAE = 0.486, 0.573, 0.813) are also best thus indicating better forecasting of low, moderate and peak inflows. The time series and scatter plot of observed inflows with ANN(6-3-3) model predicted inflow is shown in Figure 5.8(a) – (f) respectively and the figure shows that the higher inflows are accurately predicted by ANN(6-3-3) model for all the three reservoirs. Thus, current and one day antecedent inflow together with recurrent nature of dynamic TLRN, BPTT algorithm and short-term gamma memory is found suitable to model the highly complex, non-linear, daily full year and seasonal inflows into the multi-reservoirs, without exogenous inputs also.

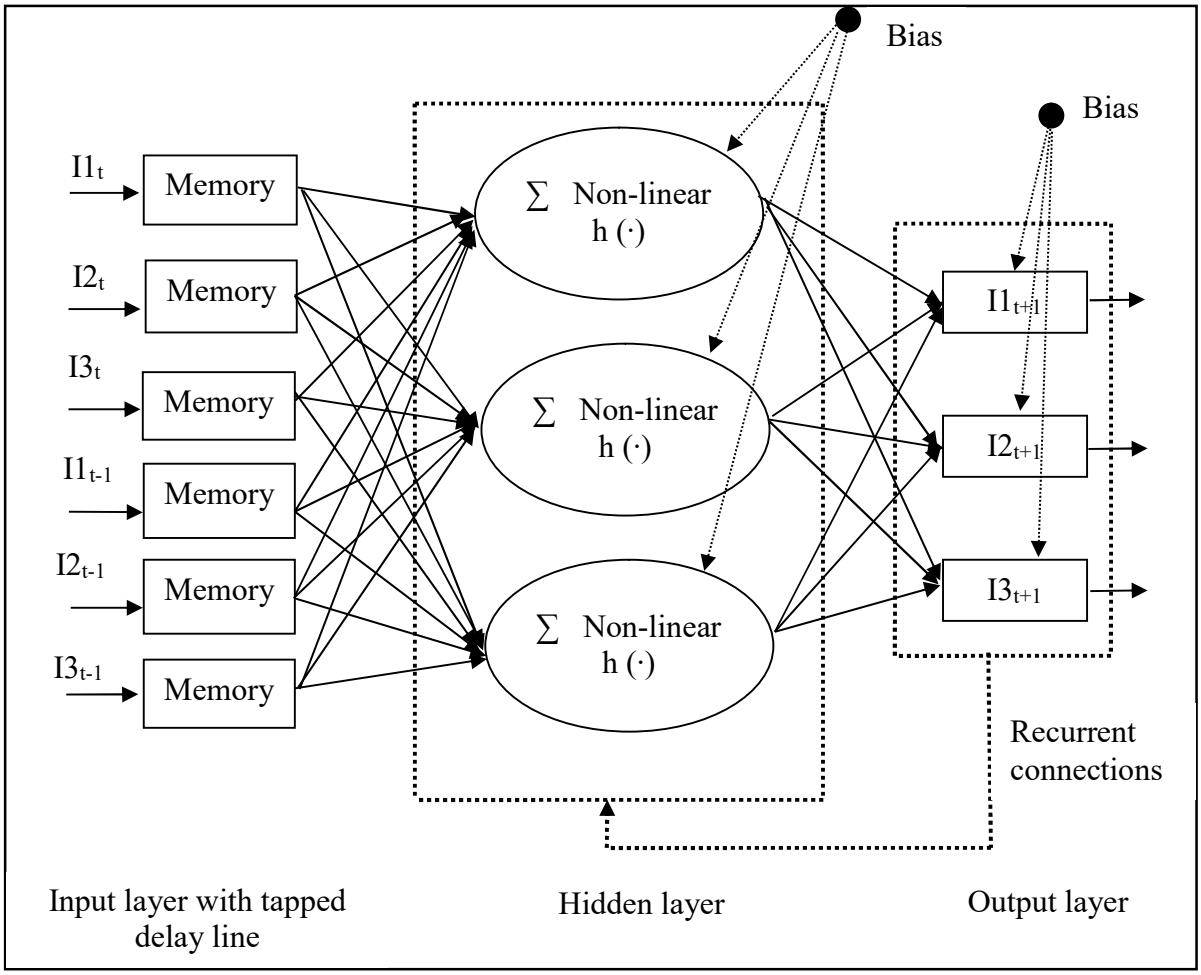

Figure 5.7 Architecture of concurrent daily seasonal ANN(6-3-3) model

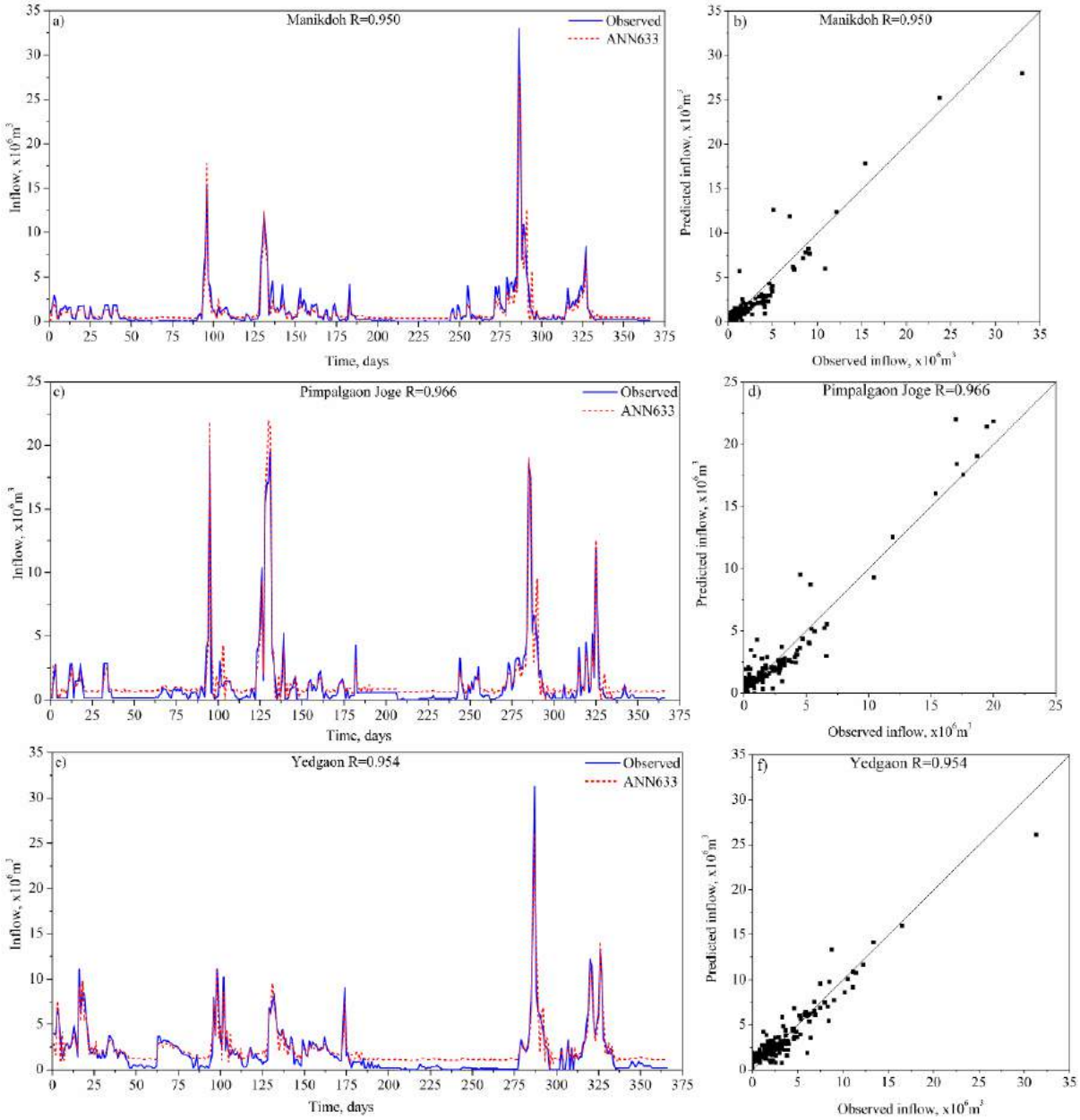

Figure 5.8(a) – (f) Time series and scatter plot of concurrent daily seasonal ANN(6-3-3) model with data pre-processing during testing period

5.1.3 Concurrent Multi-reservoir ANN Model with Exogenous Inputs

In the previous section, concurrent inflow into multi-reservoirs has been predicted without considering the exogenous inputs and is satisfactorily accepted by the watershed manager. But a policy maker needs a model which can concurrently predict the future inflow considering the exogenous variables such as releases from upstream reservoirs, surplus and continuous import from adjacent watershed reservoirs as the input to the model. Thus the

modeller needs to develop a comprehensive model which can predict the future inflow as accurately as possible by considering the exogenous inputs. Thus in the present case the one-step-ahead inflow into the multi-reservoirs are predicted using the ANN technique. Only ANN modelling is included in prediction as the conventional stochastic model involves large parameter posing analytical and computational problem. The ANN model is developed by including the inputs of imports from adjacent Dimbhe and Wadaj reservoir basins (IMt) during Kharif and rabi seasons (1st June - 29th February) in addition to inflow into the three reservoirs and corresponding releases to downstream reservoir. Surplus release from Chilhewadi (St) during monsoon season (1st July - 30th September) to Yedgaon reservoir is also an input node to the ANN model.

The output node consists of one-step-ahead inflow into the three reservoirs and in another case, it is one-step-ahead inflow into upstream reservoirs (reservoirs in parallel) and three-step-ahead inflow into downstream reservoir. It is to be noted that the travel time from one reservoir to another is less than one day. Thus the releases and antecedent releases from upstream reservoirs are also considered as input to the network. Since the time of travel is less than a day from upstream to downstream there is no dispute due to delay time of release and inflow realization in the downstream reservoir. Three-day-ahead prediction into the future is considered only in case of Yedgaon reservoir in order to study the combined effect of releases and surplus from the upstream and adjacent reservoirs and its own independent inflow. Such a study for upstream reservoirs is not necessary as the inflow is un-controlled in these reservoirs. The concurrent one-step-ahead inflow and concurrent multi-step-ahead inflow prediction are discussed separately in the following sections.

5.1.3.1 Concurrent Daily One-step-ahead ANN Model

In this case, the network includes additional input nodes due to import and surplus from adjacent watersheds i.e. IMt and St, together with reservoir inflows and releases I1t, I2t, I3t, R1t, and R2t for full year and seasonal data. The MLP and TLRN networks with trial and error procedure are configured and trained to forecast one-step-ahead inflow in the reservoirs. The large number of zero inflow values in the time series adds to the complexity of ANN modelling which is overcome with data pre-processing of raw daily inflows as seen in the previous section. The performance indicators given in Table 5.10 shows the best models developed by MLP and TLRN networks from number of trials using pre-processed full year

and seasonal data. Hidden nodes are varied from 1 - 20 by trial and error till best configuration is achieved. The TLRN model is performing very well for the case of full year as well as seasonal data series than the MLP network. It is also seen that MLP model could not perform better even with large hidden nodes. The dynamic nature of TLRN has shown remarkable improvement over MLP model in both training and testing phases with lesser number of hidden nodes.

The gamma memory of TLRN for ANN(7-4-3) model has remembered the inflows' past with efficiency and modelled the daily full year inflow quite good. The input for this network consists of inflow in these three reservoirs, releases from upstream reservoirs and surplus as well as import from adjacent watersheds. The ANN architecture for ANN(7-4-3) model is given in Figure 5.9. Forecasting in all the reservoirs showed good performance with R = 0.917, 0.912 and 0.925 during testing phase for Manikdoh, Pimpalgaon Joge and Yedgaon reservoirs respectively (Table 5.10). The MSE and MAE measures are also better (MSE = 0.596, 0.913, 0.802 and MAE = 0.359, 0.357, 0.654) for this model.

Table 5.10 Summary of performance of concurrent daily one-step-ahead ANN models during training and testing period

Phase	Error criteria	ANN(7-19-3) {MLP}			ANN(7-4-3) {TLRN with gamma memory)		
		Manikdoh	Pimpalgaon Joge	Yedgaon	Manikdoh	Pimpalgaon Joge	Yedgaon
Performance of daily full year data							
Training	MSE, 1012 m6	1.455	1.139	1.283	0.450	0.415	0.802
	MAE, 106 m3	0.572	0.423	0.659	0.388	0.309	0.669
	R	0.841	0.857	0.926	0.954	0.950	0.961
Testing	MSE, 1012 m6	1.314	2.026	0.859	0.596	0.913	0.802
	MAE, 106 m3	0.487	0.458	0.589	0.359	0.357	0.654
	R	0.810	0.796	0.915	0.917	0.912	0.925
Performance of daily seasonal data							
Phase	Error criteria	ANN(7-7-3) {MLP}			ANN(7-6-3) {TLRN with gamma memory)		

		Manikdoh	Pimpalgaon Joge	Yedgaon	Manikdoh	Pimpalgaon Joge	Yedgaon
Training	MSE, 1012 m6	2.119	2.132	3.815	0.869	0.801	1.801
	MAE, 106 m3	0.731	0.706	1.023	0.627	0.616	1.002
	R	0.887	0.866	0.879	0.959	0.957	0.951
Testing	MSE, 1012 m6	2.129	5.078	2.056	1.339	2.673	1.813
	MAE, 106 m3	0.611	0.807	0.812	0.694	0.794	0.952
	R	0.859	0.771	0.866	0.915	0.878	0.896

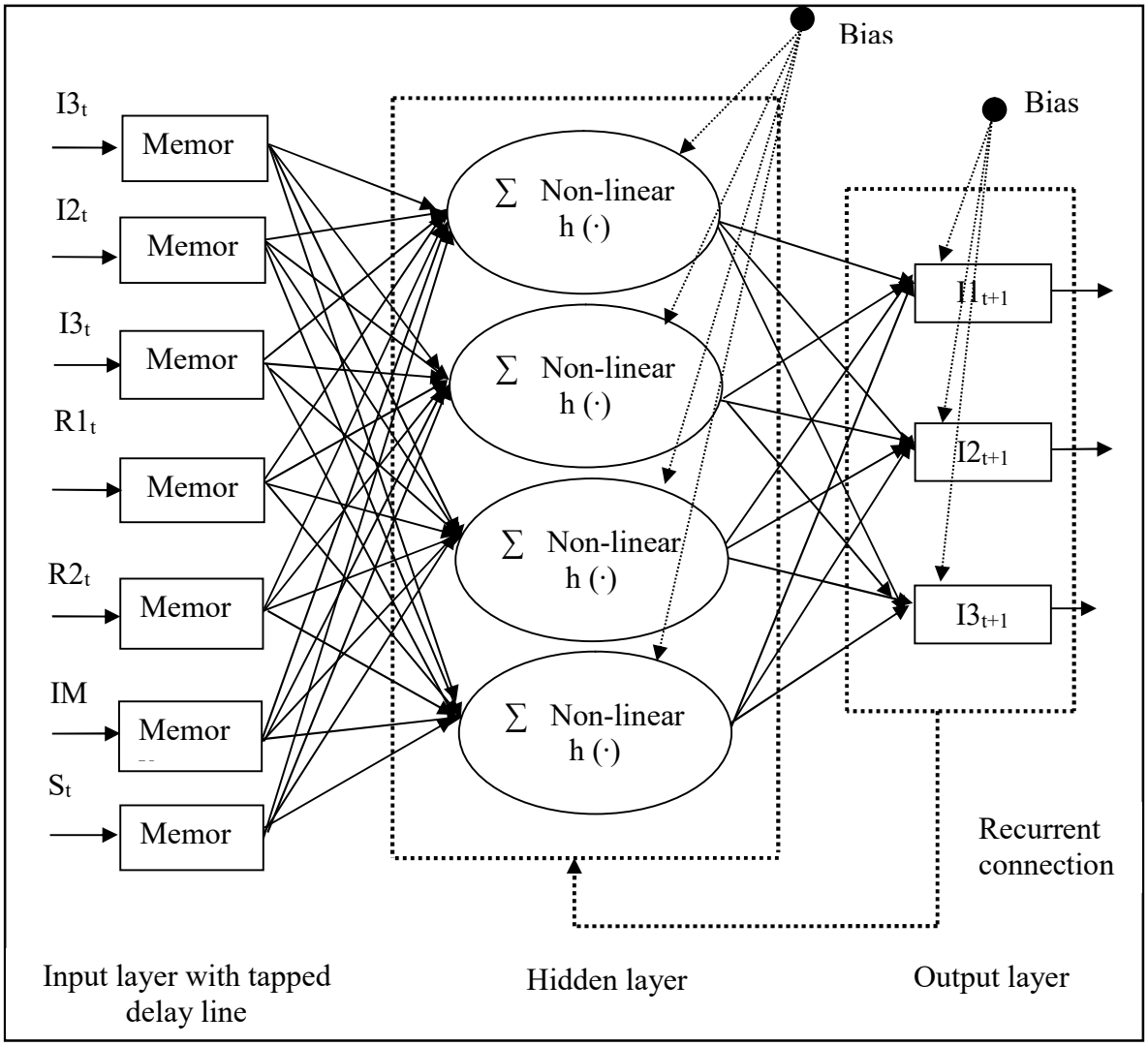

Figure 5.9 Architecture of concurrent daily full year one-step-ahead ANN(7-4-3) model

The performance of ANN(7-4-3) model is further compared with observed series with the help of time series and scatter plot as shown in Figure 5.10(a) – (f). Time series and scatter plots of inflow predictions with this model show that all the points are satisfactorily mapped for the three reservoirs except slight under-predictions of highest inflows of upstream reservoirs. The reason may be that these peak magnitudes are not there in training data set. Thus it may be concluded that daily multi-reservoir inflow could be predicted very well by considering the exogenous inputs.

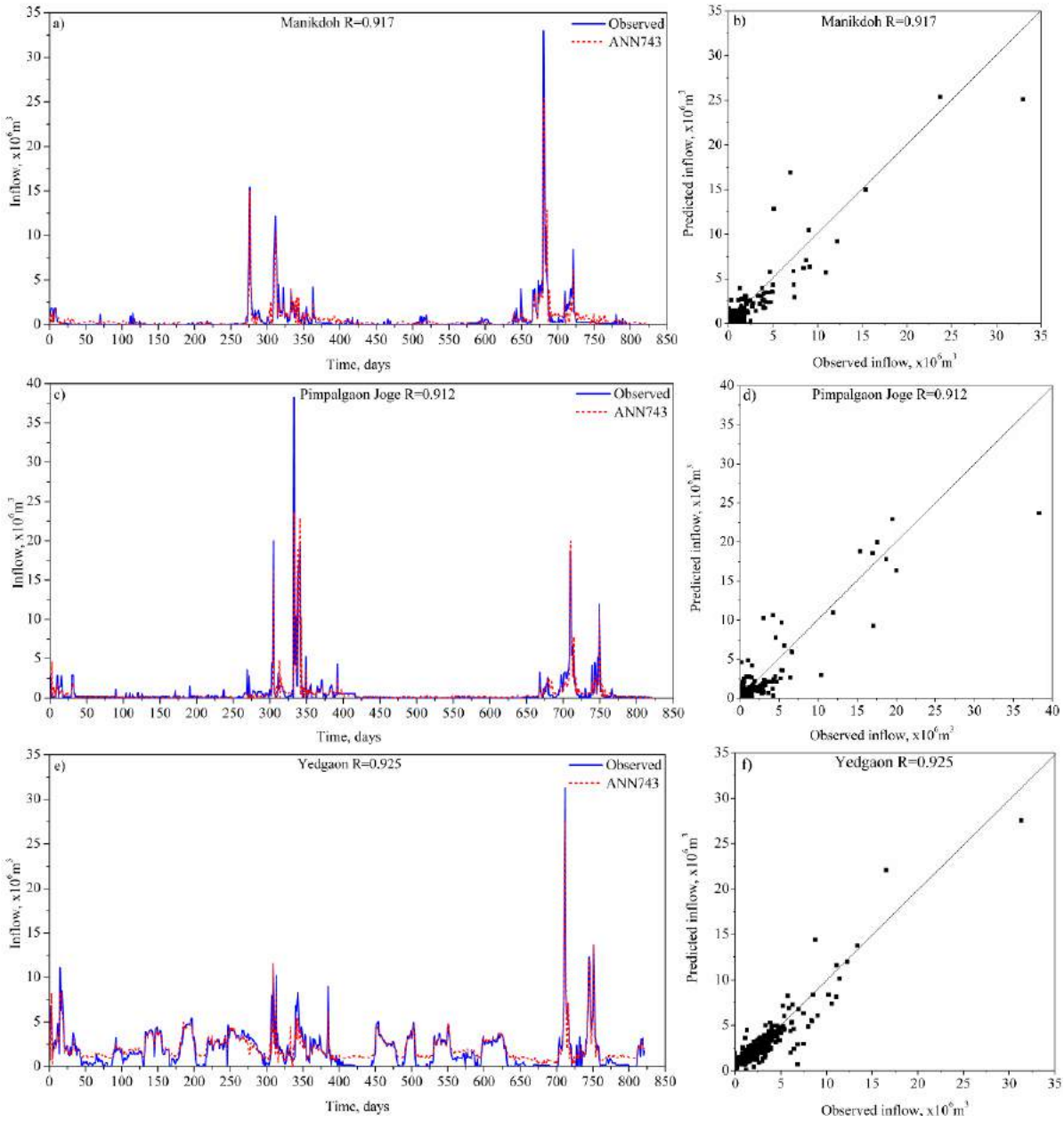

Figure 5.10(a) – (f) Time series and scatter plot of concurrent daily full year one-step-ahead ANN(7-4-3) model during testing period

5.1.3.2 Concurrent Daily Multi-step-ahead ANN Model

The multi-time-step-ahead inflow forecasting into Yedgaon reservoir will give the dam authority, few-days-ahead warning of the sudden floods due to controlled and un-controlled inflows into Yedgaon reservoir. Since the Yedgaon reservoir acts as a distribution reservoir, it is also found necessary to develop a multi-step-ahead forecasting into the reservoir. Multi-step-ahead forecasting using ANN is a challenging and complex task which tries to make predictions several steps into the future. In full year data series, there are large number of zero inflow values in the time series, the input nodes (inclusive of exogenous inputs) are more and the output nodes are higher i.e. 5 thereby leading to complex, non-linear ANN model. Mainly, MLP and TLRN networks are trained with different input nodes and hidden nodes to forecast three-step-ahead inflow in case of Yedgaon reservoir and one-step-ahead inflow in case of Manikdoh and Pimpalgaon reservoirs. Momentum and CG learning rule with sigmoid as well as hyperbolic transfer functions are tried for training the network. Hidden nodes are varied from 1 - 15 by trial and error till best ANN configuration is achieved.

Figure 5.11 shows the best MLP and TLRN networks resulting from number of trials for full year and seasonal data. From the Table 7.11 in this case also TLRN network is performing better than MLP network with full year as well as seasonal data input. The resulting best MLP and TLRN models for seasonal data viz. ANN(7-11-5) and ANN(7-5-5) model are shown in Figure 5.11. These models have shown sufficient capabilities in forecasting the daily seasonal data especially the multi-step-ahead inflows in Yedgaon reservoir. However, TLRN network could perform better because non-linearity exists within the nodes and within the layers. That is the reason TLRN learns better with the same number of input nodes. Among the TLRN models trained using full year and seasonal data, full year ANN(7-6-5) model showed improved performances during both training and testing phases. It is also found that TLRN network performance has not changed with additional number of output nodes.

The input nodes consist of I1t, I2t, I3t, R1t, R2t, IMt, and St. Except for Pimpalgaon Joge reservoir, the other two reservoir forecasting have shown improvement with MSE = 0.553, MAE = 0.361, R = 0.925 for Manikdoh reservoir and MSE = 0.606, MAE = 0.443 and R = 0.939 for Yedgaon reservoir during testing phase (Table 5.11). The two-day-ahead forecasting (I3t+2) is fairly good with R = 0.884 but has deteriorated for three-day-ahead

forecasting (I3t+3) with R = 0.760 as seen in Table 5.11. This may be due to the travel time of released water from upstream reservoirs to downstream reservoir being less than a day, leading to less correlation with previous time stepped releases.

Table 5.11 Summary of performance of concurrent daily multi-step-ahead ANN models during training and testing period

Phase	Error criteria	ANN(7-15-5) {MLP}					ANN(7-6-5) {TLRN with gamma memory)				
		Manikdoh	Pimpalgaon Joge	Yedgaon			Manikdoh	Pimpalgaon Joge	Yedgaon		
		1 day-ahead	1 day-ahead	1 day-ahead	2 day-ahead	3 day-ahead	1 day-ahead	1 day-ahead	1 day-ahead	2 day-ahead	2 day-ahead
Performance of daily full year inflow data											
Training	MSE, 10^{12} m^6	1.331	1.118	1.099	1.773	4.022	0.373	0.449	0.565	0.906	3.103
	MAE, 10^6 m^3	0.479	0.403	0.453	0.636	1.025	0.355	0.323	0.467	0.601	1.031
	R	0.855	0.860	0.937	0.896	0.744	0.963	0.945	0.967	0.951	0.814
Testing	MSE, 10^{12} m^6	1.139	2.067	0.711	0.951	2.49	0.553	1.098	0.606	1.243	2.293
	MAE, 10^6 m^3	0.412	0.451	0.360	0.503	0.808	0.361	0.413	0.443	0.615	0.925
	R	0.833	0.789	0.924	0.897	0.760	0.925	0.905	0.939	0.884	0.760
Performance of daily seasonal inflow data											
Phase	Error criteria	ANN (7-11-5) {MLP}					ANN(7-5-5) {TLRN with gamma memory)				
		Manikdoh	Pimpalgaon Joge	Yedgaon			Manikdoh	Pimpalgaon Joge	Yedgaon		
		1 day-ahead	1 day-ahead	1 day-ahead	2 day-ahead	3 day-ahead	1 day-ahead	1 day-ahead	1 day-ahead	2 day-ahead	3 day-ahead
Training	MSE, 10^{12}	2.092	2.141	3.460	7.066	10.088	1.202	0.753	2.870	6.144	9.044

	m^6										
	MAE, 10^6 m^3	0.762	0.724	0.917	1.395	1.653	0.767	0.574	1.119	1.456	1.701
	R	0.888	0.866	0.891	0.761	0.631	0.946	0.957	0.919	0.803	0.682
Testing	MSE, 10^{12} m^6	1.957	5.107	2.116	4.553	6.141	2.040	2.137	3.607	5.139	6.740
	MAE, 10^6 m^3	0.635	0.846	0.707	1.139	1.336	0.881	0.748	1.048	1.299	1.502
	R	0.869	0.761	0.868	0.710	0.565	0.884	0.893	0.803	0.724	0.567

Thus, it can be concluded that ANN(7-6-5) model for full year data is the best model for multi-step-ahead prediction and the corresponding model architecture is shown in the Figure 5.11. The number of nodes in the input layer is 7 which include current reservoir inflows, upstream releases and import as well as surplus from adjacent reservoirs. The number of hidden nodes required is 6 to predict multi-step-ahead inflow using non-linear transformation of inputs having hyperbolic-tangent activation function. The time series and scatter plot of ANN(7-6-5) model with the observed series is displayed in Figure 5.12(a) – (j). The plots show that all the observed inflows are satisfactorily mapped for the three reservoirs, especially I3t+1. But the I3t+2 and I3t+3 have not learnt the required observed pattern for high inflows. The network which has learnt the complex and spatio-temporal data is the dynamic TLRN with BPTT algorithm and global feedback from output layer to the hidden layer. The input to the network is also delayed with the tapped delay line at the input layer resulting in static memory for the network.

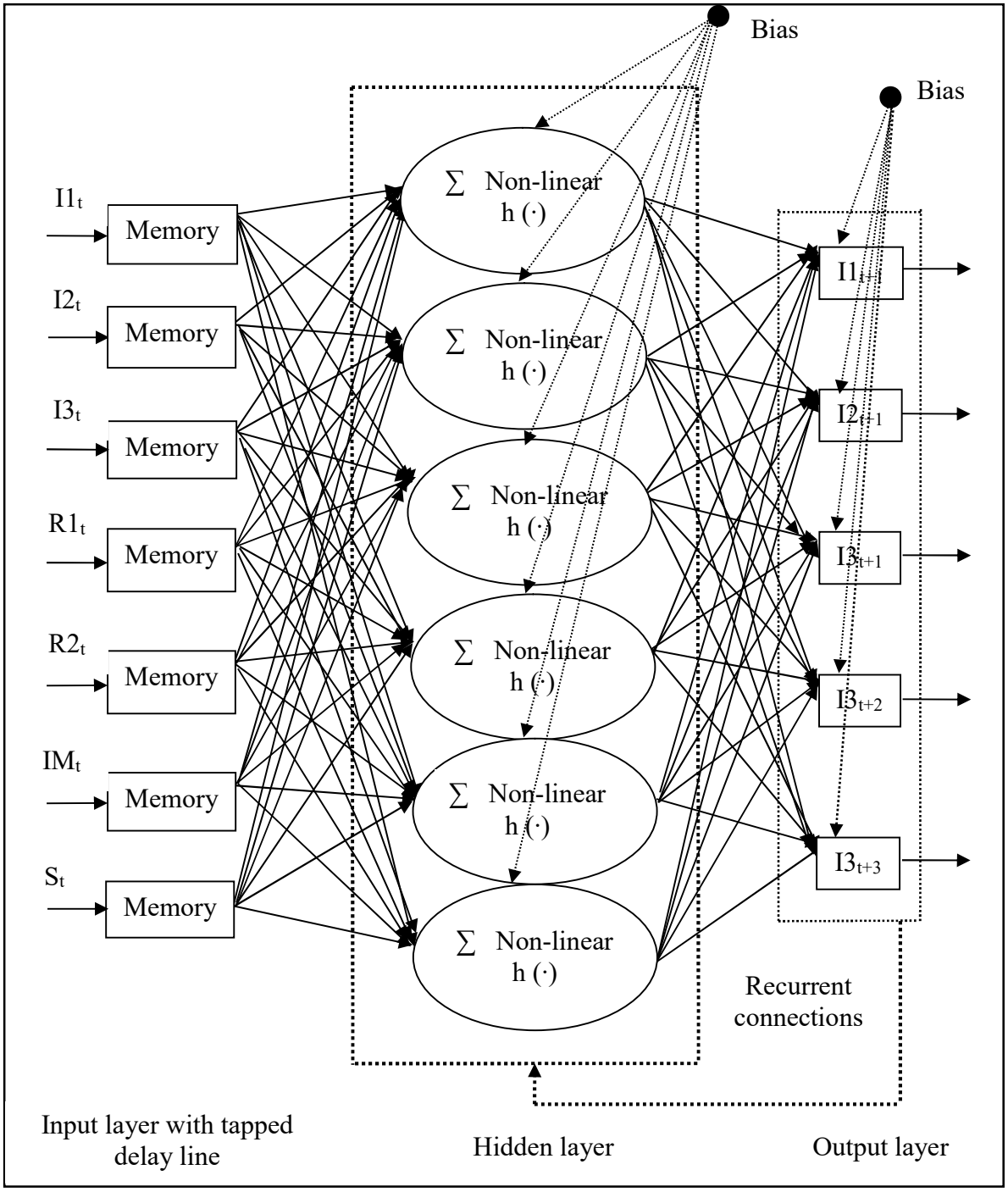

Figure 5.11 Concurrent multi-step-ahead daily full year ANN(7-6-5) model

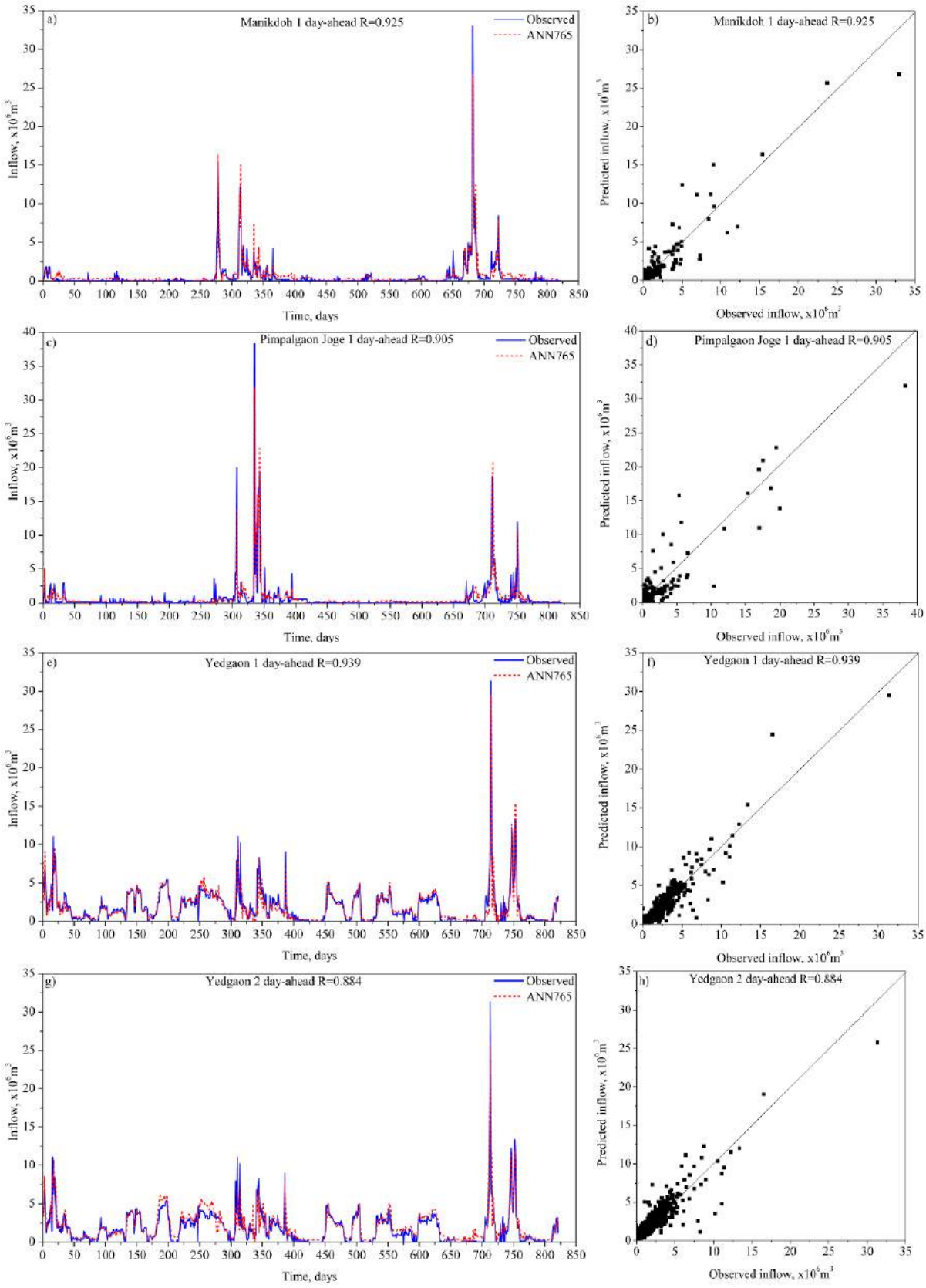
a)
Manikdoh 1 day-ahead R=0.925
Observed
ANN765
Inflow, x10^6m^3
Time, days
b)
Manikdoh 1 day-ahead R=0.925
Predicted inflow, x10^6m^3
Observed inflow, x10^6m^3
c)
Pimpalgaon Joge 1 day-ahead R=0.905
Observed
ANN765
Inflow, x10^6m^3
Time, days
d)
Pimpalgaon Joge 1 day-ahead R=0.905
Predicted inflow, x10^6m^3
Observed inflow, x10^6m^3
e)
Yedgaon 1 day-ahead R=0.939
Observed
ANN765
Inflow, x10^6m^3
Time, days
f)
Yedgaon 1 day-ahead R=0.939
Predicted inflow, x10^6m^3
Observed inflow, x10^6m^3
g)
Yedgaon 2 day-ahead R=0.884
Observed
ANN765
Inflow, x10^6m^3
Time, days
h)
Yedgaon 2 day-ahead R=0.884
Predicted inflow, x10^6m^3
Observed inflow, x10^6m^3

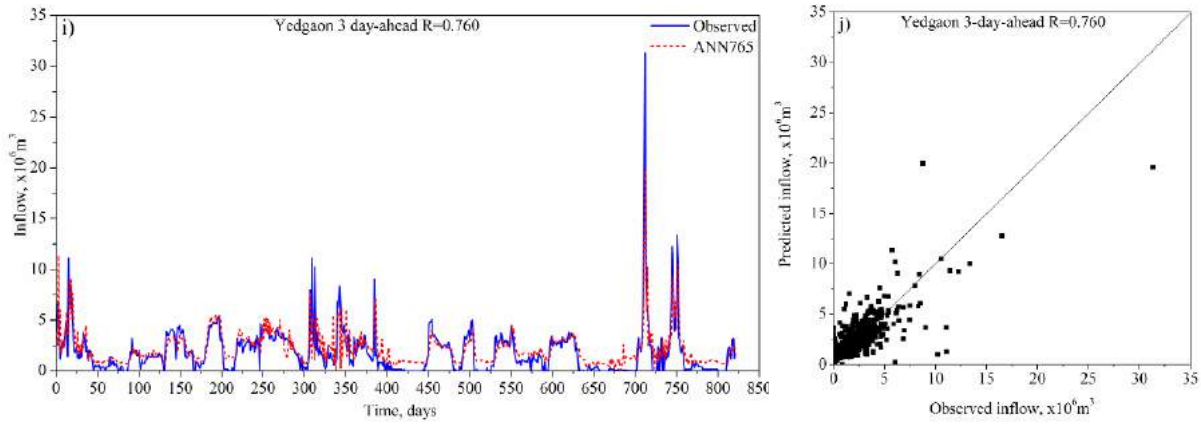

Figure 5.12(a) – (j) Time series and scatter plot of concurrent daily full year multi-step-ahead ANN(7-6-5) model during testing period

5.2 Koyna Project Electric Project

This part of the study describes the models developed for multi-time-step ahead daily reservoir inflow prediction for Koyna Hydro Electric Project (KHEP). The models are developed using daily lumped and distributed input data collected from Koyna watershed. Different soft computing technique such as ANN, ANFIS and LGP have been developed and applied along with stochastic (ARIMA) and deterministic (MLR) linear models as an initial step. Finally the developed models are inter compared to select a best model for real life application.

5.2.1 ARIMA Models (Stochastic Models)

Stochastic modelling helps the water resources engineers to forecast the observed inflow series. In these stochastic models, only reservoir inflow is used, there is no separate lumped and distributed data models and hence reported separately. Various regressive models are available in the literature like AR (p), MA(q), ARMA(p,q) and ARIMA (p,d,q) based on their p, q and d. Since the data available for the present study is non-stationary, the basic requirement to develop the AR and ARMA models could not be satisfied. Hence ARIMA model, which could handle non-stationarity in the data is used to predict multi-time-step ahead daily inflow into Koyna Reservoir.

The ARIMA time-series analysis used lags and shifts in the historical data (e.g. moving averages, seasonality) to predict the future values. It is to be noted that separate models are to be developed for different multi-time-step ahead daily inflow prediction. Since the autocorrelation function (ACF) and the partial autocorrelation function (PACF) have not provided clear idea on selection of the order of autoregressive (p), moving average (q) and differencing (d) parameters for ARIMA modelling, trial and error procedure is adopted to select the best parameters (p, d and q). Various combinations of p, d and q are tried and the models that have resulted in better combination are only presented here. The values of the parameters are chosen such that the sum of squared residuals (SSR) between the observed data and the estimated values are as small as possible. The ARIMA models are developed using 70% length of the data and remaining 30% length of data is used for testing. The commercially available software SPSS 16.0 was used for ARIMA model development. The analysis was initialized with one parameter at a time, then their combination and so on.

Even though large numbers of models are developed, only better ARIMA models with various combinations of p, q and d with a lead period of 1 day, 2 day and 3 day are depicted in Table 5.12. From Table 5.12, it is apparent that performances of the models are slightly deteriorating with increase in lead time. This may be due to poor correlation of current inflow with 2 day and 3 day lagged inflows. The prediction of 1 day ahead inflow is quite satisfactory because the input space contains the most recent information. It can also be observed that ARIMA(2,1,2) model performed better than any other combination for all lead periods and the best statistics obtained R, E, RMSE, are 0.66, 0.56 and 14.99 respectively. It is also found that the model performance is not increasing with the increase in p, q and d.

The time-series and scatter plot of observed and predicted inflow (1 day lead period) during testing period resulted from ARIMA(2,1,2) model are presented in Figure 5.13(a)-(b) respectively. From the time-series and scatter plot it can be seen that only low flows are predicted reasonably accurate, medium inflows are over predicted and high inflows are under predicted. The reason may be due to non-linear behaviour of medium and high inflows. Hence there is a strong need for better models to predict the non-linear peak inflow. Nevertheless ARIMA model can provide first hand information about the process of inflow prediction. In the following section MLR and soft computing techniques like ANN, ANFIS and LGP are applied to handle the non-linearity nature of the reservoir inflow.

Table 5.12. Performance measures of daily time-step ARIMA models

Models	Performance Criteria	Development			Testing		
		1 day	2day	3 day	1 day	2day	3 day
ARIMA 1-1-1	R	0.62	0.56	0.52	0.60	0.54	0.50
	E	0.58	0.55	0.47	0.57	0.51	0.45
	RMSE	17.89	17.95	18.02	18.23	18.32	18.37
	AIC	34656.17	34696.4	34743.16	14952.8	14978.17	14992.21
	BIC	34663.56	34703.79	34753.44	14959.35	14984.71	14998.75
ARIMA 2-2-2	R	0.65	0.59	0.56	0.62	0.57	0.54
	E	0.57	0.56	0.52	0.55	0.52	0.48
	RMSE	14.97	15.13	15.05	15.32	15.43	15.49
	AIC	32515.17	32642.9	32579.21	14057.17	14094.02	14114
	BIC	32522.56	32650.3	32589.31	14063.72	14100.56	14120.55
ARIMA 1-2-1	R	0.63	0.58	0.56	0.64	0.57	0.54
	E	0.54	0.56	0.55	0.51	0.54	0.50
	RMSE	15.12	15.33	15.59	15.46	15.49	15.49
	AIC	32634.96	32800.69	33002.76	14104.02	14114	14114
	BIC	32642.35	32808.08	33012.9	14110.57	14120.55	14120.55
ARIMA 1-2-2	R	0.61	0.58	0.50	0.59	0.52	0.50
	E	0.52	0.49	0.45	0.51	0.50	0.43
	RMSE	15.26	15.78	15.88	15.31	15.39	15.46
	AIC	32745.7	33148.3	33224.2	14053.81	14080.65	14104.02
	BIC	32753.09	33155.69	33234.36	14060.35	14087.19	14110.57
ARIMA 2-1-1	R	0.64	0.55	0.51	0.63	0.52	0.50
	E	0.59	0.52	0.45	0.58	0.50	0.43
	RMSE	15.01	15.03	15.10	15.14	15.20	15.30
	AIC	32547.23	32563.23	32619.06	13996.3	14016.67	14050.44
	BIC	32554.62	32570.62	32629.17	14002.85	14023.22	14056.99
ARIMA 2-1-2	R	0.64	0.60	0.62	0.66	0.62	0.60
	E	0.58	0.50	0.51	0.56	0.53	0.55
	RMSE	14.01	14.12	14.19	14.99	15.12	15.19
	AIC	31718.85	31812.82	31872.24	13945.02	13989.49	14013.28
	BIC	31726.25	31820.21	31882.28	13951.57	13996.04	14019.83
ARIMA 3-2-2	R	0.45	0.47	0.44	0.43	0.45	0.43
	E	0.47	0.42	0.41	0.45	0.41	0.39
	RMSE	15.18	15.32	15.72	16.10	16.12	16.22
	AIC	32682.54	32792.85	33102.53	14312.92	14319.31	14351.16
	BIC	32689.94	32800.24	33112.68	14319.47	14325.86	14357.71
ARIMA 4-1-4	R	0.45	0.43	0.41	0.43	0.41	0.39
	E	0.42	0.40	0.40	0.40	0.40	0.45
	RMSE	18.38	18.54	18.61	18.08	18.10	18.21
	AIC	34980.83	35084.97	35130.24	14910.25	14915.95	14947.15
	BIC	34988.22	35092.36	35140.56	14916.8	14922.49	14953.7

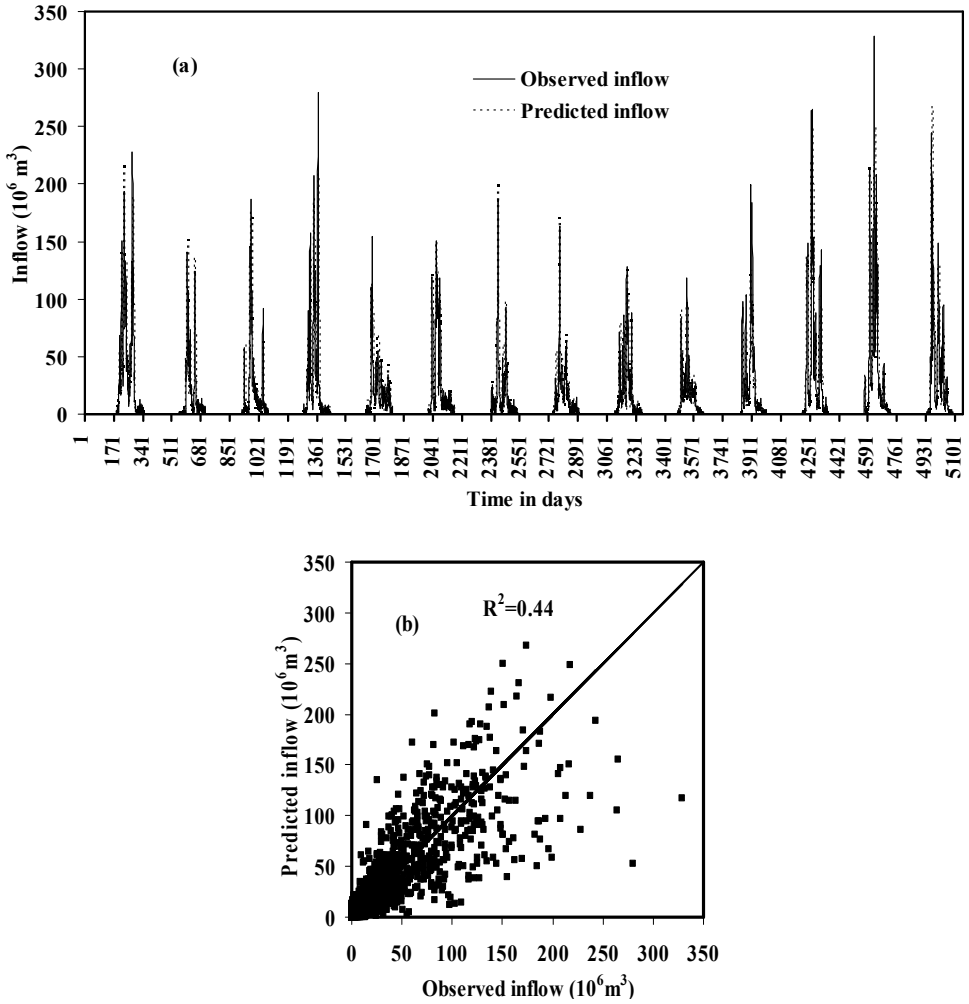

Figure 5.13. (a) Time-series and (b) scatter plot of ARIMA (2, 1, 2) model during testing period.

5.2.2 Daily Lumped Data Models

In order to develop daily lumped data models, the daily rainfall values (in mm) from the nine rain-gauge stations were spatially averaged (lumped) by Thiessen polygon method and has been used as the input. The models developed and tested using forty seven years (1961-2007) of average daily rainfall and corresponding daily inflow data are discussed below.

5.2.2.1 Daily Lumped Data MLR Models

As an initial step an attempt has been made to develop conventional MLR model for multi-time-step ahead daily inflow prediction. The forecast horizon of 1 day, 2 day and 3 day are same as that of ARIMA models (i.e.) every day ahead models are individual. This is one of

the limitations of linear stochastic and MLR models. Using statistical analysis like cross correlation, ACF and PACF twenty different models with various input combinations have been developed and applied. Each and every MLR model is developed using 70% length of the data set and remaining 30% for testing. The commercially available software SPSS 16.0 has been used for MLR model development. The performance of the lumped MLR models during training and testing period is presented in Table 5.13. From the table, it can be observed that the performance of each model during training and testing is similar indicating that the models are not over fitted and also the results are consistent and encouraging. The reason may be due to the fact that statistical properties of training data set and testing data set are similar and length of input data used for model development is sufficiently longer. From Table 5.13, it is apparent that the performances of all models are slightly deteriorating with increase in lead time. This behaviour is similar to stochastic ARIMA models. As the forecast lead period increases the correlation between desirable output and given input decreases leading to poor prediction.

For comparison the performance of time-series models (DL-MLR model 1 to DL-MLR model 7) listed in Table 5.13 are considered. From this it is observed that model performance is increasing up to a lagged input of six and then slightly decreases. Correlation coefficient (R) and Nash-Sutcliff efficiency (E) is gradually increasing and the RMSE, AIC, BIC values are decreasing with increase in number of input. Among seven models, DL-MLR model 6 with 1 day lead period which used input structure of Q(t-5),Q(t-4),Q(t-3), Q(t-2), Q(t-1),Q(t) has yielded a maximum R(0.67) and E(0.59) value and minimum RMSE (16.21), AIC (14349.81) and BIC (14356.35) values. Since AIC and BIC values are minimum than any other model, DL-MLR model 6 may be considered as a parsimonious model. This number of inputs is same as that of prominent ACF lags. Thus it may be concluded that ACF gives better indications of number of inputs in case of deterministic linear time-series modelling. The scatter plot of observed and predicted inflow by DL-MLR model 6 during testing period is shown in Figure 5.14. From this figure and performance measures it is found that this lumped time-series MLR models behave same as that of ARIMA (2-1-2) model. This may be due to large data set, which might have completely captured the stochasticity. However the overall performance is not convincing, hence to improve the performance further, the causing parameter viz. rainfall is introduced as the input in the model development and is named as cause-effect MLR models.

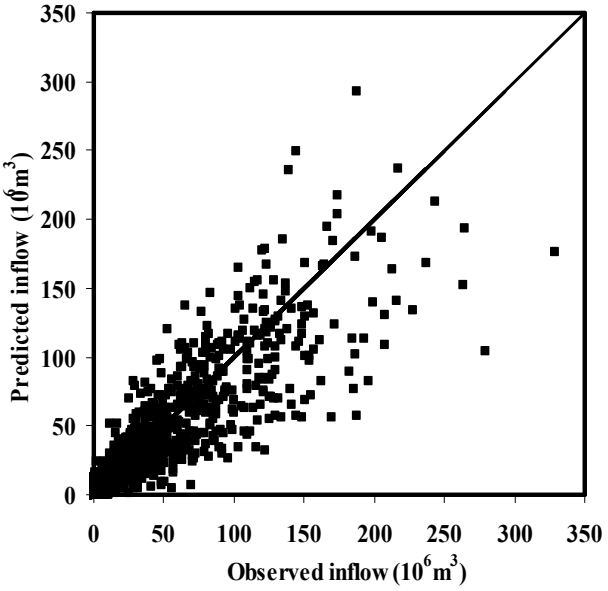

Figure 5.14. Scatter plot of observed and 1 day ahead predicted inflow by time-series DL-MLR model 6 during testing period

From Table 5.13, it can be seen that the DL-MLR model 8 to DL-MLR model 16 are cause-effect models. In this model type, it is assumed that the output (inflow in this case) is caused by the lumped rainfall (exogenous input parameter) over the entire catchment area. In this type, the models are redeveloped and from the performances during training and testing it is found that there is gradual improvement with increase in number of inputs up to 7 day lags i.e. (from DL-model 8 to DL-model 15) and thereafter the performance is decreasing. Among the cause-effect models DL-MLR model 15 which used 8 inputs has obtained best statistics than any other models. In this type also the model performance is deteriorating as lead time increases from 1 day to 3 day. This could be attributed to the low dependency between the values separated by higher lags. The number of input is same as that of prominent lag resulted from the cross correlation plot. It is also found that the time-series models are performing better than cause-effect models. The reason may be due to the better autocorrelation of inflow data than the serial correlation of rainfall. From the results it may be seen that for a linear reservoir condition where there is no prominent storage, ACF gives better indication of number of inputs required for time-series models and cross correlation plot indicates same for cause-effect models. The scatter plot of observed and predicted inflow by best cause-effect DL-MLR model 15 during testing period is shown in Table 5.13. From the Figure and performance measures it is found that cause-effect MLR models behave slightly inferior to time-series MLR models. Since the cause-effect models have not

performed satisfactorily, further improvement in the model has been sought by using combined inputs while model development.

Since, it is found that either rainfall data (causing variable) alone or inflow data (effective variable) alone is insufficient to reproduce the inflows in an effective way, both rainfall and inflow are given as input and named as combined models. The performances of the developed combined DL-MLR models i.e. DL-MLR model 17 to DL-MLR model 20 are shown in Table 5.13. From the table, it is apparent that all the combined DL-MLR models found to be better than previous time-series, and cause-effect DL-MLR models as well as ARIMA models. However among the combined models, DL-MLR model 18 which used input structure as P(t-1),P(t) and Q(t) is showing better performance. Hence, DL-MLR model 18 is selected as best MLR model among lumped input data MLR models (including time-series and cause-effect models). It is also to be noted that the number of data points during training and testing are different leading to skewed AIC and BIC values during training and testing. The combined input is responsible for the reduction in RMSE, AIC, BIC to greater extent. Thus it may be concluded that while developing a lumped reservoir inflow prediction model, having impulse response to rainfall, combined input models may result in better scenario.

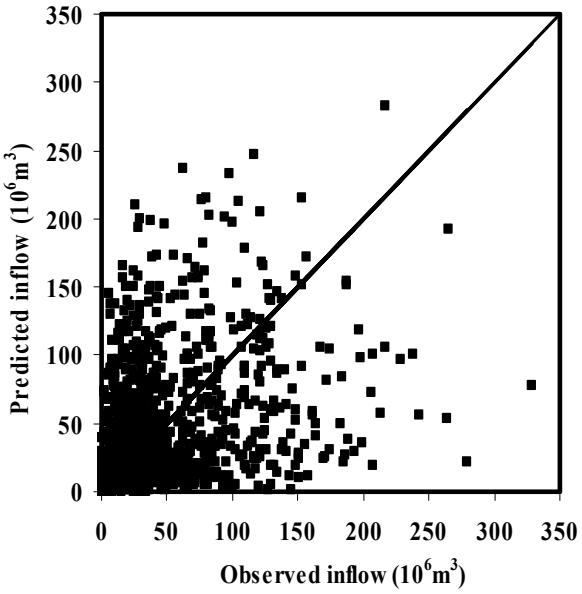

Figure 5.15. Scatter plot of observed and 1 day ahead predicted inflow by cause-effect DL-MLR model 15 during testing period

Table 5.13. Performance measures of daily lumped data MLR models

Models	Performance Criteria	Training			Testing		
		Lead period			Lead period		
		1 day	2day	3 day	1 day	2day	3 day
Time-series models							
DL-MLR Model 1	R	0.56	0.53	0.50	0.51	0.48	0.50
	E	0.54	0.53	0.48	0.50	0.47	0.52
	RMSE	17.98	18.21	18.47	18.16	18.31	18.52
	AIC	34724.36	34878.17	35042.59	14935.44	14977.69	15036.78
	BIC	34731.75	34885.56	35049.99	14941.99	14984.23	15043.33
DL-MLR Model 2	R	0.62	0.58	0.55	0.58	0.48	0.50
	E	0.56	0.55	0.50	0.47	0.47	0.52
	RMSE	17.64	17.37	18.19	17.89	18.20	18.25
	AIC	34496.71	34307.06	34863.49	14857.04	14946.96	14960.83
	BIC	34504.11	36473.33	34870.88	14863.58	14953.51	14967.37
DL-MLR Model 3	R	0.64	0.62	0.59	0.61	0.59	0.55
	E	0.61	0.53	0.51	0.58	0.52	0.51
	RMSE	17.59	17.66	18.01	17.67	17.98	18.23
	AIC	34456.66	34505.58	34743.27	14793.94	14883.04	14952.86
	BIC	34464.05	34512.97	34750.66	14800.49	14889.59	14959.4
DL-MLR Model 4	R	0.66	0.63	0.60	0.62	0.60	0.57
	E	0.63	0.60	0.58	0.59	0.55	0.54
	RMSE	16.70	16.99	17.00	17.06	17.35	17.92
	AIC	33833.89	34045.4	34050.67	14613.81	14699.78	14865.31
	BIC	33841.28	34052.87	34058.07	14620.36	14706.32	14871.85
DL-MLR Model 5	R	0.67	0.65	0.61	0.65	0.64	0.60
	E	0.63	0.62	0.59	0.63	0.62	0.62
	RMSE	16.37	16.64	16.96	16.90	16.96	17.34
	AIC	33592.2	33790.66	34022.35	14565.01	14581.17	14697.64
	BIC	33599.6	33798.06	34029.75	14571.55	14587.72	14704.18
DL-MLR Model 6	R	0.70	0.68	0.64	0.67	0.62	0.59
	E	0.66	0.60	0.53	0.59	0.57	0.56
	RMSE	15.99	17.06	18.56	16.21	17.23	18.83
	AIC	33316.25	34090.42	35106.71	14349.81	14664.83	15121.76
	BIC	33323.65	34097.82	35114.1	14356.35	14671.38	15128.3
DL-MLR Model 7	R	0.65	0.62	0.58	0.61	0.57	0.50
	E	0.61	0.58	0.55	0.58	0.56	0.45
	RMSE	15.25	16.12	17.38	15.31	15.68	15.99
	AIC	32745.65	33410.11	34312.63	14055.61	14176.87	14280.63
	BIC	32753.04	33417.51	34320.03	14062.15	14183.41	14287.18
Cause-effect models							
DL-MLR Model 8	R	0.55	0.52	0.50	0.52	0.50	0.45
	E	0.45	0.43	0.44	0.40	0.37	0.35
	RMSE	19.17	19.23	19.25	19.46	20.14	20.80
	AIC	35495.64	35530	35544.27	15291.02	15467.53	15634.03
	BIC	35503.03	35537.4	35551.67	15297.57	15474.08	15640.58

DL-MLR Model 9	R	0.58	0.55	0.52	0.55	0.52	0.48
	E	0.55	0.54	0.42	0.46	0.50	0.47
	RMSE	19.17	19.23	19.25	19.46	20.14	20.80
	AIC	35495.64	35530	35544.27	15291.02	15467.53	15634.03
	BIC	35503.03	35537.4	35551.67	15297.57	15474.08	15640.58
DL-MLR Model 10	R	0.60	0.58	0.55	0.57	0.54	0.50
	E	0.58	0.56	0.45	0.48	0.45	0.48
	RMSE	19.12	19.26	19.18	19.23	19.36	19.69
	AIC	35462.89	35546.22	35497.44	15229.13	15262.94	15351.46
	BIC	35470.28	35553.61	35504.83	15235.68	15269.49	15358
DL-MLR Model 11	R	0.62	0.58	0.56	0.58	0.55	0.53
	E	0.67	0.55	0.46	0.49	0.47	0.49
	RMSE	18.86	19.20	19.00	19.12	19.41	19.72
	AIC	35298.25	35513.74	35386.87	15200.37	15277.39	15358.08
	BIC	35305.64	35521.13	35394.26	15206.91	15283.94	15364.63
DL-MLR Model 12	R	0.62	0.58	0.56	0.59	0.55	0.54
	E	0.66	0.55	0.47	0.50	0.48	0.50
	RMSE	19.12	19.33	19.03	19.17	19.15	19.94
	AIC	35462.89	35591.07	35406.46	15213.91	15208.17	15416.98
	BIC	35470.28	35598.47	35413.86	15220.46	15214.71	15423.53
DL-MLR Model 13	R	0.63	0.59	0.58	0.58	0.56	0.56
	E	0.62	0.56	0.49	0.52	0.49	0.52
	RMSE	18.92	19.41	19.15	19.18	19.41	19.46
	AIC	35331.74	35641.18	35477.81	15215.17	15277.39	15291.02
	BIC	35339.13	35648.57	35485.21	15221.72	15283.94	15297.57
DL-MLR Model 14	R	0.63	0.60	0.55	0.62	0.57	0.55
	E	0.61	0.56	0.50	0.54	0.50	0.52
	RMSE	18.89	19.46	19.20	19.30	18.98	19.04
	AIC	35313.25	35672.66	35513.74	15249.17	15162.72	15179.16
	BIC	35320.64	35680.05	35521.13	15255.71	15169.27	15185.71
DL-MLR Model 15	R	0.66	0.64	0.60	0.63	0.58	0.56
	E	0.61	0.60	0.58	0.57	0.50	0.53
	RMSE	14.95	15.87	17.63	17.37	17.77	17.98
	AIC	32503.09	33220.9	34488.8	14706.18	14822.06	14882.32
	BIC	32510.48	33228.3	34496.19	14712.73	14828.6	14888.87
DL-MLR Model 16	R	0.54	0.53	0.52	0.50	0.50	0.45
	E	0.45	0.44	0.45	0.45	0.38	0.35
	RMSE	19.71	20.07	18.021	18.53	18.60	18.89
	AIC	35827.94	36042.87	34746.78	15038.36	15056.43	15137.03
	BIC	35835.33	32791.42	34754.18	15044.9	15062.98	15143.57
Combined models							
DL-MLR Model 17	R	0.70	0.65	0.63	0.65	0.62	0.60
	E	0.63	0.60	0.62	0.57	0.61	0.59
	RMSE	14.10	15.31	18.02	18.53	18.60	18.89
	AIC	31802.67	32791.42	34746.78	15038.36	15056.43	15137.03
	BIC	31810.06	32798.81	34754.18	15044.9	15062.98	15143.57
DL-MLR	R	0.84	0.82	0.77	0.80	0.79	0.74
	E	0.69	0.68	0.57	0.66	0.62	0.54

Model 18	RMSE	14.57	16.06	16.70	14.83	16.64	17.29
	AIC	32199.94	33363.02	33833.89	13891.64	14483.66	14680.47
	BIC	32207.33	33370.41	33841.28	13898.19	14490.21	14687.02
DL-MLR	R	0.67	0.65	0.62	0.71	0.68	0.65
	E	0.64	0.61	0.56	0.65	0.62	0.59
Model 19	RMSE	14.20	15.24	18.02	16.93	15.32	16.05
	AIC	31890.2	32734.8	34746.78	14574	14057.8	14299.57
	BIC	31897.6	32742.19	34754.18	14580.55	14064.35	14306.12
DL-MLR	R	0.65	0.62	0.60	0.69	0.66	0.63
	E	0.62	0. 59	0.50	0.66	0.65	0.61
Model 20	RMSE	14.55	14.91	18.29	16.33	15.64	15.74
	AIC	32180.12	32470.75	34928.99	14388.1	14165.53	14197.94
	BIC	32187.51	32478.14	34936.38	14394.65	14172.08	14204.48

Figure 5.16 show the scatter plots between the actual observations and corresponding predictions for different lead times of 1 day, 2 day and 3 day during testing period by combined DL-MLR model 18. Visual inspection of these Figures reveals that the performances of the models are deteriorating with increase in lead period, especially peak values. In all the MLR models, 1 day ahead prediction was found to produce more acceptable results, may be because of higher correlation with 1 day ahead input and output. The poor performance of higher lead period may be due to non-linear relationship between current inflow and higher order input variables. The other important point is that if length of data is sufficiently large, a both deterministic and stochastic linear model performs similar. Nevertheless further improvement in inflow prediction is needed to capture the complex and non-linear peak inflows. In the following section soft computing techniques like ANN, ANFIS and LGP are applied to capture the non-linear nature of the reservoir inflows and discussed.

5.2.2.2 Daily Lumped Data TDRNN Models (ANN)

Previous results of deterministic (MLR) and stochastic (ARIMA) linear models showed that the moderate and peak inflows are poorly predicted. This may due to the non-linear relationship between rainfall and inflow. Hence commonly used non-linear modelling technique such as ANN has been applied and the results are discussed in this section. Most of the ANN applications in hydrology have used a feed forward neural network, namely the standard multilayer perceptron (MLP) trained with the back-propagation algorithm. Since MLP is a static and memory less network, it often yielded suboptimal solution even though it is the most widely used network for water resource variables predictions. In fact, MLP model

does not perform temporal processing and the input vector space does not consider the temporal relationship of the inputs. In order to overcome this drawback, in the present study, the network which remembers the past pattern in the training set namely time delay recurrent neural network (TDRNN) has been used. TDRNN consist of two components first one is time-delay operators, which are arranged in an incremental order. The second components, is involving initial and past states of a system through recurrent (feedback) connection. This connection recurs either from the output layer or from the hidden layer back to a context unit and after one time step returns to the input layer. TDRNN explicitly considers temporal processing in order to perform dynamically.

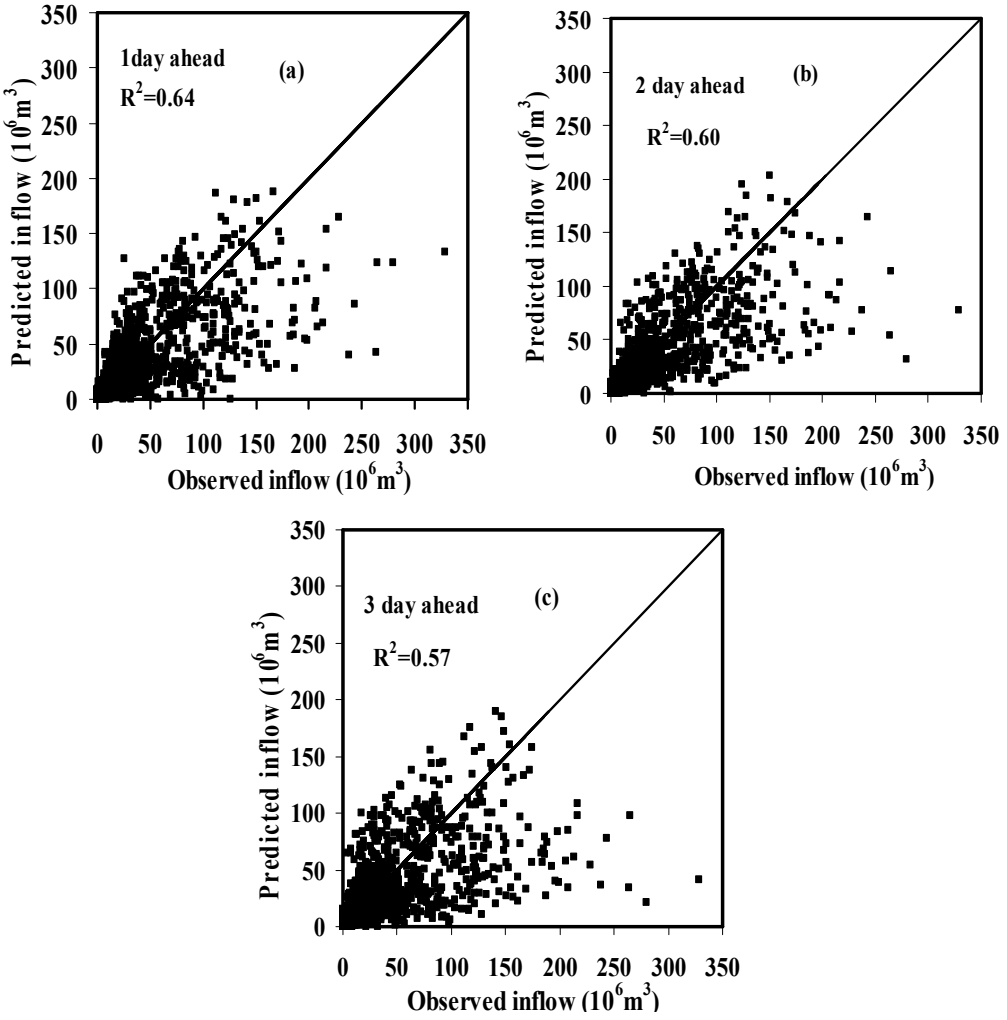

Figure 5.16. Scatter plot of observed and multi-time-step ahead predicted inflow by DL-MLR model 18 during testing period (combined input)

A major feature of TDRNN architecture is that the non-linear hidden layer receives the contents of both the input time delays and the context unit, which makes it suitable for complex sequential input learning. Despite the past work there is a need to explore effectiveness of the TDRNN models for shorter time intervals and also for Indian conditions. Multi-input multi-output (MIMO) architecture was selected, for different models for capturing the complex, dynamic, and non-linear, rainfall–inflow process in the basin. The determination of the number of neurons in each layer is also an essential task. The number of neurons in the input layer and the output layer can be specified according to the number of predictors and predictants, respectively. The output vector in the output layer is three neurons representing the inflow at 1 day, 2 day and 3 day ahead. The next step in the development of the ANN model is the determination of the optimum number of neurons in the hidden layer. The number of neurons in the hidden layer was varied from 2 to 20 and best architecture was finalized to capture the rainfall-inflow relationship. TDRNN type of network with dynamic memory of time delay, gamma and laguerre are used for improving the network performance. The performance summary of various TDRNN models developed with daily data during training and testing period is displayed in Table 5.14. Unlike MLR and ARIMA models ANN requires single model to predict the multi-time-step ahead inflow.

For comparison, initially lumped time-series ANN models namely DL-ANN model 1 to DL-ANN model 7 (Table 5.14) are considered. From this Table it is seen that model performance is improving up to a lagged input of six days and then gradually decreases. From Table 5.14 it is evident that DL-ANN model 6 with 1 day lead period has yielded best statistics and is selected as the best lumped time-series ANN model. It is observed that best time-series ANN model performed better than time-series MLR model with an improvement in ‘R’ value (of about 32%) and in ‘E’ value (38%) inspite of same numbers of inputs. It is also found that there is significant improvement in performance over the best lumped combined MLR model. Lumped ANN models overcome the limitation of the conventional approaches by extracting the desired information directly from the data and also mapping the non-linear relationship. The scatter plot of best time-series DL-ANN model 6 during testing period is shown in Figure Figure 5.17. From this Figure and the performance measures it may be concluded that this lumped time-series ANN model also failed to predict peak inflows accurately.

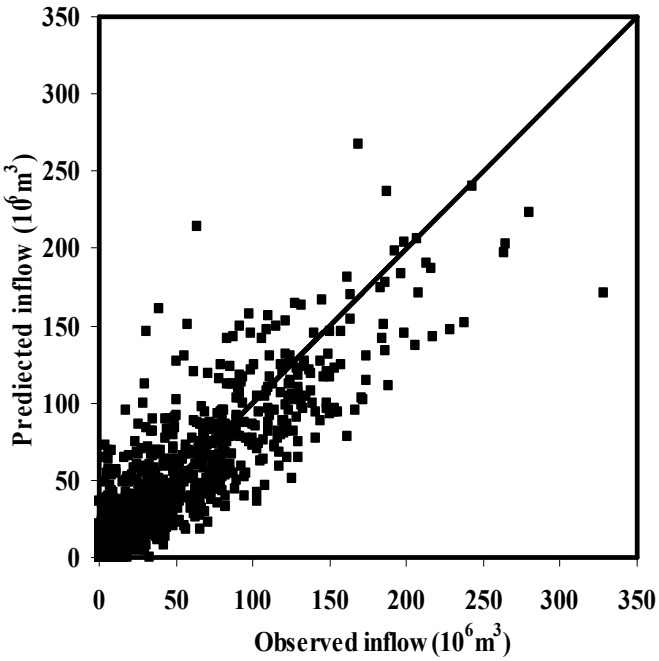

Figure 5.17. Scatter plot of observed and 1 day ahead predicted inflow by time-series DL-ANN model 6 during testing period

On studying the lumped ANN cause-effect models namely DL-ANN model 8 to DL-ANN model 16 (Table 5.14) it can be observed that the performance of the models during training and testing are comparable. In this case also the lumped cause-effect DL-ANN model 15 which used eight inputs has obtained best statistics and outperformed other lumped cause-effect models. Also as the forecast time horizon increases from 1 day to 3 day the model performance deteriorated. In this type, R value drop from 0.82 to 0.73 from 1 day to 3 day lead period. The performances of lumped ANN cause-effect models are comparatively inferior to the lumped ANN time-series models. The reason may be due to the difficulty in capturing the pattern in input and output data. The time-series models has only one pattern where as the cause-effect models have two different pattern (In time-series models the input and output has same pattern however in the cause-effect models, the pattern of input and output is different). The scatter plot of best cause-effect DL-ANN model 15 during testing period is shown in Figure 5.18. From the scatter plot and the performance it may be seen that of the cause-effect models also failed to predict the medium and high inflows accurately. Hence further combined models have been developed.

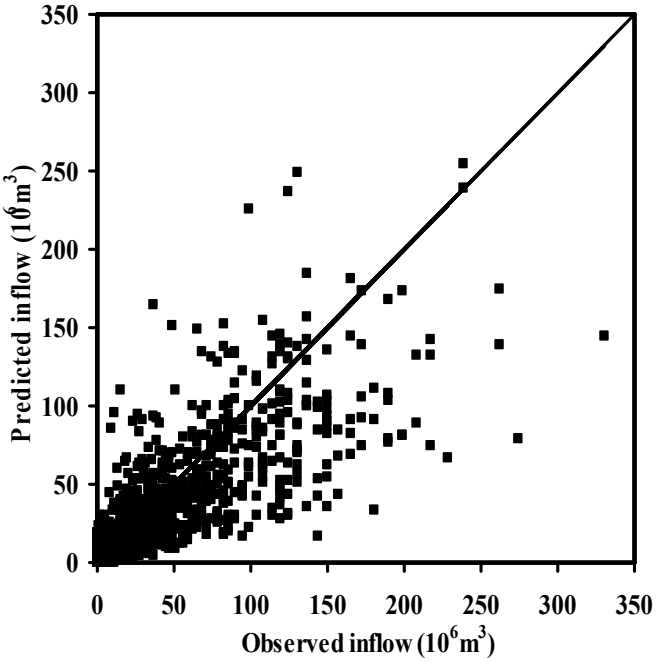

Figure 5.18. Scatter plot of observed and 1 day ahead predicted inflow by cause-effect DL-ANN model 15 during testing period

Analyzing the results of lumped combined ANN models (DL-ANN model 17 to DL-ANN model 20) showed comparable performance during training and testing (Table 5.14). From the Table, it is also clear that the overall combined DL-ANN model 18 (3-6-3) obtained best performances during training and testing. DL-ANN model 18 with a lead period of 1 day obtained maximum R (0.94), E (0.90) and minimum RMSE (8.55), AIC (11051.7) and BIC (11058.24), during testing and thus appears to be a parsimonious model. Hence, DL-ANN model 18 is selected as the best model among all the ANN models. The scatter plot of observed inflow and the multi-time-step ahead predicted inflow resulted from DL-ANN model 18 during testing period is shown in Figure 5.19. The identified lumped ANN model resulted in reasonably accurate prediction of medium inflow but not the peak inflows. The reason is that the RR inflow relationship may be highly non-linear. The shift from the ideal line may be due to the possibility of systematic errors. The resulted network architecture for ANN model with gamma memory is shown in Figure 5.20. Even though the lumped ANN models performed better than lumped MLR models there is further scope for improvement especially in moderate and peak inflow prediction. Hence ANFIS technique is employed and described in next section.

Table 5.14. Performance measures of daily lumped data ANN models (TDRNN)

Model	Model Type	Performance Criteria	Training			Testing		
			Prediction time horizon			Prediction time horizon		
			1 day	2day	3 day	1 day	2day	3 day
Time-series model								
DL-ANN Model 1	(1-3-3)	R	0.78	0.66	0.60	0.64	0.62	0.60
		E	0.76	0.64	0.56	0.63	0.59	0.50
		RMSE	12.11	12.61	13.0	13.03	13.14	13.63
		AIC	29973.06	30465.4	30830.6	13223.95	13266.3	13456.77
		BIC	29980.46	30472.8	30838.00	13230.50	13272.9	13463.32
DL-ANN Model 2	(2-5-3)	R	0.80	0.70	0.70	0.65	0.68	0.66
		E	0.78	0.66	0.64	0.70	0.65	0.62
		RMSE	11.69	12.22	12.62	12.18	12.35	12.49
		AIC	29548.95	30074.9	30465.7	12875.38	12949.31	13003.56
		BIC	29556.35	30082.3	30473.19	12881.93	12955.8	13010.11
DL-ANN Model 3	(3-5-3)	R	0.85	0.79	0.73	0.70	0.73	0.70
		E	0.83	0.76	0.70	0.73	0.74	0.58
		RMSE	11.26	11.80	11.83	11.76	12.27	12.05
		AIC	29092.62	29658.2	29686.24	12695.64	12915.35	12820.46
		BIC	29100.01	29665.65	29693.63	12702.19	12921.90	12827.01
DL Model 4	(4-3-3)	R	0.88	0.80	0.75	0.71	0.75	0.71
		E	0.85	0.78	0.71	0.74	0.64	0.60
		RMSE	10.62	11.67	12.01	11.50	11.39	11.50
		AIC	28389.24	29527.38	29871.06	12581.06	12528.36	12581.45
		BIC	28396.63	29534.78	29878.45	12587.61	12534.91	12588.00
DL-ANN Model 5	(5-4-3)	R	0.90	0.80	0.75	0.71	0.75	0.71
		E	0.80	0.78	0.71	0.74	0.66	0.61
		RMSE	10.62	11.67	12.01	11.50	11.39	11.50
		AIC	28389.2	29527.38	29871.06	12581.06	12528.36	12581.45
		BIC	28396.63	29534.78	29878.45	12587.61	12534.91	12588.00
DL-ANN Model 6	(6-4-3)	R	0.88	0.78	0.75	0.89	0.76	0.73
		E	0.81	0.69	0.63	0.82	0.66	0.60
		RMSE	12.79	12.35	11.00	11.06	11.25	11.06
		AIC	13127.6	12947.3	12351.16	12378.68	12467.86	12379.10
		BIC	13134.1	12953.8	12357.71	12385.23	12474.41	12385.65
DL Model 7	(7-4-3)	R	0.88	0.80	0.73	0.86	0.80	0.74
		E	0.81	0.72	0.70	0.73	0.78	0.72
		RMSE	10.80	11.24	11.63	11.48	13.29	12.81
		AIC	28597.72	29073.62	29483.56	12569.36	13326.80	13137.29
		BIC	28605.11	29081.01	29490.96	12575.90	13333.35	13143.84
Cause-effect models								
DL-ANN Model	(1-3-3)	R	0.78	0.72	0.70	0.77	0.75	0.74
		E	0.73	0.70	0.67	0.68	0.72	0.65
		RMSE	12.4	12.62	12.94	12.68	12.86	12.98

8		AIC	30324.57	30464.28	30766.36	13084.86	13155.73	13201.87
		BIC	30331.96	30471.68	30773.75	13091.40	13162.28	13208.42
DL-ANN Model 9	(2-4-3)	R	0.83	0.73	0.68	0.81	0.74	0.72
		E	0.74	0.70	0.65	0.68	0.66	0.63
		RMSE	12.35	12.22	12.14	12.53	12.66	12.58
		AIC	30207.57	30074.57	30002.07	13020.03	13076.68	13044.21
		BIC	30214.96	30081.97	30009.46	13026.57	13083.23	13050.75
DL-ANN Model 10	(3-4-3)	R	0.81	0.77	0.72	0.80	0.75	0.74
		E	0.75	0.72	0.66	0.70	0.68	0.65
		RMSE	12.35	12.42	12.59	12.62	12.70	12.78
		AIC	30207.17	30272.59	30434.40	13058.31	13092.05	13123.93
		BIC	30214.57	30279.98	30441.79	13064.86	13098.60	13130.48
DL-ANN Model 11	(4-3-3)	R	0.81	0.76	0.72	0.80	0.75	0.74
		E	0.75	0.73	0.66	0.70	0.68	0.65
		RMSE	12.35	12.42	12.59	12.62	12.30	12.38
		AIC	30207.17	30272.59	30434.40	13058.31	12927.29	12961.26
		BIC	30214.57	30279.98	30441.79	13064.86	12933.83	12967.81
DL-ANN Model 12	(5-4-3)	R	0.80	0.76	0.72	0.80	0.74	0.73
		E	0.73	0.70	0.66	0.68	0.68	0.63
		RMSE	12.23	12.42	12.63	12.58	12.38	12.46
		AIC	30087.85	30272.59	30472.20	13042.25	12960.76	12994.13
		BIC	30095.24	30279.98	30479.60	13048.80	12967.30	13000.68
DL-ANN Model 13	(6-4-3)	R	0.80	0.78	0.74	0.78	0.74	0.73
		E	0.75	0.73	0.68	0.69	0.67	0.63
		RMSE	12.06	11.55	11.71	11.80	11.89	12.20
		AIC	29924.96	29403.06	29571.76	12711.42	12752.35	12885.09
		BIC	29932.36	29410.45	29579.16	12717.96	12758.90	12891.63
DL-ANN Model 14	(7-6-3)	R	0.82	0.76	0.75	0.80	0.74	0.70
		E	0.76	0.77	0.70	0.72	0.70	0.66
		RMSE	11.94	12.09	12.17	12.18	12.22	12.34
		AIC	29798.15	29953.79	30034.58	12874.17	12892.69	12943.91
		BIC	29805.54	29961.18	30041.97	12880.71	12899.23	12950.45
DL-ANN Model 15	(8-4-3)	R	0.84	0.78	0.78	0.82	0.75	0.73
		E	0.75	0.72	0.67	0.76	0.72	064
		RMSE	11.84	11.56	12.27	11.80	11.89	12.20
		AIC	29699.35	29411.7	30128.00	12711.42	12752.35	12885.09
		BIC	29706.7	29419.1	30135.40	12717.96	12758.90	12891.63
DL-ANN Model 16	(9-5-3)	R	0.80	0.76	0.70	079	0.73	0.70
		E	0.75	0.70	0.68	0.76	0.68	0.67
		RMSE	11.63	11.71	11.88	11.84	11.88	12.21
		AIC	29484.01	29571.32	29744.79	12728.75	12747.25	12890.44
		BIC	29491.40	29578.72	29752.19	12735.30	12753.79	12896.99
Combined models								
DL-ANN Model 17	(2-4-3)	R	0.85	0.82	0.78	0.86	0.73	0.71
		E	0.80	0.77	0.73	0.77	0.82	0.80
		RMSE	10.74	10.83	11.28	10.96	11.45	11.37
		AIC	28522.60	28624.94	29117.69	12332.15	12557.60	12519.81
		BIC	28529.99	28632.33	29125.09	12338.70	12564.14	12526.35

DL-ANN Model 18	(3-6-3)	R	0.95	0.94	0.91	0.94	0.92	0.92
		E	0.92	0.87	0.83	0.90	0.85	0.82
		RMSE	8.37	10.45	10.93	8.55	10.56	10.74
		AIC	25532.96	28194.23	28743.68	11051.70	12142.23	12230.26
		BIC	25540.36	28201.62	28751.08	11058.24	12148.78	12236.80
DL-ANN Model 19	(5-4-3)	R	0.86	0.82	0.78	0.84	0.81	0.75
		E	0.78	0.76	0.70	0.80	0.71	0.65
		RMSE	9.95	10.59	11.10	10.40	10.92	11.01
		AIC	27613.12	28364.14	28924.83	12063.49	12313.65	12356.05
		BIC	27620.51	28371.53	28932.22	12070.04	12320.19	12362.60
DL-ANN Model 20	(7-3-3)	R	0.84	0.80	0.79	0.82	0.79	0.76
		E	0.77	0.73	0.69	0.74	0.69	0.69
		RMSE	10.15	11.19	11.37	10.64	11.06	11.18
		AIC	27843.95	29020.11	29214.64	12179.35	12379.10	12436.97
		BIC	27851.34	29027.51	29222.03	12185.90	12385.65	12443.51

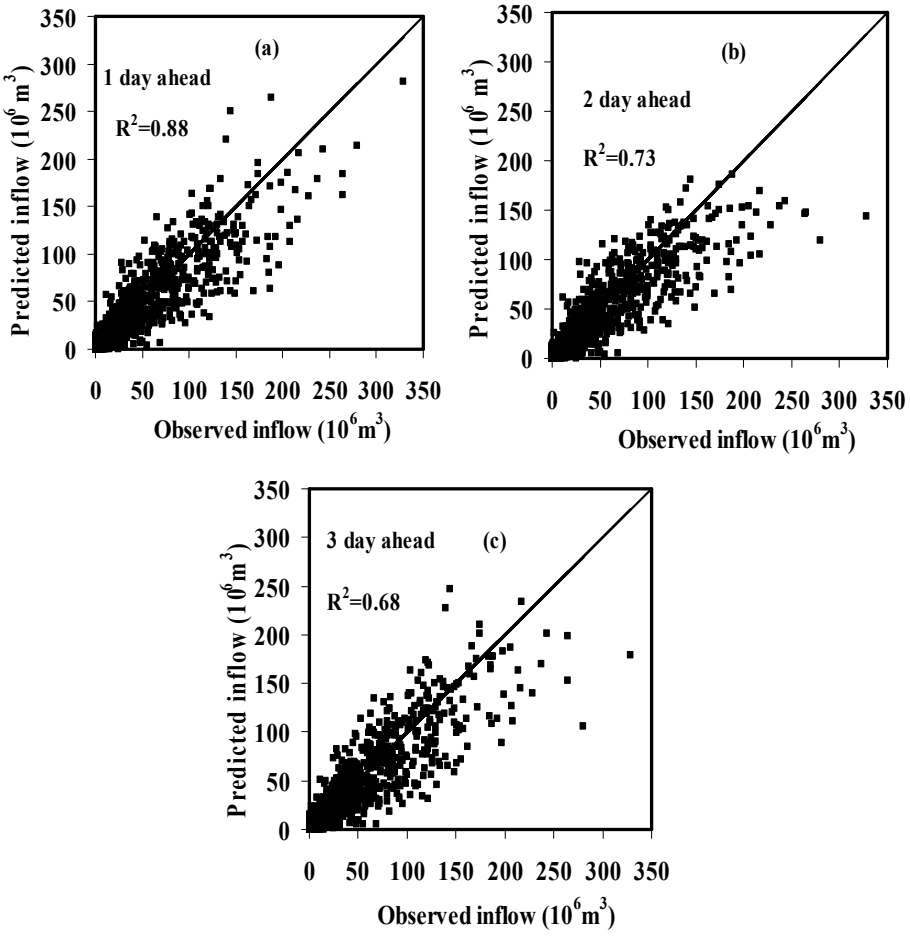

Figure 5.19. Scatter plot of observed and multi-time-step ahead predicted inflow by best DL-ANN model 18 during testing period (combined input)

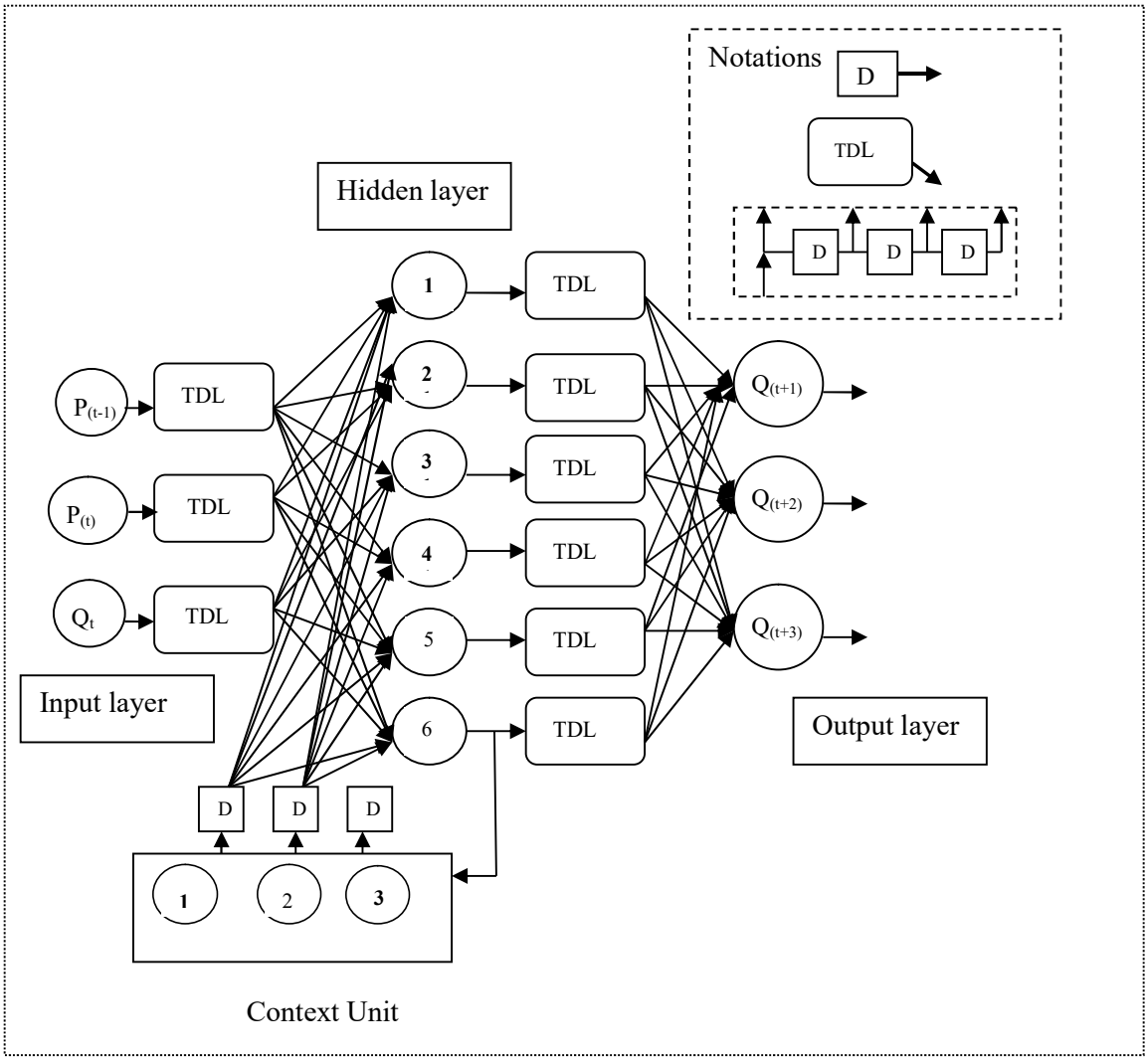

Figure 5.20. Typical ANN structure of best combined DL-ANN model 18

5.2.2.3 Daily Lumped Data ANFIS Models

The neuro-fuzzy approach combines the advantages of fuzzy logic and neural network to design an architecture that uses a fuzzy logic to represent knowledge in an interpretable manner. It also self-organizes the network structure and adapts the parameters of fuzzy system for predicting the reservoir inflow. A specific approach in neuro-fuzzy development is the adaptive neuro-fuzzy inference system (ANFIS), which has shown significant results in modelling non-linear functions. ANFIS uses the learning ability of the ANN to define the input–output relationship and constructs the fuzzy rules by determining the input structure. The system results were obtained by thinking and reasoning capability of the fuzzy logic. The hybrid-learning algorithm and subtractive function are used to determine the input structure. There are two types of fuzzy inference system in the literature: the Sugeno–Takagi (ST) inference system and the Mamdani inference system. In this study, the ST inference system is

used for hydrological time-series modelling. The most important difference between these systems is the definition of the consequence parameter. The consequence parameter in the ST inference system is a linear equation, called a 'first-order ST inference system, or a constant coefficient, called a 'zero-order ST inference system'. In the present study, various ANFIS models have been developed with input and output parameters same as that of ANN models, however the membership functions (MFs) are varied. In case of ANFIS models, number of membership function associated with each input variable is fixed by trial and error. Excess number of MFs on the input variable will increase the number of "if-then" fuzzy rules and simultaneously increases the model complexity and hence affect the model parsimony. Hence numbers of MFs are varied between two to four. The parsimonious structure that resulted in minimum error and maximum efficiency during training and testing were selected as the final form of ANFIS model. Due to smoothness and concise notation, the bell membership functions are increasingly popular for specifying fuzzy sets. The bell shaped membership functions have one more parameter than Gaussian membership functions, thus fuzzy set can be approached when the free parameter is tuned, and the same is adopted in this study. The resulted statistical performances of all the ANFIS models are shown in Table 5.15.

For comparison, initially the time-series models namely DL-ANFIS model 1 to DL-ANFIS model 7 are considered and discussed in this section (Table 5.15). From the Table, it is observed that the model performance is gradually increasing with increase in the input variables up to five and then gradually decreases. The performance of the lumped time-series DL-ANFIS model 5 has resulted in a better performance amongst all the lumped ANFIS time-series models. Since AIC and BIC values are least than any other model, indicating that DL-ANFIS model 5 is relatively parsimonious. Lumped time-series ANFIS models performed better than lumped time-series ANN model. The superiority of the ANFIS to ANN method may be due to fuzzy partioning of the inputs space and creating a rule-base to generate the output. The scatter plot of best time-series ANFIS model during testing period is shown in Figure 5.21. From this Figure, it may be observed that the lumped time-series ANFIS model failed to capture peak inflows accurately, hence for further improvement cause-effect models are developed and discussed.

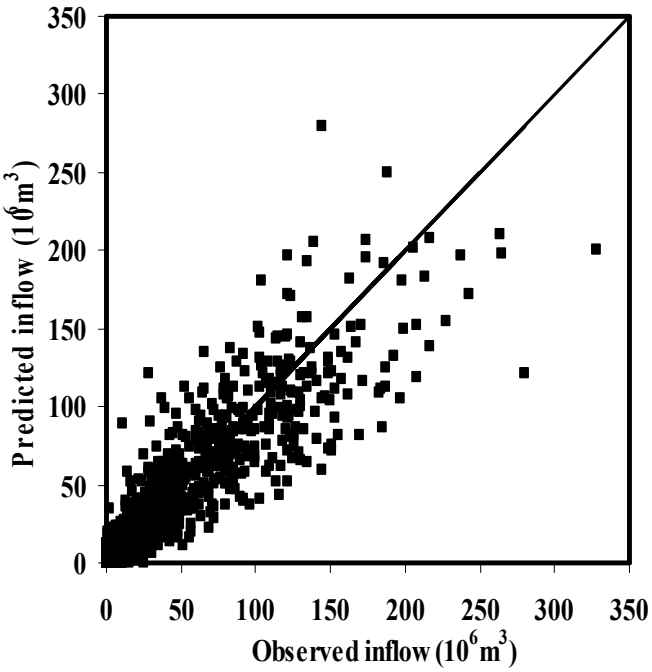

Figure 5.21. Scatter plot of observed and 1 day ahead predicted inflow by time-series DL-ANFIS model 5 during testing period

Analyzing the results of cause-effect models (Table 5.15) it is found that the performances of all the models are comparatively similar and comparable. But among the cause-effect ANFIS models, DL-ANFIS model 14 is slightly better than any other cause-effect ANFIS models. DL-ANFIS model 14 with 1 day lead period displayed best statistics with maximum of R (0.92) and E (0.87). As the lead period increases from 1 day, 2 day to 3 day the R value drops from (0.92) to (0.81). Hence it is found that there is gradual deterioration in performances from 1 day lead period to 3 day lead period.

The scatter plot of observed and predicted inflow of the best cause-effect DL-ANFIS model 14 during testing period is shown in Figure 5.22. From this figure it is found that the performances of both time-series and cause-effect model are almost similar and no significant improvement is found in the peak inflow prediction. Thus it may be concluded that the ANFIS model has resulted in equal performance for time-series and cause-effect input data.

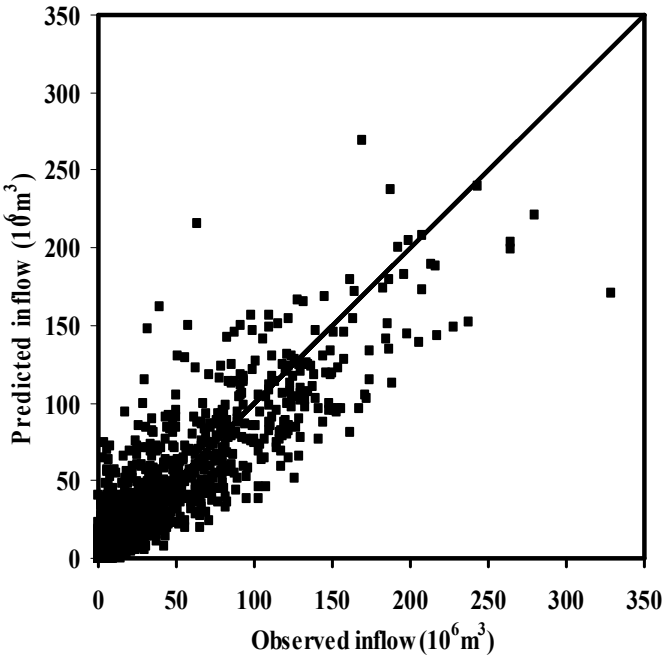

Figure 5.22. Scatter plot of observed and 1 day ahead predicted inflow by cause-effect DL-ANFIS model 14 during testing period

Studying the performance of combined models (DL-ANFIS model 17 to DL-ANFIS model 20) it is found that DL-ANFIS model 18 performed better than any other model. It is also observed that all the lumped time-series and lumped combined ANFIS models performed better with three membership functions where as cause-effect models performed better with two memberships function. The combined DL-ANFIS model 18 with 1 day lead period obtained best values of R (0.96), E (0.91), RMSE (8.07), AIC (10753.42) and BIC (10759.97). Thus from the above results, it may be concluded that the lumped DL-ANFIS model 18, which used 3 inputs outperformed the other ANFIS models. The scatter plot of DL-ANFIS model 18 with lead period of 1 day, 2 day and 3 day is shown in Figure 5.11. From the scatter plots it can be seen that low and medium inflows are well predicted by the model but peak inflows are under predicted. It is also observed that prediction of ANFIS model at higher lead period (3 day) is found to be better than those from other lumped ANN and lumped MLR models. The final ANFIS structure for the best DL-ANFIS model 18 with five layers is shown in Figure 5.24. The initial and final membership function for DL-ANFIS model 18 is shown in Figure 5.25(a) and Figure 5.25(b). From this membership functions it is seen that the inflows (60 to 200 X 10^6 m^3) has large number fuzzy rules and predicted well. But still the peak inflows are under predicted. To improve the peak inflow prediction, applicability of LGP technique is employed and described.

Table 5.15. Performance measures of daily lumped data ANFIS models

Models	Membership function	Performance Criteria	Training			Testing		
			Lead period			Lead period		
			1 day	2day	3 day	1 day	2day	3 day
Time-series models								
DL-ANFIS Model 1	3	R	0.83	0.78	0.69	0.68	0.67	0.66
		E	0.79	0.75	0.70	0.67	0.64	0.63
		RMSE	11.90	12.30	12.74	12.84	13.14	13.07
		AIC	29764.75	30155.36	30577.54	13146.84	13266.36	13240.13
		BIC	29772.14	30162.75	30584.94	13153.39	13272.91	13246.67
DL-ANFIS Model 2	3	R	0.84	0.79	0.71	0.70	0.70	0.68
		E	0.82	0.72	0.73	0.74	0.69	0.63
		RMSE	11.10	11.59	12.95	11.01	11.10	12.54
		AIC	28929.21	29443.00	30772.10	12357.96	12399.23	13026.75
		BIC	28936.61	29450.39	30779.49	12364.51	12405.78	13033.30
DL-ANFIS Model 3	3	R	0.87	0.82	0.79	0.76	0.74	0.72
		E	0.85	0.79	0.74	0.71	0.73	0.58
		RMSE	11.03	11.59	11.67	11.72	12.35	12.17
		AIC	28851.74	29438.08	29526.50	12677.33	12945.26	12873.13
		BIC	28859.13	29445.47	29533.89	12683.88	12951.81	12879.67
DL-ANFIS Model 4	3	R	0.91	0.87	0.85	0.85	0.80	0.76
		E	0.87	0.79	0.75	0.79	0.74	0.69
		RMSE	11.07	11.76	11.46	11.11	11.62	11.23
		AIC	28895.01	29614.08	29308.67	12404.45	12634.99	12455.63
		BIC	28902.41	29621.47	29316.07	12410.99	12641.54	12462.18
DL-ANFIS Model 5	3	R	0.94	0.88	0.86	0.90	0.88	0.85
		E	0.87	0.85	0.82	0.84	0.81	0.82
		RMSE	10.28	11.19	11.54	10.60	11.39	11.63
		AIC	28004.05	29020.59	29392.70	12159.02	12528.56	12639.18
		BIC	28011.44	29027.99	29400.09	12165.57	12535.11	12645.73
DL-ANFIS Model 6	3	R	0.92	0.87	0.85	0.86	0.83	0.81
		E	0.85	0.79	0.73	0.81	0.80	0.76
		RMSE	10.52	10.79	11.46	11.50	11.69	11.76
		AIC	28280.60	28578.12	29303.64	12581.06	12663.61	12695.64
		BIC	28287.99	28585.51	29311.03	12587.61	12670.16	12702.19
DL-ANFIS Model 7	3	R	0.90	0.86	0.82	0.88	0.82	0.76
		E	0.85	0.80	0.77	0.75	0.82	0.76
		RMSE	10.66	11.10	11.63	11.73	13.07	13.20
		AIC	28441.25	28929.21	29483.56	12684.07	13237.87	13289.53
		BIC	28448.64	28936.61	29490.96	12690.62	13244.41	13296.07
Cause-effect models								
DL-ANFIS Model 8	2	R	0.83	0.78	0.75	0.82	0.79	0.77
		E	0.78	0.73	0.69	0.72	0.72	0.69
		RMSE	12.27	12.30	12.94	12.28	12.70	12.86
		AIC	30126.69	30154.17	30766.36	12919.62	13092.69	13155.58
		BIC	30134.08	30161.56	30773.75	12926.17	13099.23	13162.12
DL-	2	R	0.90	0.85	0.78	0.88	0.82	0.79

ANFIS Model 9		E	0.82	0.80	0.71	0.75	0.79	0.69
		RMSE	12.27	11.84	12.14	12.36	12.55	12.30
		AIC	30125.89	29700.39	30002.07	12953.53	13028.06	12927.80
		BIC	30133.28	29707.79	30009.46	12960.07	13034.60	12934.34
DL-ANFIS Model 10	2	R	0.85	0.81	0.77	0.84	0.80	0.79
		E	0.79	0.78	0.71	0.73	0.72	0.69
		RMSE	12.27	12.34	12.26	12.70	12.82	12.70
		AIC	30126.29	30194.16	30122.30	13090.45	13139.18	13091.57
		BIC	30133.68	30201.56	30129.69	13097.00	13145.72	13098.12
DL-ANFIS Model 11	2	R	0.83	0.80	0.76	0.84	0.82	0.79
		E	0.78	0.76	0.72	0.74	0.75	0.69
		RMSE	12.31	12.26	12.18	12.26	12.22	12.30
		AIC	30167.66	30113.90	30041.47	12908.85	12893.03	12926.95
		BIC	30175.05	30121.30	30048.86	12915.39	12899.58	12933.49
DL-ANFIS Model 12	2	R	0.85	0.83	0.80	0.84	0.82	0.79
		E	0.79	0.77	0.69	0.75	0.80	0.69
		RMSE	12.23	12.42	12.63	12.58	12.38	12.46
		AIC	30087.85	30272.59	30472.20	13042.25	12960.76	12994.13
		BIC	30095.24	30279.98	30479.60	13048.80	12967.30	13000.68
DL-ANFIS Model 13	2	R	0.87	0.84	0.82	0.84	0.81	0.79
		E	0.81	0.78	0.75	0.79	0.85	0.69
		RMSE	12.06	12.17	12.22	11.59	12.30	12.26
		AIC	29924.96	30034.18	30083.02	12621.61	12925.76	12909.87
		BIC	29932.36	30041.57	30090.42	12628.16	12932.30	12916.42
DL-ANFIS Model 14	2	R	0.93	0.90	0.88	0.92	0.87	0.81
		E	0.89	0.85	0.79	0.87	0.76	0.69
		RMSE	11.41	11.55	11.71	11.80	11.89	12.20
		AIC	29257.69	29403.06	29571.76	12711.42	12752.35	12885.09
		BIC	29265.08	29410.45	29579.16	12717.96	12758.90	12891.63
DL-ANFIS Model 15	2	R	0.90	0.85	0.81	0.84	0.82	0.77
		E	0.87	0.82	0.76	0.76	0.76	0.69
		RMSE	11.94	12.09	12.17	12.18	12.22	12.34
		AIC	29798.15	29953.79	30034.58	12874.17	12892.69	12943.91
		BIC	29805.54	29961.18	30041.97	12880.71	12899.23	12950.45
DL-ANFIS Model 16	2	R	0.89	0.82	0.78	0.85	0.80	0.76
		E	0.75	0.79	0.69	0.80	0.76	0.72
		RMSE	11.63	11.71	11.88	11.84	11.88	12.21
		AIC	29484.01	29571.32	29744.79	12747.25	12747.25	12890.44
		BIC	29491.40	29578.72	29752.19	12753.79	12753.79	12896.99
Combined Models								
DL-ANFIS Model 17	2	R	0.90	0.87	0.85	0.88	0.82	0.79
		E	0.88	0.82	0.80	0.79	0.79	0.75
		RMSE	10.74	10.83	11.28	10.96	11.45	11.37
		AIC	28522.60	28624.94	29117.69	12332.15	12557.60	12519.81
		BIC	28529.99	28632.33	29125.09	12338.70	12564.14	12526.35
DL-ANFIS	3	R	0.94	0.92	0.90	0.96	0.95	0.93
		E	0.91	0.89	0.87	0.91	0.91	0.90

Model 18		RMSE	7.94	7.88	8.37	8.07	8.26	8.43
		AIC	24899.67	24809.44	25535.54	10753.42	10874.04	10982.75
		BIC	24907.07	24816.83	25542.93	10759.97	10880.59	10989.30
DL-ANFIS	3	R	0.92	0.89	0.88	0.91	0.82	0.79
		E	0.85	0.81	0.82	0.89	0.79	0.69
Model 19		RMSE	9.95	10.59	11.10	10.40	10.92	11.01
		AIC	27613.12	28364.14	28924.83	12063.49	12313.65	12356.05
		BIC	27620.51	28371.53	28932.22	12070.04	12320.19	12362.60
DL-ANFIS	3	R	0.89	0.85	0.82	0.86	0.84	0.82
		E	0.83	0.79	0.75	0.79	0.70	0.78
Model 20		RMSE	10.15	11.32	11.27	9.46	11.22	11.54
		AIC	27843.95	29161.44	29110.60	11571.79	12453.79	12599.29
		BIC	27851.34	29168.83	29118.00	11578.33	12460.34	12605.84

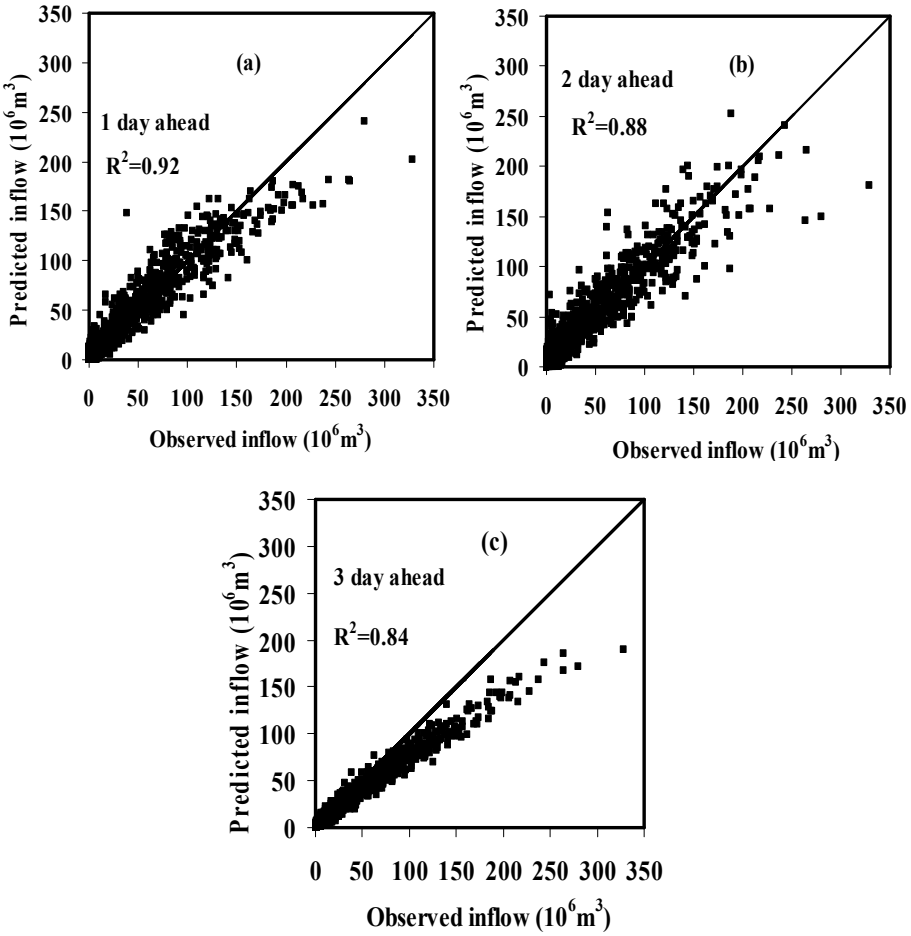

Figure 5.23. Scatter plot of observed and multi-time step ahead predicted inflow by DL-ANFIS model 18 during testing period (combined input)

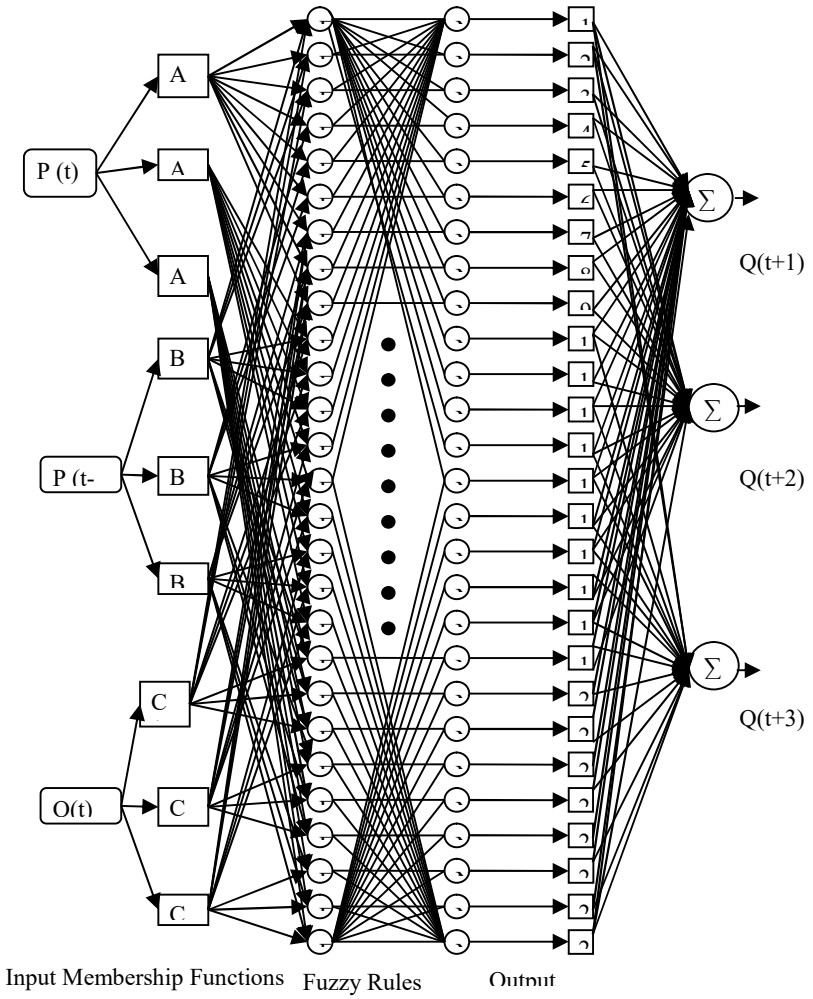

Figure 5.24. Final ANFIS structure of the combined DL-ANFIS model 18

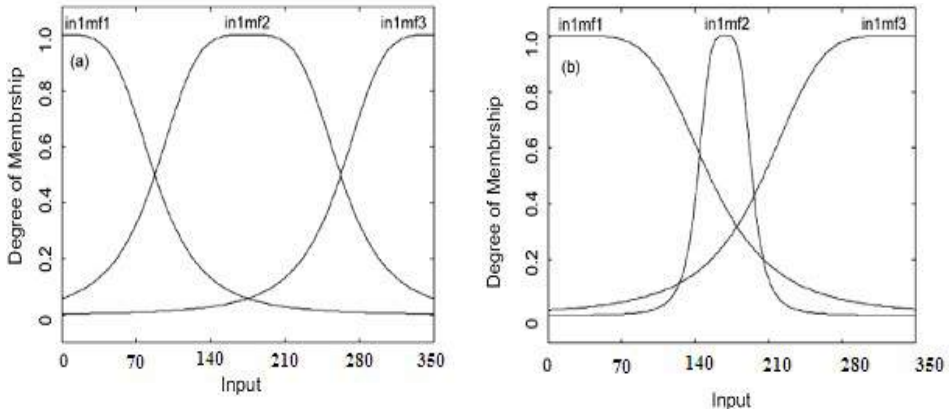

Figure 5.25. (a) Initial membership function and (b) Final membership function of combined DL-ANFIS model 18

5.2.2.4 Daily Lumped Data LGP Models

The LGP technique, which provides input-output relationship in the form of computer programs, has also been employed for prediction of multi-time step ahead daily reservoir (1day, 2 day and 3 day) inflow prediction. For LGP modelling, Discipulus software package Pro Version Lite 4.0, was applied. The codes are defined in terms of functions and terminal sets that modify the contents of internal memory and program counter. LGP algorithm produces multiple lists of programs representing models with the best fit to its training and calibrating data.

Twenty different models, same as that of previous techniques with various input combinations have been developed using LGP. After several trials, the functional set and operational parameters used in LGP model are given in Table 5.16. The population size of 500 provided high search space for LGP solution. The parameter "initial program size" and "maximum program size" indicate the maximum size of the program of the initial population and of the population from subsequent generations, respectively. From various trials, it was observed that a large initial program size, which leads to good initial exploration of the search space, resulted better. The objective function was to generate the computer program with least MSE. The statistical performance resulted from lumped LGP models are presented in Table 5.17. The relative comparison of different models in terms of performance is described in the following section.

Table 5.16. Parameters of the LGP model

Parameter	Values
Population size	500
Function set	+, -, *, /, √, ln(x),sin, cos, tan
Initial program size	80
Maximum program size	512
Crossover rate (%)	50
Homologous crossover (%)	50-95
Mutation rate (%)	90

For comparison, initially time-series models namely DL-LGP model 1 to DL-LGP model 7 (Table 5.17) are considered. From these models, it is observed that model performance increases as number of input variables increases from one (DL-LGP model 1) to six (DL-LGP model 6) and then slightly decreases. R and E value gradually increases and the RMSE, AIC,

BIC values decreases as the number of inputs are increased from one to six. Among seven time-series models, DL-LGP model 6 with 1 day lead period which used input structure of Q(t-5),Q(t-4),Q(t-3),Q(t-2), Q(t-1),Q(t) has yielded with maximum R(0.90) and E(0.86) and minimum RMSE (10.56), AIC (12142.69) and BIC (12149.24) values respectively. Since AIC and BIC values are least than any other models, time-series DL-LGP model 6 is considered relatively parsimonious model. In comparison with lumped time-series ANFIS models, lumped LGP time-series models performed better. The reason may be due to fewer mathematical functions and better build in capacity used in LGP. The scatter plot of best time-series DL-LGP model 6 during testing period is presented in Figure 5.26. From this Figure it is clear that the peak inflows are better predicted than earlier ANN and ANFIS but still are not convincing hence it may be concluded that lumped time-series LGP models also failed to predict the peak inflows. Further the effect of cause-effect models are also assessed and presented.

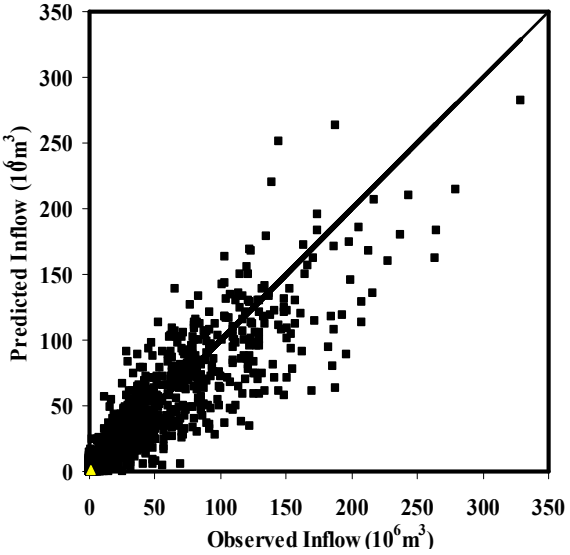

Figure 5.26. Scatter plot observed and 1 day ahead predicted inflow by time-series DL-LGP model 6 during testing period

On studying the cause-effect models namely DL-LGP model 8 to DL-LGP model 16 (Table 5.17), it can be seen that the performance of the models during training and testing are comparable and there is gradual improvement in performances with increase in input up to 6 day lags i.e. (from DL-LGP model 8 to DL-LGP model 14) and thereafter the performance is slightly deteriorated. In this case, cause-effect DL-LGP model 14 which used input structure of P(t-7),P(t-6),P(t-5),P(t-4),P(t-3),P(t-2),P(t-1),P(t) (8 inputs) has obtained best statistics and

outperformed other models. In this type also the performances deteriorated as lead time increased from 1 day to 3 day. The scatter plot of best cause-effect DL-LGP model during testing period is depicted in Figure 5.27. From the performance and scatter plot, it may be seen that the performance of lumped cause-effect LGP model is almost similar to that of lumped time-series LGP and both the models are unable to capture the peak inflows. For further improvement in the performance, combined models have been developed and applied.

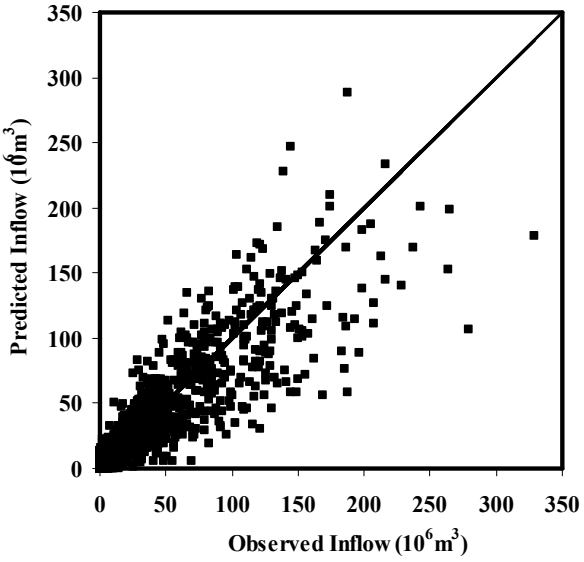

Figure 5.27. Scatter plot observed and 1 day ahead predicted inflow by cause-effect DL-LGP model 14 during testing period

On analyzing the results of combined models, Table 5.17. Performance measures of daily lumped data LGP models (DL-LGP model 17 to DL-LGP model 20) showed comparable performance during training and testing. From the table, it is apparent that all the DL-LGP combined models provide satisfactorily results showing almost comparable values of goodness of fit criteria. From the table it can be revealed that DL-LGP model 18 with 1 day ahead obtained the best statistics of R (0.98), E (0.93), RMSE (6.95), AIC (9989.05), and BIC (9995.60). Lumped combined LGP model produced excellent results for 1 day ahead and accepted prediction results for 2 day ahead and reasonably accurate results for 3 day ahead prediction. There is no significant difference in R and E value from 1 day, 2 day and 3 day ahead prediction. Looking at relative performances of combined models, DL-LGP combined model 18 is selected as the best model among all the LGP models. The scatter plot of this best combined DL-LGP model 18 for 1 day, 2 day and 3 day ahead prediction is shown in Figure 5.28. From scatter plots it is observed that LGP technique performed very well for

inflow prediction with shorter lead prediction while failed to produce very good results for inflow prediction with lead period of 2 day and 3 day. Smaller lead periods have more accurate predictions owing to their higher dependence on the preceding observation. LGP has certain advantages over the ANN and ANFIS as fewer controlling mathematical functions (and hence more flexibility in data mining) and a built-in capacity to handle a large amount of data. It is observed that a combination of rainfall and inflow variables in the input vector significantly improved the model performances.

Table 5.17. Performance measures of daily lumped data LGP models

Models	Performance Criteria	Training			Testing		
		Lead period			Lead period		
		1 day	2day	3 day	1 day	2day	3 day
Time-series models							
DL-LGP Model 1	R	0.87	0.79	0.75	0.84	0.81	0.76
	E	0.83	0.62	0.53	0.84	0.65	0.76
	RMSE	11.24	11.65	12.53	11.15	11.72	12.97
	AIC	29073.62	29508.83	30379.54	12420.86	12679.21	13198.66
	BIC	29081.01	29516.23	30386.94	12427.4	12685.75	13205.21
DL-LGP Model 2	R	0.89	0.84	0.74	0.86	0.92	0.75
	E	0.82	0.79	0.54	0.83	0.84	0.72
	RMSE	11.10	11.59	12.95	11.01	11.10	12.54
	AIC	28929.21	29443.00	30772.10	12357.96	12399.23	13026.75
	BIC	28936.61	29450.39	30779.49	12364.51	12405.78	13033.30
DL-LGP Model 3	R	0.90	0.78	0.75	0.83	0.80	0.75
	E	0.86	0.60	0.53	0.87	0.63	0.75
	RMSE	10.92	12.24	12.49	11.28	12.21	12.30
	AIC	28722.54	30095.88	30341.92	12478.42	12889.75	12925.07
	BIC	28729.94	30103.27	30349.3`	12484.96	12896.30	12931.62
DL-LGP Model 4	R	0.92	0.67	0.71	0.86	0.80	0.83
	E	0.82	0.66	0.12	0.76	0.63	0.80
	RMSE	10.65	11.11	11.46	11.11	11.62	11.23
	AIC	28422.20	28934.57	29308.67	12404.45	12634.99	12455.63
	BIC	28429.59	28941.96	29316.07	12410.99	12641.54	12462.18
DL-LGP Model 5	R	0.90	0.81	0.73	0.85	0.82	0.63
	E	0.83	0.64	0.65	0.84	0.65	0.63
	RMSE	10.88	11.08	11.73	11.02	11.28	11.58
	AIC	28680.54	28901.38	29584.44	12361.57	12480.24	12616.24
	BIC	28687.94	28908.77	29591.84	12368.11	12486.79	12622.79
DL-LGP Model 6	R	0.92	0.80	0.66	0.90	0.81	0.68
	E	0.86	0.63	0.43	0.86	0.65	0.68
	RMSE	10.96	11.50	12.47	10.56	11.21	11.54
	AIC	28775.76	29348.33	30319.16	12142.69	12450.11	12596.78
	BIC	28783.15	29355.73	30326.55	12149.24	12456.65	12603.32
DL-LGP Model 7	R	0.89	0.80	0.56	0.89	0.81	0.75
	E	0.80	0.62	0.29	0.84	0.62	0.75

	RMSE	11.39	11.83	11.91	10.92	10.13	11.70
	AIC	29233.19	29689.67	29770.26	12314.08	11925.4	12668.13
	BIC	29240.59	29697.06	29777.65	12320.63	11931.95	12674.68
Cause-effect models							
DL-LGP Model 8	R	0.80	0.79	0.74	0.83	0.77	0.75
	E	0.77	0.58	0.50	0.83	0.55	0.75
	RMSE	12.23	12.81	11.49	12.06	12.38	12.06
	AIC	30087.04	30645.29	29342.88	12826.48	12960.59	12824.36
	BIC	30094.44	30652.69	29350.27	12833.03	12967.14	12830.91
DL-LGP Model 9	R	0.88	0.78	0.37	0.84	0.81	0.55
	E	0.75	0.57	0.08	0.83	0.81	0.55
	RMSE	12.27	11.84	12.14	12.36	12.55	12.30
	AIC	30125.89	29700.39	30002.07	12953.53	13028.06	12927.80
	BIC	30133.28	29707.79	30009.46	12960.07	13034.60	12934.34
DL-LGP Model 10	R	0.87	0.82	0.81	0.83	0.83	0.76
	E	0.80	0.63	0.76	0.79	0.64	0.54
	RMSE	12.21	11.37	11.41	11.76	12.82	12.70
	AIC	30071.75	29216.03	29256.77	12697.13	13139.18	13091.57
	BIC	30079.15	29223.43	29264.16	12703.68	13145.72	13098.12
DL-LGP Model 11	R	0.88	0.80	0.56	0.83	0.82	0.60
	E	0.81	0.64	0.30	0.78	0.68	0.60
	RMSE	12.00	11.29	11.66	11.72	12.46	11.95
	AIC	29859.80	29128.07	29515.46	12678.46	12994.30	12779.70
	BIC	29867.20	29135.46	29522.86	12685.00	13000.84	12786.25
DL-LGP Model 12	R	0.88	0.80	0.56	0.83	0.83	0.67
	E	0.82	0.63	0.29	0.79	0.66	0.34
	RMSE	11.85	11.46	11.98	11.68	13.05	12.06
	AIC	29713.23	29308.67	29838.48	12659.65	13231.22	12823.12
	BIC	29720.63	29316.07	29845.88	12666.20	13237.77	12829.67
DL-LGP Model 13	R	0.88	0.80	0.75	0.84	0.82	0.76
	E	0.82	0.63	0.56	0.78	0.66	0.76
	RMSE	11.80	11.56	11.63	11.59	11.30	12.04
	AIC	29658.25	29416.55	29487.12	12621.61	12489.73	12818.33
	BIC	29665.65	29423.95	29494.51	12628.16	12496.28	12824.88
DL-LGP Model 14	R	0.94	0.81	0.75	0.92	0.83	0.76
	E	0.87	0.65	0.54	0.86	0.67	
	RMSE	10.58	11.01	12.05	10.46	12.73	12.44
	AIC	28344.84	28829.49	29915.46	12091.65	13102.88	12986.66
	BIC	28352.23	28836.89	29922.85	12098.20	13109.43	12993.21
DL-LGP Model 15	R	0.90	0.80	0.76	0.88	0.77	0.77
	E	0.86	0.63	0.65	0.84	0.55	0.63
	RMSE	11.53	11.34	13.00	11.11	12.38	12.72
	AIC	29382.31	29183.90	30820.30	12401.74	12959.41	13100.97
	BIC	29389.71	29191.29	30827.69	12408.28	12965.96	13107.52
DL-LGP Model 16	R	0.88	0.80	0.75	0.92	0.82	0.76
	E	0.80	0.64	0.55	0.84	0.67	0.76
	RMSE	11.90	11.29	12.61	10.95	12.63	12.09
	AIC	29758.39	29131.37	30457.49	12326.79	13064.77	12836.73
	BIC	29765.78	29138.76	30464.88	12333.33	13071.32	12843.27
Combined models							

DL-LGP Model 17	R	0.90	0.80	0.76	0.95	0.83	0.76
	E	0.83	0.64	0.56	0.90	0.66	0.56
	RMSE	10.49	11.13	13.34	7.64	11.84	12.50
	AIC	28242.49	28953.04	31136.18	10475.34	12732.24	13008.68
	BIC	28249.88	28960.43	31143.57	10481.89	12738.79	13015.23
DL-LGP Model 18	R	0.97	0.96	0.96	0.98	0.96	0.95
	E	0.95	0.92	0.92	0.93	0.92	0.92
	RMSE	6.80	7.43	7.69	6.95	7.43	7.69
	AIC	23043.53	24102.04	24518.15	9989.05	10331.1	10509.50
	BIC	23050.9	24109.44	24525.54	9995.60	10337.71	10516.05
DL-LGP Model 19	R	0.91	0.81	0.76	0.90	0.83	0.76
	E	0.87	0.74	0.68	0.81	0.62	0.76
	RMSE	7.83	11.20	11.46	8.27	11.26	12.60
	AIC	24724.70	29035.93	29307.76	10882.34	12469.49	13050.05
	BIC	24732.10	29043.32	29315.15	10888.88	12476.04	13056.60
DL-LGP Model 20	R	0.92	0.80	0.76	0.93	0.82	0.70
	E	0.85	0.64	0.56	0.80	0.67	0.62
	RMSE	8.62	11.32	11.27	9.46	11.22	11.54
	AIC	25884.32	29161.44	29110.60	11571.79	12453.79	12599.29
	BIC	25891.72	29168.83	29118.00	11578.33	12460.34	12605.84

The impact of each input vector was analyzed and is presented in Table 5.18. A value of 100 % in the frequency column indicates that the particular input variable appeared in set of all best programs. The average and maximum effect of removing all the instances of a particulars input from each best program is also presented. The results are scaled between 0 to 1. A value of 1 represents the largest impact value possible. It is seen that the lag one rainfall and inflow has the highest impact in predicting the future inflow. Thus based on the results it may be concluded that the LGP model has a great ability to learn from input-output patterns and work efficiently for reservoir inflow prediction with greater accuracy. The proposed LGP model can be attributed as a more practicable and robust than ARIMA, MLR, ANN and ANFIS models.

Table 5.18. Impact of each input variable in the combined DL-LGP model 18

Input Parameters	Frequency %	Average Impact	Maximum Impact
P(t-1)	63	0.018	0.039
P(t)	83	0.132	0.246
Q(t)	100	0.255	0.745

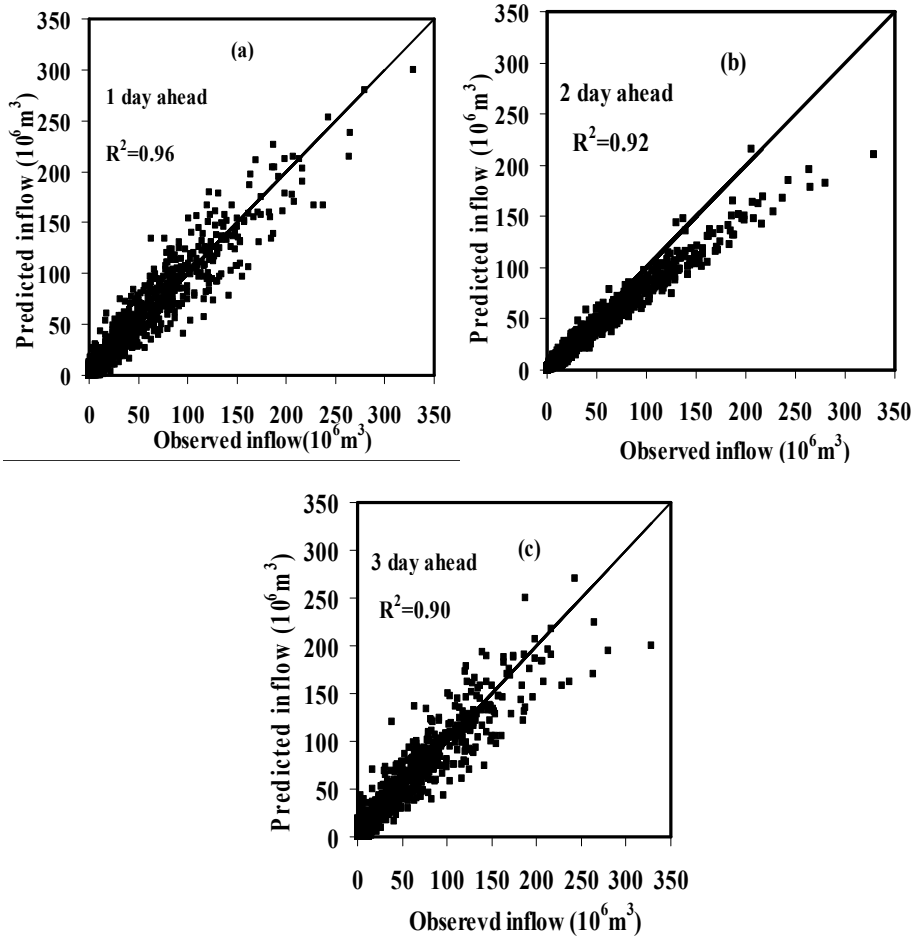

Figure 5.28. Scatter plot of observed and multi-time-step ahead predicted inflow by DL-LGP model 18 during testing period (combined input)

5.2.3 Daily Distributed Data Models

Unlike lumped data models, in distributed data models the rainfall from different sources or stations are not averaged, but considered as individual inputs for the model development. In this study the models are called distributed data models because the rainfall data obtained from nine stations are used "as it is" as the input data. In order to develop daily distributed data models, 15 years (1993-2007) of continuous daily rainfall data from nine rain-gauge stations and corresponding inflow data has been used. Twenty different models viz cause-effect and combined models have been developed with various input combinations (same numbers as that of lumped data models). All the models were developed using 70% length of the total data set and remaining 30% has been used for testing. Further different techniques such as MLR, ANN, ANFIS and LGP are applied and their performance is assessed in the subsequent section.

5.2.3.1 Daily Distributed Data MLR Models

As an initial step, conventional MLR models have been developed using distributed data and their performances evaluated. The commercially available software SPSS 16.0 is used for MLR model development. The resulted performances of the twenty models during training and testing period are analyzed and are depicted in Table 5.19. From Table 5.19, it can be observed that, the overall performance of the models during training and testing is similar and the results are consistent. It reveals that the training procedure is successful without overtraining and the proposed models have good generalization ability to predict the reservoir inflow. From Table 5.19, it is also noticed that the performances of all the models are slightly deteriorating when lead time is increased from 1 day to 3 day.

On studying the distributed cause-effect models, namely DD-MLR model 1 to DD-MLR model 7 (Table 5.19), it can be observed that the performance of the models during training and testing are comparable and there is gradual improvement in performances of input up to 4 day lags i.e. (from DD-MLR model 1 to DD-MLR model 5) and thereafter the performance has slightly deteriorated. The other limitation of DD-MLR model is when the number of inputs increased, the model becomes cumbersome, time consuming along with lengthy equation. The scatter plot of observed and predicted inflow for best cause-effect DD-MLR model 5 during testing period is depicted in Figure 5.29.

Analyzing the results of combined models in, Table 5.19 (DD-MLR model 8 to DD-MLR model 20), it is apparent that all the combined models show satisfactory results during training and testing. However the combined DD-MLR model 17 outperformed all the models. Combined DD-MLR model 17 with 1 day lead period during testing which used 29 input variable showed best performances (testing) as evident from the highest R (0.76) and E (0.71). Hence, DD-MLR model 17 is selected as the best model among combined models as well as among the cause-effect models. In comparison with the best cause-effect DD-MLR model 5 to best model DD-MLR model 17 ‘R’ value is increased from (0.62 to 0.76) and ‘E’ value is increased from (0.55 to 0.62). The numbers of input variables are reduced from 45 to 29 which show that the distributed combined models performed better than distributed cause-effect models even with lesser number of inputs.

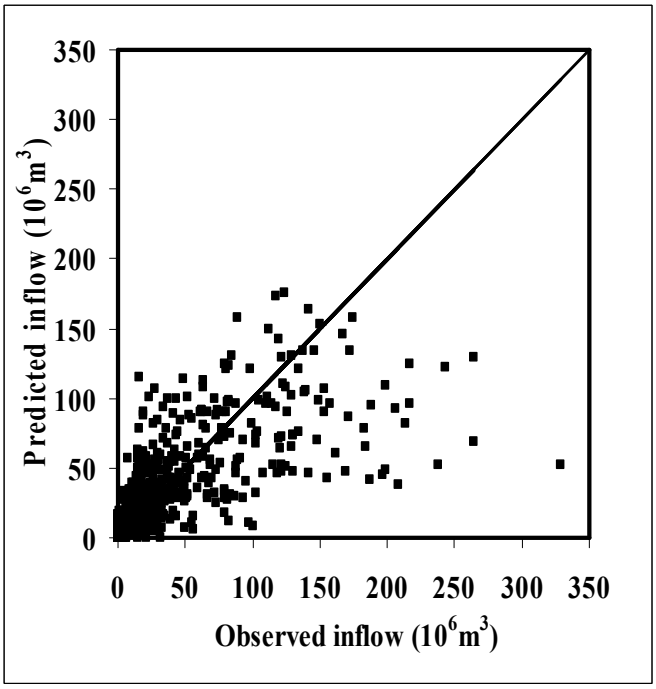

Figure 5.29. Scatter plot of observed and 1 day ahead predicted inflow by cause-effect DD-MLR model 5 during testing period

The scatter plot of the observed inflow and the predicted inflow from combined DD-MLR model 17 during testing period with a lead period of 1 day, 2 day and 3 day is shown in Figure 5.30. Visual inspection of figures reveals that as the lead period increases the performance deteriorated. The identified MLR model performed fairly better in the prediction of low inflow but failed in prediction of non-linear peak inflows. Even though large variation and trials have been carried out in the cause-effect model, the performance is not encouraging and also inferior to the lumped data models. Hence in the following section soft computing techniques like ANN, ANFIS and LGP are applied to predict peak inflow.

Table 5.19. Performance measures of daily distributed data MLR models

Models	Performance Criteria	Training			Testing		
		Lead period			Lead period		
		1 day	2day	3 day	1 day	2day	3 day
Cause-effect models							
DD-MLR Model 1	R	0.45	0.42	0.40	0.42	0.41	0.45
	E	0.42	0.40	0.42	0.35	0.38	0.35
	RMSE	21.15	22.27	23.14	22.98	23.87	25.76
	AIC	11705.04	11902.93	12049.89	5152.19	5214.62	5339.82
	BIC	11711.29	11909.18	12056.14	5157.59	5220.02	5345.22
DD-	R	0.51	0.48	0.42	0.48	0.43	0.46

MLR Model 2	E	0.45	0.46	0.38	0.42	0.40	0.42
	RMSE	20.16	21.98	22.76	21.87	22.16	23.80
	AIC	11521.19	11852.66	11986.39	5070.85	5092.49	5339.82
	BIC	11527.44	11858.91	11992.64	5076.25	5220.02	5345.22
DD-MLR Model 3	R	0.55	0.52	0.50	0.50	0.48	0.43
	E	0.51	0.46	0.48	0.45	0.42	0.40
	RMSE	19.12	19.30	20.21	20.54	21.32	22.87
	AIC	11318.07	11354.00	11530.69	4967.76	5029.00	5144.30
	BIC	11324.32	11360.25	11536.94	4973.17	5034.40	5149.71
DD-MLR Model 4	R	0.60	0.58	0.53	0.58	0.55	0.53
	E	0.57	0.55	0.44	0.52	0.51	0.49
	RMSE	19.86	21.87	22.54	19.87	19.98	20.32
	AIC	11463.69	11833.42	11949.14	4913.27	4922.34	4950.07
	BIC	11469.95	11839.67	11955.39	4918.68	4927.75	4955.47
DD-MLR Model 5	R	0.64	0.62	0.59	0.62	0.56	0.55
	E	0.59	0.56	0.55	0.55	0.50	0.52
	RMSE	15.92	16.23	18.61	18.33	18.75	18.91
	AIC	10615.65	10689.61	11214.39	4780.73	4817.95	4831.91
	BIC	10621.91	10695.87	11220.64	4786.13	4823.36	4837.32
DD-MLR Model 6	R	0.58	0.55	0.50	0.50	0.48	0.43
	E	0.55	0.52	0.48	0.45	0.42	0.40
	RMSE	18.12	19.30	20.21	20.54	21.32	22.87
	AIC	11112.06	11354.00	11530.69	4967.76	5029.00	5144.30
	BIC	11118.31	11360.25	11536.94	4973.17	5034.40	5149.71
DD-MLR Model 7	R	0.54	0.50	0.50	0.52	0.51	0.42
	E	0.48	0.46	0.48	0.43	0.40	0.39
	RMSE	18.98	19.01	20.21	20.14	21.12	22.67
	AIC	11289.88	11295.94	11530.69	4935.45	5013.51	5129.87
	BIC	11296.14	11302.19	11536.94	4940.85	5018.92	5135.28
Combined models							
DD-MLR Model 8	R	0.65	0.62	0.60	0.61	0.56	0.54
	E	0.60	0.52	0.50	0.58	0.45	0.46
	RMSE	19.82	19.61	19.11	18.89	19.27	19.76
	AIC	11455.96	11415.11	11316.06	4830.17	4862.90	4904.15
	BIC	11462.21	11421.36	11322.31	4835.58	4868.30	4909.56
DD-MLR Model 9	R	0.67	0.65	0.62	0.64	0.59	0.55
	E	0.63	0.55	0.55	0.61	0.58	0.48
	RMSE	18.15	18.69	18.91	18.89	18.98	17.31
	AIC	11118.40	11230.84	11275.71	4830.17	4837.98	4686.66
	BIC	11124.65	11237.09	11281.97	4835.58	4843.39	4692.06
DD-MLR Model 10	R	0.69	0.66	0.61	0.63	0.61	0.59
	E	0.65	0.57	0.54	0.60	0.58	0.52
	RMSE	16.08	16.34	16.57	18.29	18.68	18.35
	AIC	10654.00	10715.52	10769.12	4777.14	4811.81	4782.52
	BIC	10660.26	10721.77	10775.37	4782.54	4817.21	4787.93
DD-MLR Model	R	0.72	0.69	0.63	0.69	0.65	0.61
	E	0.69	0.59	0.56	0.63	0.58	0.56
	RMSE	15.98	15.14	14.23	15.66	16.54	17.54

11	AIC	10630.08	10423.00	10185.28	4522.07	4611.90	4708.35
	BIC	10636.33	10429.25	10191.53	4527.48	4617.30	4713.75
DD-MLR Model 12	R	0.73	0.68	0.59	0.69	0.66	0.63
	E	0.61	0.57	0.52	0.56	0.64	0.56
	RMSE	16.29	17.38	17.75	16.29	16.76	17.89
	AIC	10703.76	10952.15	11032.94	4586.88	4633.61	4740.81
	BIC	10710.02	10958.40	11039.19	4592.28	4639.01	4746.21
DD-MLR Model 13	R	0.70	0.65	0.57	0.62	0.60	0.58
	E	0.60	0.55	0.50	0.55	0.54	0.54
	RMSE	16.60	17.67	17.94	16.41	16.68	18.03
	AIC	10776.06	11015.61	11073.77	4598.93	4625.75	4753.62
	BIC	10782.31	11021.87	11080.02	4604.34	4631.15	4759.02
DD-MLR Model 14	R	0.72	0.70	0.68	0.68	0.65	0.63
	E	0.58	0.65	0.62	0.61	0.63	0.67
	RMSE	15.89	16.04	16.76	15.89	16.04	16.76
	AIC	10608.42	10644.45	10812.85	4546.03	4561.47	4633.61
	BIC	10614.67	10650.71	10819.10	4551.43	4566.87	4639.01
DD-MLR Model 15	R	0.76	0.72	0.66	0.75	0.71	0.70
	E	0.70	0.65	0.68	0.71	0.69	0.66
	RMSE	16.87	16.14	16.23	16.66	16.38	17.32
	AIC	10837.93	10668.29	10689.61	4623.78	4595.93	4687.61
	BIC	10844.19	10674.54	10695.87	4629.18	4601.33	4693.01
DD-MLR Model 16	R	0.75	0.72	0.66	0.75	0.71	0.70
	E	0.72	0.65	0.68	0.71	0.69	0.66
	RMSE	16.51	16.64	16.73	18.07	16.93	16.87
	AIC	10755.21	10785.29	10805.98	4757.26	4650.19	4644.36
	BIC	10761.46	10791.54	10812.23	4762.66	4655.59	4649.76
DD-MLR Model 17	R	0.80	0.82	0.75	0.76	0.72	0.70
	E	0.67	0.68	0.65	0.62	0.61	0.52
	RMSE	16.03	16.62	18.56	16.87	19.25	21.76
	AIC	10642.06	10780.68	11204.07	4644.36	4861.19	5062.56
	BIC	10648.31	10786.93	11210.32	4649.76	4866.59	5067.96
DD-MLR Model 18	R	0.76	0.73	0.67	0.72	0.65	0.62
	E	0.62	0.60	0.59	0.58	0.57	0.51
	RMSE	18.03	18.62	19.03	18.06	18.65	18.98
	AIC	11092.96	11216.45	11299.97	4756.35	4809.17	4837.98
	BIC	11099.21	11222.70	11306.23	4761.75	4814.57	4843.39
DD-MLR Model 19	R	0.70	0.66	0.63	0.65	0.60	0.57
	E	0.60	0.57	0.54	0.58	0.58	0.50
	RMSE	18.87	19.65	19.76	19.05	19.62	19.87
	AIC	11267.59	11422.93	11444.33	4844.03	4892.47	4913.27
	BIC	11273.85	11429.18	11450.59	4849.44	4897.88	4918.68
DD-MLR Model 20	R	0.68	0.61	0.57	0.61	0.57	0.55
	E	0.59	0.55	0.54	0.55	0.53	0.49
	RMSE	15.76	17.21	18.98	19.52	19.66	19.89
	AIC	10576.92	10914.46	11289.88	4884.08	4895.82	4914.93
	BIC	10583.17	10920.71	11296.14	4889.48	4901.22	4920.33

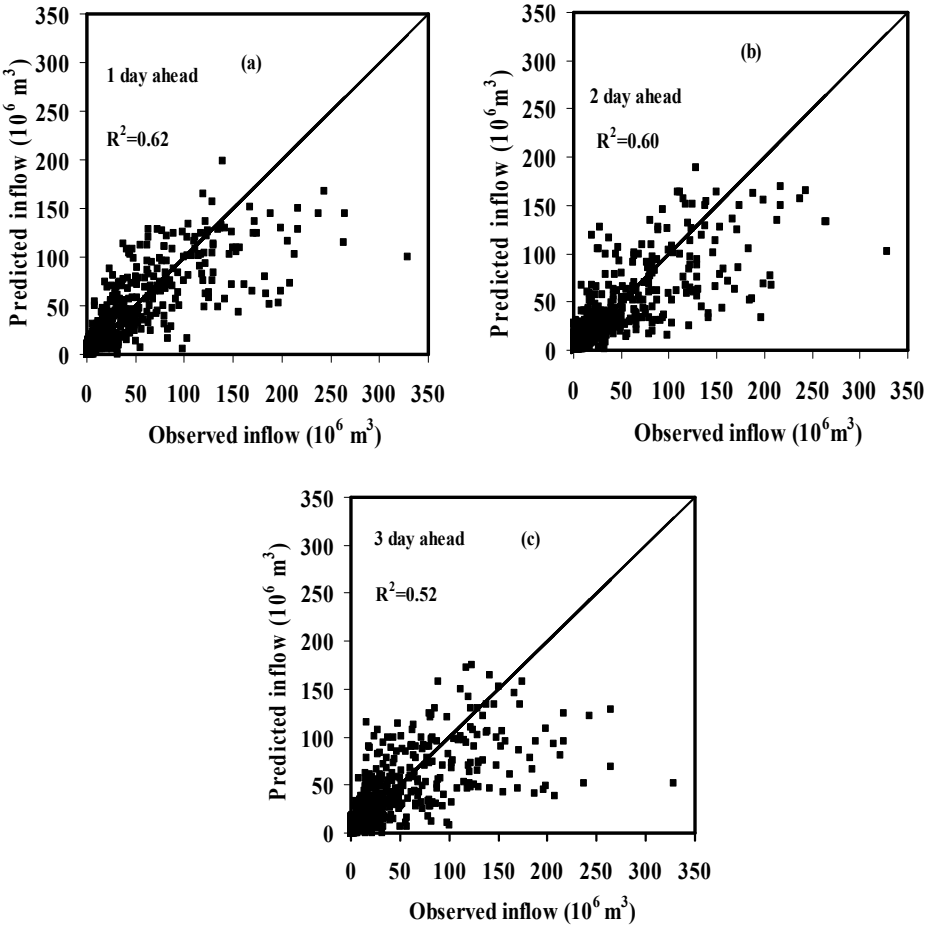

Figure 5.30. Scatter plot of observed and multi-time-step ahead predicted inflow by best DD-MLR model 17 during testing (combined input)

5.2.3.2 Daily Distributed Data TDRNN Models (ANN)

From the previous results, it is observed that the conventional DD-MLR models failed to predict the observed inflows, especially peak and moderate inflows. In order to model the non-linearity and improve the peak inflow prediction, comprehensive multi-input multi-output (MIMO) and TDRNN type of networks (same as that of lumped data models) are developed. The neurons in the output layer represented the inflow at 1 day, 2 day and 3 day ahead. The number of neurons in the hidden layer was varied from 5 to 50 and best architecture was finalized to capture the rainfall-inflow relationship. The performance summary of TDRNN models developed with full year data during training and testing phases are given in Table 5.20

For comparison, initially distributed data cause-effect ANN models namely DD-ANN model 1 to DD-ANN model 7 (Table 5.20) are studied. From the results it can be observed that

performance of the models during training and testing are comparable. The DD-ANN model 3 which required 27 inputs and obtained best statistics and outperformed other models. As forecast horizon increases from 1 day to 3 day lead period the performance gradually decreases i.e. 'R' value dropped from 0.75 to 0.70. In comparison with the previous DD-MLR models, it is found that the performance of the models has improved with ANN technique. It is also observed that increasing the input variables beyond 27, the model becomes very complex and training time increased and subsequently performance reduced. The scatter plot of observed and predicted inflow of DD-ANN model 3 during testing period is shown in Figure 5.31. From the scatter plot it may be seen that the results are similar to DD-MLR model 17(the best DD-MLR model) and no significant improvement is found in moderate and peak inflow prediction.

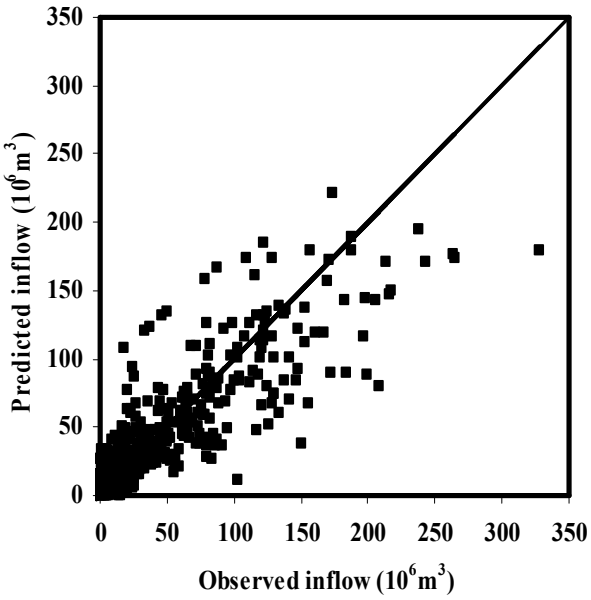

Figure 5.31. Scatter plot of observed and 1 day ahead predicted inflow by cause-effect DD-ANN model 3 during testing period

Analyzing the results of combined models (models 8 to 20) it is also apparent that overall DD-ANN model 15, obtained best performance during testing. This model required 25 inputs less than cause-effect models. The scatter plot of observed inflow and the predicted inflow from (DD-ANN model 15) during testing period with lead period of 1 day, 2day and 3 day is depicted in Figure 5.32. From these Figures it is visualized that, as lead period increases the performance deteriorated. The identified DD-ANN model 15 (1 day ahead) behaves reasonably accurate in the prediction of medium flow but not in prediction of non-linear peak

flows and outliers. In ANN technique also DL models performed slightly better than DD-ANN models, because of reduced noise due to lumping the inputs.

Table 5.20. Performance measures of daily distributed data TDRNN models (ANN)

Model	Performance Criteria	Training			Testing		
		Lead period			Lead period		
		1 day	2day	3 day	1 day	2day	3 day
Cause-effect models							
DD-ANN Model 1 (9-10-3)	R	0.71	0.65	0.63	0.68	0.63	0.62
	E	0.69	0.62	0.59	0.62	0.59	0.57
	RMSE	21.15	22.27	23.14	22.98	23.87	25.76
	AIC	11705.04	11902.93	12049.89	5152.19	5214.62	5339.82
	BIC	11711.29	11909.18	12056.14	5157.59	5220.02	5345.22
DD-ANN Model 2 (18-12-3)	R	0.74	0.69	0.64	0.69	0.65	0.61
	E	0.70	0.63	0.60	0.68	0.66	0.59
	RMSE	20.16	21.98	22.76	21.87	22.16	23.8
	AIC	11521.19	11852.66	11986.39	5070.85	5092.49	5209.79
	BIC	11527.44	11858.91	11992.64	5076.25	5097.89	5215.20
DD-ANN Model 3 (27-18-3)	R	0.82	0.81	0.78	0.75	0.72	0.70
	E	0.71	0.70	0.68	0.73	0.71	0.65
	RMSE	11.72	11.90	12.07	12.48	12.76	12.56
	AIC	9441.07	9499.52	9553.92	4149.14	4185.60	4159.64
	BIC	9447.33	9505.78	9560.17	4154.55	4191.00	4165.04
DD-ANN Model 4 (36-20-3)	R	0.76	0.75	0.72	0.76	0.72	0.69
	E	0.71	0.69	0.69	0.69	0.65	0.60
	RMSE	12.23	15.78	16.38	12.84	19.98	16.34
	AIC	9604.43	10581.78	10724.89	4195.86	4922.34	4591.91
	BIC	9610.68	10588.03	10731.15	4201.27	4927.75	4597.32
DD-ANN Model 5 (45-25-3)	R	0.77	0.75	0.73	0.75	0.72	0.69
	E	0.70	0.71	0.71	0.69	0.67	0.65
	RMSE	12.26	14.65	15.38	13.02	15.23	16.87
	AIC	9613.82	10296.83	10483.32	4218.74	4476.33	4644.36
	BIC	9620.07	10303.08	10489.57	4224.14	4481.73	4649.76
DD-ANN Model 6 (54-30-3)	R	0.79	0.77	0.75	0.78	0.75	0.72
	E	0.73	0.70	0.65	0.75	0.70	0.68
	RMSE	12.18	15.75	16.26	12.96	13.27	16.34
	AIC	9588.71	10574.48	10696.70	4211.15	4249.99	4591.91
	BIC	9594.97	10580.73	10702.95	4216.55	4255.39	4597.32
DD-ANN Model 7 (63-40-3)	R	0.75	0.71	0.68	0.72	0.67	0.65
	E	0.73	0.68	0.58	0.67	0.66	0.61
	RMSE	12.86	16.10	16.35	12.76	21.32	16.38
	AIC	10654.00	10715.52	10769.12	4777.14	4811.81	4782.52
	BIC	10660.26	10721.77	10775.37	4782.54	4817.21	4787.93
Combined models							
DD-ANN	R	0.75	0.70	0.67		0.69	0.66

Model 8					0.71		
(10-15-3)	E	0.70	0.68	0.62	0.68	0.60	0.55
	RMSE	11.38	12.21	12.62	12.23	13.21	13.44
	AIC	9328.17	9598.15	9724.81	4115.89	4242.54	4270.90
	BIC	9334.43	9604.40	9731.06	4121.30	4247.94	4276.30
DD-ANN	R	0.77	0.72	0.71	0.72	0.70	0.68
Model 9	E	0.73	0.69	0.65	0.70	0.68	0.62
(19-14-3)	RMSE	11.02	11.65	11.78	11.98	12.01	12.65
	AIC	9204.89	9418.10	9460.66	4081.96	4086.07	4171.37
	BIC	9211.15	9424.35	9466.91	4087.37	4091.47	4176.78
DD-ANN	R	0.80	0.78	0.73	0.73	0.70	0.69
Model 10	E	0.78	0.76	0.69	0.70	0.68	0.65
(20-16-3)	RMSE	10.80	11.36	11.81	11.76	12.27	12.45
	AIC	9127.56	9321.43	9470.41	4051.5	4121.26	4145.19
	BIC	9133.81	9327.68	9476.66	4056.91	4126.66	4150.59
DD-ANN	R	0.83	0.79	0.76	0.79	0.74	0.65
Model 11	E	0.74	0.72	0.69	0.70	0.69	0.65
(21-16-3)	RMSE	11.59	14.66	14.22	12.44	12.76	12.56
	AIC	9398.30	10299.45	10182.58	4143.87	4185.60	4159.64
	BIC	9404.55	10305.70	10188.83	4149.27	4191.00	4165.04
DD-ANN	R	0.87	0.83	0.80	0.79	0.77	0.71
Model 12	E	0.82	0.78	0.73	0.75	0.68	0.65
(22-16-3)	RMSE	10.13	11.23	11.58	11.06	11.38	11.54
	AIC	8881.95	9277.29	9394.99	3950.68	3997.54	4020.48
	BIC	8888.20	9283.54	9401.24	3956.08	4002.95	4025.89
DD-ANN	R	0.85	0.82	0.81	0.78	0.75	0.72
Model 13	E	0.81	0.79	0.70	0.75	0.69	0.63
(23-16-3)	RMSE	10.98	11.79	12.21	11.68	11.81	11.92
	AIC	9190.95	9463.91	9598.15	4040.29	4058.48	4073.71
	BIC	9197.20	9470.16	9604.40	4045.70	4063.88	4079.12
DD-ANN	R	0.80	0.76	0.69	0.78	0.76	0.74
Model 14	E	0.75	0.69	0.65	0.74	0.71	0.62
(24-15-3)	RMSE	14.02	14.18	14.97	14.88	14.71	14.91
	AIC	10128.26	10171.78	10379.69	4438.13	4419.25	4441.44
	BIC	10134.51	10178.03	10385.95	4443.53	4424.66	4446.84
DD-ANN	R	0.92	0.85	0.81	0.90	0.82	0.77
Model 15	E	0.88	0.82	0.78	0.84	0.79	0.65
(25-15-3)	RMSE	13.00	10.78	11.14	12.22	10.79	11.06
	AIC	9838.58	9120.45	9246.43	4114.55	3910.07	3950.68
	BIC	9844.83	9126.70	9252.68	4119.95	3915.48	3956.08
DD-ANN	R	0.80	0.76	0.74	0.71	0.69	0.65
Model 16	E	0.69	0.69	0.63	0.70	0.67	0.62
(28-16-3)	RMSE	11.68	12.95	13.28	12.84	11.89	12.62
	AIC	9427.96	9823.80	9920.30	4195.86	4069.57	4167.47
	BIC	9434.21	9830.05	9926.56	4201.27	4074.98	4172.87
DD-ANN	R	0.80	0.74	0.72	0.71	0.66	0.65
Model 17	E	0.69	0.69	0.63	0.70	0.67	0.62
(29-16-3)	RMSE	11.51	11.97	12.13	11.62	13.65	13.83

	AIC	9368.40	9522.02	9572.94	4031.83	4296.37	4317.90
	BIC	9374.65	9528.27	9579.19	4037.24	4301.78	4323.30
DD-ANN	R	0.78	0.74	0.70	0.76	0.73	0.72
Model 18	E	0.71	0.72	0.68	0.74	0.70	0.68
(30-16-3)	RMSE	12.65	12.76	13.02	12.87	13.12	13.23
	AIC	9733.92	9767.12	9844.48	4199.70	4231.31	4245.03
	BIC	9740.17	9773.37	9850.73	4205.10	4236.71	4250.43
DD-ANN	R	0.82	0.79	0.73	0.80	0.76	0.70
Model 19	E	0.71	0.76	0.65	0.74	0.70	0.63
(39-20-3)	RMSE	13.52	13.68	14.43	12.46	16.76	17.03
	AIC	9988.99	10034.11	10238.80	4146.51	4633.61	4659.87
	BIC	9995.24	10040.36	10245.05	4151.91	4639.01	4665.27
DD-ANN	R	0.83	0.77	0.72	0.76	0.68	0.65
Model 20	E	0.72	0.70	0.62	0.70	0.66	0.59
(48-30-3)	RMSE	11.64	14.73	14.89	12.64	19.62	16.01
	AIC	9414.81	10317.71	10359.15	4170.07	4892.47	4558.
	BIC	9421.06	10323.97	10365.40	4175.48	4897.88	4563.79

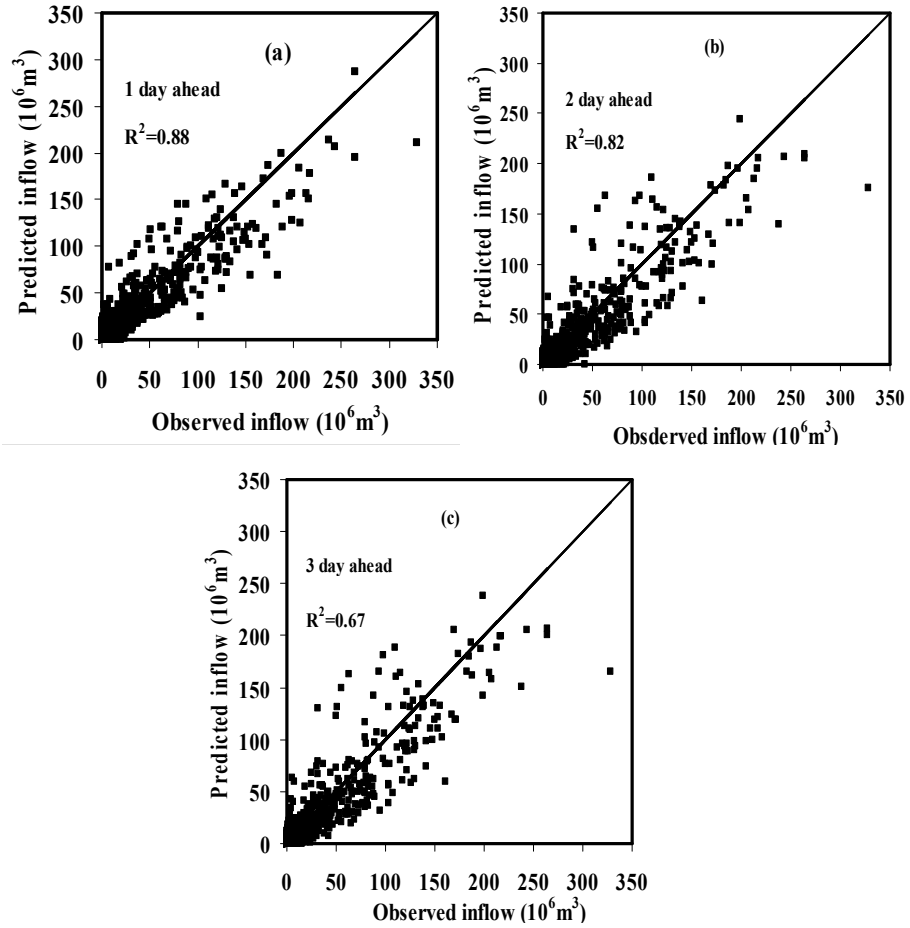

Figure 5.32. Scatter plot of observed and multi-time-step ahead predicted inflow by best DD-ANN model 15 during testing period (combined input)

5.2.3.3 Daily Distributed Data ANFIS Models

Since TDRNN technique has not resulted in encouraging results, especially the peak inflow prediction, the ANFIS techniques is tried. In this case various twenty ANFIS models have been developed, same as previous sections by changing the input parameters and membership functions. The membership function varied between 2 to 4. The resulted statistical performances of all twenty models are shown in Table 5.21. In this type also, model performance has deteriorated as the lead period increases from 1 day to 3 day. In case of ANFIS models, number of membership function associated with each input variable is fixed by trial and error. The increased number of input variables and MF on the input variable also increased the number of fuzzy "if-then" rules and simultaneously increased the model complexity, and parsimony. Hence in this case subtractive fuzzy clustering method has been used to classify the input data because of large input variables. The type of membership function used for all the models is a generalized bell type, which is direct generalization of Cauchy distribution used in the probability theory. The relative comparison of performance criteria of cause-effect and time-series models are discussed below.

Analyzing the results of distributed cause-effect models (Table 5.21) DD-ANFIS model 1 to DD-ANFIS model 7 it is found that relative performance of all the models are comparatively consistent in both training as well as testing. In this case, cause-effect DD-ANFIS model 4 which used input structure has obtained best statistics and outperformed other ANN and ANFIS models. The superiority of the ANFIS technique to TDRNN may be due to fuzzy partioning of the inputs space and for creating a rule-base to generate the output. The scatter plot of the observed and predicted inflow by best cause-effect DD-ANFIS model 4 during testing period is presented in Figure 5.33. From the Figure, it can be observed that that the peak inflows are still under predicted hence for further improvement combined models have been developed.

Studying the performance of combined models (DD-ANFIS model 7 to DD-ANFIS model 20) it is found that the DD-ANFIS model 16 (28 inputs) outperformed all other models. It is also found that the all the combined models ANFIS models performed better with three membership functions where as the cause-effect models performed better with 2 memberships function. The scatter plot of observed and the predicted inflows by DD-ANFIS model 16 with a lead period of 1 day, 2 day and 3 day is shown in Figure 5.34. From the scatter plots, it

can be seen that low and medium inflows are well predicted by the model but peak inflows are still under predicted. In ANFIS model it is found that there is only marginal difference between DL and DD-ANFIS models

Table 5.21. Performance measures of daily distributed data ANFIS models

Models	Membership function	Performance Criteria	Training			Testing		
			Lead period			Lead period		
			1 day	2day	3 day	1 day	2day	3 day
Cause-effect models								
DD-ANFIS Model 1	2	R	0.77	0.74	0.68	0.64	0.62	0.60
		E	0.74	0.70	0.61	0.61	0.58	0.55
		RMSE	12.15	12.62	13.40	13.77	13.58	14.10
		AIC	9579.26	9724.81	9954.80	4310.75	4287.93	4349.67
		BIC	9585.51	9731.06	9961.05	4316.16	4293.33	4355.07
DD-ANFIS Model 2	2	R	0.79	0.76	0.71	0.66	0.64	0.62
		E	0.76	0.74	0.63	0.60	0.59	0.58
		RMSE	12.11	12.54	13.28	13.74	13.55	13.74
		AIC	9566.61	9700.42	9920.30	4307.17	4284.29	4307.17
		BIC	9572.86	9706.67	9926.56	4312.58	4289.70	4312.58
DD-ANFIS Model 3	2	R	0.82	0.80	0.76	0.80	0.77	0.71
		E	0.79	0.76	0.66	0.78	0.71	0.62
		RMSE	11.69	12.45	13.13	13.37	13.21	13.41
		AIC	9431.24	9672.80	9876.74	4262.32	4242.54	4267.23
		BIC	9437.50	9679.05	9882.99	4267.73	4247.94	4272.63
DD-ANFIS Model 4	2	R	0.91	0.84	0.82	0.87	0.85	0.81
		E	0.87	0.82	0.78	0.79	0.73	0.73
		RMSE	11.16	11.58	12.11	12.59	12.79	12.89
		AIC	9253.31	9394.99	9566.61	4163.56	4189.45	4202.25
		BIC	9259.56	9401.24	9572.86	4168.96	4194.86	4207.65
DD-ANFIS Model 5	2	R	0.89	0.84	0.81	0.84	0.79	0.76
		E	0.84	0.79	0.63	0.76	0.75	0.69
		RMSE	11.16	12.41	12.74	13.27	13.43	13.32
		AIC	9253.31	9660.46	9761.10	4249.99	4269.68	4256.17
		BIC	9259.56	9666.71	9767.36	4255.39	4275.08	4261.57
DD-ANFIS Model 6	2	R	0.89	0.84	0.81	0.84	0.79	0.76
		E	0.81	0.79	0.63	0.75	0.75	0.69
		RMSE	11.25	12.41	12.74	13.02	13.18	13.27
		AIC	9284.11	9660.46	9761.10	4218.74	4238.80	4249.99
		BIC	9290.36	9666.71	9767.36	4224.14	4244.21	4255.39
DD-ANFIS Model 7	2	R	0.84	0.81	0.78	0.80	0.72	0.69
		E	0.80	0.78	0.74	0.74	0.63	0.62
		RMSE	12.02	12.41	13.13	13.37	13.91	14.10
		AIC	9538.00	9660.46	9876.74	4262.32	4327.37	4349.67
		BIC	9544.26	9666.71	9882.99	4267.73	4332.78	4355.07

Combined models								
DD-ANFIS Model 8	3	R	0.73	0.70	0.68	0.62	0.60	0.57
		E	0.65	0.62	0.61	0.54	0.52	0.51
		RMSE	13.58	13.79	14.08	16.69	15.87	17.29
		AIC	10005.97	10064.82	10144.64	4626.73	4543.96	4684.76
		BIC	10012.23	10071.08	10150.89	4632.14	4549.36	4690.17
DD-ANFIS Model 9	3	R	0.75	0.72	0.70	0.73	0.69	0.62
		E	0.66	0.64	0.62	0.63	0.59	0.56
		RMSE	13.21	13.42	13.72	13.15	12.19	16.31
		AIC	9900.04	9960.52	10045.31	4235.06	4110.51	4588.89
		BIC	9906.29	9966.77	10051.56	4240.47	4115.92	4594.30
DD-ANFIS Model 10	3	R	0.75	0.72	0.70	0.73	0.69	0.62
		E	0.66	0.64	0.62	0.63	0.59	0.56
		RMSE	13.21	13.42	13.72	16.39	18.32	17.31
		AIC	9900.04	9960.52	10045.31	4596.93	4779.83	4686.66
		BIC	9906.29	9966.77	10051.56	4602.34	4785.24	4692.06
DD-ANFIS Model 11	3	R	0.78	0.75	0.73	0.75	0.71	0.66
		E	0.69	0.66	0.65	0.66	0.62	0.59
		RMSE	13.17	13.46	14.08	15.77	17.93	16.73
		AIC	9888.41	9971.94	10144.64	4533.57	4744.48	4630.67
		BIC	9894.66	9978.19	10150.89	4538.98	4749.88	4636.07
DD-ANFIS Model 12	3	R	0.80	0.76	0.75	0.76	0.73	0.69
		E	0.75	0.73	0.66	0.69	0.65	0.62
		RMSE	13.05	13.42	14.10	14.38	18.75	16.42
		AIC	9853.30	9960.52	10150.08	4381.97	4817.95	4599.94
		BIC	9859.55	9966.77	10156.33	4387.38	4823.36	4605.34
DD-ANFIS Model 13	3	R	0.79	0.75	0.73	0.77	0.72	0.70
		E	0.76	0.71	0.67	0.70	0.66	0.68
		RMSE	13.13	13.50	14.10	14.38	16.20	16.12
		AIC	9876.74	9983.31	10150.08	4381.97	4625.75	4753.62
		BIC	9882.99	9989.57	10156.33	4387.38	4631.15	4759.02
DD-ANFIS Model 14	3	R	0.82	0.79	0.75	0.78	0.76	0.74
		E	0.77	0.76	0.69	0.76	0.68	0.70
		RMSE	13.21	13.54	14.14	14.38	21.12	16.42
		AIC	9900.04	9994.66	10160.94	4381.97	5013.51	4599.94
		BIC	9906.29	10000.91	10167.20	4387.38	5018.92	4605.34
DD-ANFIS Model 15	3	R	0.84	0.80	0.76	0.80	0.74	0.71
		E	0.75	0.71	0.69	0.75	0.71	0.62
		RMSE	13.01	11.55	11.71	11.79	12.45	12.50
		AIC	9841.53	9385.04	9437.80	4055.69	4145.19	4151.77
		BIC	9847.78	9391.29	9444.05	4061.10	4150.59	4157.18
DD-ANFIS Model 16	3	R	0.94	0.89	0.88	0.92	0.88	0.85
		E	0.85	0.76	0.72	0.89	0.76	0.69
		RMSE	10.34	11.91	13.73	11.31	13.15	13.19
		AIC	8960.64	10780.68	11204.07	4757.26	4861.19	5062.56
		BIC	8966.89	10786.93	11210.32	4762.66	4866.59	5067.96
DD-ANFIS	3	R	0.72	0.74	0.71	0.67	0.62	0.59
		E	0.71	0.73	0.68	0.63	0.58	0.49

Model 17		RMSE	14.11	13.56	14.04	12.22	14.65	15.05
		AIC	10152.80	10000.32	10133.73	4114.55	4412.54	4456.79
		BIC	10159.05	10006.57	10139.98	4119.95	4417.94	4462.20
DD-ANFIS		R	0.83	0.81	0.79	0.81	0.79	0.74
		E	0.76	0.73	0.71	0.69	0.59	0.68
Model 18	3	RMSE	13.38	13.48	13.68	13.80	14.66	11.63
		AIC	9949.07	9977.63	10034.11	4314.33	4413.66	4033.25
		BIC	9955.33	9983.88	10040.36	4319.73	4419.06	4038.65
DD-ANFIS		R	0.83	0.81	0.75	0.79	0.74	0.69
		E	0.72	0.74	0.70	0.73	0.69	0.62
Model 19	3	RMSE	12.61	12.03	13.78	12.62	16.65	18.63
		AIC	9721.77	9541.19	10062.04	4167.47	4622.79	4807.40
		BIC	9728.02	9547.44	10068.29	4172.87	4628.19	4812.81
DD-ANFIS		R	0.81	0.77	0.72	0.74	0.70	0.67
		E	0.73	0.70	0.67	0.68	0.66	0.60
Model 20	3	RMSE	13.12	13.83	14.14	16.10	18.62	17.33
		AIC	9873.82	10075.93	10160.94	4567.60	4806.52	4688.56
		BIC	9880.07	10082.18	10167.20	4573.00	4811.92	4693.96

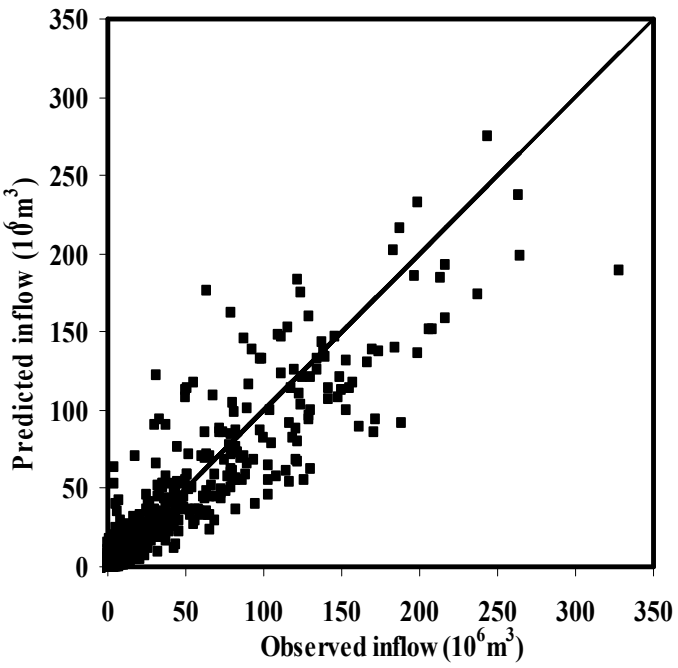

Figure 5.33. Scatter plot of observed and 1 day ahead predicted inflow by cause-effect DD-ANFIS model 4 during testing period

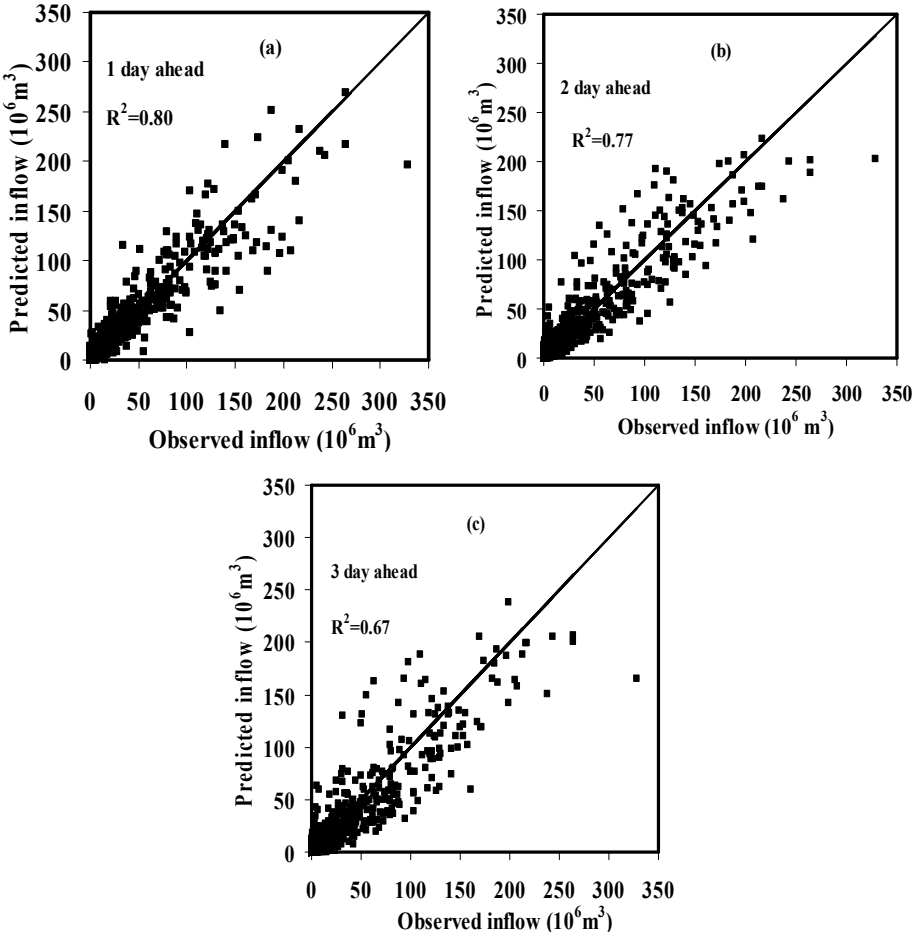

Figure 5.34. Scatter plot of observed and multi-time-step ahead predicted inflow by best DD-ANFIS model 16 during testing period (combined input)

5.2.3.4 Daily Distributed Data LGP Models

The procedure adopted in daily distributed data LGP is same as that of daily lumped data LGP models. Twenty different models same as that of previous techniques with various input combinations have been developed with LGP techniques. The statistical performance measures of twenty different models are also presented in Table 5.22. The relative comparison of different models in terms of performance is described in following section.

On studying the cause-effect models namely DD-LGP model 1 to DD-LGP model 7 (Table 5.22) it can be seen that the performance of the models during training and testing are comparable and there is a gradual improvement in performances with increase in input up to 3 day lags i.e. (from DD-LGP model 1 to DD-LGP model 5) and thereafter the performance is slightly deteriorated. In this case, DD-LGP model 5 (45 inputs) has obtained best statistics

and outperformed all other models. In this type also, the model performance deteriorated as lead time increases from 1 day to 3 day. The scatter plot of the observed and predicted inflows by best cause-effect DD-LGP model 5 during testing period is shown in Figure 5.35. From this figure it is understood that the there is some improvement in moderate to peak inflow prediction than previous DD-ANFIS models. Even though the correlation is similar the model is slightly inferior to daily lumped data models, because of very high variations in the distributed data. In case of lumped data the variation is average leading to much smoother pattern.

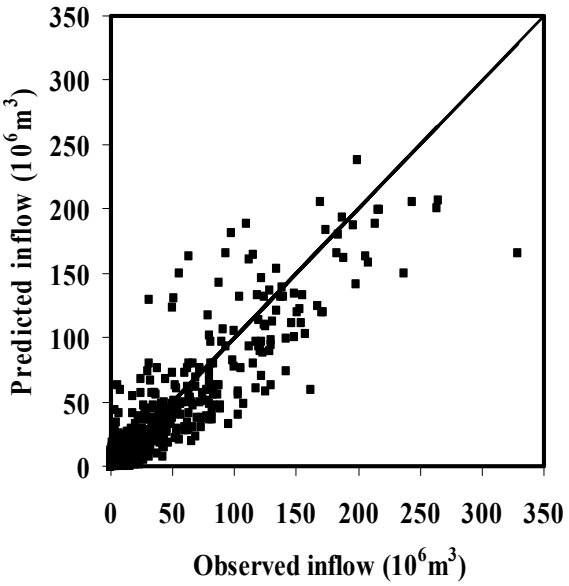

Figure 5.35. Scatter plot of observed and 1 day ahead predicted inflow by cause-effect DD-LGP model 5 during testing period

Analyzing the results of combined models, Table 5.22 (DD-LGP model 8 to DD-LGP model 20) showed comparable performance during training and testing. From the Table 5.22 it is also apparent that all the combined models show satisfactory results. From the Table 5.22 it can be revealed that the combined DD-LGP model 16 with 1 day lead period during testing obtained the best statistics. The scatter plot of the observed and predicted inflow by best combined DD-LGP model 16 with 1 day, 2 day and 3 day ahead prediction is shown in Figure 5.36. From the scatter plot it is found that the LGP technique performed very well for inflow prediction with shorter lead prediction while failed to produce very good results for inflow prediction with lead period of 3 day. But it can be seen that low, medium and high inflows are well predicted than previous models even for higher lead period. It is observed that a

combination of rainfall and inflow variables in the input vector significantly improves the model performances. The LGP models have a great ability to learn from input-output patterns and work efficiently in reservoir inflow prediction with great accuracy. In this case also the impact of rainfall and inflow are similar to lumped data set. Also, there is only marginal difference between DL and DD-LGP models.

Table 5.22. Performance measures of daily distributed data LGP models

Models	Performance Criteria	Training			Testing		
		Lead period			Lead period		
		1 day	2day	3 day	1 day	2day	3 day
Cause-effect models							
DD-LGP Model 1	R	0.72	0.71	0.68	0.69	0.65	0.61
	E	0.72	0.61	0.59	0.62	0.57	0.55
	RMSE	13.75	14.96	17.92	14.67	15.60	16.02
	AIC	10053.68	10377.13	11069.49	4414.78	4515.77	4559.42
	BIC	10059.94	10383.38	11075.75	4420.18	4521.17	4564.82
DD-LGP Model 2	R	0.76	0.75	0.71	0.75	0.72	0.69
	E	0.70	0.64	0.61	0.69	0.62	0.59
	RMSE	14.53	14.67	14.83	14.67	15.60	16.02
	AIC	10265.29	10302.06	10343.66	4414.78	4515.77	4559.42
	BIC	10271.54	10308.31	10349.91	4420.18	4521.17	4564.82
DD-LGP Model 3	R	0.80	0.78	0.75	0.82	0.81	0.78
	E	0.75	0.73	0.69	0.78	0.79	0.57
	RMSE	14.12	14.23	14.38	14.16	14.75	15.66
	AIC	10155.52	10185.28	10225.49	4356.64	4423.71	4522.07
	BIC	10161.77	10191.53	10231.74	4362.05	4429.12	4527.48
DD-LGP Model 4	R	0.72	0.74	0.71	0.67	0.62	0.59
	E	0.71	0.73	0.68	0.63	0.58	0.49
	RMSE	14.11	13.56	14.04	12.22	14.65	15.05
	AIC	10152.80	10000.32	10133.73	4114.55	4412.54	4456.79
	BIC	10159.05	10006.57	10139.98	4119.95	4417.94	4462.20
DD-LGP Model 5	R	0.87	0.74	0.66	0.89	0.77	0.68
	E	0.74	0.54	0.41	0.81	0.57	0.42
	RMSE	14.56	14.96	16.48	16.70	15.37	16.15
	AIC	10273.20	10377.13	10748.24	4627.72	4491.36	4572.69
	BIC	10279.45	10383.38	10754.49	4633.12	4496.77	4578.10
DD-LGP Model 6	R	0.83	0.75	0.66	0.81	0.77	0.68
	E	0.74	0.54	0.40	0.79	0.56	0.42
	RMSE	17.25	14.96	16.56	14.58	16.07	16.36
	AIC	10923.36	10377.13	10766.81	4404.67	4564.54	4073.71
	BIC	10929.61	10383.38	10773.06	4410.07	4569.94	4079.12
DD-LGP Model 7	R	0.80	0.70	0.62	0.78	0.76	0.62
	E	0.72	0.52	0.41	0.65	0.50	0.40
	RMSE	17.26	15.64	16.38	14.29	14.58	16.26
	AIC	10925.58	10547.60	10724.89	4371.66	4404.67	4583.85

	BIC	10931.83	10553.86	10731.15	4377.06	4410.07	4589.25
Combined models							
DD-LGP Model 8	R	0.77	0.71	0.64	0.66	0.62	0.63
	E	0.63	0.48	0.38	0.51	0.53	0.40
	RMSE	14.79	16.96	15.61	15.21	13.87	17.13
	AIC	10333.30	10858.34	10540.24	4474.17	4322.64	4669.49
	BIC	10339.56	10864.59	10546.49	4479.57	4328.05	4674.89
DD-LGP Model 9	R	0.79	0.71	0.64	0.66	0.62	0.63
	E	0.63	0.48	0.38	0.51	0.53	0.40
	RMSE	14.68	16.96	15.61	15.21	16.16	17.13
	AIC	10304.67	10858.34	10540.24	4474.17	4573.71	4669.49
	BIC	10310.93	10864.59	10546.49	4479.57	4579.12	4674.89
DD-LGP Model 10	R	0.78	0.73	0.65	0.68	0.67	0.64
	E	0.64	0.49	0.39	0.53	0.55	0.42
	RMSE	14.45	14.75	15.64	14.88	14.32	14.61
	AIC	10244.11	10322.92	10547.60	4438.13	4375.10	4408.04
	BIC	10250.37	10329.17	10553.86	4443.53	4380.51	4413.45
DD-LGP Model 11	R	0.87	0.76	0.65	0.85	0.79	0.71
	E	0.73	0.55	0.39	0.81	0.57	0.44
	RMSE	14.13	14.64	16.85	16.71	16.78	15.24
	AIC	10158.23	10294.21	10833.38	4628.70	4635.57	4477.41
	BIC	10164.48	10300.46	10839.64	4634.10	4640.97	4482.81
DD-LGP Model 12	R	0.87	0.36	0.75	0.86	0.36	0.78
	E	292.31	0.03	0.55	0.81	0.78	0.67
	RMSE	13.09	13.78	14.58	16.58	17.75	17.61
	AIC	9865.04	10062.04	10278.46	4615.87	4727.90	4714.89
	BIC	9871.29	10068.29	10284.71	4621.27	4733.31	4720.30
DD-LGP Model 13	R	0.87	0.74	0.76	0.88	0.78	0.73
	E	0.74	0.63	0.56	0.82	0.61	0.64
	RMSE	16.11	15.34	15.43	16.32	16.43	17.65
	AIC	10661.15	10473.33	10495.76	4589.90	4600.94	4718.62
	BIC	10667.41	10479.58	10502.01	4595.30	4606.34	4724.02
DD-LGP Model 14	R	0.87	0.75	0.81	0.89	0.79	0.86
	E	0.74	0.55	0.64	0.79	0.60	0.69
	RMSE	15.59	15.42	14.27	15.17	16.12	16.23
	AIC	10535.32	10493.28	10196.04	4469.84	4569.64	4580.81
	BIC	10541.58	10499.53	10202.29	4475.25	4575.04	4586.22
DD-LGP Model 15	R	0.84	0.71	0.67	0.81	0.77	0.61
	E	0.72	0.51	0.52	0.78	0.58	0.55
	RMSE	14.34	15.76	16.02	15.91	15.76	15.87
	AIC	10214.81	10576.92	10639.67	4548.10	4532.53	4543.96
	BIC	10221.06	10583.17	10645.92	4553.50	4537.94	4549.36
DD-LGP Model 16	R	0.94	0.92	0.93	0.95	0.90	0.91
	E	0.87	0.86	0.86	0.90	0.84	0.82
	RMSE	10.22	10.83	11.01	10.89	12.66	13.91
	AIC	8915.87	9138.20	9201.41	3925.23	4172.67	4327.37
	BIC	8922.12	9144.45	9207.67	3930.63	4178.07	4332.78
DD-	R	0.87	0.74	0.72	0.85	0.78	0.76

LGP Model 17	E	0.75	0.64	0.59	0.80	0.69	0.63
	RMSE	13.32	13.48	14.65	14.04	14.87	15.02
	AIC	9931.84	9977.63	10296.83	4342.66	4437.03	4453.52
	BIC	9938.09	9983.88	10303.08	4348.06	4442.43	4458.92
DD-LGP Model 18	R	0.80	0.70	0.61	0.72	0.68	0.61
	E	0.72	0.50	0.50	0.65	0.58	0.55
	RMSE	15.02	15.44	16.31	15.91	15.65	15.59
	AIC	10392.48	10498.25	10708.47	4548.10	4521.02	4514.71
	BIC	10398.73	10504.50	10714.72	4553.50	4526.43	4520.12
DD-LGP Model 19	R	0.87	0.75	0.72	0.85	0.77	0.73
	E	0.74	0.55	0.52	0.82	0.58	0.62
	RMSE	17.11	17.68	18.87	16.27	18.65	19.11
	AIC	10892.11	11017.78	11267.59	4584.86	4809.17	4849.20
	BIC	10898.36	11024.04	11273.85	4590.26	4814.57	4854.60
DD-LGP Model 20	R	0.87	0.85	0.74	0.83	0.80	0.75
	E	0.71	0.82	0.55	0.71	0.79	0.71
	RMSE	14.11	14.21	14.31	14.34	15.62	16.19
	AIC	10152.80	10179.88	10206.78	4377.40	4517.87	4576.76
	BIC	10159.05	10186.13	10213.03	4382.80	4523.28	4582.16

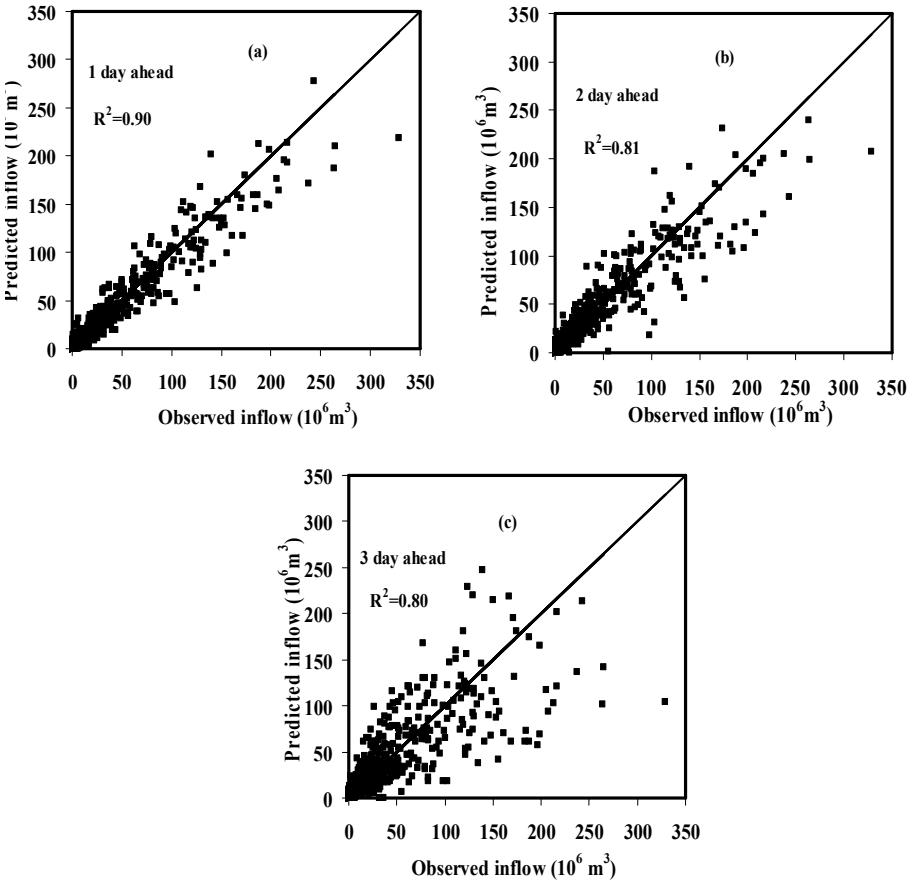

Figure 5.36. Scatter plot of observed and multi-time-step ahead predicted inflow by DD-LGP model 16 during testing period

5.3 Summary

This chapter addressed the application of conventional and AI techniques single and multi-reservoir inflow prediction. Performance measures such as R, RMSE, E, AIC and BIC are explored to check the accuracy and adequacy of the models. For KIP system, the non-linear AI models performed very well using the MA data pre-processing technique for full year and seasonal data inflow prediction in the case of multi-reservoirs considering each reservoir independently. Concurrent inflow prediction using ANN(6-3-3) model without considering exogenous inputs showed R values of 0.950, 0.966 and 0.954 for Manikdoh, Pimpalgaon Joge and Yedgaon reservoirs respectively in case of seasonal data. The one-step-ahead daily full year ANN(7-4-3) model with TLRN network and gamma memory has performed better than MLP network. The accuracy of one-step-ahead prediction was very good for all the reservoirs but the 2-day and 3-day-ahead is slightly less which may be due to the highly non-linear relationship in the input data, which the TLRN model itself could not predict. Thus, based on the results from the independent and concurrent predictions, it can be summarized that the TLRN type of ANN network with short-term gamma memory structure is suitable for forecasting concurrent multi-reservoir inflows for daily full year and daily seasonal data.

For KHEP, model 18 with 1 day ahead resulted better among lumped data models for all the modelling techniques (except ARIMA). It is also observed that lumped daily data models slightly performed better distributed data models. The reason may be length of data available for distributed model is less than lumped data models. On the other hand large number of input variables increased the complexity of the model and reduced the performance. The results showed that ANN has resulted in better scenario during training as well testing than that of MLR models. It is observed that the performance of the models has been increased by introducing choice of membership function in ANFIS models. It is concluded that the poor performance of the ANNs in comparison with the ANFIS may be due to the lack of explanatory power. LGP model captured linear as well as non-linear inflow accurately than ANN and ANFIS. The reason could be that LGP can automatically select input and appropriate relationship and thus produced parsimonious results. LGP models responded well to most fluctuations within the data and provided the closest mapping for peak inflows. It is concluded that the capability of LGP to generate innumerable new values and assess their usefulness efficiently seems to give it an edge over the ANN and ANFIS models.

Chapter 6

Multi-Objective Optimization of a Multi-Reservoir System

6.1 General

Irrigated agriculture is the largest consumer of water and has high significance in developing countries like India, since majority of the peoples depend on it. However, the uncertainty over rainfall and uneven distribution of water causes serious challenge to agriculture. The temporal variation in water requirement for different crops under multiple canals calls for an efficient operation of an irrigation system, especially for large scale irrigation projects. Thus, irrigation water management is becoming a key issue in sustainable agricultural development. In case of multi-reservoir systems, the sustainability in irrigation may be achieved by sharing water among the reservoirs. In most of such cases, water is transferred from the upstream reservoirs to cater the demands at the downstream reservoir. This intra basin water sharing necessitates an integrated operation of multi-reservoir system rather than considering them as an individual reservoir system. This urges the planners to arrive at an optimal crop plan for integrated operation of multi-reservoir system through efficient management of irrigation demands under various canals. Thus, optimizing the operations of a multi-reservoir irrigation system for an integrated operation has become essential, especially in India. This chapter describes the development and application of simulation and optimization models for an integrated operation of multi-reservoir system namely Kukadi Irrigation Project (KIP), Maharashtra, India.

6.2 Simulation Model for Crop Planning

The importance of each components of a system can be studied by simulating the system for various scenarios using a simulation model. Hence, a monthly simulation model is developed to analyse the behaviour of the KIP multi-reservoir system, especially to study the intra basin water transfer based on the standard operating policy (SOP). To study the existing operation, the simulation model first reads the input such as inflow, initial storage and crop area under each canal. The available storage for each reservoir is then estimated by detecting the evaporation and losses. Then, gross water requirement for each canal at the canal head is estimated from the net water requirement and the crop area under each canal incorporating the transmission losses. Thus, the total irrigation demand is estimated based on the crop area planned as per KIPR (1990). The releases are then made according to the SOP as per the demand for each canal in a reservoir for the time period '*t*'. If the available water is less than the demand, then the deficits are estimated for each canal. The possibility of intra basin water transfer is then checked and released. Finally, the surplus and final storage for each reservoir are estimated. This procedure is repeated for all the upstream reservoirs. The water transfer from the upstream reservoir is added with the inflow to the downstream reservoir while estimating the available storage and releases are made as per SOP. This procedure is repeated for total simulation period. The behaviour of the system based on its long term operation is assessed using the statistical performance indices such as reliability, resilience and vulnerability. The results of the simulation model are discussed in the following section.

6.2.1 Results of the Simulation Model

Kukadi Irrigation Project (KIP) is a complex system with five reservoirs and ten canals. Dimbhe, Wadaj, Manikdoh and Pimpalgaon Joge are the upstream reservoirs and are in parallel to each other. Yedgaon is at the downstream of these reservoirs and is in series with all the upstream reservoirs. Almost 60% of the cultivable area in the KIP is irrigated through Kukadi left bank canal (KLBC) from Yedgaon reservoir. However, the water available in Yedgaon reservoir is not sufficient to cater the irrigation demands of KLBC on its own. Therefore, water is transferred from all the upstream reservoirs to the Yedgaon reservoir through canals and rivers. This intra basin water allocation makes the system complex. The present simulation model is developed to study the multi-reservoir irrigation releases and the water transfer releases in the system. The reservoir operations are simulated for the

commonly available eleven years of observed inflow data. The releases to the canals and the end month storage levels of each reservoir resulted from the simulation model are discussed below.

The results of monthly irrigation releases to all the ten canals in KIP from the simulation model is shown in Figure 6.1. It is observed that all the canals have satisfied the irrigation demands during most of the time periods. It is also observed that there is clear distinction of releases between two seasons, namely Kharif (Jun – Sep) and Rabi (Oct – Feb) in all the canals. It is observed that the releases during Rabi season are higher than Kharif, since the crop area assigned during Rabi is higher than Kharif season as per the project proposal. Also, the rainfall during Kharif season makes less water requirement for irrigation. It is observed that MLBC and KLBC have frequently resulted in deficit during some months due to inadequate inflow and less storage. This deficit occurred mostly during the Rabi season (non-monsoon season). The failure of KLBC shows that the water transfer from the upstream reservoirs is not optimal and also not at appropriate time. It is also to be noted that more water cannot be transferred to the Yedgaon reservoir during monsoon season because of its less storage capacity. This calls for an efficient reallocation of water transfer from one reservoir to other reservoir, both spatially as well as temporally. This efficient spatial and temporal reallocation can be achieved through multi-objective reservoir optimization model.

The reliability of irrigation releases from the reservoirs of KIP system is given in Table 6.1. The time reliability shows that the DRBC, DLBC, GBC, MBC, WRBC, MFC, PLBC and PC of upstream reservoirs have satisfactorily released the irrigation demands. However, the time reliability of MLBC under major upstream reservoir Manikdoh is low indicating the releases are not timely in spite of having good volume reliability. The reliability of KLBC under Yedgaon reservoir is very less compared to other reservoirs in the system. This shows that most of the time, it has not satisfied the irrigation releases. It can also be inferred that the water transfer from the upstream reservoir is not at appropriate time and temporal allocation need to be revised.

The mean and maximum resilience of the canals in KIP system are given in Table 6.1. A resilience index close to one indicates that the system is capable to recover quickly from a failure state and vice versa. The resilience index of canals of Dimbhe reservoir varies significantly. Wadaj reservoir canals have high resilience than other canals in the system.

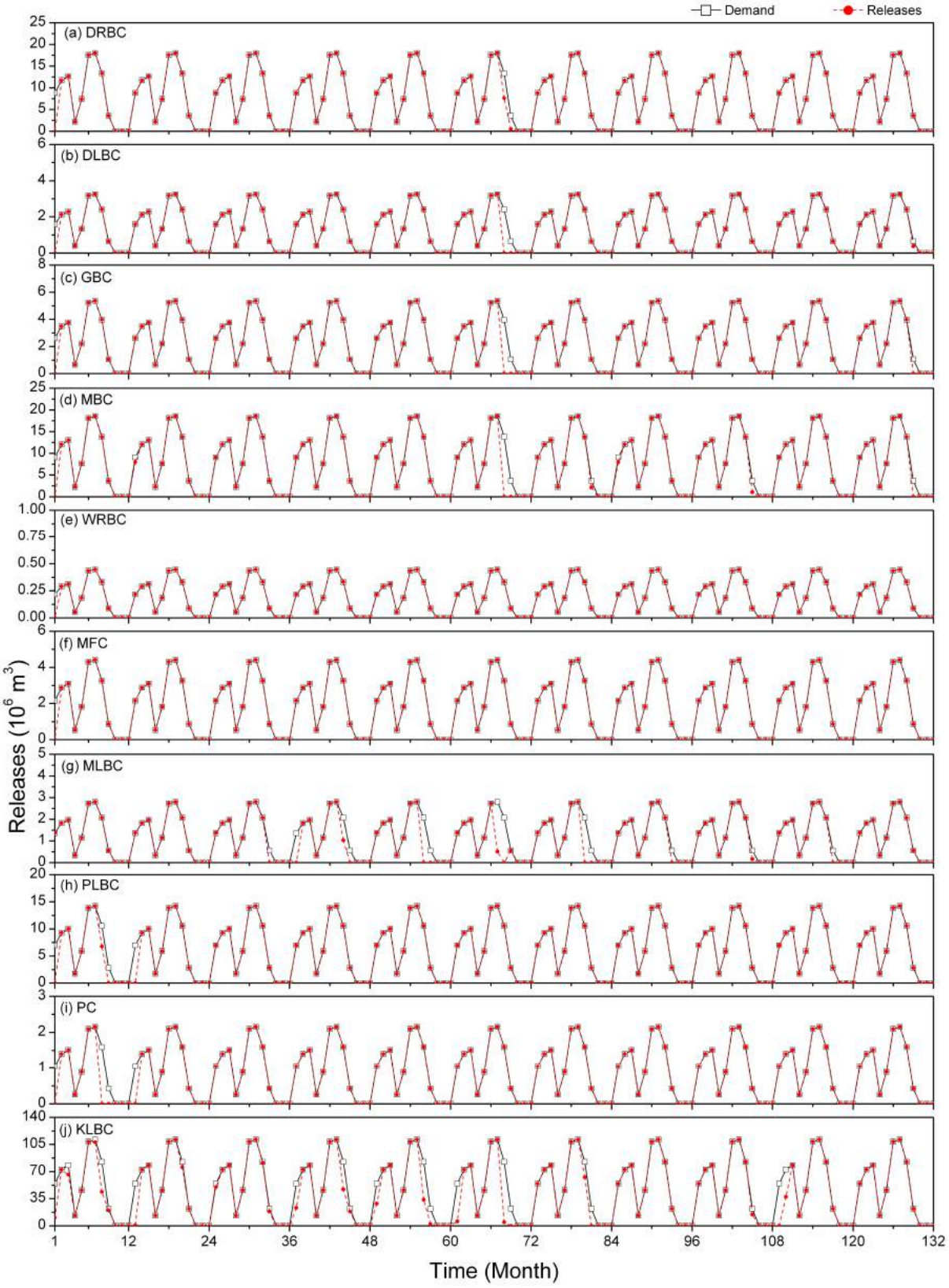

Figure 6.1 Results of monthly irrigation releases to all the ten canals in KIP from the simulation model

This shows that these canals have failed only in one month and the canals are likely return to the satisfactory state quickly. Hence, the reliability and resilience of Wadaj reservoir canals are higher compared to other canals. The canals of Manikdoh and Pimpalgaon reservoirs have very low resilience indices. The KLBC under Yedgaon reservoir has the least resilience compared to the other canals in the system. This shows that the failure occurred very frequently and probable return to satisfactory state is also slow. These results indicate that more water need to be allocated to KLBC.

The mean and maximum vulnerability of the canals and in KIP system is given in Table 6.1. The vulnerability indices of canals under Dimbhe reservoir varies significantly for each canal. Among the four canals under Dimbhe, DRBC is having higher vulnerability, since it irrigates more area. The canals under Wadaj reservoir is having less vulnerability index compared to other canals in the system. The vulnerability index shows that the KLBC is highly vulnerable with a maximum vulnerability of 117.53×10^6 m^3.

Table 6.1. Reliability, resilience and vulnerability indices of KIP canals for irrigation releases

Canals	Dam	Reliability		Resilience		Vulnerability (10^6 m^3)	
		Time	Volume	Mean	Maximum	Mean	Maximum
DRBC	Dimbhe	0.98	0.98	0.67	0.50	8.81	8.83
DLBC	Dimbhe	0.97	0.97	0.50	0.50	2.46	3.05
GBC	Dimbhe	0.97	0.97	0.75	0.50	2.90	5.02
MBC	Dimbhe/Wadaj	0.94	0.97	0.88	0.50	5.22	17.42
WRBC	Wadaj	0.99	0.99	1.00	1.00	0.22	0.22
MFC	Wadaj	0.99	0.99	1.00	1.00	2.16	2.16
MLBC	Manikdoh	0.75	0.91	0.30	0.20	1.46	4.37
PLBC	Pimpalgaon	0.93	0.98	0.33	0.17	6.84	13.57
PC	Pimpalgaon	0.93	0.97	0.33	0.17	1.37	3.07
KLBC	Yedgaon	0.70	0.90	0.28	0.14	56.72	117.53

The reliability, resilience and vulnerability indices of the reservoirs in KIP with respect water transfer to Yedgaon reservoir is given in Table 6.2. Dimbhe and Manikdoh are the two reservoirs from where the major quantity of water is transferred to the Yedgaon reservoir. From Table 6.2, it is found that three reservoirs (Dimbhe, Wadaj and Pimpalgaon) have satisfactorily succeeded in water transfer, except Manikdoh. The performance indices show that the water transfer from Manikdoh is not as per the demand because of less inflow in to the reservoir. The time reliability index of Manikdoh shows that the water transfer is not

timely. This may be due to the less rainfall and inflow in the catchment area of Manikdoh reservoir (Siddamal and Birajdar, 2012). The mean and maximum resilience index is also low compared to other reservoirs. A very high vulnerability of 114.35×10^6 m^3 has been observed for Manikdoh reservoir, which is around 40% of live storage capacity. Dimbhe reservoir has also resulted in a high vulnerability next to Manikdoh. These two are the major reservoirs which significantly contributed the water transfer to the Yedgaon reservoir.

Table 6.2. Reliability, resilience and vulnerability indices of KIP dams for Yedgaon water transfer

Dam	Reliability		Resilience		Vulnerability (10^6 m^3)	
	Time	Volume	Mean	Maximum	Mean	Maximum
Dimbhe	0.91	0.88	0.50	0.33	43.67	92.43
Wadaj	0.99	0.99	1.00	1.00	2.24	2.24
Manikdoh	0.59	0.72	0.24	0.14	60.30	114.35
Pimpalgaon	0.94	0.92	0.38	0.20	0.99	1.49

6.3 Formulation of Optimal Crop Planning Model

The spatial and temporal variation in irrigation water requirement and its increasing demand calls for an efficient integrated operation and management of multi-reservoir irrigation system. A suitable cropping pattern and optimal allocation of water for various crops is required for sustainable operation of multi-reservoir irrigation system. Hence, an optimal crop planning model has been formulated to arrive at a sustainable crop planning for the integrated operation of the multiple reservoirs in KIP system.

6.3.1 Multi-Objective Functions

In the present study, two objectives, *viz* maximizing net benefits and maximizing the crop production from the crops cultivated in the command area of KIP system are considered. These two objectives are widely used as multi-objective functions in deriving optimal crop planning studies (Maji and Heady, 1980; Raju and Duckstein, 2003). These two objectives are also conflicting because, the maximum crop production may not yield maximum net benefit but that crop may be a sociologically relevant crop. These two objectives are

subjected to various physical and economic constraints. The multi-objectives and constraints formulated for KIP are explained in the following section.

6.3.1.1 Objective 1: Maximizing the Net Benefits

The first objective is to maximize the net benefit obtained by growing multiple crops under various canals of KIP system during both Kharif and Rabi seasons. It can be expressed as:

$$\text{Maximize} \qquad NB = \sum_{j=1}^{10}\sum_{i=1}^{6} CK_i AK_{i,c} + \sum_{j=1}^{10}\sum_{i=7}^{13} CR_i AR_{i,c} \tag{6.1}$$

where i = Crop index [1 = Jowar Hybrid (K), 2 = Bajra Hybrid (K), 3 = Paddy (K), 4 = Groundnut (K), 5 = Chillies (K), 6 = Vegetables (K), 7 = Wheat (R), 8 = Jowar Local (R), 9 = Jowar Hybrid (R), 10 = Jowar Rabi (Rattoon) (R), 11 = Peas (R), 12 = Vegetables (R) and 13 = Potatoes (R), K = Kharif, R = Rabi].

NB = Total Net benefits (Indian Rupees)

CK_i = Gross benefits from the Kharif crop 'i' from the command area of KIP

CR_i = Gross benefits from the Rabi crop 'i' from the command area of KIP

The net benefits are estimated after deducting the appropriate input charges from the gross benefits.

$AK_{i,c}$ = Area of Kharif crop 'i' grown in the command area of canal 'c'

$AR_{i,c}$ = Area of Rabi crop 'i' grown in the command areas of canal 'c'

c = canal index [1= Dimbhe Right Bank Canal (DRBC), 2 = Dimbhe Left Bank Canal (DLBC), 3 = Ghod Branch Canal (GBC), 4 = Meena Branch Canal (MBC), 5 = Wadaj Right Bank Canal (WRBC), 6 = Meena Feeder Canal (MFC), 7 = Manikdoh Left Bank Canal (MLBC), 8 = Pimpalgaon Joge Canal (PLBC), 9 = Pushpawathi Canal (PC), 10 = Kukadi Left Bank Canal (KLBC)]

6.3.1.2 Objective 2: Maximizing the Crop Production

The second objective of the multi-objective optimization is to maximize the production of various crops from the command area of KIP system grown during Kharif and Rabi seasons and is given by

$$\text{Maximize} \qquad CP = \sum_{c=1}^{10}\sum_{i=1}^{6} Y_i AK_{i,c} + \sum_{c=1}^{10}\sum_{i=7}^{13} Y_i AR_{i,c} \tag{6.2}$$

Y_i = average yield of the crop '*i*' in tonnes/ha.

6.3.2 Constraints

The above formulated objective functions are subjected to the following constraints.

6.3.2.1 Seasonal Crop Area Constraint

The total area under various crops should not be more than the total area available for cultivation in command area during different crop seasons. The total sowing area constraint during Kharif and Rabi seasons is given by

During Kharif season:

$$\sum_{c=1}^{10}\sum_{i=1}^{6} AK_{i,c} \le CCA_K \tag{6.3}$$

During Rabi season:

$$\sum_{c=1}^{10}\sum_{i=7}^{13} AR_{i,c} \le CCA_R \tag{6.4}$$

where CCA_K and CCA_R is the maximum area available for cultivation during Kharif and Rabi seasons respectively.

6.3.2.2 Canal Area Constraint

The total crop area under each canal should not be more than the maximum area available for irrigation under that canal.

During Kharif Crops:

$$\sum_{i=1}^{6} AK_{i,c} \leq CCAK_c \qquad c = 1,\ldots,10 \qquad (6.5)$$

During Rabi Crops :

$$\sum_{i=7}^{13} AR_{i,c} \leq CCAR_c \qquad c = 1,\ldots,10 \qquad (6.6)$$

where $CCAK_c$ and $CCAR_c$ is the maximum area available under each canal for cultivation during Kharif and Rabi seasons respectively.

6.3.2.3 Minimum Sowing Area Constraint

The minimum crop area constraint is given to ensure that all the crops in the existing cropping pattern and also mentioned in the project report (KIPR, 1990) enters into optimal cropping pattern. These crops are staple crops required to fulfil the sociological requirements. The minimum sowing area constraint for staple crops are given by:

During Kharif season:

$$AK_{i,c} \geq AK_{i,c}^{\min} \qquad i = 1,\ldots,6;\ c = 1,\ldots,10 \qquad (6.7)$$

During Rabi season:

$$AR_{i,c} \geq AR_{i,c}^{\min} \qquad i = 7,\ldots,13;\ c = 1,\ldots,10 \qquad (6.8)$$

where $AK_{i,c}^{\min}$ and $AR_{i,c}^{\min}$ are the minimum area to be cultivated under crop 'i' in canal 'c' during Kharif and Rabi seasons respectively.

6.3.2.4 Crop Water Requirement Constraint

The water requirement for various crops under each canal is estimated by multiplying the gross irrigation requirement ($WR_{i,t}$) of the crop 'i' with its corresponding area during the time period 't'. The net irrigation requirement is estimated using Modified Penman method (Given in Table 4.3) and gross irrigation requirement is estimated after accounting for water loss during transmission (KIPR, 1990). The efficiency of different canals is incorporated accordingly. The crop water requirement constraint covering two seasons is given in Eq. 6.9 and Eq. 6.10:

For Kharif season:

$$R_{t,c} \geq \sum_{i=1}^{6} WR_{i,t} AK_{i,c} \qquad t = 1,\ldots,4;\ c = 1,\ldots,10 \qquad (6.9)$$

For Rabi season:

$$R_{t,c} \geq \sum_{i=7}^{13} WR_{i,t} AR_{i,c} \qquad t = 5,\ldots,8;\ c = 1,\ldots,10 \qquad (6.10)$$

where $R_{t,c}$ is the release to canal 'c' during the time period 't', $WR_{i,t}$ is the gross irrigation requirement for crop 'i' during the time period 't', $AK_{i,c}$ and $AR_{i,c}$ are the area of crop 'i' during Kharif and Rabi seasons respectively.

6.3.2.5 Canal Capacity Constraint

Irrigation release from the reservoir during any time period 't' should not be more than the canal carrying capacity. This constraint is given as:

$$R_{t,c} \leq CCC_c \qquad t = 1,\ldots,12;\ c = 1,\ldots,10 \qquad (6.11)$$

where CCC_C is the carrying capacity of the canal 'c'.

6.3.2.6 Reservoir Evaporation Constraint

The evaporation loss ($E_{n,t}$) from the reservoir 'n' during the period 't' is expressed as a function of initial and final storage during that particular time period (Jothiprakash *et al.*, 2011a). This constraint is expressed as:

$$E_{n,t} = a_{n,t} \times \frac{\left(S_{n,t} + S_{n,t+1}\right)}{2} + b_{n,t} \qquad n = 1,\ldots,5;\ t = 1,\ldots,12 \qquad (6.12)$$

where $a_{n,t}$ and $b_{n,t}$ are the regression co-efficient for the reservoir 'n' during the time period 't' estimated by the regression analysis. $S_{n,t}$ and $S_{n,t+1}$ are the initial and final storages of the reservoir 'n' during the time period 't'.

6.3.2.7 Mass Balance Constraint

The mass balance constraint balances the input and output of each reservoir during each time period 't'. This continuity constraint applied to each reservoirs is given as:

Dimbhe:

$$S_{1,t+1} = S_{1,t} + I_{1,t} - R_{1,t} - R_{2,t} - R_{3,t} - R_{4,t} - E_{1,t} - O_{1,t} - YR_{1,t} \qquad t = 1,\ldots,12 \qquad (6.13)$$

Wadaj:

$$S_{2,t+1} = S_{2,t} + I_{2,t} - R_{5,t} - R_{6,t} - E_{2,t} - O_{2,t} - YR_{2,t} \qquad t = 1,\ldots,12 \qquad (6.14)$$

Manikdoh:

$$S_{3,t+1} = S_{3,t} + I_{3,t} - R_{7,t} - E_{3,t} - O_{3,t} - YR_{3,t} \qquad t = 1,\ldots,12 \qquad (6.15)$$

Pimpalgaon Joge:

$$S_{4,t+1} = S_{4,t} + I_{4,t} - R_{8,t} - R_{9,t} - E_{4,t} - O_{4,t} - YR_{4,t} \qquad t = 1,\ldots,12 \qquad (6.16)$$

The mass balance constraint applied to Yedgaon reservoir is given in Eq. 6.17. This reservoir includes the intra basin water transfer as well as surplus from upstream reservoir as input apart from inflow from its own catchment.

Yedgaon:

$$S_{5,t+1} = S_{5,t} + I_{5,t} + \sum_{n=1}^{4} \eta_n YR_{n,t} + \sum_{n=3}^{4} \gamma_n O_{n,t} - R_{10,t} - E_{5,t} - O_{5,t} \qquad t = 1,\ldots,12 \qquad (6.17)$$

In the above equations, $S_{n,t}$ is the initial storage of reservoir 'n' during the time period 't'; $S_{n,t+1}$ is the final storage of reservoir 'n' during the time period 't'; $I_{n,t}$ is the inflow in to the reservoir 'n' during the time period 't'; $O_{n,t}$ is the overflow from reservoir 'n' during the time period 't'; $E_{n,t}$ is the evaporation from reservoir 'n' during the time period 't'; $R_{c,t}$ is the release to the canal 'c' during the time period 't'; $YR_{n,t}$ is the water transfer from upstream reservoirs 'n' to Yedgaon reservoir during the time period 't'; η_n and γ_n are the transmission efficiency of canals and rivers of reservoir 'n' (KIPR, 1990).

6.3.2.8 Minimum and Maximum Storage Constraint

Reservoir storage during any time period should not be more than the capacity of the reservoir, and also should not be less than the dead storage. This physical constraint is given as:

$$S_{n,\min} \le S_{n,t} \le S_{n,\max} \qquad n = 1,\ldots,5;\ t = 1,\ldots,12 \qquad (6.18)$$

where $S_{n,min}$ and $S_{n,max}$ are the dead storage and capacity of reservoir 'n'.

6.3.2.9 Overflow Constraint

The overflow occurs when the storage exceed the maximum storage (capacity) of the reservoir. If no constraint on overflow is included in the LP model, it may result in overflow even when the reservoir storage is less than the capacity and hence the overflow constraint developed by Chávez-Morales (1987) is used in the present study. This overflow constraint is given as:

$$O_{n,t} = S_{n,t+1} - S_{n,\max} \qquad n = 1,\ldots,5;\ t = 1,\ldots,12 \qquad (6.19)$$

$$O_{n,t} \ge 0 \qquad n = 1,\ldots,5;\ t = 1,\ldots,12 \qquad (6.20)$$

where $O_{n,t}$ is the overflow from the reservoir 'n' during the time period 't'.

As explained in the methodology chapter, the above developed optimization model is solved using different techniques. Initially, both the objectives of the crop planning model are solved individually using linear programming technique. This LP optimization model has 178

variables and 712 constraints. Then, the fuzziness in the objectives is considered and solved using multi-objective fuzzy linear programming approach. Both the objectives are simultaneously solved using multi-objective evolutionary algorithms. Then, the chaos is coupled with multi-objective evolutionary algorithms and used for deriving optimal crop plans. The results obtained from all the models are inter-compared and discussed in the following section.

6.4 Multi-objective Fuzzy Linear Programming Model

In the present study, the objectives are considered as imprecise variable and modelled using multi-objective fuzzy linear programming (MOFLP) approach. The objectives of the LP model are converted to a fuzzy variable using a linear membership function over the tolerance range (Zimmermann, 1996). The linear membership function for an objective function '*Z*' is given as:

$$\mu_Z(X) = \begin{cases} 0 & Z < Z_L \\ \dfrac{Z - Z_L}{Z_U - Z_L} & Z_L \le Z \le Z_U \\ 1 & Z > Z_U \end{cases} \tag{6.21}$$

where Z_U and Z_L are maximum and minimum values of the objective functions obtained from the LP model. The LP model is transferred to MOFLP model with the objective of maximizing the degree of satisfaction.

$$\text{Maximise } \lambda \tag{6.22}$$

Subject to

$$\mu_{Z(j)}(X) \ge \lambda \qquad j = 1,2,... \tag{6.23}$$

where λ is the degree of satisfaction and $0 \le \lambda \le 1$; j is the number of objectives. In addition to this all other existing constraints (Eq. 6.3 to 6.20 of LP model) has to be used while solving MOFLP model. Thus, the first objective of maximizing the net benefits is converted in to a fuzzy constraint as:

$$\frac{NB - NB_L}{NB_U - NB_L} \geq \lambda \tag{6.24}$$

The second objective of maximizing the crop production is converted in to a fuzzy constraint as:

$$\frac{CP - CP_L}{CP_U - CP_L} \geq \lambda \tag{6.25}$$

In the above equations, λ is the degree of satisfaction which varies between 0 and 1. NB_U, NB_L are the upper and lower limits of net benefits. CP_U and CP_L are the upper and lower limits of crop production. The values of NB_U, NB_L, CP_U and CP_L are obtained from the results of crisp LP model. In addition to the above fuzzy constraints, all the constraints considered in LP model is also considered while solving the fuzzy model.

6.5 Results of MOFLP Optimal Crop Planning Model

Using the above developed optimization model, optimal crop planning has been derived for the sustainable integrated operation of Kukadi multi-reservoir irrigation system using multi-objective fuzzy linear programming (MOFLP) approach. The optimization model is solved using global solver in Language for Interactive General Optimization (LINGO) package. The global solver combines a series of range bounding and range reduction techniques within a branch and bound framework to find global solutions to non-convex non-linear programs (Lingo, 2006). As a first step, the two individual objectives namely (i) maximizing the net benefits and (ii) maximizing the crop production from the crops grown in the command area of KIP are optimized separately using crisp linear programming (LP) technique for different dependable inflow levels. The objectives are optimized separately for three inflow scenarios, (i) 50% dependable inflow scenario, (ii) 75% dependable scenario and (iii) 90% dependable inflow scenarios using deterministic LP. The results of the LP model for various inflow scenarios are given in Table 6.3. From the table, it is found that both the net benefits and crop production are high for 50% dependable inflow level. The maximum net benefit obtained is Rs. 2753.28 Millions ($45.77 Millions) and crop production is 2031.90 thousand tonnes for 50% dependable inflow level. The 75% dependable inflow resulted in a net benefit of Rs.

1893.83 Millions ($31.48 Millions) and 1385.01 thousand tonnes of crop production. On comparing with 50% dependable inflow scenario, both the net benefits and crop production are decreased by 31% in 75% dependable inflow scenario. The 90% dependable inflow has resulted a net benefit of Rs. 928.79 Millions ($15.44 Millions) and 574.33 thousand tonnes of crop production. On comparing with 50% dependable inflow scenario, the net benefit is decreased by 66.27% and crop production by 71.73% in 90% dependable inflow scenario. Similarly, there is a reduction of 50.96% net benefits and 58.53% crop production with 90% dependable inflow scenario compared to 75% dependable inflow scenario. The reduction in crop area as well as crop production is due to the reduction in the inflow.

Table 6.3. Resulted net benefits and crop production from LP models

Objectives	Net Benefits (Million Rupees)			Crop Production (1000 Tonnes)		
Inflow	50%	75%	90%	50%	75%	90%
Objective value	2753.28	1893.83	928.79	2031.90	1385.01	574.33
1$ = Rs. 60.14, As on 27th March 2014						

The multi-objectives developed in the present study are considered as fuzzy variables and are fuzzified using linear membership function as shown in Figure 6.2. From the results of crisp LP models, the upper and lower limits for the fuzzified equation of net benefits and crop production are fixed for MOFLP model. Then the fuzzified equations are considered as constraints and the fuzzy model is solved for maximizing the level of satisfaction (λ) along with other constraints using 75% dependable inflow. The MOFLP model has resulted in a degree of satisfaction of 0.46 for the integrated operation of multi-reservoir system with the total net benefit of Rs. 1909.92 Millions ($31.75 Millions) and total crop production of 1191.30 thousand tonnes. It is found that the net benefit is decreased by 30.52% and crop production by 41.37% in MOFLP model compared to 50% dependable inflow scenario of crisp LP model. On comparing the results with the 75% dependable inflow, there is an increase of 1% in net benefits and 13.99% decrease in crop production. It is also found that both the net benefits and crop production are significantly more by 51.37% in MOFLP model compared to 90% dependable inflow scenario LP model.

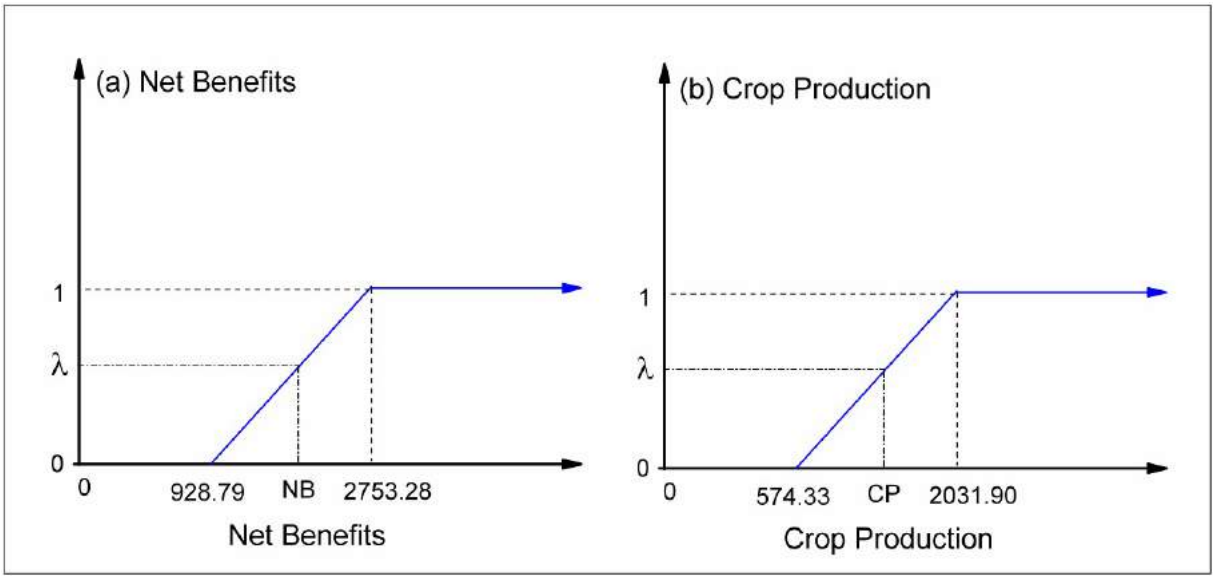

Figure 6.2. Membership functions used for (a) Net Benefits and (b) Crop Production

6.5.1 Optimal Crop Area Resulted from LP and MOFLP Models

The resulted optimal crop area under various canals from LP and MOFLP models are given in Table 6.4. Overall, the objective II has resulted in higher total crop area than objective I for 50% and 75% dependable inflow scenario. On contradicting to the project proposal, the total crop area resulted during Kharif season is higher than Rabi season for all the three inflow scenarios. This may be due to less water requirement for crops during Kharif season, because of more contribution from rainfall. It is seen that in LP model, both the 50% and 75% dependable inflows resulted in same crop area for most of the canals, except PLBC, PC and KLBC. This shows that the upstream reservoirs are capable of irrigating optimal area up to 75% dependable inflow. Further increase in the dependability reduces the crop area. The 50% dependable inflow has resulted in a maximum irrigation intensity of 137.67%. The MOFLP model has resulted in an irrigation intensity of 102.18% with a total crop area of 149232.10 ha. Since, the objectives are considered as fuzzy in MOFLP model, there is a reduction in total crop area and irrigation intensity compared to LP model. The MOFLP model also resulted higher crop area during Kharif (86429.31 ha) than Rabi (62802.79 ha).

Table 6.4. Resulted total crop area (ha) for each canal by LP and MOFLP models

Objective	LP Model						MOFLP
	Maximization of Net Benefits			Maximization of Crop Production			
Inflow	50%	75%	90%	50%	75%	90%	75%
DRBC	22306.54	22306.54	15567.43	22306.54	22306.54	16842.55	20605.07
DLBC	4078.05	4078.05	4078.05	4078.05	4078.05	4078.05	3462.33
GBC	6628.52	6628.52	4633.10	6628.52	6628.52	4633.10	6001.90
MBC	23006.73	23006.73	17455.51	23006.73	23006.73	16064.98	21270.02
WRBC	537.35	537.35	385.20	550.36	537.35	385.20	503.45
MFC	5525.75	5525.75	3814.55	5525.75	5525.75	3814.55	4397.95
MLBC	3474.93	3474.93	2423.55	3474.93	3474.93	2423.55	3038.95
PLBC	17055.34	11970.40	6560.70	17055.34	11855.30	6560.70	11954.78
PC	2375.72	2073.40	991.80	2375.72	2313.34	991.80	1998.89
KLBC	110894.96	73190.58	63963.19	116073.57	75145.09	63963.19	75998.76
Kharif	116217.24	89076.61	62305.12	124111.53	93090.24	61288.82	86429.31
Rabi	79666.65	63715.63	57567.96	76963.98	61781.35	58468.85	62802.79
Total	195883.89	152792.24	119873.08	201075.51	154871.59	119757.67	149232.10
Irrigation Intensity (%)	134.12	104.61	82.08	137.67	106.04	82.00	102.18

The resulted optimal crop area from LP and MOFLP models for various crops is given in Figure 6.3. The crop index 1-6 shows the Kharif crops and 7-13 are Rabi crops. All the crops proposed in the project report (KIPR, 1990) have entered the optimal solution because of minimum sowing area constraint. It is observed that out of the total crop area, around 60% resulted during Kharif season and remaining 40% resulted during Rabi season for all the LP and MOFLP models. From the figure, it is observed that there is a wide variation in optimal area for different inflow scenarios for various crops. Only Paddy and Chillies during Kharif season and Jowar rattoon during Rabi season have same area irrespective of inflow scenarios. It is also found that these crops have resulted only the minimum sowing area due to the more crop water requirement. All the models have resulted in a higher vegetable crop area during Kharif season, since the crop water requirement is less and high net return compared to other water intensive crops. Thus, there is wide variation in area for different inflow scenarios. Among Kharif crops, Vegetables resulted around 20%, Jowar Hybrid around 14% and Groundnut around 12% of total crop area in MOFLP model. Other crops resulted less than 3% of total crop area during Kharif in MOFLP model. Among Rabi crops, wheat has resulted in more area followed by Jowar local and Jowar hybrid. All the models have resulted in same area for Jowar rattoon during Rabi season. Among Rabi crops, both Wheat and Jowar local resulted around 12% and Jowar Hybrid resulted 10% of total crop area in MOFLP model. All other crops accounts for less than 2% in MOFLP model during Rabi season.

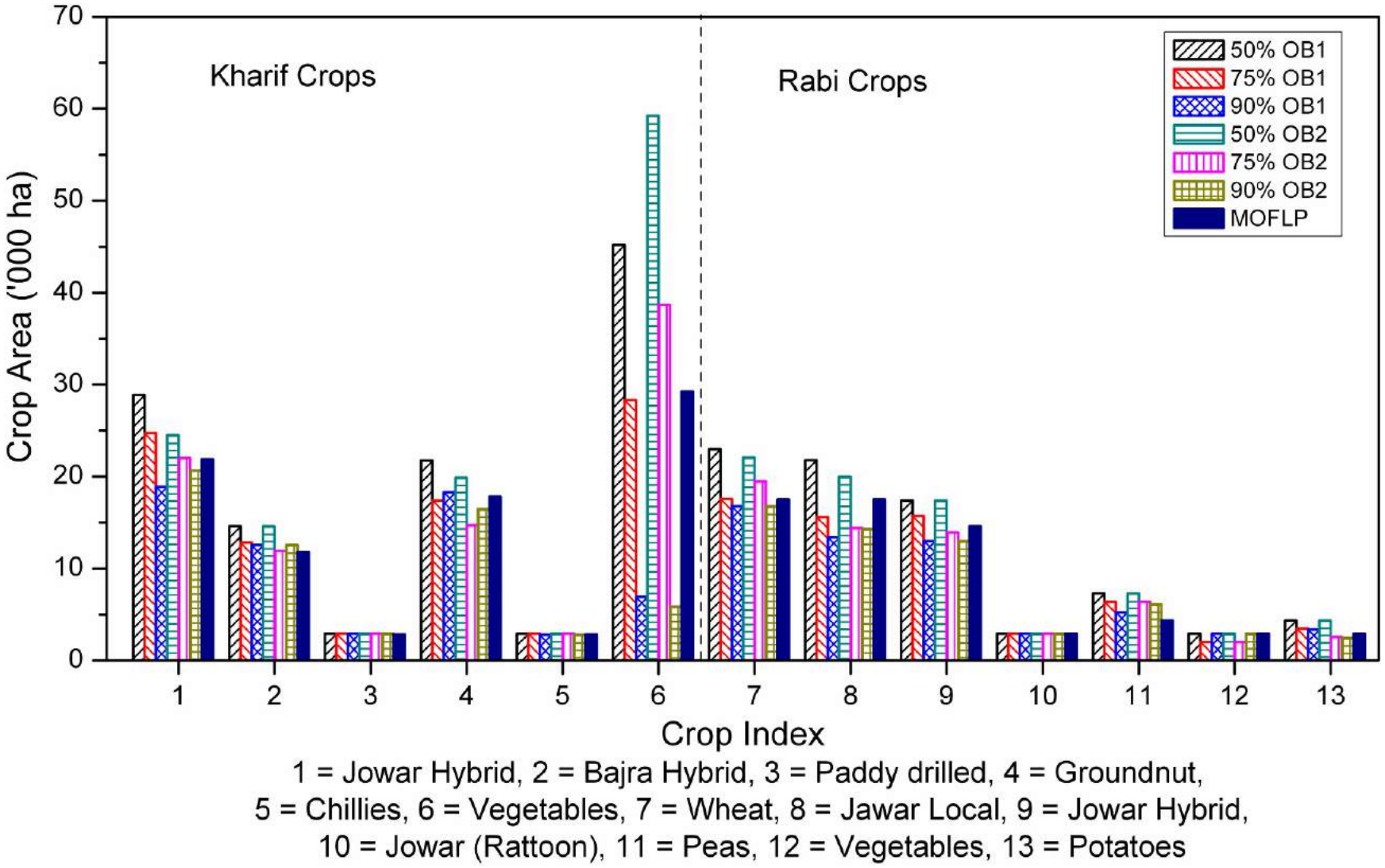

Figure 6.3. Resulted optimal total crop area for LP and MOFLP models

6.5.2 Monthly Irrigation Releases from LP and MOFLP Models

The optimal releases resulted from LP and MOFLP model to different canals during various time periods are given in Figure 6.4. The releases during Kharif season are higher than the releases during Rabi, since all the models have resulted higher crop area during Kharif season than Rabi. This may be due to less crop water requirement during Kharif season because of the contribution from rainfall. For DRBC, DLBC, GBC, MBC, WRBC and MLBC, there is clear distinction of two groups. One is all models except 90% dependable inflow and second group is 90% dependable inflow. This shows that theses canals are capable of irrigating same area up to 75% dependable inflow and further decreases in inflow reduces the crop area and releases. For all these canals, the MOFLP model follows the first group. It is also observed that there is large variation in releases among models occurred in MLBC, PLBC, PC and KLB canals. Thus, these are the canals which are mostly affected by decrease in inflow in to the reservoir. The MOFLP model has resulted in higher releases during Rabi season than Kharif season for KLBC. This may be due to that the resulted crop area during Kharif and Rabi are almost same for KLBC and the releases are less in Kharif due to rainfall. It is also observed that all the models have not resulted in any canal release during non-cropping season.

6.5.3 Water Transfer to Yedgaon Reservoir from LP and MOFLP Models

The releases to Yedgaon reservoir from different models are given in Figure 6.5. From the figure, it is found that all the models have resulted significant water transfer during Kharif and Rabi seasons, but for only one month in each season. During Kharif season, releases are significant in July month and in December during Rabi season. However, there is a wide variation in releases among the models. This is due to the variation in the resulted crop area. Dimbhe and Manikdoh have contributed significantly in water transfer. Wadaj has contributed equally during the July and December. The contribution from Dimbhe is high during Kharif season and from Manikdoh during Rabi season. Pimpalgaon has resulted very less water transfer, mostly during Kharif (starting of monsoon season) indicating that it is just a self sufficient reservoir.

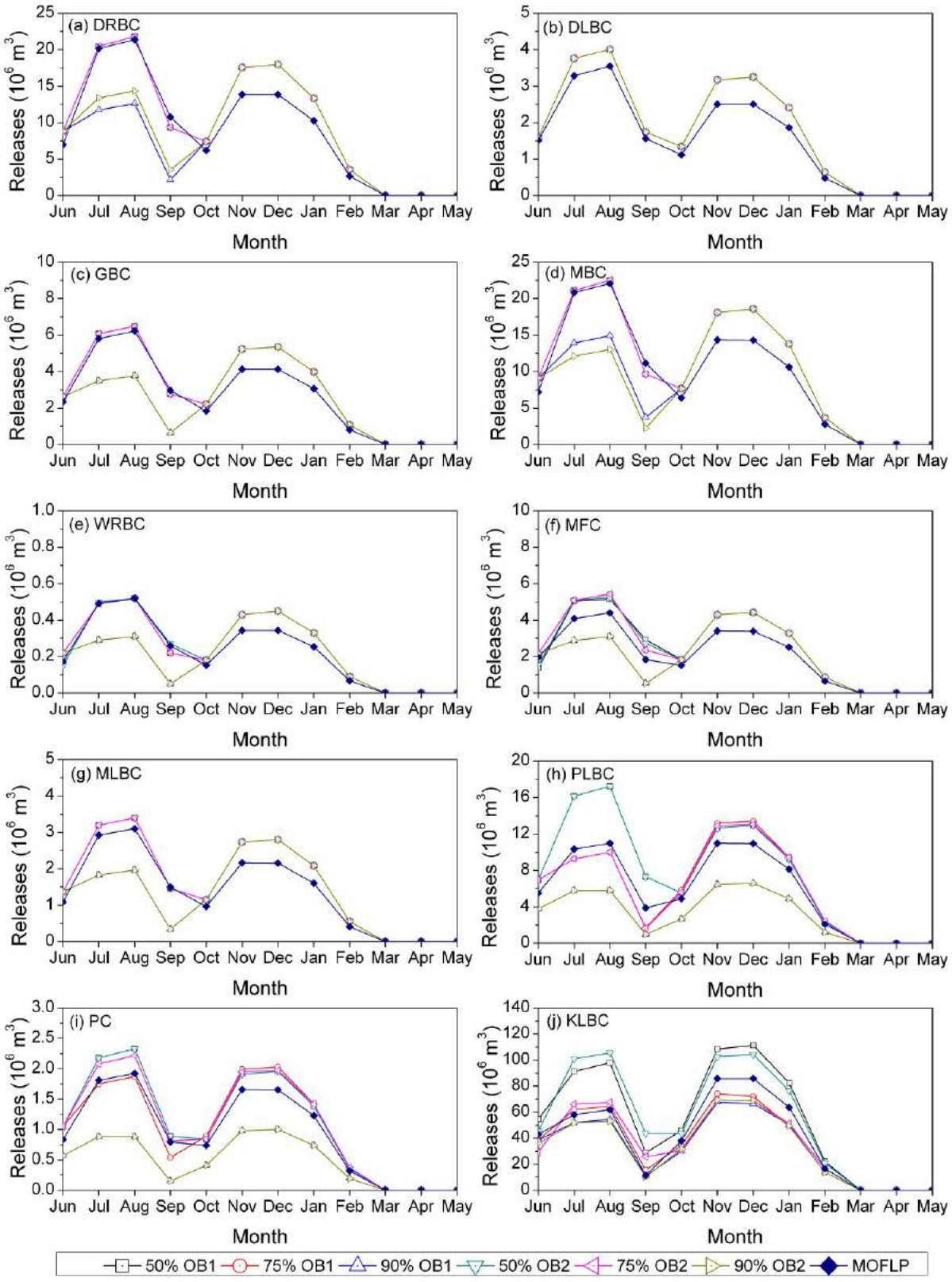

Figure 6.4. Resulted optimal releases to various canals from different LP and MOFLP models

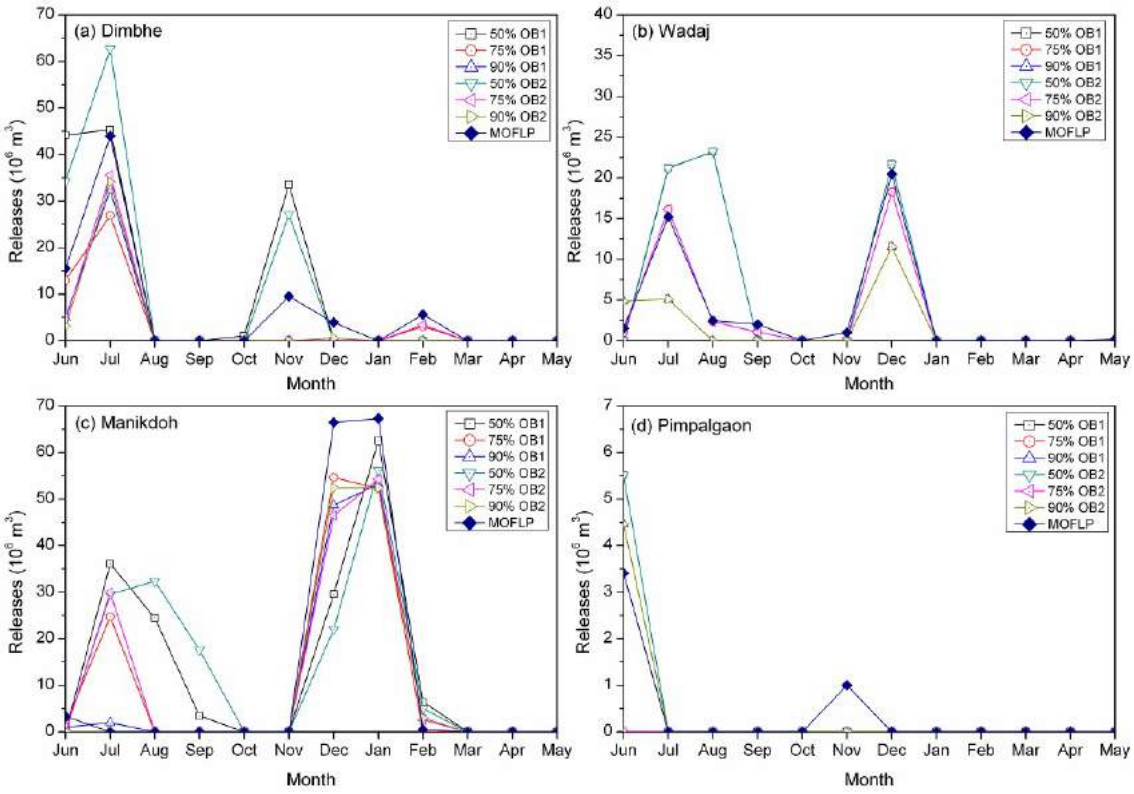

Figure 6.5. Water transfer to Yedgaon resulted from different LP and MOFLP models

6.5.4 End of Month Storage Levels from LP and MOFLP Models

The resulted final storage levels from different models for the five reservoirs in the KIP are given in Figure 6.6. All the models have resulted in high storage during monsoon and the storage gradually depletes during the non-monsoon season. This shows that all the reservoirs are intermittent reservoirs which receive inflow during the monsoon season. Even though, the storage levels are higher during monsoon, none of the reservoir except Yedgaon resulted in overflow. It is observed that 50% dependable inflows have resulted in higher storage levels due to high inflow. Also, the high storage in 50% dependable inflows scenario has resulted in more evaporation. The storage levels resulted from MOFLP model are almost similar to that of 75% dependable level. The storage levels significantly vary for all reservoirs, except Wadaj. The variation in storage level of Yedgaon reservoir during monsoon season is due to delay and variation in receiving the water from the upstream reservoirs. It is also to be noted that the live storage of Yedgaon is very less compared to other reservoirs and hence it resulted in overflow during monsoon season. Thus, more water cannot be stored in Yedgaon reservoir for irrigation during Rabi season. The storage of Yedgaon reservoir resulted from all LP

models is same during non-monsoon periods, since Yedgaon completely depends on upstream reservoir releases to cater the demands for Rabi season.

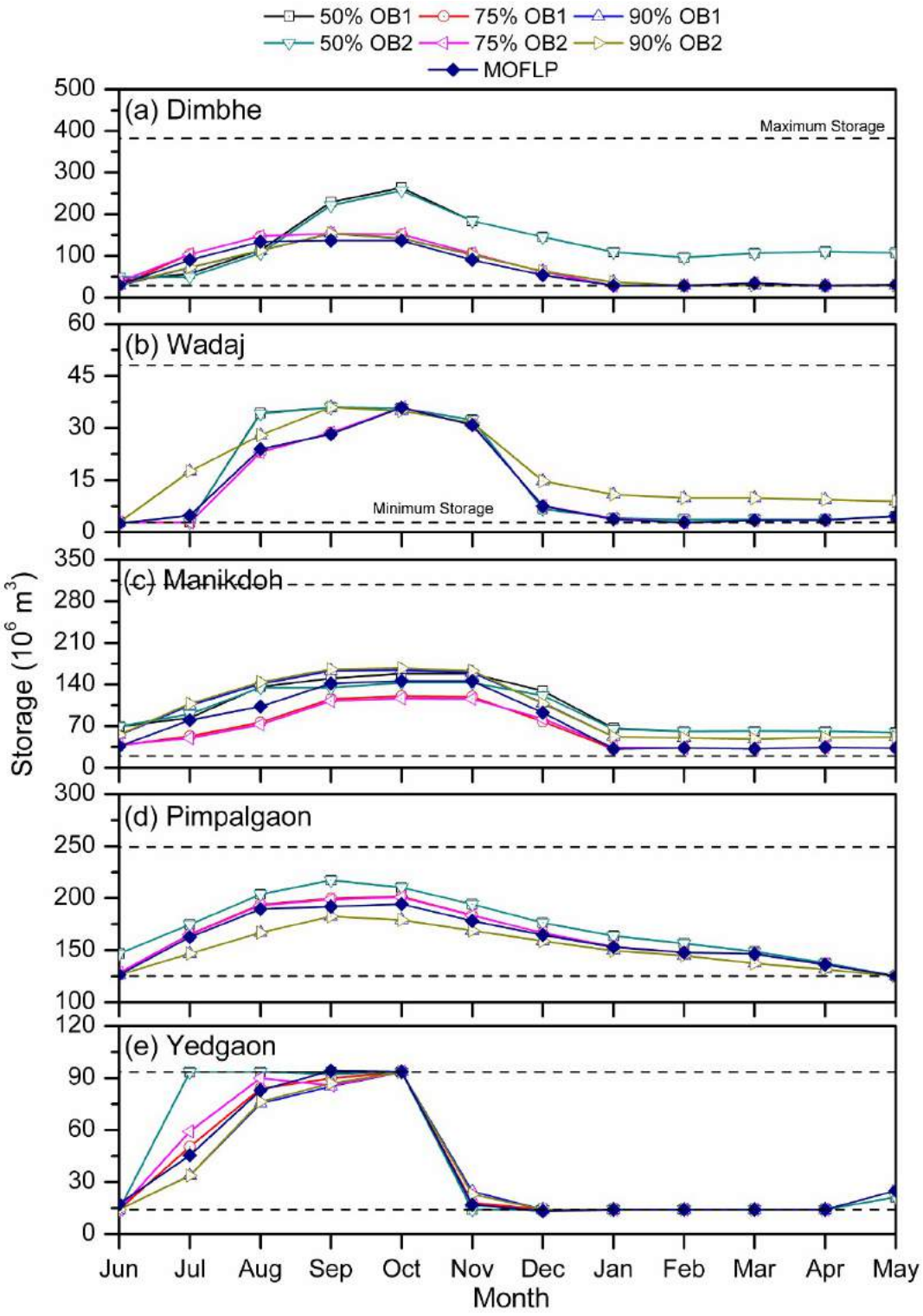

Figure 6.6. Resulted end of month storage level for various dams from different LP and MOFLP models

6.5.5 Simulation of Optimal MOFLP Results

The optimal crop area resulted from MOFLP model is simulated for 11 years of observed monthly inflow to evaluate the performance of the results. The various performance measures such as MFID, AFID, AAID and PAID reported by Jothiprakash and Shanthi (2009) is used. Monthly Frequency of Irrigation Deficit (MFID) is the ratio of the number of months deficit occurred to the total number of simulated months. Monthly Average Irrigation Deficit (MAID) is the ratio of the sum of the monthly deficit occurred in each month to the total number of simulated deficit months. Percentage Monthly Irrigation Deficit (PMID) is the ratio of the monthly average irrigation deficit to the monthly demand. Annual Frequency of Irrigation Deficit (AFID) is the ratio of number of years deficit occurred to the total simulated years. Annual Average Irrigation Deficit (AAID) is the ratio of sum of the irrigation deficit occurred in each year to number of deficit year. Percentage Annual Irrigation Deficit (PAID) is the ratio of annual average irrigation deficit to the total annual demand. In addition, reliability, resilience and vulnerability are estimated to evaluate behaviour the optimal policy for longer period. The results of the performance indices are given in Table 6.5. It is found that the optimal crop plans resulted from the MOFLP model has performed well over the period of year. The canals under Dimbhe reservoir failed in only one month out of the total simulated 132 months. The failure occurred in the first month of the simulation period for all the canals. It is also found that the MLBC under Manikdoh has resulted in irrigation releases as per the demand throughout the simulation period. This shows that the reservoir is a surplus reservoir and also significantly contributes to the water transfer to Yedgaon reservoir. Only the PLBC, PC and KLBC have resulted in deficits around 7 months out of 132 months of simulation. However, the MAID of PLBC and PC is very less and deficit occurred during June and February. Only KLBC resulted in irrigation deficits for 6 years with AAID of 12.79 $\times 10^6$ m^3.

The reliability, resilience and vulnerability for irrigation releases of various canals are given in Table 6.6. The time reliability shows that all the canals have satisfactory irrigation releases throughout the simulation period. Even though KLBC has resulted in irrigation deficits, the time reliability is higher. This shows that failure occurred only in a particular month every year. Even though the reliability of the canals under Dimbhe reservoir are high, vulnerability index of DRBC show that they are slightly vulnerable if failure occurs, since it irrigates more area. The MLBC under Manikdoh reservoir shows no vulnerability since it has satisfied the

irrigation demand in all the simulated period. The vulnerability index shows that KLBC is most vulnerable than other canals with high vulnerability.

Table 6.5. Performances of MOFLP policies for various canals

Canals	Dam	MFID	AFID	AAID (10^6 m^3)	PAID (%)
DRBC	Dimbhe	1/132	1/11	0.63	0.60
DLBC	Dimbhe	1/132	1/11	0.14	0.75
GBC	Dimbhe	1/132	1/11	0.21	0.68
MBC	Dimbhe/Wadaj	1/132	1/11	0.65	0.60
WRBC	Wadaj	5/132	2/11	0.04	1.72
MFC	Wadaj	6/132	3/11	0.53	2.24
MLBC	Manikdoh	0/132	0/11	0.00	0.00
PLBC	Pimpalgaon	7/132	2/11	1.19	1.76
PC	Pimpalgaon	7/132	2/11	0.18	1.65
KLBC	Yedgaon	7/132	6/11	12.79	2.75

Table 6.6. Reliability, resilience and vulnerability indices of MOFLP policies for various canals of KIP

Canal	Dam	Reliability		Resilience		Vulnerability (10^6 m^3)	
		Time	Volume	Mean	Maximum	Mean	Maximum
DRBC	Dimbhe	0.99	0.99	1.00	1.00	6.97	6.97
DLBC	Dimbhe	0.99	0.99	1.00	1.00	1.51	1.51
GBC	Dimbhe	0.99	0.99	1.00	1.00	2.32	2.32
MBC	Dimbhe/Wadaj	0.99	0.99	1.00	1.00	7.19	7.19
WRBC	Wadaj	0.96	0.98	0.60	0.50	0.25	0.32
MFC	Wadaj	0.95	0.98	0.50	0.33	1.95	3.17
MLBC	Manikdoh	1.00	1.00	0.00	0.00	0.00	0.00
PLBC	Pimpalgaon	0.95	0.98	0.43	0.20	4.38	7.62
PC	Pimpalgaon	0.95	0.98	0.43	0.20	0.66	1.15
KLBC	Yedgaon	0.95	0.97	0.86	0.50	23.46	36.64

The reliability, resilience and vulnerability indices of the reservoirs in KIP contributing to Yedgaon water transfer is given in Table 6.7. Dimbhe and Manikdoh are the two reservoirs from where the major quantity of water is transferred to the Yedgaon reservoir. From the table, it is found that all the four reservoirs have satisfactorily succeeded in water transfer to Yedgaon reservoir. The time reliability index of all the four reservoirs is above 0.94, which shows that the demands are met most of the simulation period. The volume reliability is also high for all the four reservoirs. A high vulnerability of 15.56×10^6 m^3 is observed for Dimbhe reservoir.

Table 6.7. Reliability, resilience and vulnerability indices of MOFLP policies for Yedgaon water transfer

	Reliability		Resilience		Vulnerability (10^6 m^3)	
Dam	Time	Volume	Mean	Maximum	Mean	Maximum
Dimbhe	0.99	0.99	1.00	1.00	15.56	15.56
Wadaj	0.94	0.96	0.50	0.33	4.45	9.97
Manikdoh	0.98	0.99	1.00	1.00	1.49	2.85
Pimpalgaon	0.95	0.86	0.43	0.20	2.27	3.41

6.6 Optimal Crop Planning using Multi-objective Evolutionary Algorithms

Application of Multi-objective Evolutionary Algorithm (MOEA) for deriving optimal crop plans for Indian scenario very minimal. In addition, it has been found from the literature review that no work has been reported in deriving optimal crop plans for multi-reservoir system using MOEA coupled with chaos. The MOEAs namely, non-dominated genetic algorithm (NSGA-II) and multi-objective differential evolution (MODE) algorithm are coupled with chaos in deriving optimal crop plans using multi-objective analysis. The chaos technique is introduced in generating initial population, crossover and mutation in NSGA-II and is referred as chaotic NSGA-II (CNSGA-II). In, MODE, the chaos is used in generating only in initial population and henceforth referred as chaotic MODE (CMODE). All the models are evaluated with 75% dependable inflow and the results are inter-compared. Further, the performances of the best optimal policy among different techniques are assessed using a simulation model for longer run, especially for estimating the irrigation deficits.

6.6.1 Chaotic Non-dominated Sorting Genetic Algorithm–II

The CNSGA–II uses chaotic initial population generation, tournament selection, chaotic simulated binary crossover and chaotic mutation developed by Arunkumar and Jothiprakash (2013). The chaos technique is introduced in simulated binary crossover to enhance the search in GA and in mutation to keep the population diversity. The optimal crossover probability for CNSGA-II is fixed by varying it from 0.50 to 0.95 with an increment of 0.05. It is found that both the net benefits and crop production is high for a crossover probability of 0.85. Both the net benefits and crop production decreases at higher crossover probability indicating that the offsprings are different from the parents losing its genetic material. The

mutation probability is fixed as the ratio of the number of variable (Deb, 2001). The same crossover probability and mutation probability are used in simple NSGA-II.

6.6.2 Chaotic Multi-Objective Differential Evolution Algorithm

Based on the initial analysis, it is found that the strategy '*CMODE/rand/2/bin*' is performing better among different strategies of MODE, since it satisfied all the constraints and converged quickly. Hence, the strategy '*CMODE/rand/2/bin*' has been used for all scenarios of both CMODE and simple MODE in present study. The optimal scale factor '*F*' and crossover factor '*CR*' in MODE is fixed based on sensitivity analysis. The scale factor (*F*) is varied from 0.1 to 0.5 with an increment of 0.10 while the crossover factor is varied between 0.50 and 0.90 with an increment of 0.10. It is found that *F* of 0.20 and *CR* value 0.90 resulted in a better net benefits and crop production.

All the techniques used in the study are evaluated up to 1000 generation with a population size of 250. All the constraints are handled by penalty function approach in all the techniques applied. Different penalty values were assumed based on the significance of the constraint and heavy penalties are imposed on fitness function upon violation. All the models are optimised repeatedly for several times and only the best optimal solution resulted from each technique is reported. The optimal fitness function values resulted from different techniques is given in Table 6.8.

Table 6.8. Optimal results from different MOEA models

	CMODE	CNSGA-II	MODE	NSGA-II
Net Benefits (Million Rupees)	1921.77	1918.26	1916.26	1915.09
Crop Production (1000 Tones)	1201.55	1198.35	1196.35	1195.99
Irrigation Intensity (%)	106.29	104.64	104.57	103.69
No. of Non-inferior solutions	2	4	2	6

6.6.3 Optimal Crop Area from Multi-objective Evolutionary Algorithm

The optimization model is optimized using multi-objective evolutionary algorithms coupled with chaos. The resulted total optimal crop area under various canals is given in Table 6.9. It is seen that almost all MOEAs have resulted in similar cropping pattern. The CMODE has resulted in a maximum irrigation intensity of 106.29% with total crop area of 155241.44 ha. The CNSGA-II and MODE have almost resulted in same irrigation intensity around 104%.

The NSGA-II has resulted around 103.69% irrigation intensity with a total crop area of 151436.00 ha. It is observed that the resulted total crop area during Kharif season is higher than Rabi season from all the techniques. This may be due to water requirement during Kharif season is less than Rabi season. However, there is variation in total crop area among the techniques during Kharif season. The NSGA-II has resulted in higher crop area for Rabi season that CNSGA-II and MODE. However, CMODE has resulted in higher crop area during Kharif and Rabi making it as better technique than simple NSGA-II and MODE.

Table 6.9. Resulted crop area for various canals from MOEA models

Canals	Dam	CMODE	CNSGA-II	MODE	NSGA-II
DRBC	Dimbhe	20789.52	20912.60	20749.50	20996.20
DLBC	Dimbhe	2825.71	2656.57	2529.67	2846.60
GBC	Dimbhe	4126.76	4021.06	4106.70	4218.69
MBC	Dimbhe/Wadaj	13165.89	13007.63	13066.30	13176.02
WRBC	Wadaj	566.47	540.92	514.84	572.38
MFC	Wadaj	3716.42	3342.92	3455.46	3739.89
MLBC	Manikdoh	2792.41	2455.37	2601.81	2680.95
PLBC	Pimpalgaon	10482.38	10450.04	9974.86	10495.79
PC	Pimpalgaon	2153.80	2036.01	1957.39	2160.81
KLBC	Yedgaon	94622.09	93413.06	93774.64	90548.68
Kharif		88678.46	88526.44	87950.42	85100.46
Rabi		66562.98	64309.74	64780.76	66335.54
Total		155241.44	152836.18	152731.18	151436.00
Irrigation Intensity (%)		106.29	104.64	104.57	103.69

The resulted optimal area for various crops from different models is given in Figure 6.7. The crop index 1-6 shows the Kharif crops and 7-13 are Rabi crops. All the crops proposed in the project report (KIPR, 1990) have entered the crop area because of minimum sowing area constraint. From the figure, it is observed that there is a wide variation in optimal area for different techniques for various crops. All the techniques have resulted in high crop area for vegetables during Kharif season. Around 58% of crop area during Kharif and remaining 42% area during Rabi out the total resulted crop area. On contrary to LP and MOFLP model, it is found that the variation in total crop area resulted by different MOEAs is less under each canal. Around 19% of the total crop area is vegetable crops. Since the crop water requirement is less and high net return compared to other water intensive crops. However, the resulted crop area varies among each technique. Jowar and Groundnut have also resulted in a significant crop area around 14% and 11% respectively. The water intensive crop like Paddy

has resulted in only minimum area around 2% of total crop area. Among Rabi crops, wheat and Jowar local have resulted in 11% of total crop area followed by Jowar hybrid for 10% of total crop area by different techniques. All the models have resulted in less acreage for Jowar rattoon around 2% of total crop area during Rabi season. In general, it is observed that all the techniques have resulted more acreage for vegetable crop during both Kharif and Rabi seasons due to high monetary value and also comparatively less water requirement than other crops.

6.6.4 Monthly Irrigation Releases from MOEA models

The resulted optimal releases for various canals from different techniques are given in Figure 6.8. Since, the variation in resulted crop area is not very significant among different MOEAs, the variation is releases also very less among different techniques. However, there is a wide variation in releases during Kharif and Rabi season for different canals. The canals DRBC and KLBC have resulted in a very high crop area during Kharif compared to Rabi season. Hence, the releases during Kharif are higher than Rabi season, even though rainfall during Kharif season is higher. The canals, DLBC, GBC, MBC, WRBC, MFC, PLBC and PC have resulted more or less equal crop area during Kharif and Rabi season. Hence, all the techniques have resulted in more releases during Rabi season than Kharif season for these canals. This is contrary to MOFLP releases. It is also observed that the variation in releases by different techniques is very less for DLBC, GBC, MBC and PLBC during both Kharif and Rabi seasons. The variation in releases is significant for WRBC during both Kharif and Rabi season, due to variation in crop area resulted by different techniques. There is large variation in releases to KLBC during Kharif season from different techniques due to variation in the optimal crop area. However, during the Rabi season all the techniques have resulted in same releases, since the crop area is same and also mainly depend on water supplied from the other reservoirs. It is also observed that all the models have not resulted in any release during non-cropping season.

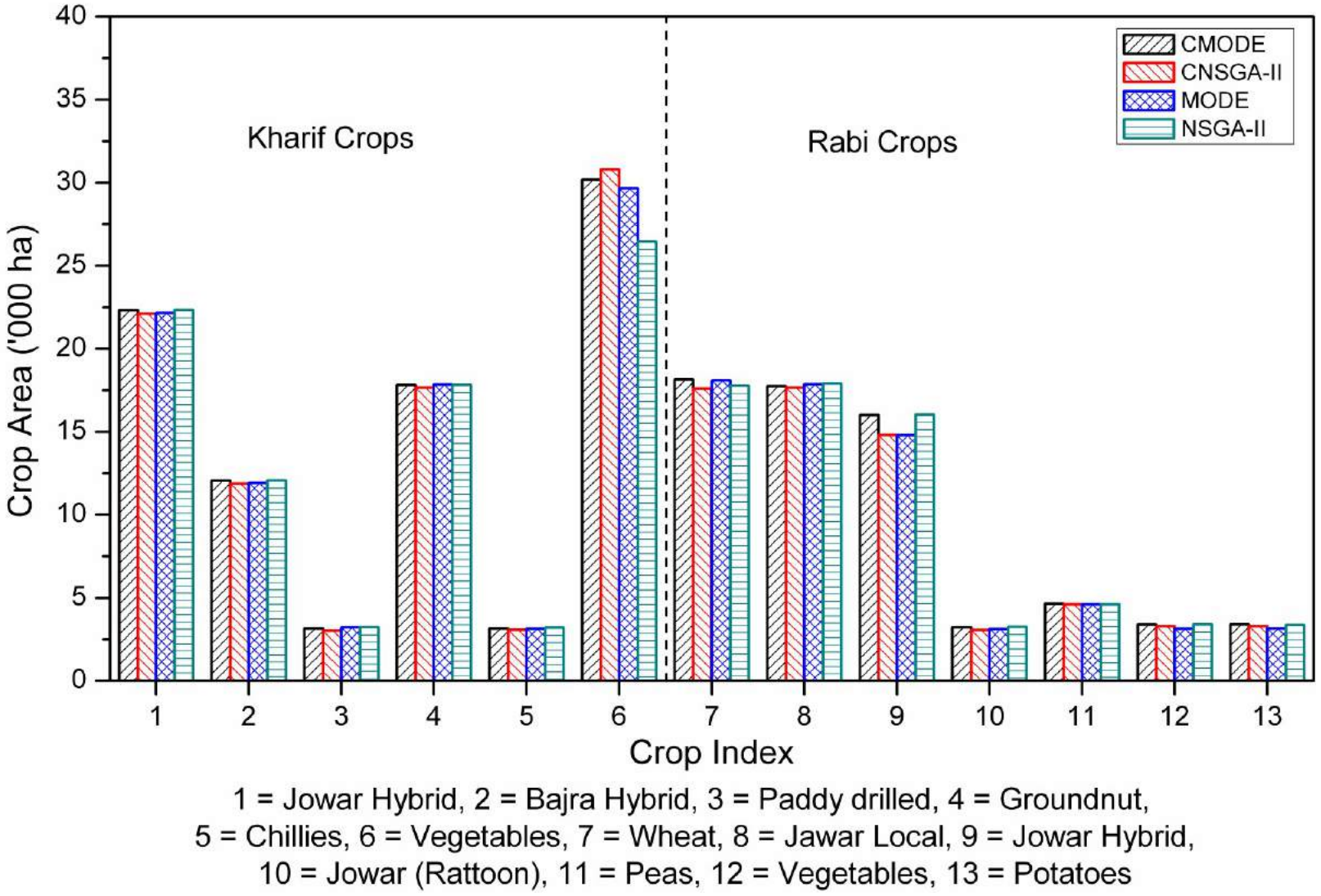

Figure 6.7. Resulted total area for each crop from different MOEA models

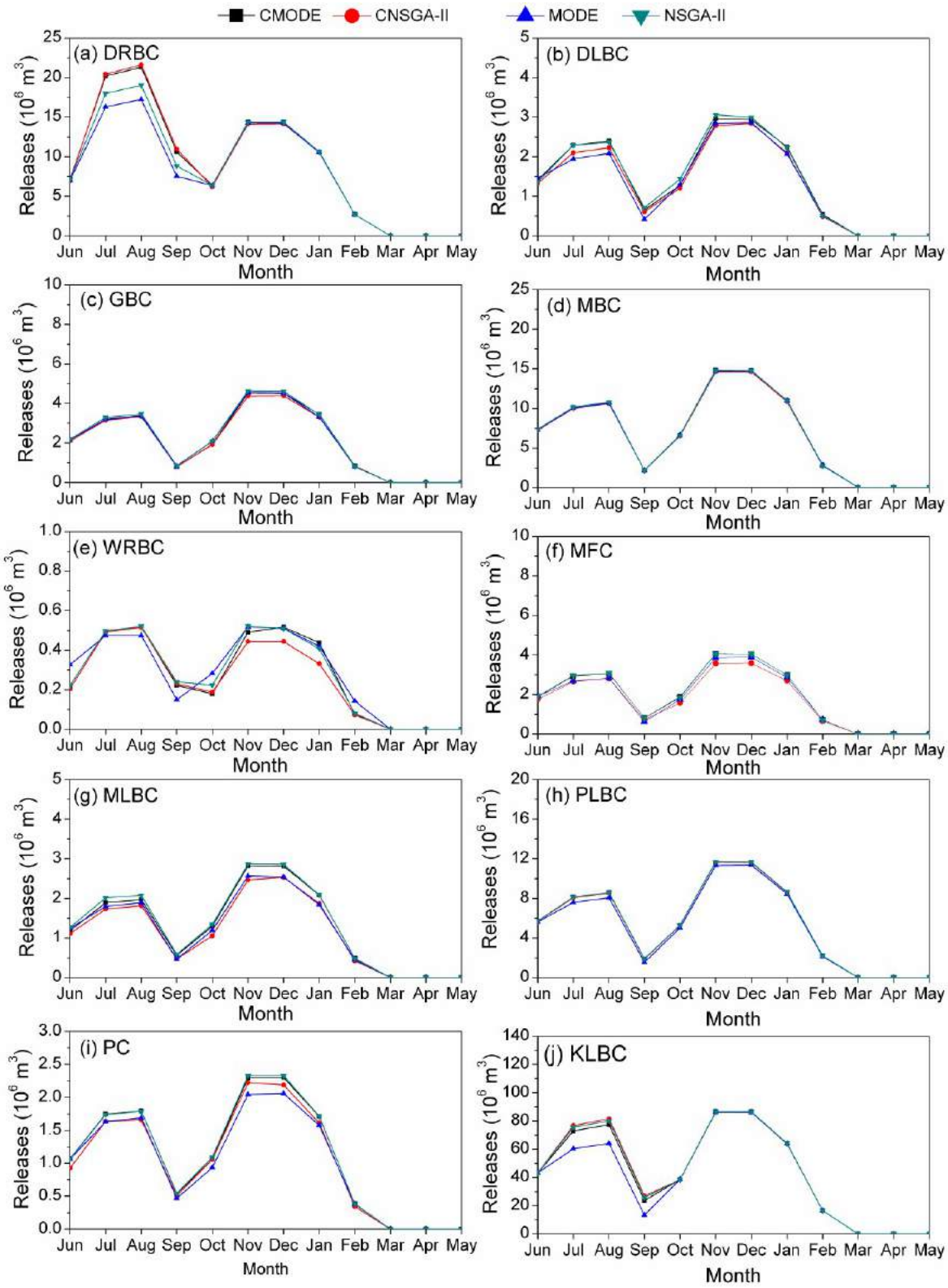

Figure 6.8. Resulted optimal releases to various canals from different MOEA models

6.6.5 Water transfer to Yedgaon Reservoir from MOEA models

The water transfer to Yedgaon reservoir resulted from different MOEA models is given in Figure 6.9. From the figure, it is found that the water transfer from all the reservoirs during Rabi season is higher than Kharif season. Both Dimbhe and Manikdoh have significantly contributed water transfer to Yedgaon reservoir. However, the water transfer from Dimbhe reservoir during Kharif season is less compared to other MOEA models. All the models have resulted in similar transfer during Rabi season from Dimbhe and Manikdoh reservoirs. All the MOEAs have resulted water transfer from Wadaj reservoir during most of the time period. All the models have resulted water transfer from Pimpalgaon only during Kharif season. Unlike MOFLP model, all the MOEA models have resulted in water transfer during most of the months indicating the optimal temporal distribution is achieved by MOEAs.

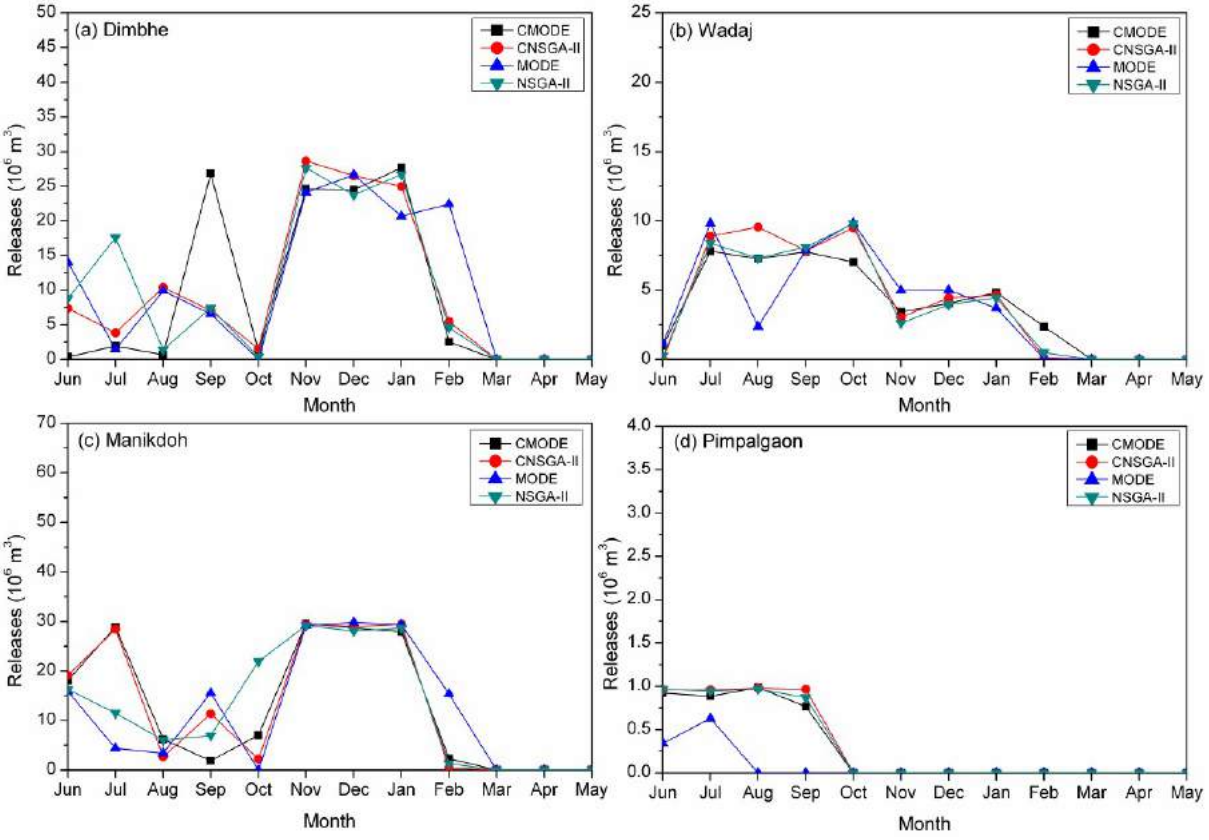

Figure 6.9. Water transfer to Yedgaon reservoir resulted from different MOEA models

6.6.6 End of Month Storage Levels from MOEA models

The end of month storage levels resulted from different techniques for all the reservoirs in the KIP are given in Figure 6.10. All the models have resulted in high storage levels during monsoon and the storage gradually depletes during the non-monsoon season. This shows that all the reservoirs are intermittent reservoirs which receive inflow only during the monsoon season. The storage level significantly varies for Manikdoh, since it is surplus reservoir and highly contributes the water transfer compared to other upstream reservoirs. For all other reservoirs the variation in storage level is minimal. All the models have resulted similar storage levels for Pimpalgaon reservoir without much variation. The storages level of Yedgaon reservoir various during monsoon season for different techniques, however during non-monsoon season it is more or less same irrespective of the techniques used. Thus, Yedgaon depends on the other reservoir especially during the non-monsoon season.

6.6.7 Simulation of Optimal CMODE Results

The optimal results obtained from CMODE are simulated to evaluate their performance over a period of time, since it is has resulted in higher net benefits and crop production compared to other techniques. Various performance measures such as MFID, AFID, AAID and PAID reported by Jothiprakash and Shanthi (2009) were used for the evaluation. In addition, reliability, resilience and vulnerability indices are also used to assess the performance. The performance indices of various canals estimated from the simulated model using 11 years of data are given in Table 6.10. It is observed that all canals have performed relatively well over the simulated period of time. The canals under Dimbhe reservoir performed very well and failed in only one month during the entire simulation period. Similarly, the canal under Manikdoh reservoir has not failed in any month during the total simulation period. This shows that these two reservoirs are surplus reservoirs and water can be satisfactorily transferred to downstream reservoir. On the other hand, the canals under Wadaj and Pimpalgaon reservoirs have failed in few months. The failure occurred mainly during the start of the season in few years where the inflow is very less. However, the AAID and PAID are very less indicating the deficit is very less compared to the demand. This shows that these two reservoirs are self sufficient reservoirs where water can be transferred only when there is excess inflow into the reservoir. The KLBC from Yedgaon reservoir has failed in five months.

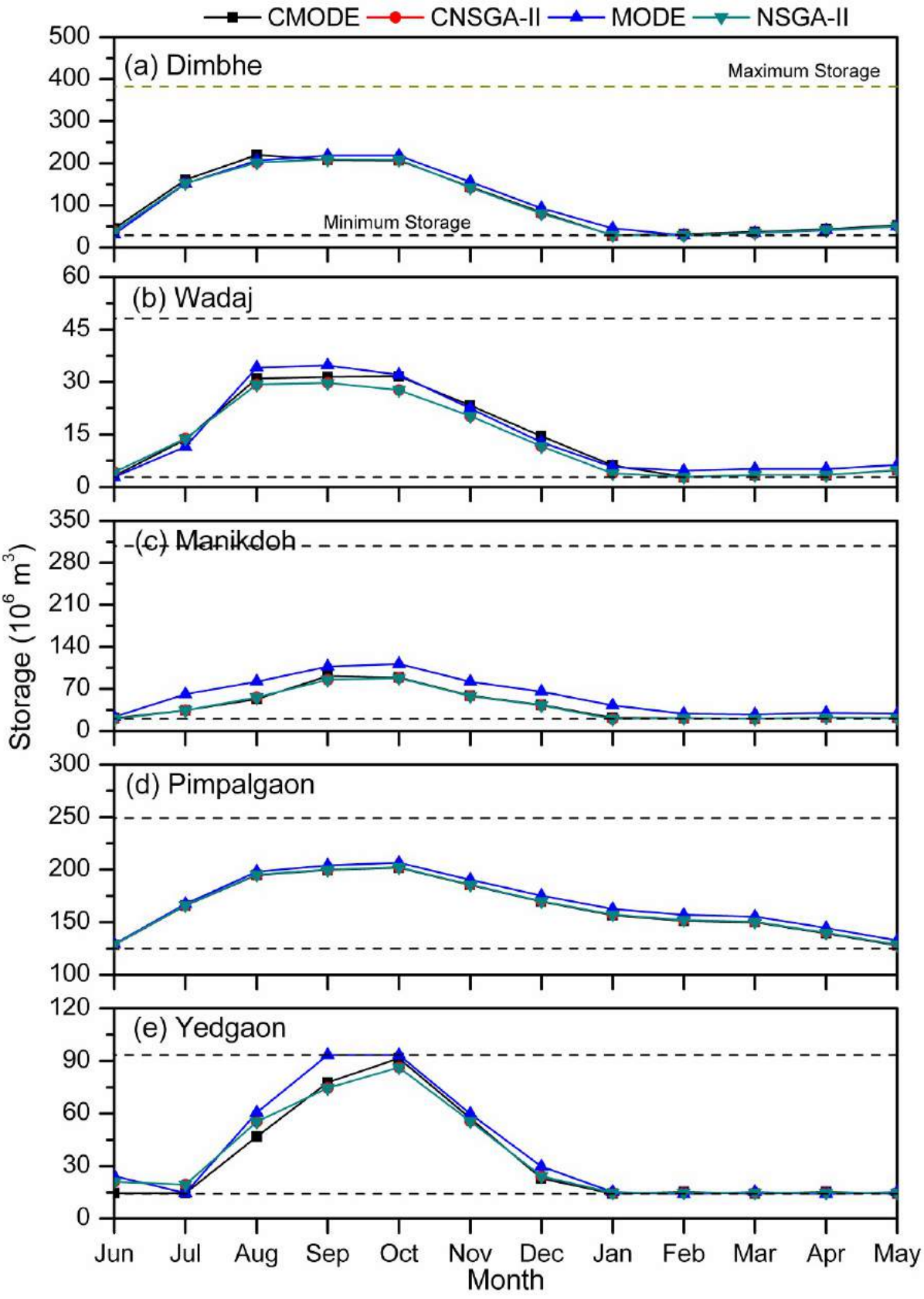

Figure 6.10. Resulted end of month storage levels from different MOEA models

The results show that the Yedgaon reservoir releases mostly depends on other reservoir during non-monsoon season due to its large command area requirement. It has resulted in an average annual irrigation deficit of 10.45×10^6 m^3. However, this deficit is also very less as the PAID is 1.94%. Thus, these indices shows the optimal policy resulted from CMODE has performed very well over the period of time. The temporal transfer from one reservoir to other reservoir is also optimal.

Table 6.10. Performances of CMODE policies for various canals of KIP

Canals	Dam	MFID	AFID	AAID (10^6 m^3)	PAID (%)
DRBC	Dimbhe	1/132	1/11	0.65	0.60
DLBC	Dimbhe	1/132	1/11	0.13	0.77
GBC	Dimbhe	1/132	1/11	0.20	0.79
MBC	Dimbhe/Wadaj	1/132	1/11	0.66	0.83
WRBC	Wadaj	5/132	2/11	0.07	2.08
MFC	Wadaj	6/132	3/11	0.57	2.54
MLBC	Manikdoh	0/132	0/11	0.00	0.00
PLBC	Pimpalgaon	7/132	2/11	1.24	1.95
PC	Pimpalgaon	7/132	2/11	0.23	1.78
KLBC	Yedgaon	5/132	3/11	10.45	1.94

The reliability, resilience and vulnerability indices estimated from simulated releases to various canals are given in Table 6.11. These indices shows that the canals under Dimbhe and Manikdoh reservoirs are reliable, since the reliability and resilience indices are high with less vulnerability. All the canals in the system shows a high reliability indicating the optimal policy performed very well over the period of time. Especially, the volume reliability shows the deficit is very less. The canals under Pimpalgaon reservoir is less compared to other reservoirs in the system. The vulnerability of KLBC is higher with a maximum vulnerability of 38.97×10^6 m^3. This is quantity can be easily achieved from Dimbhe or Manikdoh through excess transfer.

The reliability, resilience and vulnerability indices of the reservoirs in KIP contributing to Yedgaon water transfer is given in Table 6.12. Dimbhe and Manikdoh are the two reservoirs from where the major quantity of water is transferred to the Yedgaon reservoir. From the table, it is found that all the four reservoirs have satisfactorily succeeded in water transfer to Yedgaon reservoir. The time reliability index of all the four reservoirs is above 0.94, which shows that the demands are met most of the simulation period. The volume reliability is also

high for all the four reservoir. The mean and maximum resilience index of Dimbhe is one with zero vulnerability indicating that the reservoir is most reliable. A very high vulnerability of 11.71×10^6 m^3 is observed for Manikdoh reservoir.

Table 6.11. Reliability, resilience and vulnerability indices of CMODE policies for various canals of KIP

Canals	Dam	Reliability		Resilience		Vulnerability (10^6 m^3)	
		Time	Volume	Mean	Maximum	Mean	Maximum
DRBC	Dimbhe	0.99	0.99	1.00	1.00	7.13	7.13
DLBC	Dimbhe	0.99	0.99	1.00	1.00	1.42	1.42
GBC	Dimbhe	0.99	0.99	1.00	1.00	2.17	2.17
MBC	Dimbhe/Wadaj	0.99	0.99	1.00	1.00	7.29	7.29
WRBC	Wadaj	0.96	0.98	0.60	0.50	0.24	0.51
MFC	Wadaj	0.95	0.97	0.50	0.33	2.08	3.69
MLBC	Manikdoh	1.00	1.00	1.00	1.00	0.00	0.00
PLBC	Pimpalgaon	0.95	0.98	0.43	0.20	4.55	7.91
PC	Pimpalgaon	0.95	0.98	0.43	0.20	0.84	1.45
KLBC	Yedgaon	0.96	0.98	0.80	0.50	28.74	38.97

Table 6.12. Reliability, resilience and vulnerability indices of CMODE policies for Yedgaon water transfer

Dam	Reliability		Resilience		Vulnerability (10^6 $m^{3)}$	
	Time	Volume	Mean	Maximum	Mean	Maximum
Dimbhe	0.99	1.00	1.00	1.00	0.00	0.00
Wadaj	0.94	0.97	0.50	0.33	3.15	10.15
Manikdoh	0.96	0.98	0.60	0.33	10.36	11.71
Pimpalgaon	0.95	0.95	0.43	0.20	0.61	0.92

6.7 Closure

Kukadi Irrigation Project (KIP) is a complex system with five reservoirs among which four are in parallel and one in series. In order to meet the demand at the downstream reservoir, water is transferred from the upstream reservoir through rivers and canals. Dimbhe and Manikdoh are the two reservoirs from where the major quantity of water is transferred to the Yedgaon reservoir. The behaviour of the multiple reservoirs in the Kukadi Irrigation project is assessed using a simulation model based on SOP. The statistical indices such as reliability, resilience and vulnerability are assessed. It is found that the three upstream reservoirs have

satisfactorily succeeded in water transfer, except Manikdoh. The performance indices show that the water transfer from Manikdoh is not as per the demand. The time reliability index of Manikdoh shows that the water transfer is not timely. This may be due to the less rainfall than expected in the catchment area of Manikdoh reservoir.

The MOFLP model has resulted in a satisfaction level of 0.46 for the integrated operation of multi-reservoir system with an irrigation intensity of 102.18%. The total net benefit obtained from the system is Rs. 1909.92 Million and total crop production of 1191.30 thousand tonnes. It is found that CMODE has resulted in higher net benefits of Rs. 1921.77 Million ($ 31.96 Millions) and crop production of 1201.55 thousand tonnes. This has been achieved with a crop area of 88678.46 ha during Kharif and 66562.98 ha during Rabi leading to an irrigation intensity of 106.29%. The major contribution of net benefits is from the crops grown in Kharif due to the high crop area.

The comparison of simulation of optimal crop area, irrigation releases and water transfer to Yedgaon reservoir resulted from both CMODE and MOFLP shows that both the techniques have performed equally better for most of the time period. However, the MOFLP releases resulted in irrigation deficit for 7 months (7 years, one month in each year) where as the CMODE has only in 5 months (5 years) for KLBC. The reliability of KLBC for CMODE releases is higher than MOFLP release. For all other canals, both the techniques have resulted almost similar reliability levels. The Yedgaon water transfer results shows that CMODE has resulted in less vulnerability compared to MOFLP model. Thus, it may be concluded that CMODE has resulted better than MOFLP model and has achieved near global optimal solution.

Chapter 7

Single Objective Optimization of a Multi-Reservoir system

7.1 General

The water-sharing dispute in a multi-reservoir river basin forces the water resources planners to have an integrated operation of multi-reservoir system rather than considering them as a single reservoir system. Unfortunately, many existing reservoir operational policies were derived as single reservoir system and fail to consider them as a multi-reservoir system in an integrated manner, especially in India. Thus, optimizing the operation of a multi-reservoir system for an integrated operation is gaining importance and also need of the hour. The integrated operation of a multi-purpose multi-reservoir system generally requires optimal release decisions and end of month storage levels to be maintained in each reservoir during the operating time period. This can be determined by applying an optimization or simulation models or by both. This chapter describes the development and application of simulation and optimization models for the integrated operation of a multi-reservoir system, with the objective of 'maximizing the hydropower production'. The KHEP in Maharashtra, India is taken up as a case study for the single objective optimization of a multi-reservoir system. Initially, a simulation model has been developed based on standard operating policy to study the response of the system for a given input. Then, an optimization model is developed and optimized to maximize the hydropower production using soft computing techniques; the results are compared with conventional optimization technique. The results obtained from models are presented and discussed in this chapter.

7.2 Development of Simulation Model

A reservoir simulation model represents the hydrological behaviour of the system that are developed using the mass balance equation and other operating conditions (Rani and Moreira, 2010). A monthly time step rule based simulation model has been developed using the standard operating policy (SOP) to assess the power production from KHEP for various operating scenarios. The rules in the SOP are (i) if the available storage (active storage + inflow - evaporation) in the reservoir is less than the demand, then whatever storage available in the reservoir is released; (ii) if the available storage is greater than the demand, then the demand is released. Finally, the overflow is estimated if the end storage exceeds the capacity of the reservoir, else the overflow is zero. Mathematically it is given as:

$$\text{If } AS_t < D_t, \text{ then } R_t = AS_t \text{ and } O_t = 0 \tag{5.1a}$$

$$\text{Else if } D_t \leq AS_t \leq S_{max}, \text{ then } R_t = D_t,\ O_t = 0 \text{ and } S_{t+1} = AS_t - R_t \tag{5.1b}$$

$$\text{Else if } D_t \leq AS_t > S_{max}, \text{ then } R_t = D_t,\ O_t = AS_t - R_t - S_{max} \text{ and } S_{t+1} = S_{max} \tag{7.1c}$$

where AS_t is the storage available in reservoir during the time period 't', D_t is demand during the time period 't', R_t is the release during the time period 't', S_{max} is the maximum storage of the reservoir, O_t is the overflow during the time period 't' and S_{t+1} is the initial storage of time period '$t+1$'. Accordingly, the releases are made to 'n' powerhouses, if enough storage is available in the reservoir.

The power production ($P_{n,t}$) (kWh) from a powerhouse 'n' during the time period 't' is estimated using the equation (Loucks *et al.*, 1981):

$$P_{n,t} = k \times R_{n,t} \times H_{n,t} \times \eta \qquad t = 1, 2, \ldots 12;\ n = 1,2,3,4 \tag{7.2}$$

where k is the conversion constant, $R_{n,t}$ is the release to the powerhouse 'n' during the time period 't' (10^6 m^3); $H_{n,t}$ is the net head available in the reservoir for the powerhouse 'n' during the time period 't' (m) and η is the efficiency of the power plant. The net head is estimated after deducting the tail water level and other frictional losses.

The final storage of the reservoir is estimated by deducting all the releases and losses using the mass balance equation. The mass balance equation is given as:

$$S_{m,T} = S_{m,t} + I_{m,t} - \sum_{n} R_{n,t} - E_{m,t} \qquad t = 1, 2, \ldots 12;\ m = 1,2 \qquad (7.3)$$

where $S_{m,T}$ is the final storage in the reservoir 'm' during the time period 't'; $S_{m,t}$ is the initial storage in the reservoir 'm' during the time period 't'; $I_{m,t}$ is the inflow into the reservoir 'm' during the time period 't'; $R_{n,t}$ is the release to the powerhouse 'n' during the time period 't'; $E_{m,t}$ is the evaporation loss in the reservoir 'm' during the time period 't'. Koyna reservoir is having three powerhouses and hence there are three releases (n = 3). Kolkewadi reservoir is having only one powerhouse and hence only one release (n = 1). Also the tail water of Western side powerhouses (PH I and PH III) of Koyna reservoir will be additional inflow to Kolkewadi reservoir apart from the inflow from its own catchment. Overflow occurs when the final storage exceeds the reservoir capacity. Thus, the surplus is estimated using the equation:

$$O_{m,t} = S_{m,T} - S_{m,\max} \qquad t = 1, 2, \ldots, 12;\ m = 1, 2 \qquad (7.4)$$

where $S_{m,max}$ is the maximum storage (capacity) of the reservoir 'm' (10^6 m^3) and $O_{m,t}$ is the overflow in the reservoir 'm' during the time period 't'. Else, the overflow is zero. Then, the final storage is re-estimated incorporating the overflow. This final storage will be the initial storage for the next time period '$t+1$'. If the reservoir storage reaches the minimum (dead) storage, then the release to the powerhouse 'n' is zero.

In addition to these general constraints, the constraint on releases to the powerhouses on the Western side is also considered to study the system under present situation. This constraint restricts the diversion of large quantity of water towards Western side for power production from Koyna reservoir and is given as:

$$\sum_{t=1}^{12} \sum_{n=1}^{2} R_{n,t} \le R_{\max} \qquad (7.5)$$

where, R_{max} is the maximum water that can be diverted to the Western side for power production from the Koyna reservoir. Also, each powerhouse have specific minimum draw down level (MDDL), below which it cannot be operated. This constraint infers that the head available in the reservoir should be always greater than MDDL of the powerhouse '*n*' during any time period '*t*' to produce power. Mathematically this constraint is given as:

$$H_{n,t} \geq MDDL_{n,t} \qquad t = 1, 2 \ldots 12; n = 1, \ldots, 4 \qquad (7.6)$$

where $H_{n,t}$ is the average head (m) in the reservoir for the powerhouse '*n*' during the time period '*t*' and $MDDL_{n,t}$ is the minimum drawdown level for the powerhouse '*n*' during the time period '*t*'.

The above developed simulation model has been used to assess the behaviour of KHEP for different operating scenarios based on release constraint and for various powerhouse operating durations. The behaviour of the system for various scenarios in long run is assessed using the statistical performance indices such as reliability, resilience and vulnerability. The results of the simulation model and the behaviour of the system from the statistical indices are discussed in the following section.

7.3 Results of Simulation Model

Usually, hydropower releases are termed as non-consumptive, since the water can be used for some other purpose after power generation, mostly for irrigation. However in this case study, the releases to major powerhouses and irrigation are in the opposite direction which makes the operation of the system very complex. The diversion of huge quantity of water for power production towards the Western side is restricted by KWDT (2010), due to which the power production has decreased significantly. Hence, two scenarios are analysed, (a) power production without tribunal constraint on releases (unconstrained scenario) (i.e. all physical constraints are considered without constraint on releases) and (b) power production with tribunal constraint on releases (constrained scenario) to powerhouses PH I and PH III on the Western side (i.e. hard binding constraints on releases are also considered along with all physical constraints). Thus, the unconstrained scenario will assess the full power production

potential of the KHEP system for the given input and the constrained scenario will give the power production under restricted releases with SOP.

In KHEP, all the powerhouses are peak stations, except PH IV and are operated only few hours in a day and do not have any specific demand. The PH IV is operated only through irrigation releases. Based on this, three cases of simulation have been analyzed. In case 1, it is considered that the power is produced for 4 hours in a day (4 hr), in case 2, the power production is for 6 hours in a day (6 hr) and in case 3, the power is produced for 8 hours in a day (8 hr). The monthly water demand for these cases are estimated based on the maximum turbine discharge capacity, number of hours of operation in a day and number of days in a month. The KHEP operations are then simulated using 11 years of observed inflow data from 1999 – 2010 using the developed simulation model. The release to powerhouse PH III is given first priority, since the MDDL for PH III is higher than other powerhouses and also it is the major powerhouse with high capacity in the system. Then the second priority is given to PH I and third to PH IV. The results of the simulation model are discussed in the following section.

7.3.1 Power Production

The annual power production resulted from the simulation model for different duration of operation for constrained and unconstrained scenarios is given in Figure 7.1. In general, it is observed that the annual power production in unconstrained scenario is higher than the constrained scenario for all the three cases (duration of operation) considered. It is worth mentioning that constrained/ unconstrained refers only to the constraints on releases. In both the scenarios, the systems physical constraints remain the same. The high power production in case of unconstrained scenario is due to the unrestricted releases to the powerhouses on the Western side of Koyna reservoir. The variation in annual power production is less for case 1 over the years, which shows the power production is highly stable and reliable for this 4 hr duration of operation. However, there is a large variation in annual power production over the years for case 2 (6 hr) and case 3 (8 hr) in the unconstrained scenario. If the powerhouses are operated 4 hours per day, the left over storage will be carried over to subsequent years and hence there is a constant power production in all the years in case 1. It is also found that the power production largely depends on the corresponding year inflow for longer duration of

operation, since the carryover storage will be very less. Hence, there is high variation in annual power production for different years in unconstrained scenario.

The power production under constrained scenario for different cases is shown in Figure 7.1(b). It is observed that the annual power production is almost equal irrespective of duration of operation, since the total annual releases for different cases are same. This has led to a small variation in annual power production in all the years for different duration of operation. Thus, in the constrained scenario, the powerhouses can produce only restricted power and almost equal irrespective of duration of operation. However, the monthly power production varies largely. From the figure, it is also observed that the constraint on the releases has drastically reduced the power production. The total annual releases in the unconstrained scenario are 12%, 36% and 47% higher than the constrained scenario for case 1, 2 and 3, respectively. On an average, this has increased the annual power production by 12%, 30% and 35% for case 1, 2 and 3, respectively in the unconstrained scenario. The study shows that the 4 hr operation without imposing the constraints on releases can produce 12% more power than constrained scenario every year and also satisfies the irrigation demands.

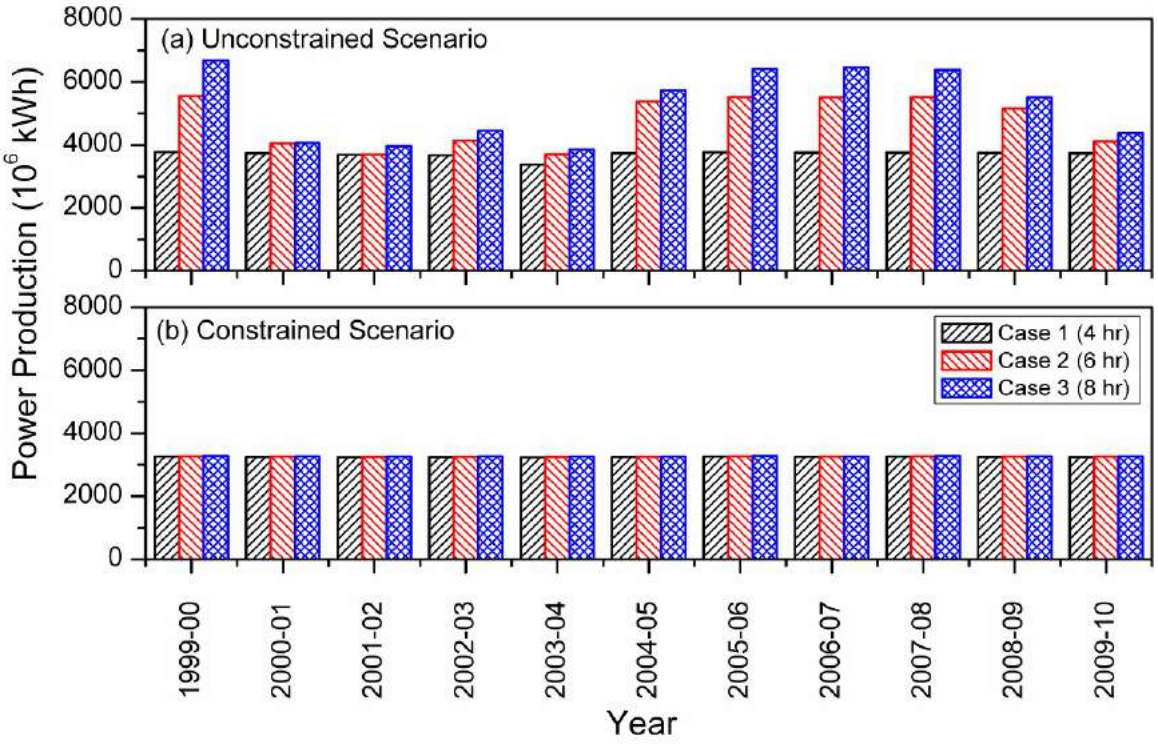

Figure 7.1. Comparison of annual power production resulted from the model (a) unconstrained and (b) constrained scenarios

The monthly power production resulted from simulation model for different cases of unconstrained and constrained scenario is given in Figure 7.2. From the figure, it is found that there is large variation in monthly power production for different duration of operations for both unconstrained and constrained scenario. The case 3 (8 hr duration of operation) resulted in more power production than case 1 and 2 for both unconstrained and constrained scenarios, but produces power only in few months of a year. The model reaches the maximum allowable limit of water diversion within few months and hence there is no continuous power production in the constrained scenario. Thus, 8 hr duration may not be viable option for power production, since peak demands need to be met throughout the year. The case 1 and 2 of unconstrained scenario has resulted power production in most of the months in a year compared to constrained scenario. The power production also varies among the months for same duration of operation due to variation in storage levels and available net head. Thus, it may be concluded the 4 hr to 6 hr operation is a viable period of power production that may satisfy the hard bound constraints on releases as well as irrigation requirements.

7.3.2 Monthly Releases

The monthly release to the powerhouses for case 1 (4 hr operation) is given in Figure 7.3. From the figure, it is observed that the unconstrained scenario has resulted in continuous releases to all the powerhouses for all the months of simulation period except in one month (May, water year 2003 – 2004). This is due to very less inflow in to the reservoir during that particular year as it was a severe drought year. The constrained scenario also has released most of the months in a year but failed to release at the end of the season in every year to the powerhouses PH I and PH III, since the total releases has reached the maximum allowable limit. Thus, the simulation results indicate that all the powerhouses can be operated only around 4 hr a day under the constrained scenario. The releases to PH II are similar to PH I and PH III, since the operations of PH II is based on PH I and PH III releases. It is also observed that the constrained scenario has resulted in irrigation releases as per the irrigation demand in all the months of the simulation period. The unconstrained scenario failed in only one month to release for irrigation due to less inflow in that year, particularly at the end of the season.

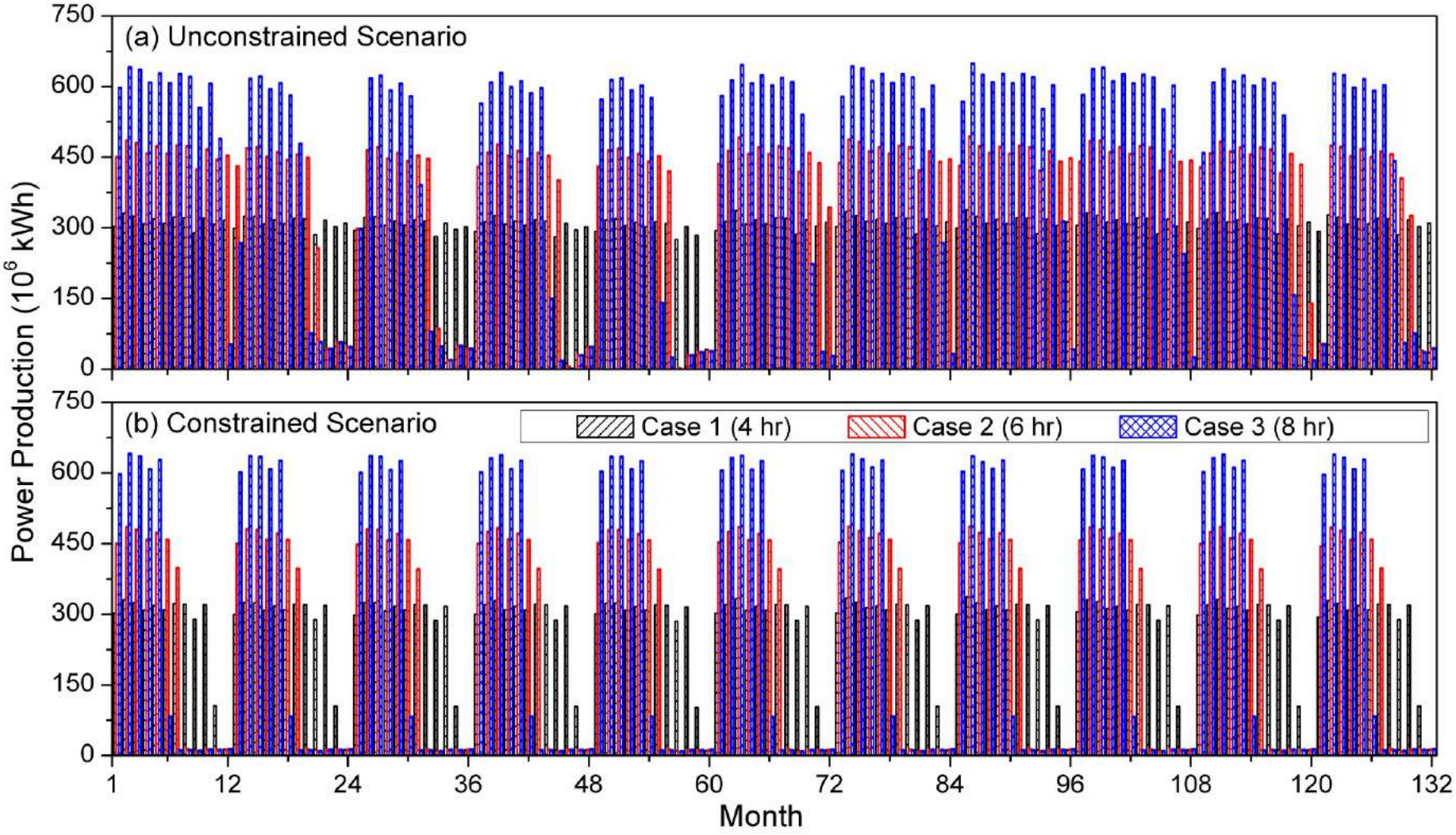

Figure 7.2. Monthly power production for different duration of operation (a) unconstrained scenario and (b) constrained scenario

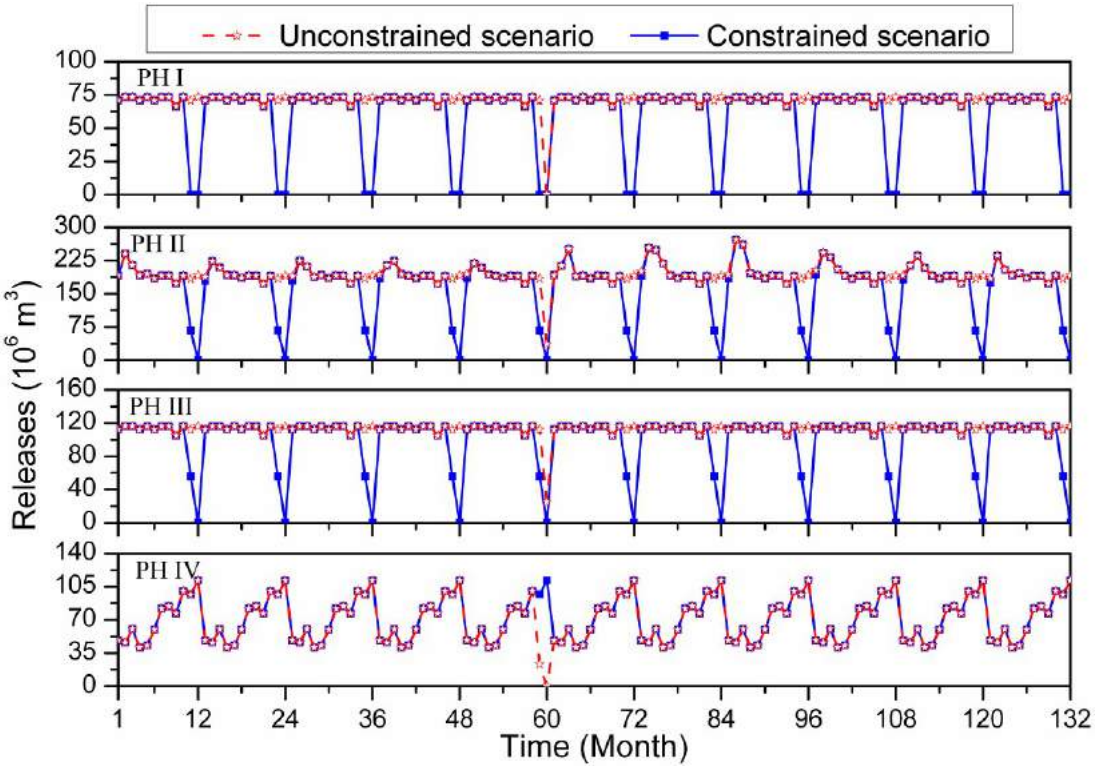

Figure 7.3. Monthly releases for 4 hours of operation of various powerhouses for the unconstrained and constrained scenarios

The monthly release to the powerhouses for unconstrained and constrained scenarios for case 2 (6 hr operation) is given in Figure 7.4. The release for case 2 is higher, since the duration of operation of power plants has increased. In case 2, both the unconstrained and constrained scenarios have released only during the start of the season in every year. However, the unconstrained scenario has resulted release in most of the months compared to the constrained scenario and failed in few months where inflow is very less during that particular year. In spite of having high storage in the reservoir, there are no releases in the constrained scenario at the end of the season for every year due to the restriction on releases. But, this has ensured the irrigation releases for all months of the simulation period in the constrained scenario. The unconstrained scenario failed in irrigation release for few months due to less inflow and also due to diversion of large quantity of water for power production. The case 3 (8 hr duration of operation) has also resulted similar to case 2 (6 hr duration of operation) for all powerhouses and is given in Figure 7.5. Thus, it may be concluded that the case 1 (4 hr duration of operation) of unconstrained scenario is viable for KHEP, since it has resulted constant and continuous power production as well as satisfied the irrigation demands in all months.

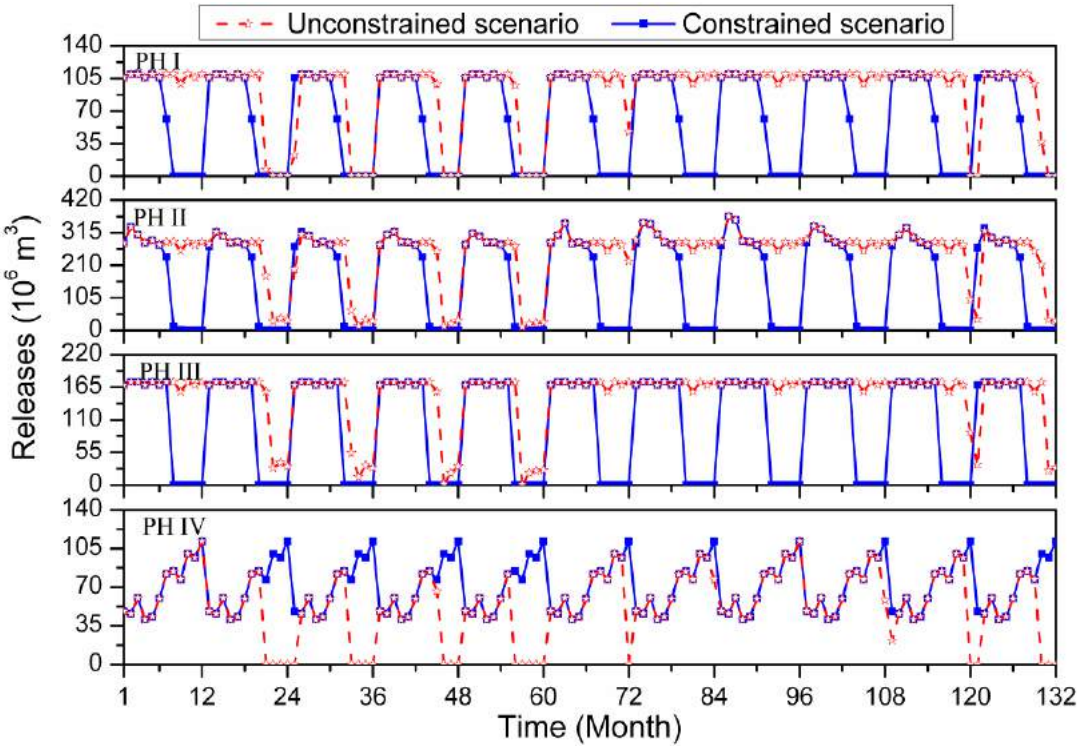

Figure 7.4. Monthly releases for 6 hours of operation of various powerhouses for the unconstrained and constrained scenarios

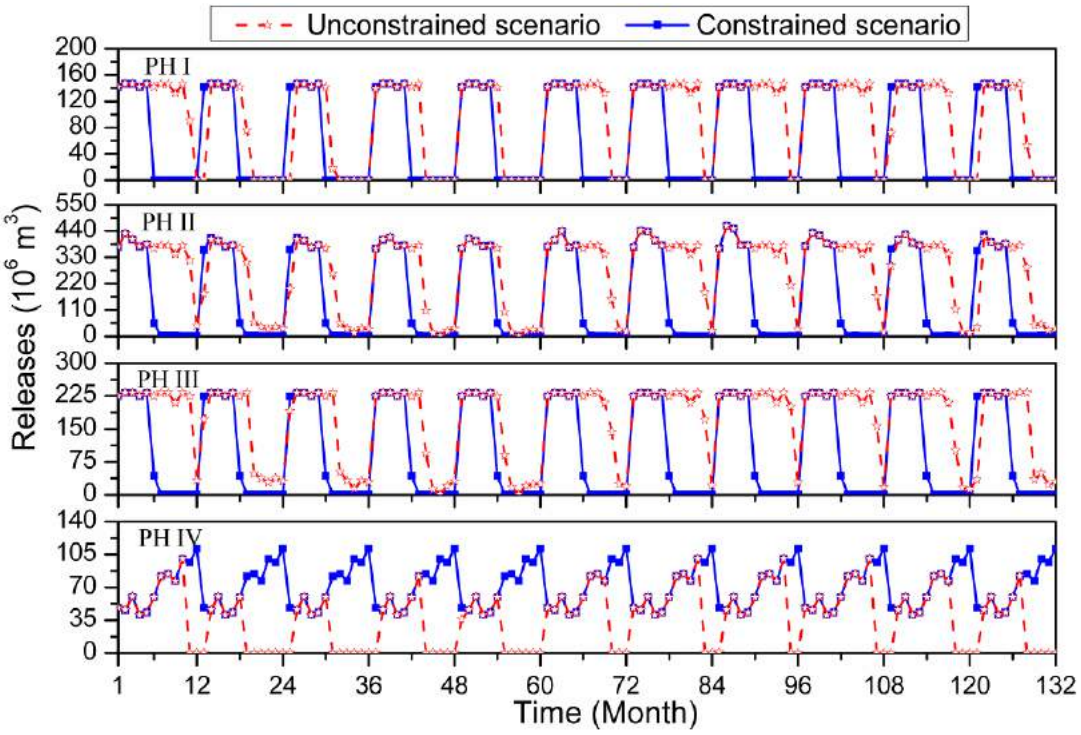

Figure 7.5. Monthly releases for 8 hours of operation of various powerhouses for the unconstrained and constrained scenarios

7.3.3 End of Month Storage Levels

The resulted end of month storage levels of Koyna reservoir from the simulation model for the unconstrained and constrained scenarios is given in Figure 7.6. From the figure, it is found that there is large variation in storage levels for different cases. It is observed that the unconstrained scenario has resulted in lesser storage levels than the constrained scenario due to unrestricted releases leading to complete utilization of available water. Thus, it can be concluded that the unconstrained scenario has fully utilized the available storage in the reservoir for power production. Figure 7.6(a) shows the end of month storage levels for case 1 (4 hr operation). There is no much variation in storage levels for most of the months in constrained and unconstrained scenarios. Both the scenarios have resulted in large storage for most of the time period due to less duration of operation and also resulted in overflow for few months. Figure 7.6(b) and Figure 7.6(c) shows the end of month storage levels for case 2 (6 hr operation) and case 3 (8 hr operation), respectively. Though both the figures looks similar, the storage level varies over the time period. It is observed that the storage depleted rapidly for case 3 (8 hr operation) due to high demand compared to case 2 (6 hr operation). For both these cases, the constrained scenario has high storage and overflow due to the restriction in releases. The total releases to the powerhouses on Western side reached their allowable limits within few months and hence the releases are zero at the end of the season every year. In the unconstrained scenario, both these cases fully utilized the available storage in the reservoir for power production and hence resulted in dead storage at the end of the season. However, the unconstrained scenario has also resulted in overflow in few months, due to exceptionally high inflow. All the models have resulted in similar storage levels for constrained scenario for the Kolkewadi reservoir. From these simulated results and figures, it may be concluded that for the integrated operation of KHEP, case 1 (4 hr daily power production) is a most viable option.

7.3.4 Reliability

The time reliability shows how far the system has satisfied the demand during the total simulation period. The volume reliability shows to what extent the demands are satisfied in terms of quantity. The reliability index close to one indicates the system is highly reliable and vice versa.

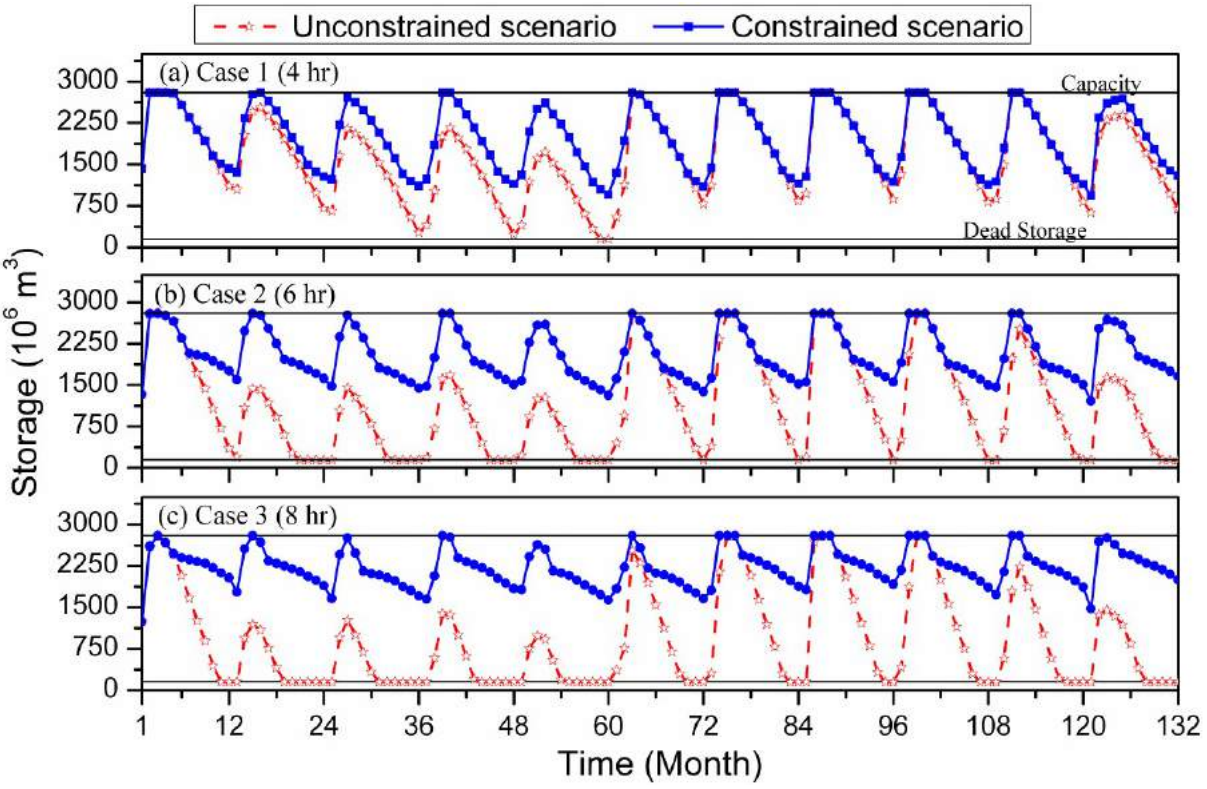

Figure 7.6. Resulted end of month storage levels of Koyna reservoir for the unconstrained and constrained scenarios

The reliability of various powerhouses and KHEP system is estimated for both the unconstrained and constrained scenarios based on time as well as volume and are depicted in Table 7.1. It is noted that the reliability is high for case 1 (4 hr duration of operation) for unconstrained scenario than the constrained scenario, since the demands are met in most of the time period in unconstrained scenario. It can also be seen that the reliability of the KHEP system is higher for the unconstrained scenario than the constrained scenario. The lesser reliability of constrained scenario is due to that the total releases to the Western side powerhouses have reached the maximum allowable limit within few months and hence there are no releases in the later part of the year. However, PH IV has resulted in a higher reliability for the constrained scenario, since the irrigation demands are satisfied throughout the simulation period in constrained scenario. The volume reliabilities are slightly higher than the time reliability in both the scenarios. This is due to that the time reliability considers the releases less than the demand as failure during that time period however; the volume reliability accounts releases during that failure time period also. From the reliability point of

view also, it may be concluded that case 1 (4 hr operation) has ensured the irrigation supply with high reliability in both constrained and unconstrained scenario and can be one of the viable operation time period.

Table 7.1. Resulted time and volume reliability for unconstrained and constrained scenarios

Cases	Unconstrained Scenario					Constrained Scenario				
	PH I	PH II	PH III	PH IV	KHEP	PH I	PH II	PH III	PH IV	KHEP
Time Reliability										
Case 1	0.99	0.99	0.99	0.98	0.98	0.83	0.83	0.83	1.00	0.83
Case 2	0.83	0.85	0.86	0.80	0.80	0.50	0.58	0.58	1.00	0.50
Case 3	0.64	0.68	0.69	0.63	0.63	0.42	0.42	0.42	1.00	0.42
Volume Reliability										
Case 1	0.99	0.99	0.99	0.98	0.99	0.83	0.87	0.87	1.00	0.89
Case 2	0.84	0.88	0.89	0.75	0.86	0.55	0.59	0.59	1.00	0.63
Case 3	0.67	0.75	0.76	0.53	0.72	0.42	0.44	0.44	1.00	0.49

7.3.5 Resilience

Resilience is the measure of how fast a system is likely to return to a satisfactory state from an unsatisfactory state. A resilience index close to one indicates the system will quickly recover from failure state and vice versa. The mean and maximum resilience for the powerhouses and the system for the unconstrained and constrained scenario are given in Table 7.2. The resilience index of unconstrained scenario is higher than the constrained scenario for all the powerhouses and KHEP system. From the table, it is observed that both the mean and maximum resilience decreases with the increase in duration of operation. Both the mean and maximum resilience are same for case 1 (4 hr duration of operation) in the unconstrained and constrained scenarios. This shows that constraints on releases have no effect for short duration of operation of powerhouses. However, there is wide variation in mean resilience among powerhouses for longer duration of operation. The constraint scenario has satisfied the irrigation demands during all the simulation periods. Hence, there are no failure events for PH IV for all the cases and hence the resilience is zero.

Table 7.2. Resulted mean and maximum resilience for the unconstrained and constrained scenarios

Case	Unconstrained Scenario					Constrained Scenario				
	PH I	PH II	PH III	PH IV	KHEP	PH I	PH II	PH III	PH IV	KHEP
Mean Resilience										
Case 1	1.00	1.00	1.00	0.50	0.50	0.50	0.50	0.50	0.00	0.50
Case 2	0.30	0.30	0.33	0.33	0.33	0.17	0.20	0.20	0.00	0.17
Case 3	0.23	0.26	0.27	0.22	0.22	0.14	0.14	0.14	0.00	0.14
Maximum Resilience										
Case 1	1.00	1.00	1.00	0.50	0.50	0.50	0.50	0.50	0.00	0.50
Case 2	0.20	0.20	0.25	0.20	0.20	0.17	0.20	0.20	0.00	0.17
Case 3	0.14	0.17	0.17	0.14	0.14	0.14	0.14	0.14	0.00	0.14

7.3.6 Vulnerability

Vulnerability is the measure of the likely damage of a failure event. The mean and maximum vulnerability of the powerhouses and the KHEP system under unconstrained and constrained scenarios is given in Table 7.3. From the table, it is observed that both the mean and maximum vulnerability increases with increase in the duration of operation. The mean and maximum vulnerability of the powerhouses and the system varies significantly for long duration of operation in the unconstrained scenario. However, it remains almost equal in the constrained scenarios. Also, the vulnerability of the powerhouses and the KHEP system is higher for longer duration of operation in constrained scenario than the unconstrained scenario, since restricting the releases leads to higher deficits in the Western side powerhouses. Thus, these performance indices such as reliability, resilience and vulnerability confirm that KHEP can be operated up to 4 hr without restricting the releases.

Table 7.3. Resulted mean and maximum vulnerability (10^6 m^3) for the unconstrained and constrained scenario

Case	Unconstrained Scenario					Constrained Scenario				
	PH I	PH II	PH III	PH IV	KHEP	PH I	PH II	PH III	PH IV	KHEP
Mean Vulnerability										
Case 1	73.21	106.73	90.81	184.95	455.70	144.06	213.83	172.46	0.00	530.35
Case 2	322.47	535.65	423.55	255.75	1146.03	582.78	1030.22	848.03	0.00	2461.03
Case 3	571.57	834.66	650.16	394.86	2451.24	1001.33	1894.30	1543.79	0.00	4439.42
Maximum Vulnerability										
Case 1	73.21	106.73	90.81	184.95	455.70	144.06	214.48	172.46	0.00	531.00
Case 2	501.54	747.39	604.20	469.52	2258.51	582.78	1031.74	848.03	0.00	2462.55
Case 3	925.41	1486.94	1186.60	599.52	4084.41	1001.33	1895.69	1543.79	0.00	4440.81

7.4 Development of Optimization Model for Hydropower Production

Hydropower is one of the potential sources for meeting the growing energy needs of the country. India is endowed with rich hydropower potential and it ranks fifth in the world in terms of usable potential. The total installed capacity in India as on 31 December 2010 was 171,644 MW among which hydropower constitutes 40,320 MW including both small and large hydropower plants (Sukhatme, 2011). However, Sukhatme (2011) reported that India needs to produce four times of the present generation to cope up the future energy demand. In India, most of the reservoirs have hydropower plants. However, many of them are not operated to their full potential. Some of the reasons highlighted by Arunkumar and Jothiprakash (2012) were (i) in most of the plants, hydropower is produced through irrigation release, hence there will be power production only when there is irrigation release; (ii) hydropower and irrigation releases are conflicting objectives and (iii) disputes in sharing available water among different stakeholders. This calls for an efficient and effective operation of reservoirs for crop and power production, considering long-term sustainability, environmental aspects, and social concerns. In the present study, the hydropower production from KHEP is optimized considering all the reservoirs in the project as a multi-reservoir system and the results are discussed.

The objective of the present study is to maximize the hydropower production from all the powerhouses of the two reservoirs. It is expressed as:

$$\text{Maximize} \qquad Z = \sum_{t=1}^{12} (\text{PH I}_t + \text{PH II}_t + \text{PH III}_t + \text{PH IV}_t) \tag{7.7}$$

where, $PH\ I_t$, $PH\ II_t$, $PH\ III_t$ and $PH\ IV_t$ is the power production from PH I, PH II, PH III, and PH IV respectively during the time period '*t*' in terms of kWh. According to Loucks *et al.* (1981), the hydropower production during any time period '*t*' is dependent on the plant capacity, flow through the turbines, average effective storage head, number of hours operation and a constant for converting the product of flow, head and plant efficiency to electrical energy. Thus, the hydropower production ($PH_{n,t}$) in terms of kilowatt-hours (kWh) during any time period '*t*' is expressed as

$$PH_{n,t} = K \times R_{n,t} \times HN_{n,t} \times \eta_n \qquad t = 1,2,..12;\ n = 1,2,3,4 \tag{7.8}$$

where, K is the constant to convert the hydropower to kWh, $R_{n,t}$ is the release to the powerhouse 'n' during the time period 't', $HN_{n,t}$ is the net head (m) during the time period 't', and η_n is the n^{th} power plant efficiency. The average head ($H_{n,t}$) available for the powerhouse 'n' during a particular time period 't' is expressed as the second order function of the storage and is given as:

$$H_{n,t} = C_{1,n}S_{n,t} + C_{2,n}S_{n,t}^2 + C_{3,n} \qquad t = 1,2,..12;\ n = 1,2,3,4 \tag{7.9}$$

The net head ($HN_{n,t}$) is estimated by deducting the tail water level and the frictional losses from the average head available in reservoir during the time period 't' from Eq. 5.9.

The above objective function (Eq. 5.7) is subjected to various physical constraints. The head available in the reservoir should be greater than the minimum drawdown level (MDDL) of the powerhouse during any time period 't'. This is expressed as

$$H_{n,t} \geq MDDL_{n,t} \qquad t = 1, 2 \ldots 12;\ n = 1, 2, 3, 4 \tag{7.10}$$

where $H_{n,t}$ is the average head (m) in the reservoir for the powerhouse 'n' during the time period 't' and $MDDL_{n,t}$ is the minimum drawdown level of the powerhouse 'n' during the time period 't'. The power production in a power plant 'n' during any time period 't' should be less than or equal to the maximum power generating capacity of the plant

$$PH_{n,t} \leq P\max_{n,t} \qquad t = 1, 2 \ldots 12;\ n = 1, 2, 3, 4 \tag{7.11}$$

where $PH_{n,t}$ is the power produced (kWh) from the powerhouse 'n' during the time period 't'; $Pmax_{n,t}$ is the maximum generation capacity (kWh) of the powerhouse 'n' during the time period 't'. Even though Koyna is one of the largest reservoir in the state of Maharashtra, India, due to its intended purpose more emphasis is being given to hydropower after meeting the irrigation demand. Hence, in the present study, irrigation demand is taken as a constraint and is made as a compulsory release. This constraint is given as the monthly irrigation release and should be greater than or equal to the monthly irrigation demand during the time period 't' and is mathematically expressed as:

$$R_{4,t} \geq ID_t \qquad t = 1, 2 \ldots 12 \qquad (7.12)$$

where $R_{4,t}$ is the irrigation release from Koyna Dam during the time period 't' and ID_t is the irrigation demand during the time period 't'.

To ensure adequate water for irrigation on Eastern side and other downstream requirements, the diversion of large quantity of water towards Western side was limited by Krishna Water Dispute Tribunal (KWDT, 2010). As per this constraint, diversion of large quantity of water to Western side for power production was restricted to 1912×10^6 m^3. The total annual release for irrigation should be 850×10^6 m^3. These constraints are given as:

$$\sum_{t=1}^{12} (R_{1,t} + R_{3,t}) \leq R_{w,\max} \qquad (7.13)$$

$$\sum_{t=1}^{12} R_{4,t} \leq AID_{\max} \qquad (7.14)$$

where, $R_{w,max}$ is the maximum water that can be diverted to the Western side for power production and AID_{max} is the maximum water to be released annually for irrigation to the Eastern side.

The storage '$S_{m,t}$' in reservoir 'm' during any time period 't' should not be less than the minimum storage ($S_{m,min}$) or dead storage and should not be more than maximum storage ($S_{m,max}$) or capacity of the reservoir. It is also essential to maintain the reservoir storage at some lower level during the monsoon season to observe the flood and to avoid flooding at the downstream. This is given by (Simonovic and Srinivasan, 1993):

$$S_{m,\min} \leq S_{m,t} \leq (S_{m,\max} - \theta_{m,t}) \qquad t = 1, 2 \ldots 12, m = 1, 2 \qquad (7.15)$$

where $\theta_{m,t}$ is the required storage to be emptied for flood during the monsoon season for the reservoir 'm' during the time period 't'. The required flood storage ($\theta_{m,t}$) for different time period 't' during the monsoon season are fixed as per downstream canal carrying capacity and time required for operating the gates of the reservoirs (KHEP, 2005).

The evaporation loss ($E_{m,t}$) from the reservoir 'm' during the period 't' is expressed as a function of initial and final storage (Arunkumar and Jothiprakash, 2012) during that particular time period. This is expressed as:

$$E_{m,t} = a_{m,t} + b_{m,t}\left(\frac{S_{m,t} + S_{m,(t+1)}}{2}\right) \qquad t = 1, 2 \ldots 12 \ ; m = 1, 2 \qquad (7.16)$$

where, $a_{m,t}$ is the constant estimated by regression analysis when evaporation is plotted against the average storage during the time period 't' and $b_{m,t}$ is the slope when evaporation is plotted against the average storage of the reservoir during the time period 't' for the reservoir 'm'.

The continuity equation for Koyna reservoir is given as:

$$S_{1,(t+1)} = S_{1,t} + I_{1,t} - \sum_{n=1}^{1,3,4} R_{n,t} - O_{1,t} - E_{1,t} \qquad t = 1, 2 \ldots 12, n = 1, 3 \ \& \ 4 \qquad (7.17)$$

where, $S_{1,(t+1)}$ is the final storage in the Koyna reservoir during the time period 't' (10^6 m^3); $S_{1,t}$ is the initial storage in the Koyna reservoir during the time period 't' (10^6 m^3); $I_{1,t}$ is the inflow into the Koyna reservoir during the time period 't'(10^6 m^3); $R_{n,t}$ is the release to the powerhouse 'n' during the time period 't' (10^6 m^3) from the Koyna reservoir; $O_{1,t}$ is the overflow from the Koyna reservoir during the time period 't'(10^6 m^3) and $E_{1,t}$ is the evaporation losses from the Koyna reservoir during the time period 't', (10^6 m^3).

The continuity equation for the Kolkewadi reservoir is given as follows:

$$S_{2,(t+1)} = S_{2,t} + I_{2,t} + R_{1,t} + R_{3,t} - R_{2,t} - O_{2,t} - E_{2,t} \qquad t = 1, 2 \ldots 12 \qquad (7.18)$$

where, $S_{2,(t+1)}$ is the final storage in the Kolkewadi reservoir during the time period 't'; $S_{2,t}$ is the initial storage during the time period 't' in Kolkewadi reservoir; $I_{2,t}$ is the inflow into the Kolkewadi reservoir from its own catchment area during the time period 't'; $R_{2,t}$ is the release to the PH II from the Kolkewadi reservoir during the time period 't'; $R_{1,t}$ is the inflow to the Kolkewadi reservoir from PH I during the time period 't'; $R_{3,t}$ is the inflow to the Kolkewadi reservoir from PH III during the time period 't'; $O_{2,t}$ is the overflow from the Kolkewadi

reservoir during the time period '*t*'; $E_{2,t}$ is the evaporation losses from the Kolkewadi reservoir during the time period '*t*'.

The overflow occurs when the final storage exceeds the reservoir capacity. This overflow constraint is given by:

$$O_{m,t} = S_{m,(t+1)} - S_{m,\max} \qquad t = 1, 2 \ldots 12;\ m = 1, 2 \qquad (7.19)$$

$$\text{and} \quad O_{m,t} \geq 0 \qquad t = 1, 2 \ldots 12;\ m = 1, 2 \qquad (7.20)$$

where, $S_{m,(t+1)}$ is the final storage in the reservoir '*m*' during time period '*t*' (10^6 m^3) and this final storage is the initial storage for the next time period '*t+1*', when there is no overflow. If overflow occurs then $S_{m,max}$ will be the initial storage for the next time period '*t+1*'.

7.5 Optimization of Multi-reservoir System

The KHEP is optimized for maximizing the hydropower production using the above developed monthly time step model considering both the Koyna and Kolkewadi reservoirs as multi-reservoir system. Based on the tribunal constraints (Eq. 5.13 and Eq. 5.14) of the above formulated model, four operating policies (Arunkumar and Jothiprakash, 2012) are analyzed. These different operating policies will be helpful in assessing the full potential of the KHEP system for power production under different release conditions. The policies considered in the present study are:

Policy 1: No binding constraint on Eastern and Western side releases (all the constraints are considered except constraint Eq. 5.12, 5.13 and 5.14) [Aim: To find the full power production potential of the system]

Policy 2: Only annual binding constraint on irrigation (Eastern side) releases (all the constraints are considered except constraint Eq. 5.12 and 5.13)

Policy 3: Both monthly and annual binding constraint on irrigation (Eastern side) releases (all the constraints are considered except constraint Eq. 5.13)

Policy 4: Both Western and Eastern side binding constraints on releases are considered as per the Tribunal (with all the hard bound constraints)

The Koyna reservoir receives 95% of the inflow during the monsoon season (Jun - Oct) and the remaining 5% during the non-monsoon period (Nov - May). This shows that this intermittent inflow Koyna reservoir completely depends on the monsoon inflow. The major inflow into Kolkewadi reservoir is the power releases from Koyna reservoir through PH I and PH III. Thus, the operation of PH III at Kolkewadi reservoir completely depends on Koyna releases to PH I and PH III. The average head available in the reservoir is represented as a quadratic function of storage and is given in Eq. 5.9. The constants of the equation, C_1, C_2 and C_3 are estimated by regression analysis from area-capacity-elevation table of the reservoirs. The developed optimization model has 48 decision variables and 264 constraints. Initially, the above optimization model has been solved using a conventional NLP technique. Then, the optimization model is solved using soft computing techniques coupled with chaos. In addition, the optimal releases of the selected policy are further tested using a simulation model for 49 years of observed inflow.

7.6 Optimization using Conventional NLP Technique

The NLP model is optimized for three different inflows scenarios, namely, scenario 1: wet scenario (50% dependable inflow), scenario 2: normal scenario (75% dependable inflow) and scenario 3: dry scenario (90% dependable inflow). The dependable inflows are estimated using Weibull's method (Chow *et al.*, 1988) from 49 years of observed inflow. The NLP optimization model is solved using global solver in Language for Interactive General Optimization (LINGO) Software. The global solver combines a series of range bounding (e.g. interval analysis and convex analysis) and range reduction techniques (e.g. linear programming and constraint propagation) within a branch and bound framework to find global solutions to non-convex non-linear programs (Lingo, 2006). The optimal releases of the developed NLP model for the above four policies under different dependable inflow scenarios are discussed in the following section.

7.6.1 Annual Power Production

In order to assess the full power production potential of the KHEP as well as under restricted releases, the formulated NLP model is solved for the above mentioned four policies using three different dependable inflow scenarios. The variation of annual power production for

different operating policies resulted from three inflow scenarios is given in Figure 7.7. It can be observed from Figure 7.7 that the power production decreases among the policy with increase in restriction on releases as well as with increase in inflow dependability. However, in case of dry inflow scenario, the annual power production is almost same for Policies 2, 3 & 4. This shows that the power production potential under dry inflow scenario remains the same irrespective of restriction on Western side releases. Among all these policies, the Policy 1 has resulted in a maximum power production of 5826.29×10^6 kWh for wet inflow scenario, since there is no restriction on the Western and Eastern side releases. Even though this Policy 1 has resulted in maximum power production through major power plants on the Western side, the releases towards Eastern side for irrigation are lower and most of the months are zero for all the inflow scenarios. This shows that with no hard bound constraints, the model reduced the irrigation release on the Eastern side to achieve full power production in the Western side power plants. Depriving irrigation release is not a viable case in practical, since irrigation is the primary occupation on the Eastern side of the reservoir and hence irrigation releases are mandatory. Thus, Policy 1 cannot be a practically implementable policy. But, Policy 1 shows the full power production potential of the KHEP system under unrestricted releases.

In order to achieve irrigation releases, the annual irrigation release constraint is considered in Policy 2. Under this Policy 2, all the three inflow scenarios have resulted in irrigation releases equal to the annual demand, but not in every month. Considering this constraint in the optimization model reduces the power production substantially for all the three inflow scenarios showing that hydropower production and irrigation are conflicting objectives. The reduction in total power production for different inflow scenarios varies between 10 – 29% compared to Policy 1. The hydropower plants in the Western side are having high net head with high generating capacity and hence produce more hydropower for same discharge compared to PH IV at the dam foot on the Eastern side. Thus, the power produced from PH IV through irrigation releases is lesser than the power produced at PH I & III for the same discharge. Even though this Policy 2 has satisfied the total annual irrigation demand, the month wise irrigation demands are not met.

In order to have irrigation release for all months, both the annual and monthly irrigation demand constraints are considered in Policy 3. The optimization model solved with Policy 3 has resulted in irrigation release in all the months as per the monthly demand and the power

production is almost similar to that of Policy 2 for all the scenarios. This Policy 3 is a practically implementable optimal solution, leading to higher power production satisfying all the physical and other demand constraints. In all these policies, the restriction on releases towards the Western side for power production is not considered for all the inflow scenarios and hence the releases are slightly more than the tribunal limit.

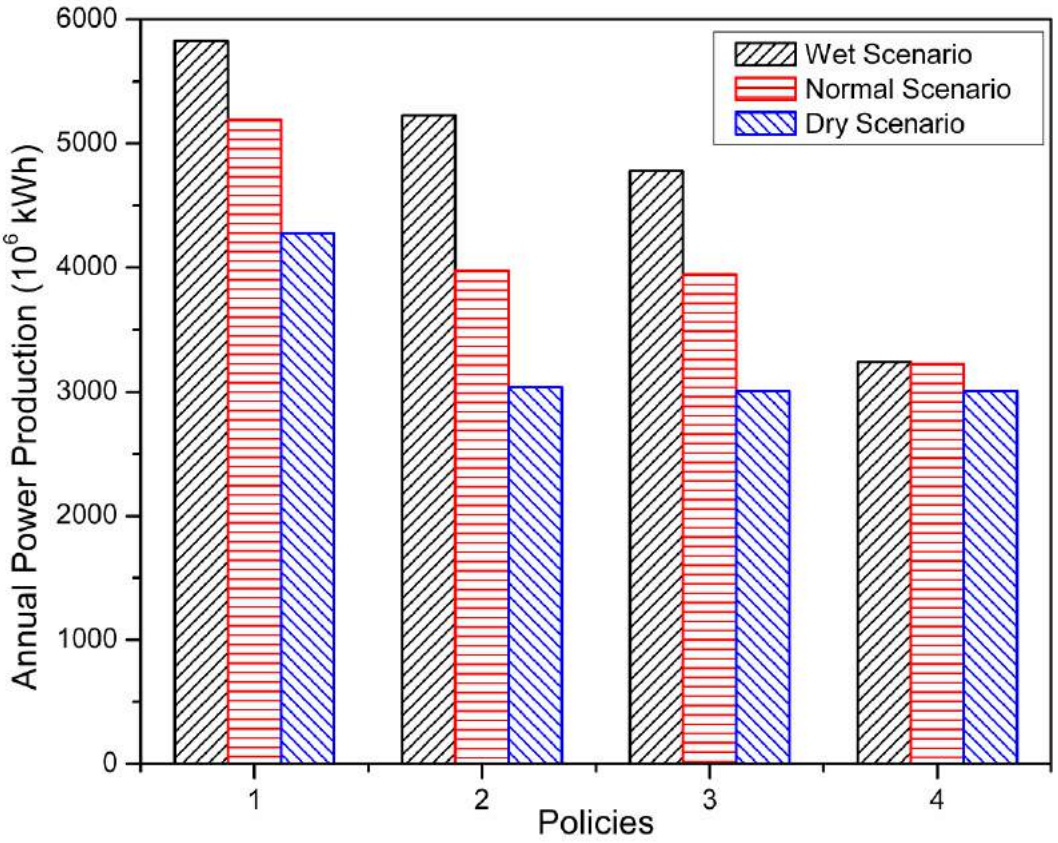

Figure 7.7. Annual power produced from various scenarios under different inflow condition using NLP technique

In Policy 4, all the binding constraints on releases are considered and thus, the model has restricted the releases for both power production and irrigation as per the tribunal limits. The limitation on releases has reduced the power production significantly for all inflow scenarios compared to other policies. Also, there is not much variation in the power production among the different inflow scenarios in this Policy 4, since the total quantity of release for power production is same. This shows that under restricted releases, the power production is same irrespective of the quantity of inflow received by the reservoir. When compared to Policy 1, the power production decreases by 44% for wet scenario, 38% for normal and 29% for dry

scenario in Policy 4. Also, there is a decrease of around 32% and 18% in power production when compared to Policy 3 for wet and normal scenarios, respectively. In Policy 4, the dry inflow scenario has produced almost the same hydropower as that of Policy 3. This shows that under dry (less) inflow scenario, the system produces almost same hydropower irrespective of tribunal release constraints and thus leading to redundancy of this constraint at low inflow scenario. On the other hand, Policy 4 increased the storage in the reservoir leading to overflow from the reservoir during normal and wet years. Based on the annual power production and satisfying various demands it may be concluded that Policy 3 is the best viable and implementable policy and is a best alternative to Policy 4.

7.6.2 Monthly Power Production

The monthly power production resulted from the NLP model for various policies are discussed scenario wise. First, the policies for wet scenario are discussed followed by normal scenario and dry scenario. A maximum of 614.74×10^6 kWh was produced in August for both Policy 1 and 2, and minimum of 98.24×10^6 kWh was produced in June for Policy 4 from the system for the wet inflow scenario. A maximum firm energy of 417.14×10^6 kWh was produced from Policy 1 and decreases with restriction on releases. Among the hydropower plants, PH III has produced maximum of 300×10^6 kWh for all policies because of high head and capacity. It is also to be observed that PH IV has produced power only in July and August. It can be inferred that there is no irrigation release during most of the months in Policy 1, since no binding constraints on releases are considered. In Policy 2, PH IV has produced power only during the monsoon season, which shows that irrigation releases are made only during the monsoon season. However, the total releases are equal to the annual irrigation demand. There is power production in PH IV in all months in Policy 3. This has lead to the satisfaction of monthly irrigation demand and annual irrigation demand. There is a wide variation in power production among the hydropower plants in Policy 4. All these variations are due to the constraint imposed on Western side releases. This wet scenario shows that Policy 3 has produced maximum power satisfying all the physical constraints including meeting the irrigation demands. Thus, Policy 3 may be considered as the better policy.

During normal inflow scenario, only the Policy 1 has resulted in considerable power production in all the months expect PH IV. Both the Policy 2 and 3 has shown a similar trend in power production with less variation in each month. A maximum of 477.76×10^6 kWh was produced in October for Policy 2, and minimum of 90.22×10^6 kWh was produced in June for Policy 2 from the system for the normal inflow scenario. The maximum firm energy of 356.33×10^6 kWh is produced from the system for Policy 1. Among the hydropower plants, PH III has produced maximum firm energy in Policy 1 because of high head and capacity. In Policy 2, not only the total power production but also the firm energy has decreased compared to Policy 1, since the annual irrigation release constraint is considered. These results show that Policy 3 is best policy for 75% dependable inflow scenario also.

Contrary to other inflow scenarios, the variation in monthly minimum power production from the system is very less among different policies under dry inflow scenario. This shows that under less inflow scenario, the restriction on releases has less impact on power production. It is observed that the Policies 2, 3 and 4 have resulted in a similar trend in monthly power production. These three policies have produced power only during the monsoon season, where there will be inflow and during non-monsoon season the power production remains constant. This shows that under dry inflow scenario, the system behaves the same way irrespective of constraints on releases. Thus, Policy 3 and Policy 4 are producing almost same results under dry inflow scenario.

In general, the wet inflow has resulted in more hydropower production than the normal and dry inflow scenario for all the policies studied. It is observed that PH III has produced maximum hydropower for all the policies and scenarios. It is also observed that the hydropower production in PH III has reduced considerably compared to the other hydropower plants due to constraints on releases. Since, Kolkewadi reservoir receives inflow mainly from PH I and PH III, the power production from PH II varies accordingly. The variation in power production among the wet, normal and dry inflow scenario is less for Policy 4 compared to other policies. The Policy 1 showed the full potential of the KHEP power production capability. The Policy 4 shows the power production under the hard bound constraints. It is found that the constraint on Eastern side and Western side releases reduced the power production from the system. But Policy 3 seems to be a much viable policy, since it obeys all the constraints but in different way, it is better to have Policy 3 rather than Policy 4.

7.6.3 Monthly Releases

The monthly releases to the powerhouses resulted from various policies solved using NLP technique is shown in Figure 7.8. From the figure, it is observed that there is wide variation in releases for different scenarios. In general, the wet scenario has releases more than other scenarios. Figure 7.8(a) shows the releases to powerhouses for Policy 1. For Policy 1, only the wet scenario has resulted in releases to PH IV for few months. This shows that when no binding constraints are considered all the releases are oriented towards the power production. Figure 7.8(b) depicts releases made by Policy 2 for different scenarios. In Policy, both the wet scenario and dry scenario resulted in releases to PH IV for few months, since the annual irrigation demand is considered. It is to be noted that the total releases in these few months is equal to the total annual demand. On the other hand, this has reduced the releases to PH I. The releases made by Policy 3 under different scenario are given in Figure 7.8(c). The Policy 3 which considers the monthly irrigation demand constraint has resulted in releases to PH IV as per the irrigation demand. All the three scenarios have resulted in irrigation releases in Policy 3. From Figure 7.8(d), it is observed that the Policy 4 has resulted almost similar releases for all scenarios to PH I in most of the time period. Compared to other policies, the releases are less in Policy 4 due to Western side release constraint. The Policy 4 also has released irrigation demands as per the requirement for all three scenarios.

7.6.4 End of Month Storage Levels

The resulted end of month Koyna reservoir storage for various operating policies is given in Figure 7.9. From Figure 7.9, it can be seen that the end storage curve of Koyna reservoir follows a similar trend for all policies. Only the wet inflow scenario reached the maximum storage in all policies, while the normal inflow scenario reached the maximum storage in Policy 4 due to the restriction in releases and storing the water in the reservoir. Figure 7.9(a) shows the resulting storage levels for Policy 1 and indicates that the available inflow and storage is fully utilized for power production, since there are no binding constraints on releases. Only the wet inflow scenario has reached the maximum capacity of the reservoir for Policy 1 in spite of high power production. The resulting storage levels for Policy 2 and 3 are shown in Figure 7.9(b) and Figure 7.9(c) respectively. Both the policies have similar storage levels. A minor difference seen is due to the irrigation release during all the months in Policy 3.

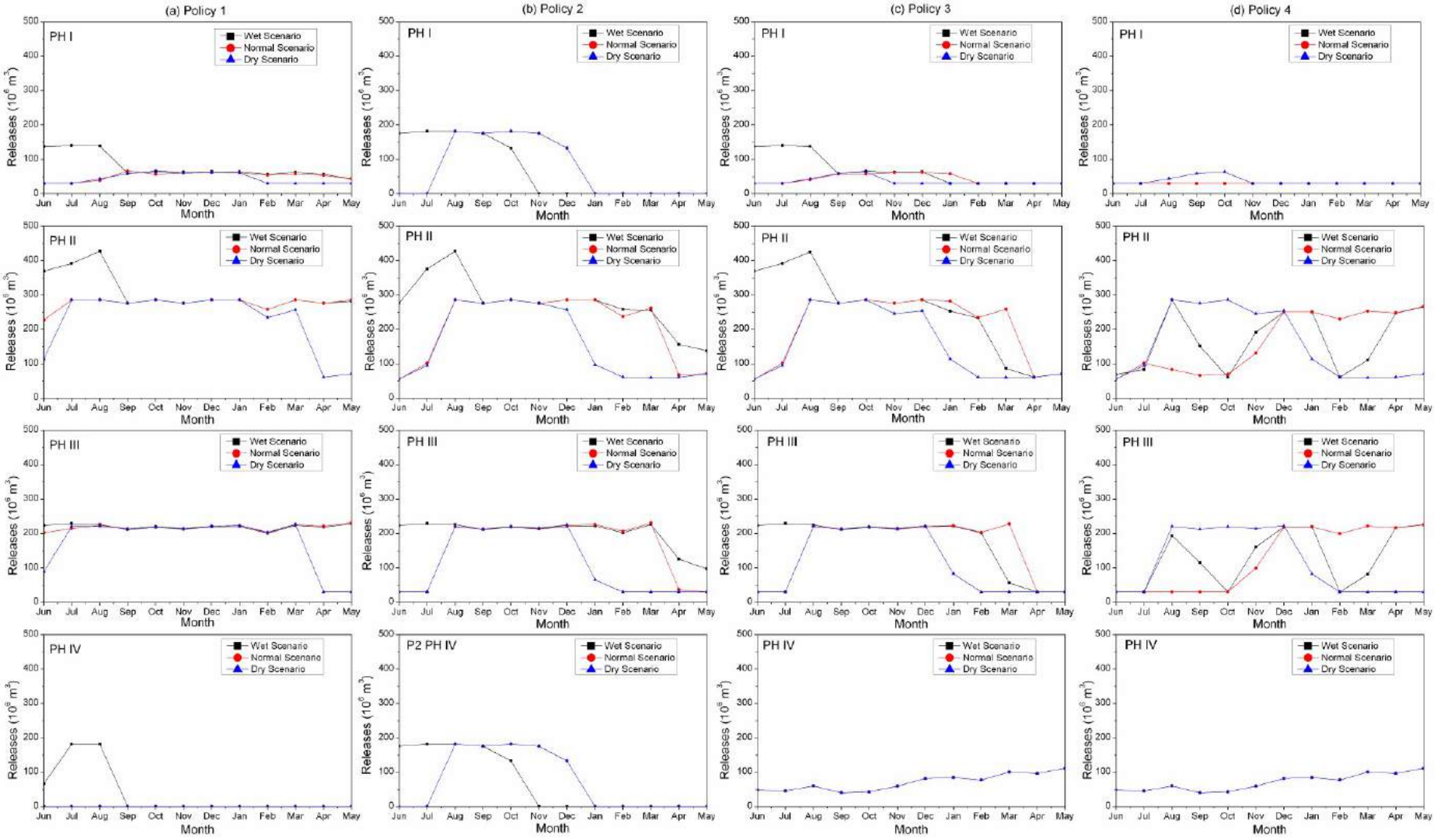

Figure 7.8. Monthly releases to different powerhouses of KHEP resulted from NLP technique

The end month storage levels for Policy 4 is shown in Figure 7.9(d), the wet and normal inflow have resulted in maximum storage leading to overflow from the reservoir, since the releases are restricted as per the Tribunal limits. The variation in storage levels for dry inflow scenario is the same as that of the other policies. Due to the restriction in releases, Policy 4 resulted in higher storage levels leading to lower power production. This indicates that policy 4 not only produces less power, it is also under utilizing the power potential created. Even though, the wet scenario of Policy 1 and Policy 2 reached the maximum storage level, they have not resulted overflow. However, the wet scenario of Policy 3 and Policy 4 have resulted 277.49 × 10^6 m^3 and 1020.28 × 10^6 m^3 overflow during the month of August from Koyna reservoir. The operations of Kolkewadi reservoir is mainly depends on tail water from PH I and PH III of Koyna reservoir. The resulted end of month storage curves of Kolkewadi reservoir is shown in Figure 7.10. It is observed that the storage rule curves are same for all the policies and also for all the three inflow scenarios. Thus, all inflows are completely utilized for power production in Kolkewadi reservoir with any overflow.

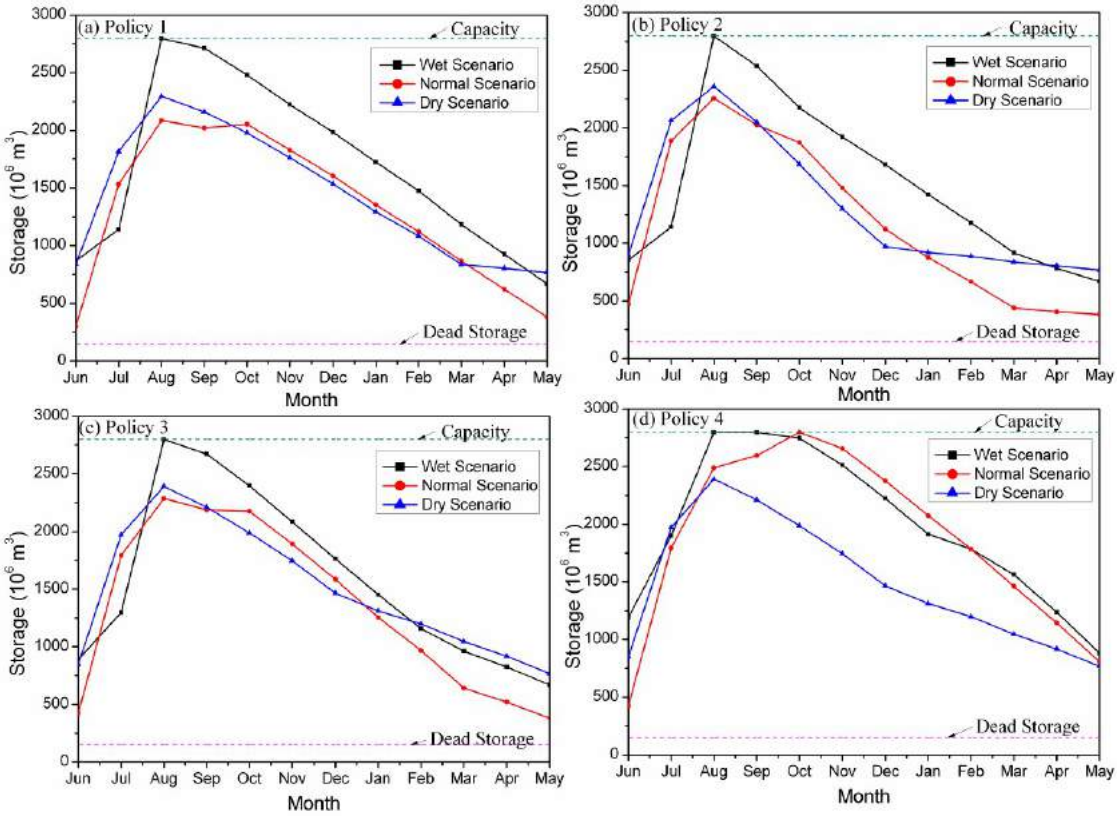

Figure 7.9. Resulted storage curves for various scenarios for Koyna reservoir using NLP technique

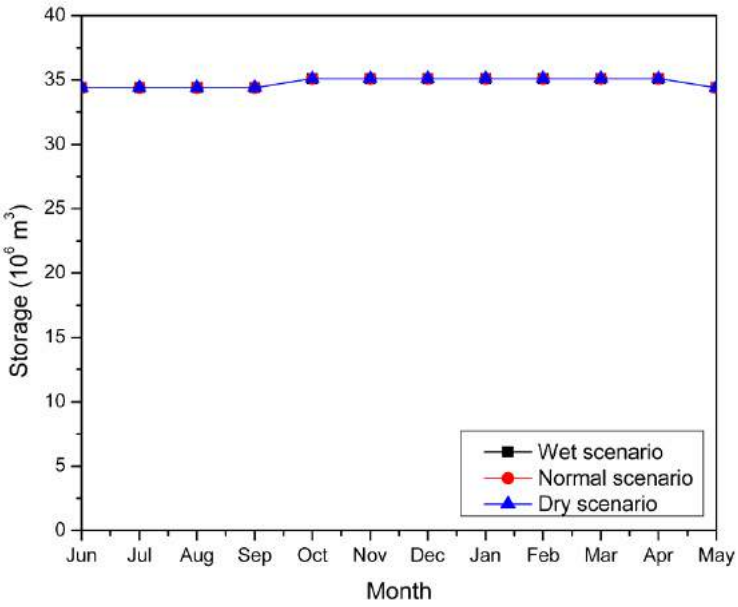

Figure 7.10. Resulted storage curves for Kolkewadi reservoir using NLP technique

7.6.5 Simulation of NLP results

Based on the above analysis, the Policy 3 is selected as the best and viable optimal result, since it has satisfied the monthly irrigation demand and also produced considerable power production compared to Policy 4. The performance of the optimal releases of Policy 3 obtained from wet inflow (referred as Scenario 1), normal inflow (referred as Scenario 2) and dry inflow (referred as Scenario 3) are assessed using a simulation model for 49 years of observed inflow. The performance of the optimal policies were evaluated using the criteria reported by Jothiprakash and Shanthi (2009). Table 7.4 shows the performance of the optimal Policy 3 for longer period. The MFID gives the number of months the deficit occurred to the total simulated months. The table shows the Scenario 1 has resulted in deficit irrigation in 45 months out of total simulated 588 months. The annual average irrigation deficit is also higher for Scenario 1. The Scenario 2 has resulted deficit irrigation release in 10 months. The Scenario 3 has not resulted in any irrigation deficit and has released as per the demand for all the time periods.

Table 7.4. Performance analyses of Policy 3 of NLP model

Scenario	MFID	AFID	AAID (10^6 m^3)	PAID (%)
Scenario 1	45/588	16/49	74.97	8.83
Scenario 2	10/588	7/49	18.60	2.19
Scenario 3	0/588	0/49	0.00	0.00

The optimal releases of Scenario 1 are higher than Scenario 2 and 3 as per the results of the optimization model. Hence, the simulation results of Scenario 1 encountered higher MFID, MAID, AFID, AAID and PAID than Scenario 2 and 3. The volume of monthly average irrigation deficit for all the scenarios is given in Figure 7.11. From the figure, it can be seen that the Scenario 1 has resulted in irrigation deficit and the Scenario 2 for few months at the end of the time period. However, the Scenario 3 has not resulted in any irrigation deficit. It is also seen that the deficits occurred mostly at the end of the year. The result shows that irrespective of the inflow, the Policy 3 performs very well for longer runs with a maximum average irrigation deficit of 8.8% over 49 years.

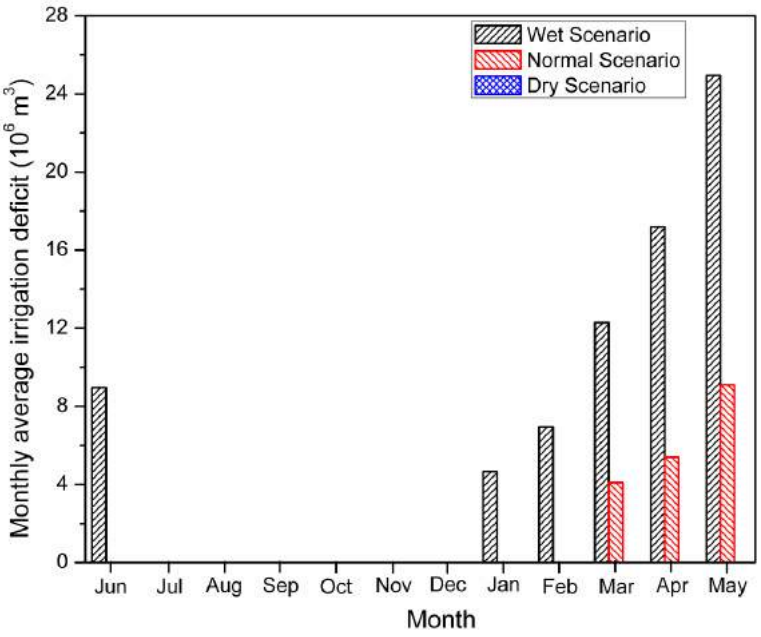

Figure 7.11. Monthly average irrigation deficit in KHEP of Policy 3 for different scenarios

The volume reliability of monthly irrigation release is given in Figure 7.12. From the figure, it is observed that all the scenarios have more than 75% reliability. Even though the Scenario 1 has resulted in deficit in few months at the end of the season, it has released more than 75% of the demand and similarly the Scenario 2 has released more than 80% of the demand in deficit months. The overall volume reliability is more than 90% for all the scenarios, which shows that the optimal results of Policy 3 are highly reliable. This study shows that the power production can be increased by slightly relaxing the power releases without compromising the irrigation releases.

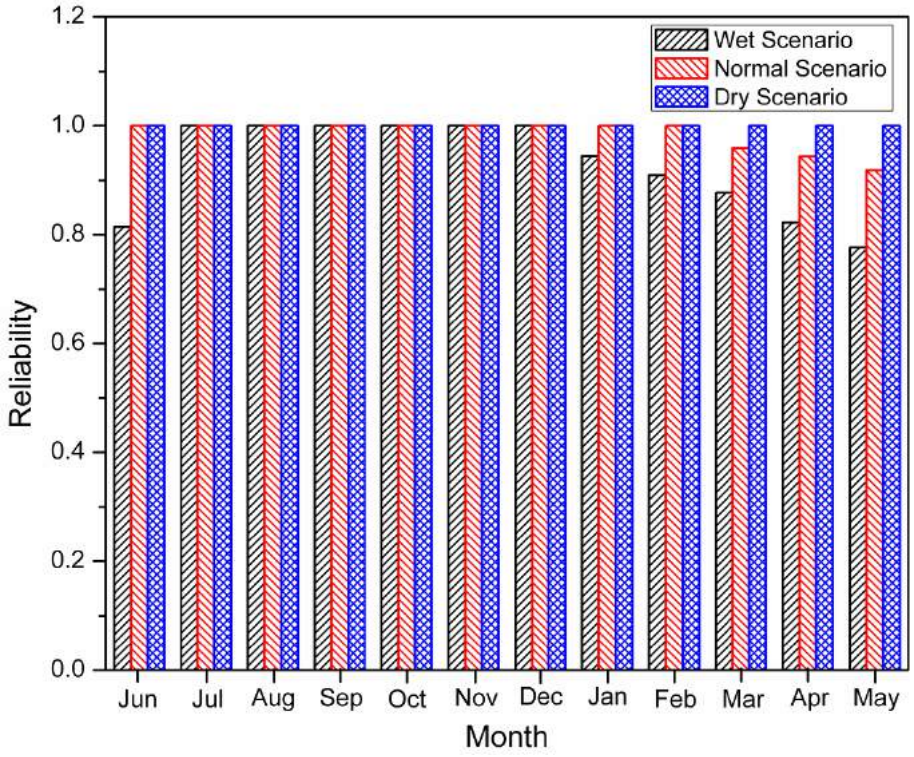

Figure 7.12. Volume reliability of monthly irrigation releases of Policy 3 for various scenarios

7.7 Optimization using Hybrid Evolutionary Algorithms

In order to overcome the drawbacks of conventional optimization techniques, the evolutionary algorithm based soft computing techniques is also applied in this study. The operations of KHEP reservoirs are optimized using chaotic evolutionary optimization algorithms. The genetic algorithm and differential evolution algorithm are used as a base optimization algorithm and are coupled with chaos technique to enhance the search by generating better initial population and other genetic operations. The chaos technique is introduced in generating initial population, crossover and mutation. All these four policies are evaluated with 75% dependable inflow using hybrid chaotic differential evolution (HCDE), chaotic genetic algorithm (HCGA), differential evolution (DE) algorithm and genetic algorithm (GA) techniques and the results are inter-compared. Further, the performances of the optimal results of best scenario are assessed using a simulation model for estimating the irrigation deficits in longer run, since agriculture is the major sector.

7.7.1 Hybrid Chaotic Genetic Algorithm

The Hybrid Chaotic Genetic Algorithm (HCGA) uses chaotic initial population generation, tournament selection, chaotic simulated binary crossover and chaotic mutation. The chaotic technique is introduced in simulated binary crossover to enhance the search in GA and in mutation to keep the population diversity. It is reported that the crossover probability should be selected such that it should not create a complete copy of parent nor completely different from the parents (Goldberg, 1989). Hence, the sensitivity analyses on crossover probability were carried out for HCGA by varying it from 0.50 to 0.95 with an increment of 0.05. The results showed that the power production was higher for a crossover probability of 0.80. The objective function fitness value, annual power production increases with the increase in crossover probability up to 0.8 and then decreases. This may be due to the reason that the offsprings are different from the parents at higher crossover probability and hence, it losses the genetic material. Jothiprakash and Arunkumar (2013) reported that a crossover probability of 0.75 resulted better power production for Koyna reservoir alone when modelled as a single reservoir system,. This shows that the increase in number of variables for a multi-reservoir system can be handled by increasing the probability of crossover (Jothiprakash *et al.*, 2011b). The mutation probability is fixed as the ratio of the number of variable (*1/n*) as suggested by Deb (Deb, 2001). The elitism is applied to preserve the best strings in the population such that it is not lost during the genetic operations. To have a true comparison between HCGA and GA, the same crossover probability and mutation probability are used in simple GA. The other GA parameters used for various scenarios are given in Table 7.5.

Table 7.5. HCGA and GA parameter used for hydropower multi-reservoir system

	Policies			
Parameters	1	2	3	4
Crossover Probability	0.80	0.80	0.80	0.80
Mutation Probability	0.021	0.021	0.021	0.021
Population size	250	250	250	250
Maximum generations	1000	1000	1000	1000
Elitism	0.1	0.1	0.1	0.1

7.7.2 Hybrid Chaotic Differential Evolution Algorithm

Jothiprakash and Arunkumar (2013) reported that the *DE/best/1/exp* strategy resulted best optimal results for a single reservoir optimization. Hence, in the present study also, the strategy '*HCDE/best/1/exp*' is used for all the policies of both HCDE and simple DE, since the best strings are used for mutation. The scale factor '*F*' and crossover factor '*CR*' are the two important factors that control global search in DE. An optimal scale factor should be such that it should not generate the parent population again nor completely different from parents. The scale factor should also ensure the diversity in the population and also retain the genetic information from the parent population. Price *et al*. (2005) reported that a scale factor (*F*) less than 0.50 is reasonable to maintain the diversity in the population and to have parent genetic information. Similarly, the crossover is also a significant factor, which controls the global search by generating new population. Price *et al*. (2005) reported that the *CR* values between 0.50 and 1 is optimal for crossover in DE. Therefore, a sensitivity analyses has been performed by varying *CR* and *F* in the above specified range with an increment of 0.10. From the figure it is found that *F* of 0.3 and *CR* value 0.6 resulted in better power production. It is also found that further increase in the *CR* value decreases the power production for all the scale factor. In addition, the power production is less for very low (0.10) scale factor and also for high (0.5) scale factor. A scale factor (*F*) of 0.30 and *CR* value of 0.60 resulted in a better power production for the single reservoir system also (Jothiprakash and Arunkumar, 2013). The other DE parameters used for various scenarios are given in Table 7.6.

Table 7.6. HCDE and DE parameters used for different policies of hydropower optimization

		Policies			
S.No	Parameters	1	2	3	4
1	F	0.30	0.30	0.30	0.30
2	CR	0.60	0.60	0.60	0.60
3	Population	250	250	250	250
4	Generation	1000	1000	1000	1000

7.7.3 Computational Efficiency of the Hybrid Search Algorithms

All the algorithms used in the study are evaluated up to 1000 generation with a population size of 250. The constraints in the optimization are handled by penalty function approach for all the techniques applied. Based on the significance of the constraint, different penalties are assumed and heavy penalties are imposed on fitness function upon violation. All the four policies are run repeatedly for several times for all the techniques and only the best optimal solution resulted from each technique is reported. The convergence of these techniques to arrive optimal solution over the generation is traced and is given in Figure 7.13. From Figure 7.13, it can be observed that the rate of convergence to optimal solution by HCGA and HCDE is faster than simple GA and DE for all the policies studied. Further, the HCGA and HCDE with chaotic initial population have higher fitness value than simple GA and DE for all the four policies. Hence, it may be concluded that hybrid chaotic evolutionary algorithm converges quickly to the global optimal solution. It is also noted that for policy 3 and policy 4, all the techniques with the tribunal binding constraints on releases have resulted in sub-optimal solution for first few generations. It is found that, imposing heavy penalties on the fitness function leads to negative fitness value and resulted in sub-optimal solution. Over the generation, all the algorithms reached the optimal solution without violating the constraints. It is very clearly seen that with hard binding constraints, the HCGA and HCDE have satisfied the constraints and reached the optimal solution in lesser generations than simple GA and DE. This also shows that when binding constraints are imposed strictly, the simple GA and DE take more generations for convergence. On the other hand, the HCGA and HCDE with better initial population with enhanced search converged quickly to the optimal solution.

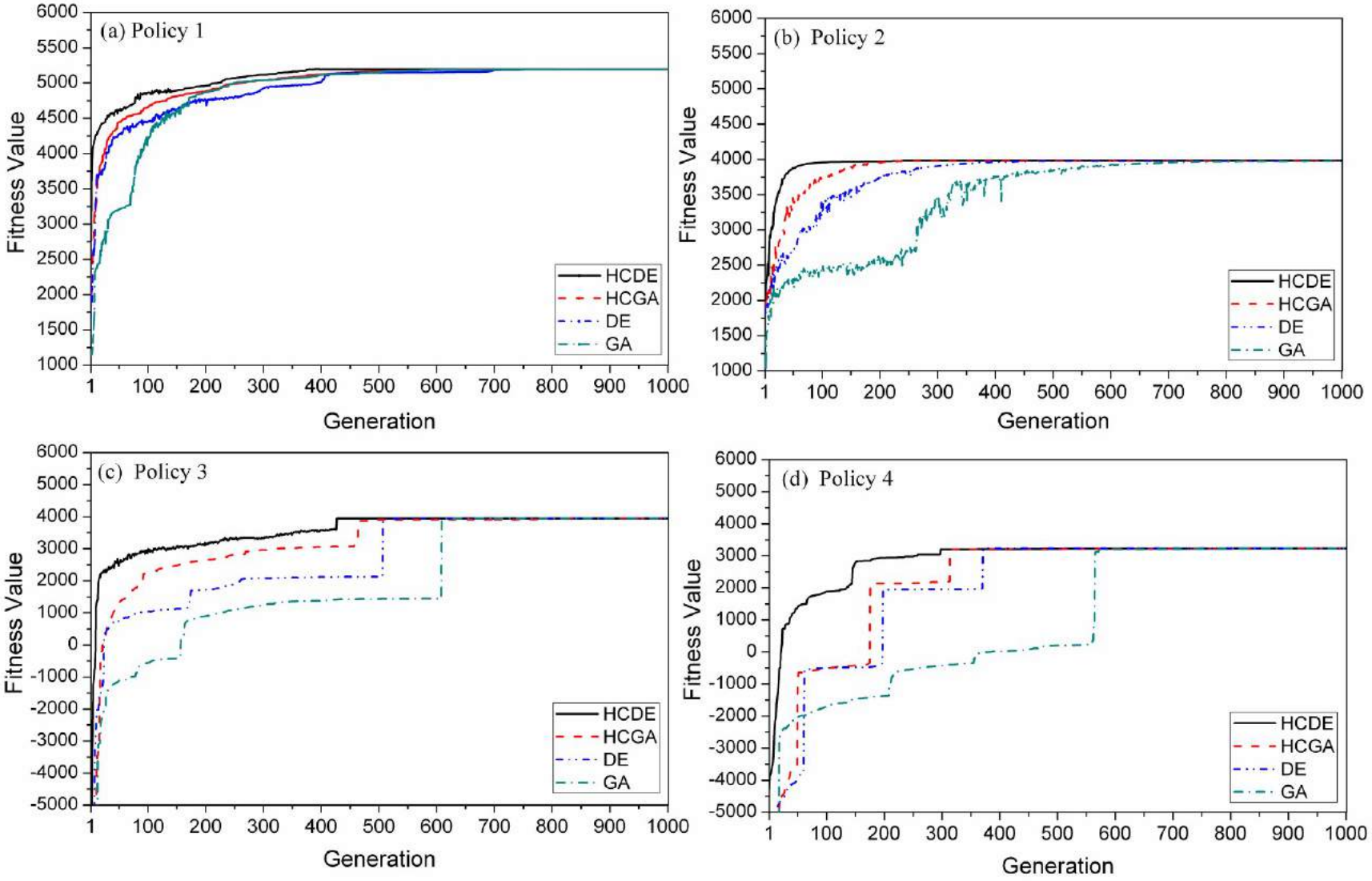

Figure 7.13. Convergence of evolutionary algorithms for different policies of KHEP

7.7.4 Annual Power Production

The annual power production resulted from various techniques for different policies are given in Table 7.1. It is observed that all the techniques have resulted in more or less same quantity of power production in their respective policies however there is large variation from one policy to the other policy. These variations in power production among the policies are due to constraint on releases. In order to assess the possible power production potential of whole KHEP, in Policy 1, no restrictions on releases to the powerhouses are considered. Under this condition, a maximum of 5195.39×10^6 kWh is generated by HCDE model. The HCGA has resulted slightly lesser power production than HCDE, however both are higher than simple DE and GA models. This shows that the chaotic algorithm coupled with general optimization algorithm has enhanced the search with better initial population. All the techniques have resulted in very less releases for Policy 1 on Eastern side for irrigation, since no binding constraint on irrigation is considered. In order to have irrigation releases, the annual irrigation release constraint is considered in Policy 2 [Eq. 5.14]. All the models are optimized with this additional constraint. From the results, it observed that all the models have resulted in irrigation releases equal to total annual irrigation demand. This has considerably reduced the total annual power production, since the releases to the powerhouses on the Western side have reduced significantly. Thus, there is a large variation in power production among the powerhouses for the same quantity of discharge.

Even though the total annual irrigation demand is achieved in Policy 2, the month wise irrigation demands are not satisfied. Hence in Policy 3, all the models are forced to release for irrigation every month by enforcing the monthly irrigation demand constraint. This hard binding constraint took few more generations for converging to a global optimal solution. The variation in releases within the months has slightly reduced the power production in Policy 3 compared to Policy 2. However, all the four models have satisfied the monthly irrigation demands as per the requirement. Thus, in the Policy 3 irrigation releases are given higher priority, since agriculture is the primary occupation and also leads to downstream flow. In Policy 4, the present situation is reproduced by restricting the releases for power production in the Western side considering the all the constraints. This has resulted in further reduction in power production with decreased release to the major powerhouses in the Western side. From the table it can also be observed that there is no much variation among models for this

Policy 4. For all the four policies, HCDE resulted in slightly higher hydropower generation compared to other techniques. On comparing with the Koyna reservoir studied by Jothiprakash and Arunkumar (2013) as a single reservoir system, there is a 20% increase in annual power production in all the policies for all the techniques. This shows that even though Kolkewadi is very small reservoir compared to Koyna, it terms of power production it contributes significantly to the KHEP, since it has the second largest powerhouse in the system with a capacity of 320 MW.

Table 7.7. Resulted annual power (10^6 kWh) production from various techniques

Policy	HCDE	HCGA	DE	GA
Policy 1	5195.39	5193.08	5192.44	5191.54
Policy 2	3980.27	3977.79	3976.23	3975.56
Policy 3	3950.93	3949.38	3947.95	3946.84
Policy 4	3226.60	3225.71	3224.89	3224.23

7.7.5 Resulted Monthly Releases

The monthly releases to the powerhouses for various policies from different optimization techniques are shown in Figure 7.14. From the figure, it is observed that all the techniques have resulted more releases to PH II than other powerhouses. This may be due to the reason that the PH II is having highest capacity in system and the net head for PH II is higher than the other powerhouses. Hence, all the models have resulted more releases to PH II. However, there is a large variation in releases to the powerhouses for every month among the models. Figure 7.14(a) shows the releases to powerhouses for Policy 1. For Policy 1, all the models have resulted no releases to PH IV, which is operated through irrigation release. This shows that when no binding constraints are considered all the releases are oriented towards the power production. The Policy 2, shown in Figure 7.14(b) depicts that the PH IV is having releases when annual irrigation demand is considered. On the other hand, this has reduced the releases to PH I subsequently. Even though the total annual irrigation releases are satisfied, the releases are not as per the monthly irrigation requirement in Policy 2. Few months have higher releases and few months have very less releases for all the models. Hence, to have the monthly irrigation releases as per the requirement, in Policy 3, the monthly irrigation requirement constraint is considered. All the models have resulted in releases as per the irrigation requirement every month as shown in Figure 7.14(c). In the last Policy 4, the releases to the powerhouses are further reduced since the binding constraint on releases

towards West and East are considered. From Figure 7.14(d), it is observed that the all the models have resulted almost similar releases to PH I and maximum release to PH II. These results show that the KHEP is under generating the hydropower beyond its capability due to hard bound constraint. If the constraint on Westward flow is relaxed by 10%, it is found that more than 14% of hydropower could be generated. Hence, based on the study it may be concluded that Policy 3 studied in the present study may be a better alternative policy to the existing policy in KHEP.

7.7.6 End of Month Storage Levels

The end of month storage levels of Koyna reservoir resulted from different techniques for various policies are shown in Figure 7.15. From the figure, it is observed that all other policies have resulted in similar storage curves, except Policy 4. In order to achieve the steady state policy, the storage in the reservoir at the end of the season is forced to meet the storage at the beginning of the season. Hence, for all the policies the final storage is equal to the initial storage, except for Policy 4. This is not possible in Policy 4, since the restriction on releases increased the storage in the reservoir and resulted in higher storage at the end of the season, thus violating the steady state policy. Hence, in order to maintain the steady state policy and to increase the power production by satisfying the irrigation demands, the available storage in the reservoir at the end of the season may be used for power production in the Western side (Policy 3). This also shows that under fully restricted release (Policy 4), the reservoir behaves as a surplus system, leading to underutilization of the potential created. This study shows that the available storage can be utilized for power production in the Western side by relaxing the restriction on releases (Policy 3), at the same time satisfying the irrigation demand in Eastern side.

The Kolkewadi reservoir operations mainly depends on the tail water releases from PH I and PH II, which in turn receives from Koyna reservoir releases. Also, the storage at the Kolkewadi is always maintained at maximum level for high head. The resulted end of month storage levels of Kolkewadi reservoir is given in Figure 7.16. The initial storage during the start of the season corresponds to the 75% dependable inflow year initial storage (June month) observed in the reservoir. However, this initial storage may not occur every year in reality. Hence to test the performance of the optimal results obtained for 75% dependable inflow, the best optimal results arrived through Policy 3 are further simulated for longer period.

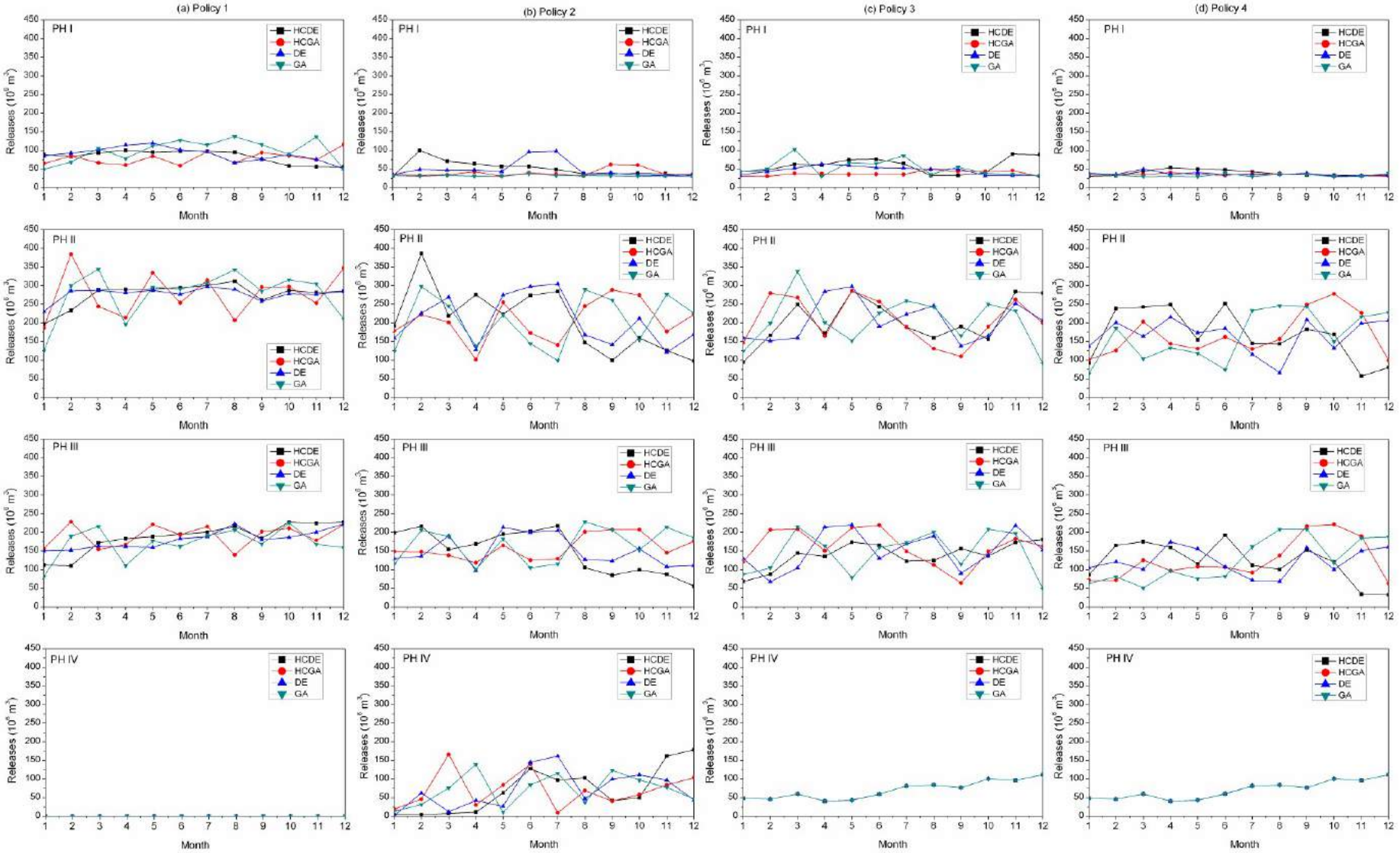

Figure 7.14. Monthly releases to different powerhouses of KHEP resulted from various techniques

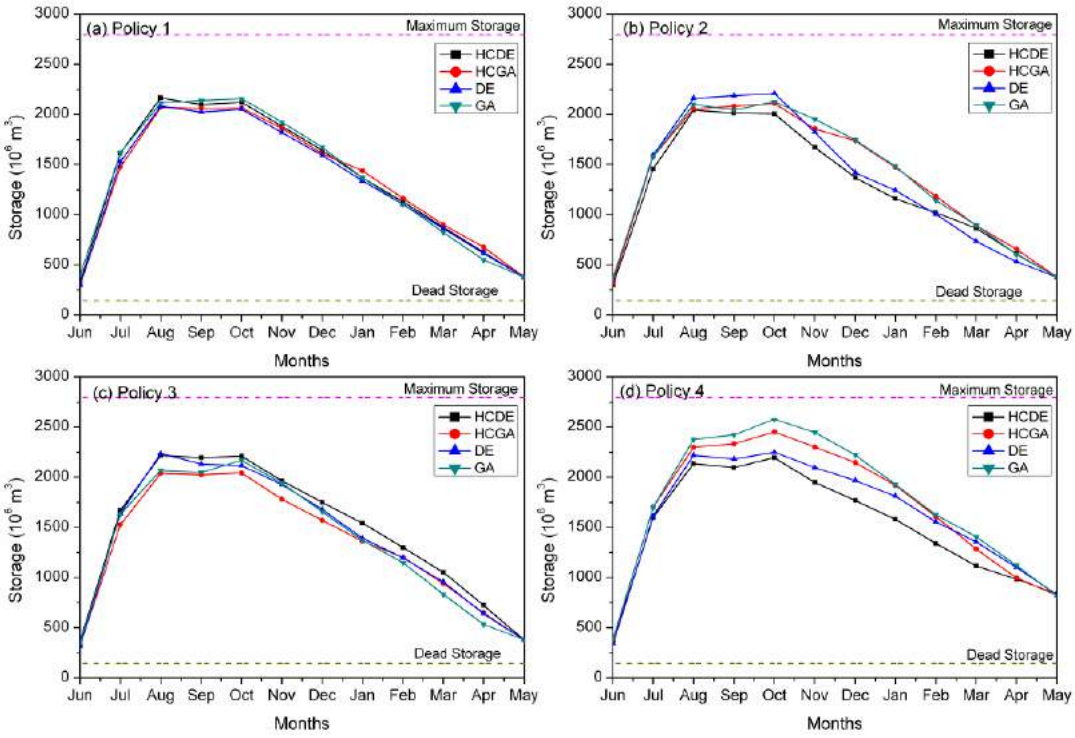

Figure 7.15. Resulted end storage curves of Koyna reservoir for various policies using evolutionary algorithms

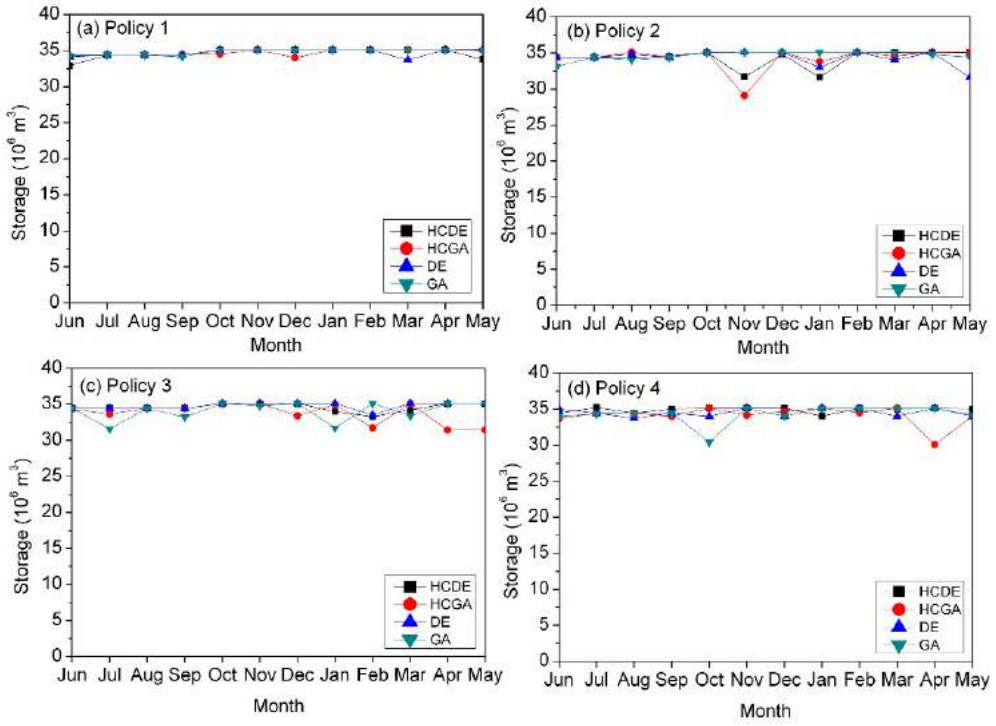

Figure 7.16. Resulted storage curves for various policies for Kolkewadi reservoir using evolutionary algorithms

7.7.7 Simulation of Optimal Releases

The Policy 3 optimized through HCDE algorithm is selected as the best optimal policy, since it has satisfied the monthly irrigation demand and also produced considerable power production compared to Policy 4. The irrigation performance is assessed for longer run using a simulation model. The performance has been assessed through a simulation model using 49 years of observed monthly inflow data. The performances indices such as the MFID, MAID, AFID and PMID reported by Jothiprakash and Shanthi (2009) is used. The simulation analysis shows that the model encountered irrigation deficit only in 8 months out of total simulated 588 months. These 8 months occurred in 6 years at the end of the season where inflows during those years are very less. The monthly average irrigation deficit resulted from the simulation model is given in Figure 7.17. The deficit occurred mostly at the end of the season, when there is no rainfall and the reservoir is to be operated with the available storage. From the figure, it is also observed that the total irrigation deficit is around 12% out of which 8% deficit occurred in May (end of the season). The average annual irrigation deficit is about 12.63×10^6 m^3, which is very meagre when compared to the storage in the Koyna dam. These results show that the Policy 3 satisfactorily meets the irrigation requirements for all the time period and performed better for longer run also.

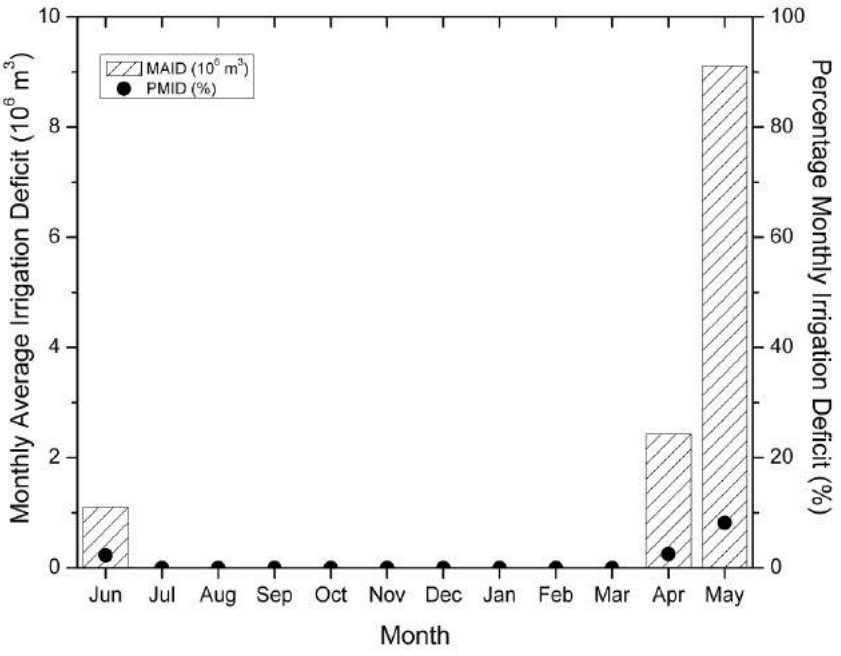

Figure 7.17. Resulted monthly average irrigation deficits in KHEP for Policy 3 in longer run

7.8 Closure

The performance of the evolutionary algorithm coupled with chaos for single objective optimization is tested by applying it to a complex multi-reservoir system, namely Koyna Hydro-Electric Project. The KHEP has four powerhouses, among which three are in the Western side and one is at the Eastern side. The irrigation releases are made through the powerhouse at the Eastern side by making the power production incidental. The complexity of the system is that the power releases and irrigation releases are in the opposite direction and cannot be complemented due to the topology. Hence, there is a need to optimize the operation of KHEP such that the power production and irrigation demands are met satisfactorily.

Initially, the behaviour of the KHEP is assessed using a monthly time step simulation model for various cases based on duration of operation under unconstrained scenario and constrained scenarios. From the simulation results, it is observed that the power production can be increased up to 12% for 12% increase in releases to the Western side powerhouses for 4 hr operation in the unconstrained scenario. The reliability indices shows that the system is more reliable for case 1 (4 hr operation of powerhouses) for the scenarios studied. The high resilience and low vulnerability indices show that the power production is more stable and continuous for case 1 in unconstrained scenario.

An optimization model has been developed with the objective of maximizing the hydropower production of KHEP. In this model, irrigation demands are given higher priority by making it as a separate constraint. The developed model is solved for four different operating policies using both conventional NLP and evolutionary algorithm techniques. In the conventional NLP technique, the optimization model is solved for three different inflow scenarios namely, wet, normal and dry inflow scenarios. On comparing the different policies, it is found that the power production can be increased upon by relaxing the release constraint slightly. Policy 3 shows an increment of 47 and 22% in power production for wet and normal inflow scenario satisfying the monthly irrigation demands compared to Policy 4. The monthly irrigation release has also slightly reduced the power production for Policy 2 and 3. On evaluating the performance of the Policy 3 using a simulation model, the results shows that the optimal releases are highly reliable on longer run.

The optimization model with same policies are again solved with evolutionary algorithms coupled with chaos. The chaotic technique is combined with the population based search algorithms namely genetic algorithm and differential evolution algorithm to enhance the global optimal search. On comparing with simple genetic algorithm and differential evolution algorithm, it is found that hybrid chaotic differential evolution algorithm and hybrid chaotic genetic algorithm resulted better. Among four policies assessed, the Policy 1 has resulted in maximum power production of 5195.39 × 10^6 kWh. However, this Policy 1 has not resulted in irrigation release. The Policy 3, which has resulted in irrigation releases as per the monthly demand as well as produced considerable hydropower, is found to be a viable option. Further, the performances of Policy 3 are evaluated using a simulation model. The simulation results of Policy 3 for longer time period show that the model satisfies the irrigation demand for most of the month and the deficit is very less.

The comparison of annual power production and annual releases resulted from different techniques for various polices are given in Table 7.8. On comparing the results, it found that the power production is slightly higher in HCDE. It is also found that the total releases vary in both NLP and HCDE techniques. In Policy 1, HCDE has resulted in higher release and in Policy 2 and 3, NLP has resulted in higher release. For Policy 4, both the techniques has resulted almost equal releases. However, HCDE has produced slightly more hydropower than NLP for all the policies. This may be due to the variation in monthly storage levels. There is a better variation in the end of month storage levels between HCDE policy and NLP policy. This indicates that soft computing techniques have resulted in a better optimal solution. Thus, the present study shows that the chaotic algorithm with general optimizer helped to achieve better global optimal solution in lesser number of generations compared to simple optimization techniques.

Table 7.8. Comparison of annual power production annual releases resulted from NLP and HCDE techniques

	Power Production (10^6 kWh)		Releases (10^6 m^3)	
Policy	HCDE	NLP	HCDE	NLP
Policy 1	5195.39	5190.45	6551.60	6547.46
Policy 2	3980.27	3974.29	5725.21	5736.13
Policy 3	3950.93	3945.82	5693.83	5703.67
Policy 4	3226.60	3223.37	4765.18	4765.08

Chapter 8

Summary and Conclusions

8.1 Summary

Water is one of the most essential natural resources not only for the human survival but also for the socio-economic development of a country. The wide variation in its availability over space and time has caused concern to use it efficiently and effectively. The surface water reservoirs play prominent role in solving the problem of spatial and temporal variation of water availability to some extent. It also serves various purposes such as irrigation, hydropower, flood control, industrial and domestic water supply, recreation, etc. Among these purposes, irrigated agriculture is the largest consumer of water and has high significance in India, since majority of the people depends on it. The varying crop water requirement for different crops under multiple canals necessitated the planners to arrive at an optimal crop planning for efficient, effective and economic operation of an irrigation system. Also, some reservoirs are having more command area but could not cater the irrigation demand on its own. In such cases, water will be shared or transferred within the basin from the upstream reservoirs to cater the demands at the downstream reservoir.

Another important purpose of impounded water in surface water reservoir is hydropower production. In India, many reservoirs have hydropower plants, but most of them are incidental, where the power production is through irrigation releases. Thus, the hydropower releases are termed as non-consumptive, since the water can be used for some other purpose

after power generation, mostly for irrigation. However, there are few reservoirs specially built for hydropower production, where the hydropower and irrigation releases are in the opposite direction. This calls for an optimal planning and operation of reservoirs for efficient and effective agricultural and hydropower production, considering the social concerns.

Over the decades, several conventional optimization techniques had been developed and applied for optimizing reservoir operation. The conventional techniques have their own merits and demerits. To overcome the drawbacks of conventional techniques, recently the evolutionary algorithm (EA) based soft computing techniques are widely used in optimizing the water resources systems. The EA that works on principle of natural genetics '*survival of the fittest*' is genetic algorithm (GA) and differential evolution (DE) algorithm. These techniques start their search from the initial population of possible solutions that are randomly generated to attain the global optimal solution over the generation. However, the simple EAs are slower in convergence and may results in sub-optimal solutions for complex problems having hardbound constraints. In order to improve the search of optimal solution and for faster convergence, recently chaos technique is being used along with other optimization algorithms. In the present study, the chaos algorithm is coupled with EAs such as GA and DE algorithm and applied for optimizing multi-reservoir operations using single and multi-objective approaches.

From the literature survey, it is found that mostly LP, NLP and DP techniques were used in optimizing reservoir operation, especially for single objective optimization. These techniques were either solved deterministically or stochastically. MOFLP has been most widely used for multi-objective optimization, especially in deriving optimal crop planning. However, studies on application of MOFLP in solving multi-objective multi-reservoir optimal crop planning model were very scanty. Among the EAs, GA had been frequently used for single objective optimization and NSGA-II for multi-objective optimization of reservoir systems. However, most of these studies pertain to single reservoir system. Studies on multi-objective multi-reservoir systems using EAs are very less, especially for Indian scenario. Few studies were found on application of chaotic evolutionary algorithm for reservoir optimization. The chaos sequences are mostly used only in generating initial population and are for single objective single reservoir optimization. Studies on application of chaotic evolutionary algorithm for multi-objective multi-reservoir system are not reported. Hence, in the present study an

attempt is made to use chaos sequence in every step of evolutionary algorithms and applied for both single and multi-objective optimization of multi-reservoir systems.

The Koyna Hydro Eclectic Project (KHEP) is chosen for the single objective optimization of a multi-reservoir system using EAs coupled with chaos. It consists of two reservoirs namely, Koyna and Kolkewadi reservoirs. In KHEP, the major powerhouses are in the Western side and the irrigation releases are on the Eastern side of Koyna reservoir. Thus, the releases to major powerhouses and irrigation are in the opposite direction and make the operation of the system very complex, which necessitates the optimal utilization of available water. The KHEP is optimized for maximizing the hydropower production considering the irrigation releases as constraints. Initially, a simulation model is developed to study the behaviour of the system. Then, the hydropower optimization model is developed with the objective of maximizing the hydropower production. The model is solved using both conventional and soft computing techniques. Finally, the optimal results obtained among various techniques are further simulated for longer period to evaluate the performance of the optimal policy.

The Kukadi Irrigation Project (KIP) is selected for multi-objective optimization of a multi-reservoir system using multi-objective evolutionary algorithms (MOEA) coupled with chaos. It is one of the major irrigation projects in Maharashtra comprising of five dams namely, Dimbhe, Wadaj, Manikdoh, Pimpalgaon Joge and Yedgaon. Dimbhe, Wadaj, Manikdoh and Pimpalgaon are the upstream reservoirs in parallel. Yedgaon is at the downstream of these reservoirs and is in series with all the reservoirs. Almost 60% of the cultivable area in the KIP is irrigated through Kukadi left bank canal (KLBC) from Yedgaon reservoir. However, the water available in Yedgaon reservoir is very minimal and is not sufficient to cater the irrigation demands. Therefore, water is transferred from all the upstream reservoirs to the Yedgaon reservoir through canals and rivers. This makes the operation of the system complex, since both the temporal and spatial water transfer is not optimal. Hence, a simulation model is developed to study the irrigation releases and the water transfer in the system. Then, the multi-reservoir crop planning model is developed with the objective of maximizing the net benefits and crop production. Initially, each objective is solved using crisp LP model. From the results of LP model, the MOFLP model is developed considering both the objectives as fuzzy in nature. The same multi-objective problem is then solved using MOEAs coupled with chaos. Finally, the best optimal result obtained from MOEAs is simulated to evaluate the performance of the optimal policy over the period of time.

8.2 Conclusions

In general, this study shows that the evolutionary algorithms coupled with chaos can be used for optimizing complex water resources systems having hard bound constraints. It is also found that the chaos algorithm has enriched the search of global optimal solution and converged quickly. It is found that solving multi-objective evolutionary optimization algorithm for longer generation results in very close global optimal solutions with very less variation in Pareto optimal solutions. It is observed that the hard bound constraints are not satisfied for less number of generations and the simple EAs resulted in sub-optimal solutions. The specific conclusions emanated from the present research work are as follows:

8.2.1 Multi-Objective Optimization for Optimal Crop Planning

The hybrid chaotic evolutionary algorithms developed for single objective optimization are suitably modified and applied to a large scale multi-objective multi-reservoir irrigation system. The specific conclusions arrived from this study is listed below:

1. The simulation models are very much useful in assessing the significance of individual reservoirs and their capability in satisfying their own demand and also their share in intra basin water transfer. The simulation of multi-reservoir crop planning model based on SOP showed that the Manikdoh and Yedgaon reservoir are not performing well in meeting the irrigation demand on its own. The reliability index for irrigation releases from these two reservoirs is 0.75 and 0.70, respectively. The Yedgaon reservoir has resulted in high vulnerability of 117.53×10^6 m^3 for the irrigation releases.
2. The simulation results also showed that the three upstream reservoirs namely, Dimbhe, Wadaj and Pimpalgaon have satisfactorily succeeded in water transfer to Yedgaon reservoir. However, Manikdoh reservoir failed to release the water at appropriate time to Yedgaon reservoir indicated that the releases are not optimal. The time reliability of water transfer for Manikdoh reservoir only 0.59 with a maximum vulnerability of 114.35×10^6 m^3.
3. The MOFLP is found to be one of the useful models in deriving optimal cropping pattern for multi-objective multi-reservoir system. The results give first hand information on optimal cropping pattern. The MOFLP optimal crop planning model

developed with the objective of maximizing the net benefits and crop production resulted a satisfaction level of 0.46 with an irrigation intensity of 102.18% for the integrated operation of KIP multi-reservoir system.

4. The total net benefit obtained from the system using MOFLP is Rs. 1909.92 Millions ($31.75 Millions) and total crop production of 1191.30 thousand tonnes. The MOFLP model has resulted a crop area of 86429.31 ha during Kharif and 62802.79 ha during Rabi season. On comparing with crisp LP model, the results of MOFLP are slightly less due to fuzzification on achieving the optimal trade-off between the objectives.

5. The sensitivity analyses of crossover probability over multi-objective optimization using CNSGA-II showed the objective values are better for a probability of 0.85. Similarly, the sensitivity analyses on scale factor (*F*) and crossover factor (*CR*) on multi-objective optimization using CMODE depicted that the net benefits and crop production are better for 0.20 and 0.90, respectively.

6. Among different MOEA techniques used, the CMODE has resulted in higher net benefits of Rs. 1921.77 Million ($ 31.96 Millions) and crop production of 1201.55 thousand tonnes for the multi-reservoir system. A crop area of 88678.46 ha during Kharif season and 66562.98 ha during Rabi season with an irrigation intensity of 106.29% is obtained from CMODE. The total crop area resulted by CMODE is 4 % (6009.34 ha) more than MOFLP. However, the total releases are only 0.65% (5.57×10^6 m^3) higher than MOFLP, indicating the CMODE achieved better optimal results than MOFLP by utilizing the available water efficiently.

7. The total water transfer resulted from CMODE is 26.46×10^6 m^3 higher than MOFLP model. In addition, CMODE has resulted in water transfer from all the reservoirs of KIP during most of the months. This has resulted in higher crop area under Yedgaon reservoir in CMODE model leading to higher net benefits and crop production for the same input. Thus, CMODE has resulted in global optimal water transfer both spatially and temporally compared to MOFLP model.

8. The simulation of optimal policies of CMODE showed that the policies performed very well for longer period. All the canals in the system resulted reliabilities more than 0.95 indicating the optimal policy performed very well over the period of time. Similarly, the reliability of water transfer is also more than 0.94 for all the reservoirs in the system.

9. This study shows that the chaos can be effectively coupled with multi-objective evolutionary algorithms for the multi-objective analysis of multi-reservoir systems.

8.2.2 Single Objective Optimization for Hydropower Production

1. In water resources system analysis, simulation model helps to ascertain the existing scenario for various operating conditions. In the present study, the simulation of KHEP for hydropower production using SOP showed that the power production potential is higher than present condition. It is also found that the power production can be increased to 12% for 12% increase in releases to the Western side powerhouses.
2. The evaluation of simulation studies through performance indicators helps in identifying the important components of water resources system.
    a. In the present study on evaluating the duration of operation of hydropower plants revealed that 4 hr operation per day produces more sustainable (reliable) hydropower for both constrained and unconstrained policies. However, unconstrained policy is the most advantageous in terms of utilization of the hydropower potential created.
    b. The high resilience and low vulnerability of 4 hr duration of operation of powerhouses depicts that the power production is more stable and continuous.
3. The chaos with general optimization algorithm helped to achieve better global optimal solution in lesser number of generations compared to simple optimization techniques for complex water resources problems with hard bound constraints. Introducing the chaos sequence in all the process of GA like initial population generation, crossover and mutation improved the search much better.
4. The hybrid chaotic differential evolution algorithm and hybrid chaotic genetic algorithm resulted in a better power production than NLP model as well as from simple genetic algorithm and differential evolution algorithm models.
5. In spite of various advantages, some of the parameters of EAs are need to be fixed using sensitivity analyses. The sensitivity analyses on scale factor (F) and crossover factor (CR) over the single objective using HCDE revealed that the power production is better for 0.30 and of 0.60, respectively. The sensitivity analyses on crossover

probability on single objective optimization in HCGA showed that the power production is high for 0.80.

6. Among different techniques used, HCDE resulted in highest power production for all the four policies considered in the study. These policies varied from the scenario of assessing full power production potential to present scenario of releases with tribunal constraint. Among the four policies assessed, the Policy 1 has resulted in maximum power production of 5195.39×10^6 kWh, which shows the full potential of the KHEP system. However, this Policy 1 has not resulted in irrigation release.
7. The Policy 3 which considers both the monthly and annual irrigation constraints is found to be a viable option than the Policy 4, since Policy 3 has produced 3950.93×10^6 kWh hydropower as well as resulted in irrigation releases as per the demand. This is 22% more than the power produced by Policy 4.
8. The Policy 3 is evaluated using a simulation model to study its performance in longer run. The simulation results showed that the model satisfied the irrigation demand for most of the month (deficit occurred only in 8 months out of 588 simulated months). The average annual irrigation deficit is about 12.63×10^6 m^3, which is very meagre when compared to the storage of the Koyna reservoir.

8.3 Research Contribution

The following are the research contributions:

1. The chaos algorithm is coupled with the evolutionary optimization algorithms such as genetic algorithm and differential evolution algorithm. The chaos is introduced in generating initial population, simulated binary crossover and random mutation in genetic algorithm. In differential evolution algorithm, chaos is introduced in initial population generation. The same is extended for multi-objective evolutionary algorithms.
2. The developed algorithms are applied to two complex multi-reservoir systems using non-linear hydropower production function and complicated multi-reservoir water sharing crop planning.

8.4 Scope for Future Work

The following are the scope for future work:

1. The study may be extended to develop optimal operating policies for conjunctive use of surface and ground water for the same basin using multi-objective analysis.
2. The derived optimal operating policies are in monthly time steps, which can be extended to weekly and daily time steps, especially for hydropower production.
3. In this study, one dimensional logistic map method is used for generating the chaos sequence. Other available methods can be used to generate chaos sequence and the results can be compared.

REFERENCES

Adeyemo, J. A. (2011). “Reservoir Operation using Multi-objective Evolutionary Algorithms - A Review.” *Asian Journal of Scientific Research*, 4(1), 16–27.

Adeyemo, J. A., and Otieno, F. A. O. (2009a). “Optimizing Planting Areas Using Differential Evolution (DE) and Linear Programming (LP).” *International Journal of Physical Sciences*, 4(4), 212–220.

Adeyemo, J. A., and Otieno, F. A. O. (2009b). “Optimum Crop Planning using Multi-Objective Differential Evolution Algorithm.” *Journal of Applied Sciences*, 9(21), 3780–3791.

Adeyemo, J. A., and Otieno, F. A. O. (2010). “Differential Evolution Algorithm for Solving Multi-Objective Crop Planning Model.” *Agricultural Water Management*, 97(6), 848–856.

Ahmed, J. A., and Sarma, A. K. (2005). “Genetic Algorithm for Optimal Operating Policy of a Multipurpose Reservoir.” *Water Resources Management*, 19(2), 145–161.

Ailing, L. (2004). “A Study on the Large-scale System Decomposition-Coordination Method Used in Optimal Operation of a Hydroelectric System.” *Water International*, 29(2), 228–231.

Alabdulkader, A. M., Al-Amoud, A. I., and Awad, F. S. (2012). “Optimization of the Cropping Pattern in Saudi Arabia Using a Mathematical Programming Sector Model.” *Agricultural Economics*, 58(2), 56–60.

Arunkumar, R., and Jothiprakash, V. (2012). “Optimal Reservoir Operation for Hydropower Generation using Non-linear Programming Model.” *Journal of The Institution of Engineers (India): Series A*, 93(2), 111–120.

Arunkumar, R., and Jothiprakash, V. (2013). “Chaotic Evolutionary Algorithms for Multi-Reservoir Optimization.” *Water Resources Management*, 27(15), 5207–5222.

Barros, M. T. L., Tsai, F. T.-C., Yang, S., Lopes, J. E. G., and Yeh, W. W.-G. (2003). “Optimization of Large-Scale Hydropower System Operations.” *Journal of Water Resources Planning and Management*, 129(3), 178–188.

Barros, M. T. L., Zambon, R. C., Lopes, J. E. G., Barbosa, P. S. F., Francato, A. L., and Yeh, W. W.-G. (2009). “Impacts of the Upstream Storage Reservoirs on Itaipu Hydropower Plant Operation.” *World Environmental and Water Resources Congress 2009*, American Society of Civil Engineers, Reston, VA, 4938–4946.

Bellman, R. E. (1957). *Dynamic Programming*. Princeton Landmarks in Mathematics, Princeton University Press, Princeton, NJ, USA, 340.

Ben Alaya, A., Souissi, A., Tarhouni, J., and Ncib, K. (2003). "Optimization of Nebhana Reservoir Water Allocation by Stochastic Dynamic Programming." *Water Resources Management*, 17(4), 259–272.

Boehle, W., Harboe, R., and Schultz, G. (1983). "Operating Rules for a Reservoir System Using Critical Storage Levels." Scientific Procedures Applied to the Planning, Design and Management of Water, Resources Systems, Proceedings of the Hamburg Symposium, IAHS Publ. No. 147, 321–329.

Bozorg Haddad, O., Moradi-Jalal, M., Mirmomeni, M., Kholghi, M. K., and Mariño, M. A. (2009). "Optimal Cultivation Rules in Multi-Crop Irrigation Areas." *Irrigation and Drainage*, 58(1), 38–49.

Braga Jr, B. P. F., Yeh, W. W.-G., Becker, L., and Barros, M. T. L. (1991). "Stochastic Optimization of Multiple Reservoir System Operation." *Journal of Water Resources Planning and Management*, 117(4), 471–481.

Burn, D. H., Venema, H. D., and Simonovic, S. P. (1991). "Risk-Based Performance Criteria for Real-Time Reservoir Operation." *Canadian Journal of Civil Engineering*, 18(1), 36–42.

Caponetto, R., Fortuna, L., Fazzino, S., and Xibilia, M. G. (2003). "Chaotic Sequences to Improve the Performance of Evolutionary Algorithms." *IEEE Transactions on Evolutionary Computation*, 7(3), 289–304.

Chang, F.-J., and Chen, L. (1998). "Real-Coded Genetic Algorithm for Rule-Based Flood Control Reservoir Management." *Water Resources Management*, 12(3), 185–198.

Chang, F.-J., Chen, L., and Chang, L.-C. (2005). "Optimizing the Reservoir Operating Rule Curves by Genetic Algorithms." *Hydrological Processes*, 19(11), 2277–2289.

Chang, L.-C. (2008). "Guiding Rational Reservoir Flood Operation Using Penalty-Type Genetic Algorithm." *Journal of Hydrology*, 354(1-4), 65–74.

Chang, L.-C., and Chang, F.-J. (2009). "Multi-Objective Evolutionary Algorithm for Operating Parallel Reservoir System." *Journal of Hydrology*, 377(1-2), 12–20.

Chang, L.-C., Chang, F.-J., Wang, K.-W., and Dai, S.-Y. (2010). "Constrained Genetic Algorithms for Optimizing Multi-Use Reservoir Operation." *Journal of Hydrology*, 390(1-2), 66–74.

Changchit, C., and Terrell, M. P. (1989). "CCGP Model for Multiobjective Reservoir Systems." *Journal of Water Resources Planning and Management*, 115(5), 658–670.

Chávez-Morales, J., Mariño, M. A., and Holzapfel, E. A. (1987). "Planning Model of Irrigation District." *Journal of Irrigation and Drainage Engineering*, 113(4), 549–564.

Chen, D., Huang, G., Chen, Q., and Jin, F. (2010). “Implementing Eco-Friendly Reservoir Operation by Using Genetic Algorithm with Dynamic Mutation Operator.” *Life System Modeling and Intelligent Computing*, Lecture Notes in Computer Science, K. Li, L. Jia, X. Sun, M. Fei, and G. Irwin, eds., Springer Berlin Heidelberg, 509–516.

Chen, L. (2003). “Real Coded Genetic Algorithm Optimization of Long Term Reservoir Operation.” *Journal of the American Water Resources Association*, 39(5), 1157–1165.

Chen, L., and Chang, F.-J. (2007). “Applying a Real-Coded Multi-Population Genetic Algorithm to Multi-Reservoir Operation.” *Hydrological Processes*, 21(5), 688–698.

Chen, L., McPhee, J., and Yeh, W. W.-G. (2007). “A Diversified Multiobjective GA for Optimizing Reservoir Rule Curves.” *Advances in Water Resources*, 30(5), 1082–1093.

Chen, Y. (1997). “Management of Water Resources Using Improved Genetic Algorithms.” *Computers and Electronics in Agriculture*, 18(2-3), 117–127.

Cheng, C.-T., Wang, W.-C., Xu, D.-M., and Chau, K. W. (2008). “Optimizing Hydropower Reservoir Operation Using Hybrid Genetic Algorithm and Chaos.” *Water Resources Management*, 22(7), 895–909.

Choudhari, S. A., and Raj, P. A. (2010). “Multiobjective Multireservoir Operation in Fuzzy Environment.” *Water Resources Management*, 24(10), 2057–2073.

Chow, V. Te, Maidment, D. R., and Mays, L. W. (1988). *Applied Hydrology*. McGraw-Hill, Inc., New York, 572.

Coello, C. A. C., Lamont, G. B., and Veldhuizen, D. A. V. (2007). *Evolutionary Algorithms for Solving Multi-Objective Problems*. Genetic and Evolutionary Computation Series, Springer US, Boston, MA, 800.

Dariane, A. B., and Momtahen, S. (2009). “Optimization of Multireservoir Systems Operation Using Modified Direct Search Genetic Algorithm.” *Journal of Water Resources Planning and Management*, 135(3), 141–148.

Darshana, Pandey, A., Ostrowski, M., and Pandey, R. P. (2012). “Simulation and Optimization for Irrigation and Crop Planning.” *Irrigation and Drainage*, 61(2), 178–188.

Dauer, J. P., and Krueger, R. J. (1980). “A Multiobjective Optimization Model for Water Resources Planning.” *Applied Mathematical Modelling*, 4(3), 171–175.

Davendra, D., Zelinka, I., and Onwubolu, G. (2010a). “Chaotic Attributes and Permutative Optimization.” *Evolutionary Algorithms and Chaotic Systems*, I. Zelinka, S. Celikovsky, H. Richter, and G. Chen, eds., Springer-Verlag Berlin Heidelberg, 481–517.

Davendra, D., Zelinka, I., and Senkerik, R. (2010b). “Chaos Driven Evolutionary Algorithms for the task of PID Control.” *Computers & Mathematics with Applications*, 60(4), 1088–1104.

Deb, K. (1999). “An Introduction to Genetic Algorithms.” *Sadhana*, 24(4-5), 293–315.

Deb, K. (2001). *Multi-Objective Optimization using Evolutionary Algorithms*. John Wiley & Sons (Asia) Pte Ltd, Singapore, 518.

Deb, K., and Agrawal, R. B. (1995). “Simulated Binary Crossover for Continuous Search Space.” *Complex Systems*, 9, 115–148.

Deb, K., Pratap, A., Agarwal, S., and Meyarivan, T. (2002). “A Fast and Elitist Multiobjective Genetic Algorithm: NSGA-II.” *IEEE Transactions on Evolutionary Computation*, 6(2), 182–197.

Devamane, M. G., Jothiprakash, V., and Mohan, S. (2006). “Nonlinear Programming Model for Multipurpose Multi-Reservoir Operation.” *Hydrology Journal*, 29(3-4), 33–46.

Devamane, M. G., Jothiprakash, V., and Mohan, S. (2009). “Storage Allocation and Release Rules for Multi- Reservoir System.” *Hydrology Journal*, 32(3-4), 208–220.

Dhar, A., and Datta, B. (2008). “Optimal Operation of Reservoirs for Downstream Water Quality Control Using Linked Simulation Optimization.” *Hydrological Processes*, 22(6), 842–853.

Ebrahimzadeh, R., and Jampour, M. (2013). “Chaotic Genetic Algorithm based on Lorenz Chaotic System for Optimization Problems.” *International Journal of Intelligent Systems and Applications*, 5(5), 19–24.

Fayaed, S. S., El-Shafie, A., and Jaafar, O. (2013). “Reservoir-System Simulation and Optimization Techniques.” *Stochastic Environmental Research and Risk Assessment*, 27(7), 1751–1772.

Feoktistov, V. (2006). *Differential Evolution: In Search of Solutions*. Springer-Verlag New York Inc, 195.

Gagnon, C. R., Hicks, R. H., Jacoby, S. L. S., and Kowalik, J. S. (1974). “A Nonlinear Programming Approach to a Very Large Hydroelectric System Optimization.” *Mathematical Programming*, 6(1), 28–41.

Gakpo, E., Tsephe, J., Nwonwu, F., and Viljoen, M. (2005). “Application of Stochastic Dynamic Programming (SDP) for the Optimal Allocation of Irrigation Water under Capacity Sharing Arrangements.” *Agrekon*, 44(4), 436–451.

Garudkar, A. S., Rastogi, A. K., Eldho, T. I., and Gorantiwar, S. D. (2011). “Optimal Reservoir Release Policy Considering Heterogeneity of Command Area by Elitist Genetic Algorithm.” *Water Resources Management*, 25(14), 3863–3881.

Goldberg, D. E. (1989). *Genetic Algorithms in Search, Optimization, and Machine Learning*. Artificial Intelligence, Addison-Wesley Longman Publishing Co., Inc., Boston, MA, USA, 412.

Gupta, A. P., Harboe, R., and Tabucanon, M. T. (2000). "Fuzzy Multiple-Criteria Decision Making for Crop Area Planning in Narmada River Basin." *Agricultural Systems*, 63(1), 1–18.

Hakimi-Asiabar, M., Ghodsypour, S. H., and Kerachian, R. (2009). "Multi-Objective Genetic Local Search Algorithm Using Kohonen's Neural Map." *Computers & Industrial Engineering*, 56(4), 1566–1576.

Hakimi-Asiabar, M., Ghodsypour, S. H., and Kerachian, R. (2010). "Deriving Operating Policies for Multi-Objective Reservoir Systems: Application of Self-Learning Genetic Algorithm." *Applied Soft Computing*, 10(4), 1151–1163.

Han, F., and Lu, Q.-S. (2008). "An Improved Chaos Optimization Algorithm and Its Application in the Economic Load Dispatch Problem." *International Journal of Computer Mathematics*, 85(6), 969–982.

Hashimoto, T., Stedinger, J. R., and Loucks, D. P. (1982). "Reliability, Resiliency, and Vulnerability Criteria for Water Resource System Performance Evaluation." *Water Resources Research*, 18(1), 14–20.

Haupt, R. L., and Haupt, S. E. (2003). *Practical Genetic Algorithms*. John Wiley & Sons, Inc., Hoboken, NJ, USA, 272.

Hınçal, O., Altan-Sakarya, A. B., and Metin Ger, A. (2011). "Optimization of Multireservoir Systems by Genetic Algorithm." *Water Resources Management*, 25(5), 1465–1487.

Holland, J. H. (1975). Adaptation in Natural and Artificial Systems: An Introductory Analysis with Applications to Biology, Control, and Artificial Intelligence. University of Michigan Press, 183.

Horn, J., Nafpliotis, N., and Goldberg, D. E. (1994). "A Niched Pareto Genetic Algorithm for Multiobjective Optimization." *Proceedings of the First IEEE Conference on Evolutionary Computation. IEEE World Congress on Computational Intelligence*, IEEE, 82–87.

Hossain, M. S., and El-Shafie, A. (2013). "Intelligent Systems in Optimizing Reservoir Operation Policy: A Review." *Water Resources Management*, 27(9), 3387–3407.

Huang, X., Fang, G., Gao, Y., and Dong, Q. (2010). "Chaotic Optimal Operation of Hydropower Station with Ecology Consideration." *Energy and Power Engineering*, 02(03), 182–189.

Jain, S. K. (2009). "Statistical Performance Indices for a Hydropower Reservoir." *Hydrology Research*, 40(5), 454–564.

Jain, S. K., Agarwal, P. K., and Singh, V. P. (2007). "Physical Environment of India." *Hydrology and Water Resources of India SE - 1*, Water Science and Technology Library, Springer Netherlands, 3–62.

Jain, S. K., and Singh, V. P. (2003). *Water Resources Systems Planning and Management*. Developments in Water Science, Elsevier Science, 882.

Jian-Xia, C., Qiang, H., and Yi-min, W. (2005). "Genetic Algorithms for Optimal Reservoir Dispatching." *Water Resources Management*, 19(4), 321–331.

Jothiprakash, V., and Arunkumar, R. (2013). "Optimization of Hydropower Reservoir Using Evolutionary Algorithms Coupled with Chaos." *Water Resources Management*, 27(7), 1963–1979.

Jothiprakash, V., and Arunkumar, R. (2014). "Multi-Reservoir Optimization for Hydropower Production using NLP Technique." *KSCE Journal of Civil Engineering*, 18(1), 344–354.

Jothiprakash, V., Arunkumar, R., and Ashok Rajan, A. (2011a). "Optimal Crop Planning Using A Chance Constrained Linear Programming Model." *Water Policy*, 13(5), 734–749.

Jothiprakash, V., and Mohan, S. (2003). "Implicit Stochastic Approach for Seasonal Planning of an Irrigation System." *Water Resources Journal*, 40–52.

Jothiprakash, V., and Shanthi, G. (2004). "Stochastic Dynamic Programming Model for Optimal Policies of a Multi-purpose Reservoir." *Journal of Indian Water Resources Society*, 24(4), 32–42.

Jothiprakash, V., and Shanthi, G. (2006). "Single Reservoir Operating Policies Using Genetic Algorithm." *Water Resources Management*, 20(6), 917–929.

Jothiprakash, V., and Shanthi, G. (2009). "Comparison of Policies Derived from Stochastic Dynamic Programming and Genetic Algorithm Models." *Water Resources Management*, 23(8), 1563–1580.

Jothiprakash, V., Shanthi, G., and Arunkumar, R. (2011b). "Development of Operational Policy for a Multi-reservoir System in India using Genetic Algorithm." *Water Resources Management*, 25(10), 2405–2423.

Karamouz, M., and Houck, M. H. (1982). "Annual and Monthly Reservoir Operating Rules Generated By Deterministic Optimization." *Water Resources Research*, 18(5), 1337–1344.

Karamouz, M., Houck, M. H., and Delleur, J. W. (1992). "Optimization and Simulation of Multiple Reservoir Systems." *Journal of Water Resources Planning and Management*, 118(1), 71–81.

Karamouz, M., and Houck, M. M. H. (1987). "Comparison of Stochastic and Deterministic Dynamic Programming for Reservoir Operating Rule Generation." *Journal of the American Water Resources Association*, 23(1), 1–9.

Karamouz, M., Szidarovszky, F., and Zahraie, B. (2003). *Water Resources Systems Analysis*. Lewis Publishers, 589.

Karamouz, M., Zahraie, B., Kerachian, R., and Eslami, A. (2008). "Crop Pattern and Conjunctive Use Management: A Case Study." *Irrigation and Drainage*, 59, 161–173.

KHEP. (2005). *Koyna Hydro Electric Project Stage - IV*. Irrigation Department, Government of Maharashtra, India.

Kim, T., and Heo, J.-H. (2004). "Multireservoir System Optimization Using Multi-Objective Genetic Algorithms." *Critical Transitions in Water and Environmental Resources Management*, S. Gerald, F. H. Donald, and K. S. David, eds., American Society of Civil Engineers, Reston, VA, 1–10.

Kim, T., and Heo, J.-H. (2006). "Application of Multi-Objective Genetic Algorithms to Multireservoir System Optimization in the Han River Basin." *KSCE Journal of Civil Engineering*, 10(5), 371–380.

Kim, T., Heo, J.-H., Bae, D.-H., and Kim, J.-H. (2008). "Single-Reservoir Operating Rules for a Year Using Multiobjective Genetic Algorithm." *Journal of Hydroinformatics*, 10(2), 163–179.

Kim, T., Heo, J.-H., and Jeong, C.-S. (2006). "Multireservoir System Optimization in the Han River Basin Using Multi-Objective Genetic Algorithms." *Hydrological Processes*, 20(9), 2057–2075.

Kim, T., Heo, J.-H., and Yi, J. (2001). "Monthly Reservoir Operating Rules Generated by Implicit Stochastic Optimization." *Watershed Management and Operations Management 2000*, F. Marshall, F. Donald, W. W. David, and Jr, eds., American Society of Civil Engineers, Reston, VA, 1–9.

KIPR. (1990). *Kukadi Irrigation Project Report, Volume I, II Revision*. Irrigation Department, Government of Maharashtra, India.

Kjeldsen, T. R., and Rosbjerg, D. (2004). "Choice of Reliability, Resilience and Vulnerability Estimators for Risk Assessments of Water Resources Systems." *Hydrological Sciences Journal*, 49(5), 755–767.

Knowles, J., and Corne, D. (1999). "The Pareto Archived Evolution Strategy: A New Baseline Algorithm for Pareto Multiobjective Optimisation." *Proceedings of the 1999 Congress on Evolutionary Computation-CEC99*, IEEE, Washington, DC, 98–105.

Konak, A., Coit, D. W., and Smith, A. E. (2006). "Multi-objective Optimization using Genetic Algorithms: A Tutorial." *Reliability Engineering & System Safety*, 91(9), 992–1007.

Koutsoyiannis, D., Efstratiadis, A., and Karavokiros, G. (2002). "A Decision Support Tool for the Management of Multi-Reservoir Systems." *Journal of the American Water Resources Association*, 38(4), 945–958.

Kumar, R., Singh, R. D., and Sharma, K. D. (2005). "Water Resources of India." *Current Science*, 89(5), 794–811.

Kumphon, B. (2013). “Genetic Algorithms for Multi-objective Optimization: Application to a Multi-reservoir System in the Chi River Basin, Thailand.” *Water Resources Management*, 27(12), 4369–4378.

Kuo, J. T., Cheng, W. C., and Chen, L. (2003). “Multiobjective Water Resources Systems Analysis Using Genetic Algorithms – Application to Chou-Shui River Basin, Taiwan.” *Water Science and Technology*, 48(10), 71–77.

KWDT. (2010). Krishna Water Disputes Tribunal: The Report of the Krishna Water Disputes Tribunal with the Decision. Ministry of Water Resources, Government of India, New Delhi.

Labadie, J. W. (2004). “Optimal Operation of Multireservoir Systems: State-of-the-Art Review.” *Journal of Water Resources Planning and Management*, 130(2), 93–111.

Li, B., and Jiang, W. (1998). “Optimizing Complex Functions by Chaos Search.” *Cybernetics and Systems*, 29(4), 409–419.

Liang, R.-H., and Hsu, Y.-Y. (1994). “Fuzzy Linear Programming: An Application to Hydroelectric Generation Scheduling.” *IEE Proceedings - Generation, Transmission and Distribution*, 141(6), 568.

Lingo. (2006). *Optimization Modeling with LINGO*. LINDO Systems, Inc, Illinois, 617.

Louati, M. H., Benabdallah, S., Lebdi, F., and Milutin, D. (2011). “Application of a Genetic Algorithm for the Optimization of a Complex Reservoir System in Tunisia.” *Water Resources Management*, 25(10), 2387–2404.

Loucks, D. P. (1992). “Water Resource Systems Models: Their Role in Planning.” *Journal of Water Resources Planning and Management*, 118(3), 214–223.

Loucks, D. P. (1997). “Quantifying Trends in System Sustainability.” *Hydrological Sciences Journal*, 42(4), 513–530.

Loucks, D. P., Stedinger, J. R., and Haith, D. A. (1981). *Water Resource Systems Planning and Analysis*. Prentice-Hall Inc., Englewood Cliffs, N.J., 559.

Lü, Q., Shen, G., and Yu, R. (2003). “A Chaotic Approach to Maintain the Population Diversity of Genetic Algorithm in Network Training.” *Computational Biology and Chemistry*, 27(3), 363–371.

Maji, C. C., and Heady, E. O. (1980). “Optimal Reservoir Management and Crop Planning Under Deterministic and Stochastic Inflows.” *Journal of the American Water Resources Association*, 16(3), 438–443.

May, R. M. (1976). “Simple Mathematical Models with Very Complicated Dynamics.” *Nature*, 261(5560), 459–467.

Mayer, D. G., Kinghorn, B. P., and Archer, A. A. (2005). "Differential Evolution – An Easy and Efficient Evolutionary Algorithm for Model Optimisation." *Agricultural Systems*, 83(3), 315–328.

Mays, L. W., and Tung, Y. K. (2002). *Hydrosystems Engineering and Management*. Water Resources Publications, LLC, 530.

McMahon, T. A., Adeloye, A. J., and Zhou, S.-L. (2006). "Understanding Performance Measures of Reservoirs." *Journal of Hydrology*, 324(1-4), 359–382.

Mehta, R., and Jain, S. K. (2009). "Optimal Operation of a Multi-Purpose Reservoir Using Neuro-Fuzzy Technique." *Water Resources Management*, 23(3), 509–529.

Mirajkar, A. B., and Patel, P. L. (2013). "Development of Sustainable Irrigation Planning With Multi-Objective Fuzzy Linear Programming for Ukai–Kakrapar Irrigation Project, Gujarat, India." *Canadian Journal of Civil Engineering*, 40(7), 663–673.

Mohan, S., and Jothiprakash, V. (2000). "Fuzzy System Modelling For Optimal Crop Planning." *Journal of the Institution of Engineers (India): Civil Engineering Division*, 81(1), 9–17.

Mohan, S., and Jothiprakash, V. (2003). "Development of Priority-Based Policies for Conjunctive Use of Surface and Groundwater." *Water International*, 28(2), 254–267.

Mohan, S., and Raipure, D. M. (1992). "Multiobjective Analysis of Multireservoir System." *Journal of Water Resources Planning and Management*, 118(4), 356–370.

Mohan, S., and Vijayalakshmi, D. P. (2009). "Genetic Algorithm Applications in Water Resources." *ISH Journal of Hydraulic Engineering*, 15(sup1), 97–128.

Momtahen, S., and Dariane, A. B. (2007). "Direct Search Approaches Using Genetic Algorithms for Optimization of Water Reservoir Operating Policies." *Journal of Water Resources Planning and Management*, 133(3), 202–209.

Moradi-Jalal, M., Bozorg Haddad, O., Karney, B. W., and Mariño, M. A. (2007). "Reservoir Operation in Assigning Optimal Multi-Crop Irrigation Areas." *Agricultural Water Management*, 90(1-2), 149–159.

Moradi-Jalal, M., Mariño, M. A., and Afshar, A. (2003). "Optimal Design and Operation of Irrigation Pumping Stations." *Journal of Irrigation and Drainage Engineering*, 129(3), 149–154.

Morankar, D. V., Raju, K. S., and Nagesh Kumar, D. (2013). "Integrated Sustainable Irrigation Planning with Multiobjective Fuzzy Optimization Approach." *Water Resources Management*, 27(11), 3981–4004.

Mousavi, S. J., Mahdizadeh, K., and Afshar, A. (2004). "A Stochastic Dynamic Programming Model with Fuzzy Storage States for Reservoir Operations." *Advances in Water Resources*, 27(11), 1105–1110.

Mujumdar, P. P., and Nirmala, B. (2007). "A Bayesian Stochastic Optimization Model for a Multi-Reservoir Hydropower System." *Water Resources Management*, 21(9), 1465–1485.

Nagesh Kumar, D., and Baliarsingh, F. (2003). "Folded Dynamic Programming for Optimal Operation of Multireservoir System." *Water Resources Management*, 17, 337–353.

Nagesh Kumar, D., Raju, K. S., and Ashok, B. (2006). "Optimal Reservoir Operation for Irrigation of Multiple Crops Using Genetic Algorithms." *Journal of Irrigation and Drainage Engineering*, 132(2), 123–129.

Naik, P. K., Awasthi, A. K., Anand, A. V. S. S., and Mohan, P. C. (2001). "Hydrogeologic Framework of the Deccan Terrain of the Koyna River Basin, India." *Hydrogeology Journal*, 9(3), 243–264.

Nicklow, J. W., Reed, P., Savic, D., Dessalegne, T., Harrell, L., Chan-Hilton, A., Karamouz, M., Minsker, B., Ostfeld, A., Singh, A., and Zechman, E. (2010). "State of the Art for Genetic Algorithms and Beyond in Water Resources Planning and Management." *Journal of Water Resources Planning and Management*, 136(4), 412–432.

Oliveira, R., and Loucks, D. P. (1997). "Operating Rules for Multireservoir Systems." *Water Resources Research*, 33(4), 839–852.

Pant, M., Thangaraj, R., Rani, D., Abraham, A., and Srivastava, D. K. (2008). "Estimation Using Differential Evolution for Optimal Crop Plan." *Hybrid Artificial Intelligence Systems*, E. Corchado, A. Abraham, and W. Pedrycz, eds., Springer Berlin Heidelberg, 289–297.

Paudyal, G. N., and Das Gupta, A. (1990). "A Nonlinear Chance Constrained Model for Irrigation Planning." *Agricultural Water Management*, 18(2), 87–100.

Price, K. V, Storn, R. M., and Lampinen, J. A. (2005). *Differential Evolution: A Practical Approach to Global Optimization*. Springer-Verlag Berlin Heidelberg, 558.

Qin, H., Zhou, J., Lu, Y., Li, Y., and Zhang, Y. (2010). "Multi-Objective Cultured Differential Evolution for Generating Optimal Trade-Offs In Reservoir Flood Control Operation." *Water Resources Management*, 24(11), 2611–2632.

Raju, K. S., and Duckstein, L. (2003). "Multiobjective Fuzzy Linear Programming for Sustainable Irrigation Planning: An Indian Case Study." *Soft Computing*, 7(6), 412–418.

Raju, K. S., and Nagesh Kumar, D. (2000a). "Optimum Cropping Pattern for Sri Ram Sagar Project: A Linear Programming Approach." *Journal of Applied Hydrology*, 8(1-2), 57–67.

Raju, K. S., and Nagesh Kumar, D. (2000b). "Irrigation Planning of Sri Ram Sagar Project Using Multi Objective Fuzzy Linear Programming." *ISH Journal of Hydraulic Engineering*, 6(1), 55–63.

Raju, K. S., and Nagesh Kumar, D. (2004). “Irrigation Planning using Genetic Algorithms.” *Water Resources Management*, 18(2), 163–176.

Raju, K. S., Vasan, A., Gupta, P., Ganesan, K., and Mathur, H. (2012). “Multi-Objective Differential Evolution Application to Irrigation Planning.” *ISH Journal of Hydraulic Engineering*, 18(1), 54–64.

Rani, D., Jain, S. K., Srivastava, D. K., and Perumal, M. (2013). “Genetic Algorithms and Their Applications to Water Resources Systems.” *Metaheuristics in Water, Geotechnical and Transport Engineering*, X.-S. Yang, A. H. Gandomi, S. Talatahari, and A. H. Alavi, eds., Elsevier, 43–78.

Rani, D., and Moreira, M. M. (2010). “Simulation–Optimization Modeling: A Survey and Potential Application in Reservoir Systems Operation.” *Water Resources Management*, 24(6), 1107–1138.

Ranjithan, S. R. (2005). “Role of Evolutionary Computation in Environmental and Water Resources Systems Analysis.” *Journal of Water Resources Planning and Management*, 131(1), 1–2.

Reddy, M. J., and Nagesh Kumar, D. (2006). “Optimal Reservoir Operation Using Multi-Objective Evolutionary Algorithm.” *Water Resources Management*, 20(6), 861–878.

Reddy, M. J., and Nagesh Kumar, D. (2007). “Multiobjective Differential Evolution with Application to Reservoir System Optimization.” *Journal of Computing in Civil Engineering*, 21(2), 136–146.

Reddy, M. J., and Nagesh Kumar, D. (2008). “Evolving Strategies for Crop Planning and Operation of Irrigation Reservoir System Using Multi-Objective Differential Evolution.” *Irrigation Science*, 26(2), 177–190.

Reddy, M. J., and Nagesh Kumar, D. (2012). “Computational Algorithms Inspired By Biological Processes and Evolution.” *Current Science*, 103(4), 370–380.

Reeves, C. (2003). “Genetic Algorithms.” *Handbook of Metaheuristics*, F. Glover and G. A. Kochenberger, eds., Kluwer Academic Publishers, Dordrecht, 55–82.

Regulwar, D. G., Choudhari, S. A., and Raj, P. A. (2010). “Differential Evolution Algorithm with Application to Optimal Operation of Multipurpose Reservoir.” *Journal of Water Resource and Protection*, 02(06), 560–568.

Regulwar, D. G., and Gurav, J. B. (2010). “Fuzzy Approach Based Management Model for Irrigation Planning.” *Journal of Water Resource and Protection*, 02(06), 545–554.

Regulwar, D. G., and Gurav, J. B. (2011). “Irrigation Planning Under Uncertainty—A Multi Objective Fuzzy Linear Programming Approach.” *Water Resources Management*, 25(5), 1387–1416.

Regulwar, D. G., and Gurav, J. B. (2012). "Sustainable Irrigation Planning with Imprecise Parameters under Fuzzy Environment." *Water Resources Management*, 26(13), 3871–3892.

Sahoo, B., Lohani, A. K., and Sahu, R. K. (2006). "Fuzzy Multiobjective and Linear Programming Based Management Models for Optimal Land-Water-Crop System Planning." *Water Resources Management*, 20(6), 931–948.

Sarker, R., and Ray, T. (2009). "An Improved Evolutionary Algorithm for Solving Multi-Objective Crop Planning Models." *Computers and Electronics in Agriculture*, 68(2), 191–199.

Savić, D. A. (2008). "Global and Evolutionary Optimization for Water Management Problems." *Practical Hydroinformatics*, R. J. Abrahart, L. M. See, and D. P. Solomatine, eds., Springer-Verlag Berlin Heidelberg, 231 – 243.

Schardong, A., Simonovic, S. P., and Vasan, A. (2013). "Multiobjective Evolutionary Approach to Optimal Reservoir Operation." *Journal of Computing in Civil Engineering*, 27(2), 139–147.

Sethi, L. N., Nagesh Kumar, D., Panda, S. N., and Mal, B. (2002). "Optimal Crop Planning and Conjunctive Use of Water Resources in a Coastal River Basin." *Water Resources Management*, 16(2), 145–169.

Sharif, M., and Wardlaw, R. (2000). "Multireservoir Systems Optimization Using Genetic Algorithms: Case Study." *Journal of Computing in Civil Engineering*, 14(4), 255–263.

Shokri, A., Bozorg Haddad, O., and Mariño, M. A. (2013). "Algorithm for Increasing the Speed of Evolutionary Optimization and its Accuracy in Multi-objective Problems." *Water Resources Management*, 27(7), 2231–2249.

Siddamal, U. V., and Birajdar, C. A. (2012). "Sustainable Development of Irrigation in Kukadi Integrated Project by Transfer of Surplus Water from One Reservoir to Other." *Sustainable Irrigation and Drainage: Management, Technologies and Policies*, H. Bjornlund, C. A. Brebbia, and S. Wheeler, eds., 403–411.

Simonovic, S. P. (1992). "Reservoir Systems Analysis: Closing Gap between Theory and Practice." *Journal of Water Resources Planning and Management*, 118(3), 262–280.

Simonovic, S. P. (2009). *Managing Water Resources: Methods and Tools for a Systems Approach*. Earthscan Publication Ltd., London, 640.

Simonovic, S. P., and Srinivasan, R. (1993). "Explicit Stochastic Approach for Planning the Operations of Reservoirs for Hydropower Production." *Extreme Hydrological Events: Precipitation, Floods and Droughts, Proceedings of the Yokohama Symposium*, IAHS Press-Intern Assoc Hydrological Science, Yokohama, Japan, 349–349.

Singh, A. (2014). "Irrigation Planning and Management Through Optimization Modelling." *Water Resources Management*, 28(1), 1–14.

Singh, A., and Panda, S. N. (2012). “Development and Application of an Optimization Model for the Maximization of Net Agricultural Return.” *Agricultural Water Management*, 115, 267–275.

Singh, D. ., Jaiswal, C. ., Reddy, K. ., Singh, R. ., and Bhandarkar, D. . (2001). “Optimal Cropping Pattern in a Canal Command Area.” *Agricultural Water Management*, 50(1), 1–8.

Sinha, A. K., Rao, B. V., and Bischof, C. H. (1999). “Nonlinear Optimization Model for Screening Multipurpose Reservoir Systems.” *Journal of Water Resources Planning and Management*, 125(4), 229–233.

Sivakumar, B. (2000). “Chaos Theory in Hydrology: Important Issues and Interpretations.” *Journal of Hydrology*, 227(1-4), 1–20.

Sivanandam, S. N., and Deepa, S. N. (2007). *Introduction to Genetic Algorithms*. Springer Verlag, Berlin Heidelberg, 442.

Skanderova, L., Zelinka, I., and Saloun, P. (2013). “Chaos Powered Selected Evolutionary Algorithms.” *Nostradamus 2013: Prediction, Modeling and Analysis of Complex Systems*, Advances in Intelligent Systems and Computing, I. Zelinka, G. Chen, O. E. Rössler, V. Snasel, and A. Abraham, eds., Springer International Publishing, Heidelberg, 111–124.

Solomatine, D. P., See, L. M., and Abrahart, R. J. (2008). “Data-Driven Modelling: Concepts, Approaches and Experiences.” *Practical Hydroinformatics SE - 2*, Water Science and Technology Library, R. Abrahart, L. See, and D. Solomatine, eds., Springer Berlin Heidelberg, 17–30.

Sreenivasan, K. R., and Vedula, S. (1996). “Reservoir Operation for Hydropower Optimization: A Chance-Constrained Approach.” *Sadhana*, 21(4), 503–510.

Srinivas, N., and Deb, K. (1994). “Muiltiobjective Optimization Using Nondominated Sorting in Genetic Algorithms.” *Evolutionary Computation*, 2(3), 221–248.

Srinivasa Prasad, A., Umamahesh, N. V., and Viswanath, G. K. (2011). “Optimal Irrigation Planning Model for an existing Storage based Irrigation system in India.” *Irrigation and Drainage Systems*, 25(1), 19–38.

Storn, R. M., and Price, K. V. (1995). Differential Evolution - A Simple and Efficient Adaptive Scheme for Global Optimization over Continuous Spaces. International Computer Science Institute-Publications-TR-95-012, Citeseer, 1–15.

Storn, R. M., and Price, K. V. (1997). “Differential Evolution – A Simple and Efficient Heuristic for Global Optimization over Continuous Spaces.” *Journal of Global Optimization*, 11(4), 341–359.

Sukhatme, S. (2011). “Meeting India’s Future Needs of Electricity through Renewable Energy Sources.” *Current Science*, 101(5), 624–630.

Tavazoei, M. S., and Haeri, M. (2007). “Comparison of Different One-Dimensional Maps as Chaotic Search Pattern in Chaos Optimization Algorithms.” *Applied Mathematics and Computation*, 187(2), 1076–1085.

Tejada-Guibert, J. A., Stedinger, J. R., and Staschus, K. (1990). “Optimization of Value of CVP’s Hydropower Production.” *Journal of Water Resources Planning and Management*, 116(1), 52–70.

Thatte, C. D. (2012). “Impacts of Koyna Dam, India.” *Impacts of Large Dams: A Global Assessment*, Water Resources Development and Management, C. Tortajada, D. Altinbilek, and A. K. Biswas, eds., Springer Berlin Heidelberg, 329–356.

Tilmant, A., Fortemps, P., and Vanclooster, M. (2002). “Effect of Averaging Operators in Fuzzy Optimization of Reservoir Operation.” *Water Resources Management*, 16(1), 1–22.

Tospornsampan, J., Kita, I., Ishii, M., and Kitamura, Y. (2005). “Optimization of a Multiple Reservoir System Operation Using a Combination of Genetic Algorithm and Discrete Differential Dynamic Programming: A Case Study in Mae Klong System, Thailand.” *Paddy and Water Environment*, 3(1), 29–38.

Tzimopoulos, C., Balioti, V., Evangelides, C., and Yannopoulos, S. (2011). “Irrigation Network Planning Using Linear Programming.” *Proceedings of the 12th International Conference on Environmental Science and Technology*, A–1939–A–1946.

Umadevi, P. P., Padikkal, S., and James, E. J. (2013). “Sustainability Considerations of Irrigation Systems: A Case Study of Inter-State Systems in the Aliyar Sub-Basin, India.” *ISH Journal of Hydraulic Engineering*, 19(3), 154–163.

Valunjkar, S. S. (2007). “Optimization of Water Resources for Cropping Pattern under Sustainable Conditions through Fuzzy Logic System.” *Sustainable Development and Planning III*, WIT Transactions on Ecology and the Environment, Vol 102, A. Kungolos, C. . Brebbia, and E. Beriatos, eds., WIT Press, Southampton, UK, 883–892.

Vasan, A., and Raju, K. S. (2007). “Application of Differential Evolution for Irrigation Planning: An Indian Case Study.” *Water Resources Management*, 21(8), 1393–1407.

Vedula, S., and Mohan, S. (1990). “Real-Time Multipurpose Reservoir Operation: A Case Study.” *Hydrological Sciences Journal*, 35(4), 447–462.

Vedula, S., Mohan, S., and Shrestha, V. S. (1986). “Improved Operating Policies for Multipurpose Use: A Case Study of Bhadra Reservoir.” *Sadhana*, 9(3), 157–176.

Vedula, S., and Mujumdar, P. P. (2005). *Water Resources Systems: Modelling Techniques and Analysis*. Tata McGraw-Hill, New Delhi, 279.

Vucetic, D., and Simonovic, S. P. (2013). “Evaluation and Application of Fuzzy Differential Evolution Approach for Benchmark Optimization and Reservoir Operation Problems.” *Journal of Hydroinformatics*, 15(4), 1456–1473.

Wardlaw, R., and Bhaktikul, K. (2001). “Application of a Genetic Algorithm for Water Allocation in an Irrigation System.” *Irrigation and Drainage*, 50(2), 159–170.

Wardlaw, R., and Sharif, M. (1999). “Evaluation of Genetic Algorithms for Optimal Reservoir System Operation.” *Journal of Water Resources Planning and Management*, 125(1), 25–33.

Williams, G. P. (1997). *Chaos Theory Tamed*. Joseph Henry Press, Washington, D.C., 499.

Wu, X., Huang, X., Fang, G., and Kong, F. (2011). “Optimal Operation of Multi-Objective Hydropower Reservoir with Ecology Consideration.” *Journal of Water Resource and Protection*, 03(12), 904–911.

Wurbs, R. A. (1993). “Reservoir-System Simulation and Optimization Models.” *Journal of Water Resources Planning and Management*, 119(4), 455–472.

Wurbs, R. A., and Carriere, P. E. (1993). “Hydrologic Simulation of Reservoir Storage Reallocations.” *International Journal of Water Resources Development*, 9(1), 51–64.

Xianfeng, H., Dongguo, S., and Wenquan, G. (2008). “Multi-Objective Chaotic Optimization Algorithm and Its Application in Optimal Water Resources Deployment.” *Kybernetes*, 37(9/10), 1374–1382.

Yang, C.-C., Chang, L.-C., Chen, C.-S., and Yeh, M.-S. (2009). “Multi-objective Planning for Conjunctive Use of Surface and Subsurface Water Using Genetic Algorithm and Dynamics Programming.” *Water Resources Management*, 23(3), 417–437.

Yeh, W. W.-G. (1985). “Reservoir Management and Operations Models: A State-of-the-Art Review.” *Water Resources Research*, 21(12), 1797–1818.

Yeh, W. W.-G., and Becker, L. (1982). “Multiobjective Analysis of Multireservoir Operations.” *Water Resources Research*, 18(5), 1326–1336.

Yin, L., and Liu, X. (2009). “Optimal Operation of Hydropower Station by Using an Improved DE Algorithm.” *Proceedings of the Second Symposium International Computer Science and Computational Technology(ISCSCT ’09)*, 071–074.

Yuan, X., Yuan, Y., and Zhang, Y. (2002). “A Hybrid Chaotic Genetic Algorithm for Short-Term Hydro System Scheduling.” *Mathematics and Computers in Simulation*, 59(4), 319–327.

Yuan, X., Zhang, Y., Wang, L., and Yuan, Y. (2008). “An Enhanced Differential Evolution Algorithm for Daily Optimal Hydro Generation Scheduling.” *Computers & Mathematics with Applications*, 55(11), 2458–2468.

Yurtal, R., Seckin, G., and Ardiclioglu, G. (2005). “Hydropower Optimization for the Lower Seyhan System in Turkey using Dynamic Programming.” *Water International*, 30(4), 522–529.

Zadeh, L. A. (1965). “Fuzzy Sets.” *Information and Control*, 8(3), 338–353.

Zahraie, B., and Hosseini, S. M. (2009). “Development of Reservoir Operation Policies Considering Variable Agricultural Water Demands.” *Expert Systems with Applications*, 36(3), 4980–4987.

Zahraie, B., Kerachian, R., and Malekmohammadi, B. (2008). “Reservoir Operation Optimization Using Adaptive Varying Chromosome Length Genetic Algorithm.” *Water International*, 33(3), 380–391.

Zambon, R. C., Barros, M. T. L., Lopes, J. E. G., Barbosa, P. S. F., Francato, A. L., and Yeh, W. W.-G. (2012). “Optimization of Large-Scale Hydrothermal System Operation.” *Journal of Water Resources Planning and Management*, 138(2), 135–143.

Zeng, X., Kang, S., Li, F., Zhang, L., and Guo, P. (2010). “Fuzzy Multi-Objective Linear Programming Applying To Crop Area Planning.” *Agricultural Water Management*, 98(1), 134–142.

Zhang, H., Zhou, J., Zhang, Y., Fang, N., and Zhang, R. (2013). “Short Term Hydrothermal Scheduling Using Multi-Objective Differential Evolution with Three Chaotic Sequences.” *International Journal of Electrical Power & Energy Systems*, 47, 85–99.

Zimmermann, H. J. (1996). *Fuzzy Set Theory - And Its Applications*. Allied Publishers Limited, New Delhi, 399.

Zitzler, E., and Thiele, L. (1999). “Multiobjective Evolutionary Algorithms: A Comparative Case Study and the Strength Pareto Approach.” *IEEE Transactions on Evolutionary Computation*, 3(4), 257–271.

LIST OF PUBLICATIONS FROM THE PRESENT WORK

International Journals

1. Magar, R.B., and Jothiprakash, V. (2011). Intermittent reservoir daily-inflow prediction using lumped and distributed data multi-linear regression models. *Journal of Earth System Science,* 120(6), 1067-1084.
2. Jothiprakash, V., Arunkumar, R. and A. Asokarajan. (2011). Optimal Crop Planning using Chance Constraint Linear Programming Model. *Water Policy,* 13(5), 734–749.
3. Jothiprakash, V., Shanthi, G., and Arunkumar, R. (2011). Development of Operational Policy for a Multi-reservoir System in India using Genetic Algorithm. *Water Resources Management*, 25(10), 2405-2423.
4. Jothiprakash, V., Nirmala, J. and Arunkumar, R. (2012). Performance assessment of storage policies of the Vaigai Reservoir using a simulation model. *Water International,* 37(3), 319 - 333.
5. Jothiprakash, V., and, Magar R.B. (2012). Multi-time-step ahead daily and hourly intermittent reservoir inflow prediction by artificial intelligent technique using lumped and distributed data. *Journal of Hydrology,* 450-451, 293-307.
6. Arunkumar, R. and Jothiprakash, V. (2013). Reservoir Evaporation Prediction Using Data Driven Techniques. *Journal of Hydrologic Engineering*, ASCE, 18(1), 40 – 49.
7. Jothiprakash, V and T.A. Fathima, (2013). Chaotic Analysis of Daily Rainfall Series in Koyna Reservoir Catchment Area. *Stochastic Environmental Research and Risk Assessment,* 27(6), 1371-1381.
8. Jothiprakash, V. and Arunkumar, R. (2013). Optimizing Hydropower Reservoir using Evolutionary Algorithm coupled with Chaos. *Water Resources Management,* 27(7), 1963-1979.
9. Arunkumar, R. and Jothiprakash, V. (2013). Chaotic evolutionary algorithms for multi-reservoir optimization. *Water Resources Management*, 27(15), 5207-5222.
10. Jothiprakash, V. and Arunkumar, R. (2014). Multi-Reservoir Optimization for hydropower generation using NLP Technique. *KSCE Journal of Civil Engineering*, 18(1), 344–354.

National Journal

11. Arunkumar, R. and Jothiprakash, V., (2011). Artificial Neural Network Models For Shivajisagar Lake Evaporation Prediction. *National Journal on Chembiosis*, 2(1), 35 - 42.
12. Arunkumar, R. and Jothiprakash, V. (2012). Optimal Reservoir Operation for Hydropower Generation Using Non-Linear Programming Model. *Journal of Institution of Engineers (India) Series A, 93(2), 111 – 120.*
13. Mandal, T., and Jothiprakash, V. (2012). Short term rainfall prediction using ANN and MT techniques. *ISH Journal of Hydraulic Engineering,* 18(1), 28-37.
14. Arunkumar, R. and Jothiprakash, V. (2014). Evaluation of a multi-reservoir hydropower system using a simulation model. *ISH Journal of Hydraulic Engineering*, 20(2), 177-187.
15. Magar R.B, and V. Jothiprakash, (2014) Nash IUH parameters estimation using method of moments - a case study, *Journal of Indian Water Resources Society,* 34(2), 1-8.

Book Section

16. Arunkumar, R., and Jothiprakash, V. (2014). "Improving the Performance of the Optimization Technique Using Chaotic Algorithm." *Proceedings of the Second International Conference on Soft Computing for Problem Solving (SocProS 2012)*, December 28-30, 2012 SE - 27, Advances in Intelligent Systems and Computing, B. V Babu, A. Nagar, K. Deep, M. Pant, J. C. Bansal, K. Ray, and U. Gupta, eds., Springer India, 243–250.

International Conferences

17. Arunkumar, R. and Jothiprakash, V., (2012). Optimal Reservoir Operation for Hydropower Generation using Differential Evolution Algorithm. 2nd International Conference on Water Resources (ICWR-2012), 5-9 November 2012, Langkawi, Malaysia.
18. Arunkumar, R. and Jothiprakash, V., (2012). Improving the performance of the optimization technique using chaotic algorithm. *International Conference on Soft Computing for Problem Solving* (SocPros 2012) at The Institute of Engineering and Technology, JK Lakshmipat University, Jaipur (India) during December 28-30, 2012.
19. Arunkumar, R. and Jothiprakash, V., (2013). Deriving Optimal Crop Plan For Dimbhe Reservoir – A Fuzzy Multi-Objective Approach. International Conference on 'Advances in Water Resources Development and Management (AWRDM-2013)' at Panjab University, Chandigarh, October 23-27, 2013. Pp. 38.
20. Arunkumar, R. and Jothiprakash, V., (2013). Deriving Optimal Crop Planning For the Command Area of Dimbhe Reservoir, Maharashtra. Proceedings of 'XVIII Conference

on Hydraulics, Water Resources, Coastal and Environmental Engineering (HYDRO 2013 INTERNATIONAL)' December 04-06, 2013, IIT Madras, India, pp. 1285 – 1293.

National Conferences

21. Arunkumar, R and V. Jothiprakash (2010) 'A Review on Reservoir Optimization Models using Genetic Algorithm Technique', Proceeding of '*National conference on Hydraulics, Water Resources, Coastal and Environmental Engineering – HYDRO 2010*', pp. 719 - 725.
22. Jothiprakash, V., Arunkumar, R., and J. Nirmala (2010) Evaluation of Vaigai Reservoir Operating Rules Using a Simulation Model" in the 14th *National symposium on Hydrology* with focal theme of '*Management of Water Resources under Drought Situation*', Dec 21 – 22, 2010, MNIT, Jaipur.
23. Arunkumar, R., and Jothiprakash, V., (2011) Reservoir evaporation prediction using Artificial Neural Network" in the abstract volume of the '*Annual convention on the Geo-spatial Technologies and Applications*, Geo Summit 2011', July 27 – 29, 2011, Sathyabama University, Chennai, pp. 35.
24. Arunkumar, R., and Jothiprakash, V. (2011) Simulation Studies on a Large Scale Hydropower Reservoir. *National Conference on Hydraulics and Water Resources* – HYDRO 2011, held during 29-30 Dec 2011 at SVNIT, Surat, pp. 828 – 836.
25. Arunkumar, R., and Jothiprakash, V. (2012) Optimal Reservoir Operation for Hydropower Generation. *National Symposium on Water Resources Management in Changing Environment* (WARMICE – 2012) held during 8-9 Feb 2012 at NIH, Roorkee, pp. 311 – 317.
26. Arunkumar, R. and Jothiprakash, V., (2012). Optimal Reservoir Operation for Hydropower Generation using Genetic Algorithm. *National Conference on Hydraulics, Water Resources, Costal and Environmental Engineering* (HYDRO-2012), during Dec 7 & 8, 2012 at IIT Bombay, India, pp. 1419 - 1426.
27. Arunkumar, R. and Jothiprakash, V., (2013). Sustainable Crop Planning For A Multi-Reservoir System Using Fuzzy Multi-Objective Approach. *National Conference on Sustainable Water Resources Development and Management* (SWARDAM-2013), Government College of Engineering, Aurangabad, 30 Sept. - 01 Oct. 2013, pp. 236-242.
28. Jothiprakash, V., and Arunkumar, R. (2013). Soft Computing Techniques in Reservoir Optimization. *National Conference on Sustainable Water Resources Development and Management* (SWARDAM-2013), Government College of Engineering, Aurangabad, 30 Sept. - 01 Oct. 2013, pp. 273-282.
29. Arunkumar, R. and Jothiprakash, V., (2014). Optimizing Reservoir Operation Using Hybrid Chaotic Genetic Algorithm. *Research Scholar and Alumni Symposium (RSAS-*

2014), during 7 - 8th March 2014 held at Indian Institute of Technology Bombay, Mumbai, Maharashtra. Pp. 59.

ACKNOWLEDGEMENTS

I take this opportunity to thank Ministry of Water Resources, Government of India for sponsoring this project through Indian National Committe of Surface Water, erstwhile Indian National Committee on Hydrology. I thank HOD, Department of Civil Engineering, Dean (R&D), Industrial Research & Consultancy Centre (IRCC), IIT Bombay for the help and support to implement this project. I also thank Indian Institute of Technology Bombay for providing the facilities to carry out this project.

I thank Mr. D. N. Modak, Chief Engineer, Koyna Hydroelectric Project, Mr. Siddhamal, Executive Engineer, Koyna Dam and Mr. Gokale, Executive Engineer, Kolkewadi Dam for providing the necessary data. I thank Mr. A. S. Nanaware, Superintending Engineer, Command Area Development Authority, Pune for providing permission and Mr. S. P. Mahamane, Administrative officer, Command Area Development Authority, Pune for their help in data collection. I also thank Mr. Y. R. Kathal, Executive Engineer, Kukadi Irrigation Circle 1, Narayangaon for providing the necessary data of Kukadi Irrigation Project. I also express my heartfelt thanks to Mr. Tushar Pawar, Section Engineer and Mr. Shrimandilkar, Kukadi Project Irrigation Circle 1, Narayangaon for their kind help during my visits to Narayangaon to collect the necessary data.

I would like to thank my research scholars Dr. Alka Kote, Dr. R. B. Magar and Dr. R. Arunkumar for their work in this project.

Dr. V. Jothiprakash